This document was prepared in conjunction with work accomplished under Contract No. DE-AC09-96SR18500 with the U. S. Department of Energy.

DISCLAIMER

WSRC-TR-2005-00074
Revision 0

KEY WORDS: Performance Assessment
Low-level Radioactive Waste Disposal

SPECIAL ANALYSIS: REVISION OF SALTSTONE VAULT 4 DISPOSAL LIMITS (U)

PREPARED BY:
James R. Cook
Elmer L. Wilhite
Robert A. Hiergesell
Gregory P. Flach

MAY 26, 2005

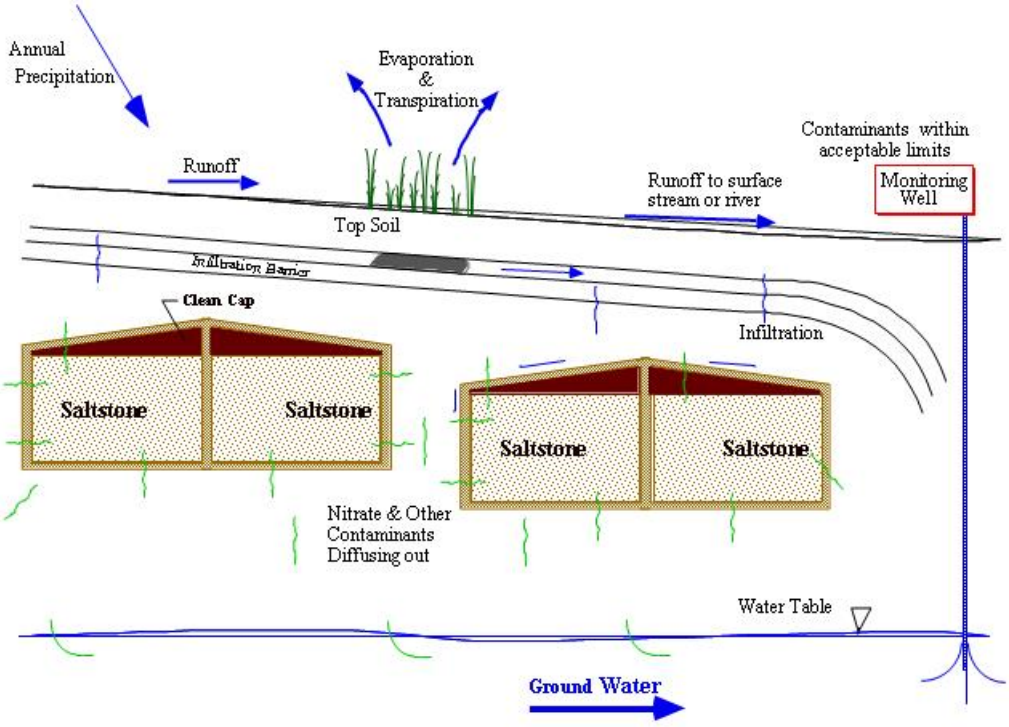

Westinghouse Savannah River Company
Savannah River Site
Aiken, SC 29808

Prepared for the U.S. Department of Energy Under Contract Number DE-AC09-96SR18500

SRNL
SAVANNAH RIVER NATIONAL LABORATORY

WSRC-TR-2005-00074
Revision 0

KEY WORDS: **Performance Assessment**
Low-level Radioactive Waste Disposal

SPECIAL ANALYSIS: REVISION OF SALTSTONE VAULT 4 DISPOSAL LIMITS (U)

MAY 26, 2005

PREPARED BY:
James R. Cook
Elmer L. Wilhite
Robert A. Hiergesell
Gregory P. Flach

Westinghouse Savannah River Company
Savannah River Site
Aiken, SC 29808

Prepared for the U.S. Department of Energy Under Contract Number DE-AC09-96SR18500

SRNL
SAVANNAH RIVER NATIONAL LABORATORY

THIS PAGE INTENTIONALLY LEFT BLANK

REVIEWS AND APPROVALS

Authors

J. R. Cook, Author, Waste Disposal and Environmental Development Group Date

E. L. Wilhite, Author, Waste Processing Technology Department Date

R. A. Hiergesell, Author. Waste Disposal and Environmental Development Group Date

G. P. Flach, Author. Environmental Sciences and Technology Department Date

SRNL Approvals

B. T. Butcher, Level 4 Manager, Waste Processing Technology Department Date

W. E. Stevens, Level 3 Manager, Waste Processing Technology Department Date

Waste Solidification Area Project and Additional Approvals

D. G. Thompson, Facility Operations Safety Committee Chairman Date

M. S. Miller, Waste Solidification Chief Engineer Date

W. T. Goldston, Solid Waste Division Date

THIS PAGE INTENTIONALLY LEFT BLANK

EXECUTIVE SUMMARY

New disposal limits have been computed for Vault 4 of the Saltstone Disposal Facility based on several revisions to the models in the existing Performance Assessment and the Special Analysis issued in 2002. The most important changes are the use of a more rigorous groundwater flow and transport model, and consideration of radon emanation. Other revisions include refinement of the aquifer mesh to more accurately model the footprint of the vault, a new plutonium chemistry model accounting for the different transport properties of oxidation states III/IV and V/VI, use of variable infiltration rates to simulate degradation of the closure system, explicit calculation of gaseous releases and consideration of the effects of settlement and seismic activity on the vault structure. The disposal limits have been compared with the projected total inventory expected to be disposed in Vault 4. The resulting sum-of-fractions of the 1000-year disposal limits is 0.2, which indicates that the performance objectives and requirements of DOE 435.1 will not be exceeded. This SA has not altered the conceptual model (i.e., migration of radionuclides from the Saltstone waste form and Vault 4 to the environment via the processes of diffusion and advection) of the Saltstone PA (MMES 1992) nor has it altered the conclusions of the PA (i.e., disposal of the proposed waste in the SDF will meet DOE performance measures). Thus a PA revision is not required and this SA serves to update the disposal limits for Vault 4. In addition, projected doses have been calculated for comparison with the performance objectives laid out in 10 CFR 61. These doses are 0.05 mrem/year to a member of the public and 21.5 mrem/year to an inadvertent intruder in the resident scenario over a 10,000-year time-frame, which demonstrates that the 10 CFR 61 performance objectives will not be exceeded. This SA supplements the Saltstone PA and supersedes the two previous SAs (Cook et al. 2002; Cook and Kaplan 2003).

THIS PAGE INTENTIONALLY LEFT BLANK

TABLE OF CONTENTS

LIST OF FIGURES

LIST OF TABLES

LIST OF APPENDICES

LIST OF ACRONYMS AND ABBREVIATIONS

ACRONYMS

ARP	Actinide Removal Process
CFR	Code of Federal Regulations
CRC	Chemical Rubber Company
DOE	Department of Energy
DWPF	Defense Waste Processing Facility
EDE	effective dose equivalent
ETP	Effluent Treatment Project
FACT	Subsurface Flow and Contaminant Transport code
GCL	geosynthetic clay liner
GSA	General Separations Area
HELP	Hydrologic Evaluation of Landfill Performance code
HLW	high-level waste
ITP	In-Tank Precipitation
LLC	Limited Liability Company
LAW	low-activity waste
LLW	low-level waste
MCL	maximum contaminant level
MEI	maximally exposed individual
MMES	Martin Marietta Energy Systems, Inc.
NCRP	National Council on Radiation Protection and Measurements
NDAA	National Defense Authorization Act
NPDES	National Pollutant Discharge Elimination System
NRC	Nuclear Regulatory Commission
PA	Performance Assessment
RPA	Radiological Performance Assessment
SA	Special Analysis
SDCF	scenario dose conversion factor
SDF	Saltstone Disposal Facility
SOF	sum-of-fractions
SPF	Saltstone Processing Facility
SRS	Savannah River Site
SWPF	Salt Waste Processing Facility
TCLP	toxicity characteristic leaching procedure
TEDE	total effective dose equivalent
TPB	Tetraphenylborate
TRU	transuranic
USDA	United States Department of Agriculture
USDOE	United States Department of Energy
USEPA	United States Environmental Protection Agency
USNRC	United States Nuclear Regulatory Commission
WSRC	Westinghouse Savannah River Company

ABBREVIATIONS

μ	micro
Ci	Curie
cm	centimeter
d	day
ft	feet
g	gram
in	inch
m	meter
mL	milliliter
mrem	millirem
mSv	milliSievert
p	pico
sec	second
Sv	Sievert
wt%	weight percent
yr	year

THIS PAGE INTENTIONALLY LEFT BLANK

1.0 INTRODUCTION

This Special Analysis report describes a study to update the disposal limits for Vault 4 in the Saltstone Disposal Facility, originally presented in the Z-Area Performance Assessment (MMES et al. 1992) and subsequent Special Analyses (Cook et al. 2002; Cook and Kaplan 2003). This SA uses the same conceptual model (i.e., migration of radionuclides from the Saltstone waste form and Vault 4 to the environment via the processes of diffusion and advection) employed in the earlier assessments. Relative to the former PA and SAs, this analysis incorporates the following specific revisions:

- evaluation of additional radionuclides based on a recent updated screening analysis (Cook 2004),
- a revised treatment of Pu chemistry in the groundwater pathway, in which Pu(III/IV) and Pu(V/VI) are modeled separately with differing geochemical properties (Cook 2002, Kaplan 2004),
- updated soil-solute distribution coefficients (K_d 's) for various elements and soil/waste types (Kaplan 2004),
- a revised infiltration time history to reflect the present Z-Area closure plan and a cover degradation analysis (Phifer and Nelson 2003),
- refinement of the aquifer model computational mesh,
- groundwater flow field results from a new GSA/PORFLOW model that replaces the previous GSA/FACT model (Flach 2004),
- an expanded radon analysis considering Ra-226, Th-230, U-238 and Pu-238 as parents of Rn-222 in addition to U-234, which was the only precursor considered in the 2002 SA (Cook et al. 2002),
- application of atmospheric pathway screening to define the suite of radionuclides considered in the air pathway analysis (Crapse and Cook 2004),
- updated meteorology parameters and dose factors (Simpkins 2004) in the air pathway analysis, and
- use of an automated intruder analysis that uses updated *Federal Guidance Report 11* and 12 dose conversion factors (Koffman 2004).

Disposal limits are computed based on analyses of groundwater, inadvertent intruder, and air pathways for potential exposure and radon emanation. Each pathway analysis is discussed in subsequent sections of the report, followed by presentation of disposal limits, and conclusions and recommendations. All disposal limits are given in the Appendices, though only those less than 1E20 are brought into the report Sections, since limits greater than 1E20 curies are equivalent to "no limit need be considered". The evaluation demonstrates that disposal of the waste planned for Vault 4 will meet the performance objectives of DOE Order 435.1, and, thus, does not alter the conclusions of the PA.

This SA supplements the Saltstone PA and supersedes the two previous SAs (Cook et al. 2003; Cook and Kaplan 2003).

1.1 Vault Description

The two existing vaults (i.e., Vault #1 and Vault #4) are constructed of reinforced concrete containing slag (Langton 1986). Slag has also been incorporated into the Saltstone composition.

The currently active vault (Vault #4) has the dimensions of approximately 200 feet wide, by 600 feet in length, by 26 feet in height. The vault is divided into 12 cells, with each cell measuring approximately 100 ft. x 100 ft. The vault is covered with a sloped, permanent roof that has a minimum thickness of 4 inches, and a minimum slope of 0.24 inches/foot. The vault walls are approximately 1.5 feet thick, with the base mat having a thickness of 2 feet. Operationally, the cell of the vault will be filled to a height of approximately 25 feet with Saltstone, and then a layer of uncontaminated grout, with an average thickness of 2 feet, will be poured to fill in the space between the Saltstone and the sloped roof. Figure 1-1 is an aerial view of Vaults 1 and 4.

1.2 SDF Closure Concept

One of the key performance objectives of any closure of a waste disposal site is to limit moisture flux through the waste minimizing contamination of surface runoff and underlying groundwater. Because the SDF is designed as a controlled release facility, proper closure to meet the objective of limiting moisture through the waste will be an integral part of long-term acceptability of the disposal site. Because backfilling around the vaults and final closure of the SDF will be delayed for several years, a detailed closure design has not been fully developed for the SDF. Thus, an integral part of the SDF SA required that a closure concept be described and subsequently tested in models that simulate the performance characteristics of the proposed closure concept.

1.2.1 Physical Description of the SDF Closure Concept

The closure concept developed is illustrated in Figure 1-2. After an individual vault cell is filled with Saltstone, interim closure will be performed which consists of the placement of a 16-inch (0.41 m) clean grout layer between the Saltstone and the overlying concrete roof. Final closure will occur when all Saltstone vaults are filled, and will consist of the placement of a closure cap over all of the vaults. This will be followed by a 100-year period of institutional control, as described in Phifer and Nelson, 2003.

Final closure of the SDF will be accomplished by constructing a drainage system and revegetating the site. The drainage system will consist of a system of rip-rap lined ditches that intercept the gravel layer of the moisture barrier. These ditches will divert surface runoff and water intercepted by the moisture barrier away from the disposal site. The drainage ditches will be constructed between rows of vaults and around the perimeter of the SDF.

The topsoil will be revegetated with bamboo. A study conducted by the USDA Soil Conservation Service (Cook and Salvo 1992) has shown that two species of bamboo (Phyllostachys bissetii and Phyllostachys rubromarginata) will quickly establish a dense ground cover which will prevent the growth of pine trees, the most deeply rooted naturally occurring plant type at SRS. Bamboo is the shallow-rooted climax species which evapotranspirates year-around in the SRS climate removing a large amount of moisture from the soil and decreasing the infiltration into the underlying disposal system.

1.3 EXISTING VAULT 4 WASTE INVENTORY

The current radionuclide inventory in Vault 4 is given in Table 1-1.

Figure 1-1. Aerial View of Vaults 1 (Rear) and 4 (Foreground)

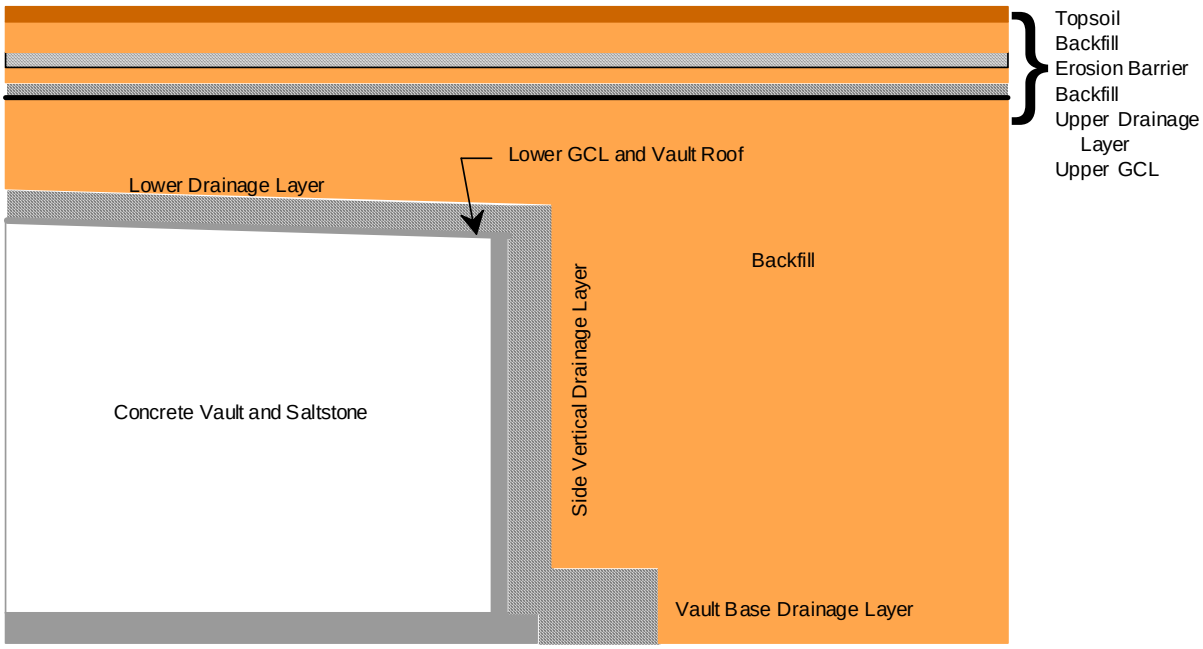

Figure 1-2. SDF Closure Cap Configuration

Table 1-1. Vault 4 Inventory as of 12/31/03

Nuclide	Ci
H-3	2.94E+01
C-14	2.35E-01
Co-57	3.43E-04*
Ni-59	<9.09E-03
Co-60	6.83E-03
Ni-63	<6.01E-02
Se-79	2.57E-02
Sr-90	3.17E-01
Nb-94	<9.91E-04
Tc-99	2.35E+01
Ru-103	2.70E-05*
Ru-106	6.14E-03
Sb-124	2.39E-02*
Sb-125	9.39E-01
Sn-126	5.66E-02
I-129	8.16E-02
Ba-133	NR[2]
Cs-134	1.32E-02*
Cs-137	1.68E+01
Ce-141	8.85E-06*
Pm-144	7.45E-03*
Pm-146	1.97E-04*
Sm-151	<9.29E-04*
Eu-152	<5.14E-03*
Eu-154	<9.03E-03
Eu-155	<1.58E-03
U-232	9.46E-03*
U-233/234	3.52E+00
U-235/236	6.81E-02
Np-237	4.87E-03
U-238	<1.10E-01
Pu-238	6.78E-01
Pu-239/240	1.33E-01
Pu-241	1.63E-02
Am-241	6.67E-02
Pu-242	<8.03E-03
Am-243	1.30E-03*
Cm-243/244	8.06E-02
Cf-251	2.47E-01*

NOTES:
*Value calculated based on available data that was not reported for one or more cells.
NR[2] Not reported on applicable sample analyses.
Source: (Crapse et al. 2004)

THIS PAGE INTENTIONALLY LEFT BLANK

2.0 GROUNDWATER ANALYSIS

2.1 Methodology

The groundwater pathway analysis for each radionuclide involves two steps. First a vadose zone flow and transport simulation is done to estimate flux to the water table for a disposed radionuclide parent and any subsequent progeny. Then saturated zone flow and transport modeling is used to estimate the groundwater concentration(s) at a hypothetical well placed 100 meters down-gradient from the disposal unit.

The vadose zone flow model was developed to reflect the current Z-Area closure concept (Phifer and Nelson 2003), which calls for a geosynthetic cover system instead of a kaolin cap as assumed in the 1992 PA. After completion of the institutional control period, infiltration is predicted to gradually increase over time as the closure system degrades due to phenomena such as intrusion of deep-rooted plants (e.g., trees) and silting of drainage layers (Phifer 2004). While it is assumed that tree root penetration will contribute to closure system degradation, tree roots should not penetrate into the Saltstone, itself, and uptake radionuclides for the following reasons:

- Several layers of the multi-layered cover system above the vault roof are frequently at or near saturation. Since tree roots are opportunistic and seek sources of water, the roots will concentrate in these layers above the vault roof, which contain significant water.
- While roots might penetrate to the vault roof, the concrete roof presents a hardened surface over which roots are more likely to extend along rather than penetrate.
- The pore fluid within Saltstone is essentially a salt solution (brackish water) which the trees could not utilize.
- It is unlikely that roots would be able to extract water from Saltstone due to the matrix potential within Saltstone.

The purpose of the deeper roots of pine trees is to seek sources of water. The multi-layered cover system will produce local zones of saturated water in the drainage layers overlying the barrier layers. The pine tree roots will tend to follow these layers rather than attempt to penetrate to deeper levels since it is much easier for the roots to extract water from saturated soil than unsaturated soil. Therefore, pine tree roots are not expected to penetrate the vault roof.

A potential PA concern is the effects of cracks developing in the Saltstone monolith over time. A structural analysis (Peregoy 2003) predicts that cracks will develop and their aperture will increase with increasing time. However, the analysis shows that the cracks will open either at the top or at the bottom and will be pinched closed at the opposite end. Therefore, no through-wall cracks will develop. A separate modeling study (Yu and Cook 2004) concluded that cracks of this nature have very little effect on contaminant transport rate. Based on this finding cracks are not considered in this SA.

The conceptual model describes the materials, layout, and dimensions of the SDF. Figure 2-1 depicts the conceptual model used for the Vault No. 4. The Saltstone monolith is approximately 200×600×25 ft. Only half of a vault in the short dimension is modeled, taking advantage of symmetry. The top of the modeling domain is the bottom of the upper GCL layer. Infiltration through this layer as a function of time is calculated by the HELP code (USEPA 1994a, 1994b). The constant infiltration rate is used as a flow boundary condition at the top of the modeling domain. The bottom of the modeling domain is the water table. Capillary pressure at the water table is set to zero to simulate 100% water saturation. The vertical boundary through the center of the vault is modeled as a no-flow boundary due to symmetry. The right boundary is also assumed to be a no-flow boundary because it is sufficiently far away from the vault and the predominant

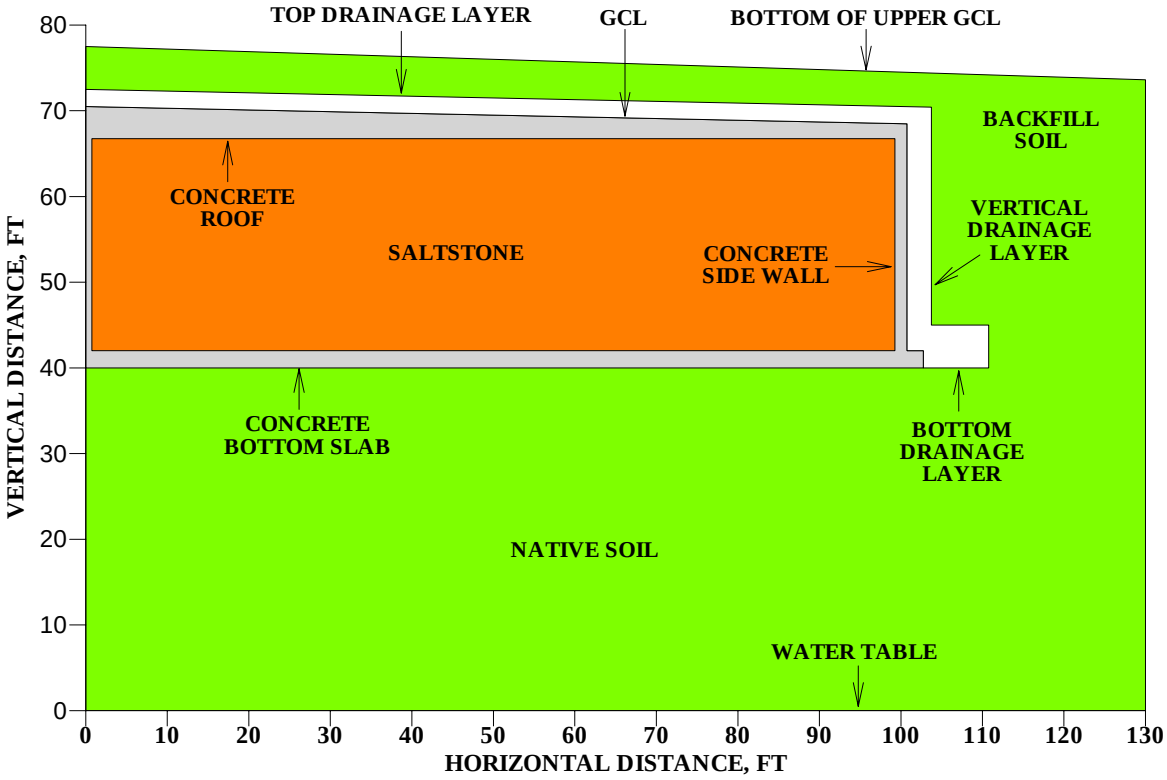

Figure 2-1. Conceptual Model for the Saltstone Vault No. 4

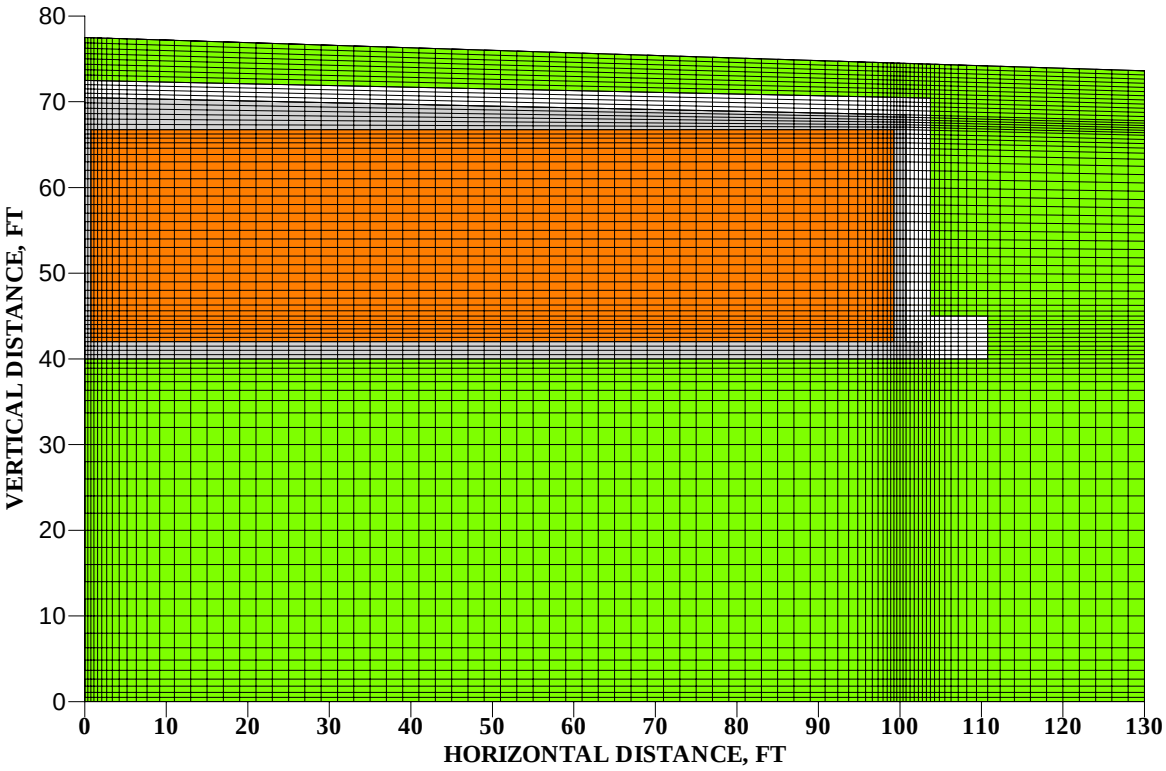

Figure 2-2. Modeling Grid

contaminant transport mechanism is downward convection. Figure 2-2 shows the gridding used in the model.

The vadose zone flow simulation was performed as a sequence of steady-state runs approximating average conditions during a number of time intervals over 10,000 years based on the HELP code results. Time zero is when closure operations are complete. Material properties were varied for each time interval to represent degradation of the closure system, the Saltstone waste form, and the vault. These properties are given in Appendix A.

A total of 45 radionuclides were selected for analysis based on a screening study for the SRS Low Level Waste Facility (Cook and Wilhite 2004). Nitrate was also run in the analysis because it occurs in high concentrations and has a relatively low groundwater limit.

The new plutonium chemistry implemented for the trench disposal units in the E-Area Low-Level Waste Facility (Cook 2002, Kaplan 2004) has been included in the present special analysis. The Pu (III/IV) oxidation state is far more abundant than Pu (V/VI), but the latter is significantly more mobile in sediments: a soil-solute distribution coefficient of K_d = 370 mL/g is assumed for Pu (III/IV) versus K_d = 15 mL/g for Pu (V/VI). Although present in trace amounts, the relatively high mobility of Pu (V/VI) could potentially lead to a significant contribution to the dose at the 100-meter well. The two pairs of oxidation states are tracked separately in the vadose zone transport simulations to accommodate the difference in mobility.

In addition to the geochemistry modifications described above, some distribution coefficients were updated to reflect current knowledge. Appendix A provides a complete listing of K_d values used in the groundwater analysis and other key input data such as, radionuclides analyzed, half-lives, atomic mass, concentration limits, solubility limits, and assumed decay chains.

The FACT code model of the General Separations Area (GSA) was recently superseded by an equivalent model using the PORFLOW code, in order to consolidate PA subsurface flow and transport modeling to a single software product (Flach 2004). The flow field computed by GSA/PORFLOW is used in the present study. GSA/PORFLOW is a regional scale model with a mesh resolution in the horizontal plane of 200 ft, compared to a width of about 200 ft for Vault 4.

Figure 2-3 illustrates locations of the existing Vaults, 1 and 4, and the aquifer model mesh. Figure 2-3 also shows the extent of the aquifer flow and transport model (blue border) and the mesh resolution in the horizontal plane (light gray dashes). Particle tracking results starting from the four corners of the combined facility indicate the groundwater flow direction. Time markers (red dots) are shown every 10 years of travel. Figure 2-3 indicates a possibility of plume overlap, which is the subject of a sensitivity study presented in Section 7.

2.2 Results

The magnitude and time of maximum concentration, the Maximum Contaminant Level (MCL) (USEPA 2004) and the Vault 4 inventory limit for the key radionuclides for two time periods of interest, 1000 years and 10,000 years, are given in Tables 2-1 and 2-2, respectively. These limits for the groundwater pathway are compared with limits derived for the other pathways and with the projected Vault 4 inventory in Section 7. For the projected Vault 4 inventory, none of the radionuclides produces a significantly large fraction of the groundwater limit.

Plots of fractional flux and concentration for each radionuclide modeled with PORFLOW are presented in Appendix A.

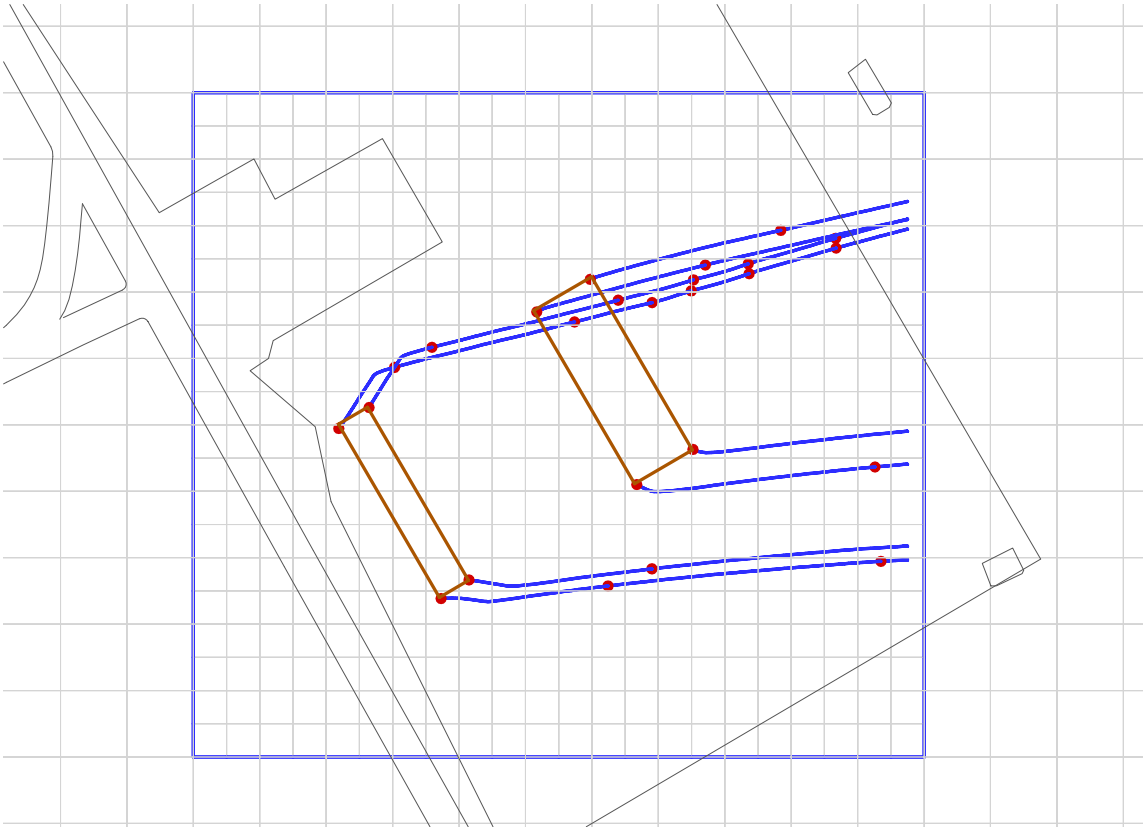

Figure 2-3. PORFLOW Model Horizontal Grids and Particle Tracking

Table 2-1. Maximum Contaminant Levels and Calculated Inventory Limits for the Radionuclides Time of Compliance = 1,000 years

Radionuclide	Peak Conc. pCi/L/Ci	Peak Time Years	MCL pCi/L	Inv. Limit Ci
Al-26	2.94E-17	1.00E+03	4.00E+02	1.36E+19
H-3	1.10E-08	1.25E+02	2.00E+04	1.82E+12
I-129	5.69E-08	1.00E+03	1.00E+00	1.76E+07
K-40	2.83E-08	1.00E+03	3.00E+02	1.06E+10
Mo-93	5.07E-07	1.00E+03	4.00E+03	7.89E+09
Se-79	3.50E-07	1.00E+03	7.00E+02	2.00E+09
Sr-90	3.35E-16	6.57E+02	8.00E+00	2.39E+16

Table 2-2. Maximum Contaminant Levels and Calculated Inventory Limits for the Radionuclides Time of Compliance = 10,000 years

Radionuclide	Peak Concentration pCi/L/Ci	Peak Time Years	MCL pCi/L	Inventory Limit Ci
Al-26	6.19E-09	1.00E+04	4.00E+02	6.46E+10
Cs-135	1.11E-11	1.00E+04	9.00E+02	8.11E+13
H-3	1.10E-08	1.25E+02	2.00E+04	1.82E+12
I-129	4.62E-03	1.00E+04	1.00E+00	2.16E+02
K-40	2.39E-03	1.00E+04	3.00E+02	1.26E+05
Mo-93	2.84E-03	1.00E+04	4.00E+03	1.41E+06
Nb-94	1.17E-17	1.00E+04	1.00E+03	8.55E+19
Ni-59	1.19E-15	1.00E+04	3.00E+02	2.52E+17
Np-237	2.28E-19	1.00E+04	1.50E+01	6.58E+19
Pd-107	9.15E-13	1.00E+04	4.00E+04	4.37E+16
Ra-226	1.05E-16	1.00E+04	5.00E+00	4.76E+16
Rb-87	1.76E-11	1.00E+04	3.00E+02	1.70E+13
Se-79	1.83E-02	1.00E+04	7.00E+02	3.83E+04
Sr-90	3.35E-16	6.57E+02	8.00E+00	2.39E+16
Tc-99	2.01E-15	1.00E+04	9.00E+02	4.48E+17
Th-230	4.36E-39	1.00E+04	1.50E+01	
Ra-226	4.04E-17	1.00E+04	5.00E+00	1.24E+17
Pb-210	9.13E-17	1.00E+04	1.00E+00	**1.10E+16**
Po-210	1.65E-16	1.00E+04	1.50E+01	9.09E+16
U-234	5.77E-25	1.00E+04	1.30E+02*	
Th-230	1.00E-27	1.00E+04	1.50E+01	
Ra-226	2.96E-19	1.00E+04	5.00E+00	1.69E+19
Pb-210	6.72E-19	1.00E+04	1.00E+00	**1.49E+18**
Po-210	1.21E-18	1.00E+04	1.50E+01	1.24E+19

NOTE: Entries in **bold type** indicate an inventory limit determined by a progeny rather than a parent radionuclide.

* Uranium "MCL" is based on 25 mrem/year rather than the 30 μg/L MCL

THIS PAGE INTENTIONALLY LEFT BLANK

3.0 INADVERTENT INTRUDER ANALYSIS

The inadvertent intruder analysis considers the radiological impacts to hypothetical persons who are assumed to intrude into Vault 4 at the SDF after institutional control ceases 100 years after facility closure.

3.1 Methodology

The intruder analysis was performed with a software tool for automated analyses (Koffman 2004) which calculates radionuclide-specific concentrations and inventory limits allowed in waste at the time of disposal. These values are based on dose assessments for credible exposure scenarios for the inadvertent intruder described in Appendix B. The tool eliminates the historical use of complex spreadsheets that require extensive design checks. Radionuclide- and scenario-specific parameters within the software tool have been researched and independently verified (Lee 2004).

The method of analysis separates the intruder analyses from the groundwater pathway analysis by disregarding leaching and only considering decay for the amount of contaminant remaining at the time of intrusion. The groundwater pathway typically uses a distribution coefficient (K_d) that is conservative for its own pathway by enhancing the release slightly. However, that value is typically slightly non-conservative for the intruder pathways, because too much release results in less contaminant remaining for the intruder to encounter. This non-conservatism has been removed with the revised method.

The method of analysis for this SA can produce a transient analysis for each type of intrusion, rather than selecting a fixed time. The decay process continually changes the amount of contaminant present in the waste zone that the intruder can encounter. While the amount of parent monotonically decreases, the amount of each progeny initially increases and ultimately decreases. As the decay process takes place, sediments and engineered materials can erode and degrade as well. Determining the time when the maximum impact on the intruder will occur is impossible, unless a rigorous examination is conducted with calculus or a transient analysis is performed. The current method has a transient analysis option that is valid across the spectrum of disposal units and does not require extensive calculations by the analyst; rather it requires the analyst to define geometry and process inputs, and then relies on the computer model to perform pathways calculations at a specified time increment that is nominally 10 years.

The automated analysis accounts for the closure system developed by Phifer and Nelson (2003) that includes a 12-inch thick erosion barrier near the top of the cap. Because the erosion barrier is assumed to never erode and all the layers between the waste and the erosion barrier always remain in place at their design thickness, approximately 11.5 ft of material always exists above the waste. Soil/cover layers overlying the vault roof were adjusted to be consistent with the current closure concept (Phifer and Nelson 2003). Appendix B provides additional information on disposal unit specific inputs to the automated intruder analysis.

Because the thickness from the top of the erosion barrier to the waste is greater than the depth of a typical basement (3 m or 10 ft), the agriculture scenario can never occur as it relies on a basement extending into the waste zone. Additionally, the concrete roof of the vault will prevent excavation and drilling through it for more than 1,000 years. For the resident scenario, the erosion barrier greatly increases the amount of material above the waste that serves to shield the residential intruder.

3.2 Results

The agriculture scenario was not evaluated because implementation of an erosion barrier during closure eliminates the potential for contact with the waste via this scenario. The post-drilling scenario was not evaluated because the reinforced concrete vault roof was assumed to prevent

drilling into the waste for the entire period of assessment. Results of the resident intruder analyses for Vault 4 for the time period of 100 – 1,000 years are provided in Table 3-1. Table 3-2 shows the results of the resident intruder analysis for the time period 100 – 10,000 years. The entry "---" in the Time of Limit column means that the dose calculation is always zero so there is no limit. For cases where there is a time given, there may be an entry "---" in one or both of the limit columns. In this case the entry "---"indicates a limit value greater than or equal to the threshold value of 1E+20. Additional details are provided in Appendix B. Because the automated method used in this SA applies a transient analysis, it calculates the lowest inventory limit for the entire time period, regardless of when it occurs.

The vault roof and upper layer of clean grout provide a minimum of a half-meter of shielding throughout the resident scenario transient. Consequently, exposure levels are relatively low compared to other disposal units at SRS (e.g., slit and engineered trenches in E Area). Limits are correspondingly high.

These limits for the intruder pathway are compared with limits derived for the other pathways and with the projected Vault 4 inventory in Section 7. For the projected Vault 4 inventory, only ^{137}Cs produces a significantly large fraction (i.e., 0.21) of the intruder limit.

Table 3-1. Intruder-Based Radionuclide Disposal Limits for Vault 4 – Resident Scenario with Transient Calculation for 100 – 1,000 Years

Radionuclide	Time of Limit (Years)	Concentration Limit ($\mu Ci/m^3$)	Inventory Limit (Ci)
Na-22	100	9.90E+16	7.80E+15
Al-26	760	2.05E+03	1.61E+02
K-40	760	4.00E+04	3.15E+03
Co-60	100	7.29E+10	5.75E+09
Kr-85	100	3.46E+12	2.73E+11
Nb-94	760	1.28E+04	1.01E+03
Tc-99	760	4.64E+14	3.66E+13
Ag-108m	760	7.21E+04	5.68E+03
Sn-126	760	1.48E+04	1.17E+03
Sb-125	100	1.79E+18	1.41E+17
Cs-134	100	---	4.12E+19
Cs-137	100	7.61E+07	5.99E+06
Ba-133	100	1.53E+11	1.21E+10
Eu-152	100	8.15E+07	6.42E+06
Eu-154	100	1.46E+09	1.15E+08
Eu-155	100	---	1.12E+19
Pb-210	100	4.99E+12	3.94E+11
Bi-207	100	3.91E+06	3.08E+05
Ra-226	760	5.34E+03	4.21E+02
Ra-228	100	4.72E+09	3.72E+08
Ac-227	100	1.11E+09	8.78E+07
Th-228	100	---	1.88E+19
Th-229	760	1.09E+05	8.61E+03
Th-230	1000	1.10E+04	8.66E+02
Th-232	760	1.98E+03	1.56E+02
Pa-231	760	2.73E+05	2.15E+04
U-232	100	1.14E+05	9.00E+03
U-233	1000	1.13E+06	8.92E+04
U-234	1000	2.23E+06	1.76E+05
U-235	1000	7.29E+06	5.75E+05
U-236	1000	4.06E+10	3.20E+09
U-238	1000	1.02E+06	8.01E+04
Np-237	1000	9.74E+05	7.68E+04
Pu-238	1000	7.90E+09	6.22E+08
Pu-239	1000	3.80E+11	3.00E+10
Pu-240	1000	2.86E+15	2.25E+14
Pu-241	1000	1.85E+11	1.46E+10
Pu-242	1000	6.56E+12	5.17E+11
Pu-244	760	4.64E+04	3.65E+03
Am-241	1000	6.05E+09	4.77E+08
Am-242m	750	1.99E+08	1.57E+07
Am-243	760	3.75E+06	2.96E+05
Cm-242	1000	1.56E+12	1.23E+11

Table 3-1. Intruder-Based Radionuclide Disposal Limits for Vault 4 – Resident Scenario with Transient Calculation for 100 – 1,000 Years

Radionuclide	Time of Limit (Years)	Concentration Limit ($\mu Ci/m^3$)	Inventory Limit (Ci)
Cm-243	100	8.88E+10	7.00E+09
Cm-244	1000	1.09E+18	8.60E+16
Cm-245	760	1.07E+08	8.42E+06
Cm-246	1000	7.41E+15	5.84E+14
Cm-247	1000	3.26E+05	2.57E+04
Cm-248	1000	5.84E+09	4.60E+08
Bk-249	760	6.24E+08	4.92E+07
Cf-249	760	1.61E+06	1.27E+05
Cf-250	1000	2.80E+18	2.21E+17
Cf-251	760	2.33E+07	1.83E+06
Cf-252	1000	7.96E+14	6.27E+13

Table 3-2. Intruder-Based Radionuclide Disposal Limits for Vault 4 – Resident Scenario with Transient Calculation for 100 – 10,000 Years

Radionuclide	Time of Limit (Years)	Concentration Limit ($\mu Ci/m^3$)	Inventory Limit (Ci)
Na-22	100	9.90E+16	7.80E+15
Al-26	760	2.05E+03	1.61E+02
K-40	760	4.00E+04	3.15E+03
Co-60	100	7.29E+10	5.75E+09
Kr-85	100	3.46E+12	2.73E+11
Nb-94	760	1.28E+04	1.01E+03
Tc-99	760	4.64E+14	3.66E+13
Ag-108m	760	7.21E+04	5.68E+03
Sn-126	760	1.48E+04	1.17E+03
Sb-125	100	1.79E+18	1.41E+17
Cs-134	100	---	4.12E+19
Cs-137	100	7.61E+07	5.99E+06
Ba-133	100	1.53E+11	1.21E+10
Eu-152	100	8.15E+07	6.42E+06
Eu-154	100	1.46E+09	1.15E+08
Eu-155	100	---	1.12E+19
Pb-210	100	4.99E+12	3.94E+11
Bi-207	100	3.91E+06	3.08E+05
Ra-226	760	5.34E+03	4.21E+02
Ra-228	100	4.72E+09	3.72E+08
Ac-227	100	1.11E+09	8.78E+07
Th-228	100	---	1.88E+19
Th-229	760	1.09E+05	8.61E+03
Th-230	9090	4.18E+03	3.29E+02
Th-232	760	1.98E+03	1.56E+02
Pa-231	760	2.73E+05	2.15E+04
U-232	100	1.14E+05	9.00E+03
U-233	10000	1.71E+05	1.35E+04
U-234	10000	5.69E+04	4.48E+03
U-235	10000	1.30E+06	1.03E+05
U-236	10000	4.02E+09	3.17E+08
U-238	10000	8.38E+05	6.60E+04
Np-237	10000	8.55E+05	6.73E+04
Pu-238	10000	1.62E+08	1.27E+07
Pu-239	10000	1.74E+11	1.37E+10
Pu-240	10000	3.75E+13	2.96E+12
Pu-241	10000	1.30E+11	1.02E+10
Pu-242	10000	6.23E+11	4.91E+10
Pu-244	760	4.64E+04	3.65E+03
Am-241	10000	4.29E+09	3.38E+08
Am-242m	10000	1.25E+08	9.83E+06
Am-243	760	3.75E+06	2.96E+05
Cm-242	10000	3.18E+10	2.51E+09
Cm-243	100	8.88E+10	7.00E+09

Table 3-2. Intruder-Based Radionuclide Disposal Limits for Vault 4 – Resident Scenario with Transient Calculation for 100 – 10,000 Years

Radionuclide	Time of Limit (Years)	Concentration Limit ($\mu Ci/m^3$)	Inventory Limit (Ci)
Cm-244	10000	1.37E+16	1.08E+15
Cm-245	760	1.07E+08	8.42E+06
Cm-246	10000	1.06E+14	8.34E+12
Cm-247	10000	3.11E+05	2.45E+04
Cm-248	10000	5.89E+08	4.64E+07
Bk-249	760	6.24E+08	4.92E+07
Cf-249	760	1.61E+06	1.27E+05
Cf-250	10000	3.87E+16	3.05E+15
Cf-251	760	2.33E+07	1.83E+06
Cf-252	10000	8.00E+13	6.31E+12

4.0 AIR ANALYSIS

The air analysis considers diffusion of volatile radionuclides from the waste zone through overlying soil layers to the ground surface. The specific radionuclides analyzed are C-14, Cl-36, H-3, I-129, Sb-125, Se-79, Sn-121m and Sn-126. Radon is assessed separately in Section 5.

4.1 Methodology

A screening analysis was conducted to produce a list of radionuclides requiring a more thorough analysis to derive disposal limits for the SDF based on the atmospheric pathway (Crapse and Cook 2004). This study used a methodology developed by the NCRP (NCRP 1996), professional judgment and process knowledge to determine this list. The list of potential radionuclides includes C-14, Cl-36, H-3, I-129, Sb-125, Se-79, Sn-121m and Sn-126.

This analysis considers the diffusion of these radionuclides upward from the Saltstone vault through the overlying soil material (anticipated closure cap) to determine emanation rates at the land surface. This mechanism was evaluated using the PORFLOW numerical model, within which reasonable, if not conservative, estimates of media and diffusive transport parameters were selected.

Using the land surface flux rates output from the soil vapor diffusion model a second air-dispersion model was utilized to calculate exposures to a Maximally Exposed Individual (MEI) at two locations at two different times. The USEPA computer code CAP88 (Beres 1990), was used to calculate dose factors in units of mrem/yr per curie/yr released at the ground surface, at the SRS site boundary and at a location 100 m from Vault 4 (Simpkins 2004). The diffusion model and the atmospheric transport dose model were thus used together to calculate disposal limits based on the atmospheric pathway dose limit of 10 mrem/yr (USDOE 1999).

4.2 Results

Table 4-1 summarizes the results for the air pathway analysis. Appendix C provides additional detail on the assumptions, parameters and methodology.

Table 4-1. Air Pathway Dose Calculations and Saltstone Vault 4 Disposal Limits

Radionuclide	Dose to MEI at SRS Boundary from 1 Ci (mrem/yr)	Dose to MEI at 100 Meters from 1 Ci (mrem/yr)	Saltstone Vault 4 Disposal Limit (Ci)
C-14	2.70E-10	2.28E-07	4.39E+07
Cl-36	9.93E-22	6.81E-19	1.47E+19
H-3	1.19E-12	1.83E-11	5.46E+11
I-129	1.39E-17	5.90E-14	1.70E+14
Se-79	2.03E-09	2.07E-06	4.84E+06

These limits for the air pathway are compared with limits derived for the other pathways and with the projected Vault 4 inventory in Section 7. For the projected Vault 4 inventory, none of the radionuclides produces a significantly large fraction of the air limit.

THIS PAGE INTENTIONALLY LEFT BLANK

5.0 RADON ANALYSIS

This section describes the investigation conducted to evaluate the potential magnitude of radon release from Vault 4 of the SDF over the 10,000-year performance assessment period of interest. The permissible radon flux for USDOE facilities is addressed in *Implementation Guide for use with DOE M 435.1-1*, DOE G 435.1-1, July 9, 1999, Appendix A. In this Appendix, Section IV. P. (c) states the radon flux limitations associated with operation and closure of a disposal facility. This requirement is that the release of radon shall be less than an average flux of 20 pCi/m^2/sec at the surface of the disposal facility. The requirements analysis states that this standard was adopted from the uranium mill tailings requirements in 40 CFR Part 192 and 10 CFR Part 40. 10 CFR Part 40 discusses both Rn-222 from uranium and Rn-220 from thorium, therefore the performance objective refers only to radon, and the correct species must be analyzed depending on the characteristics of the waste stream.

This investigation addresses only Rn-222 from uranium because screening calculations, using the numerical model developed in this analysis, indicate that the short half-life of Rn-220 (55.6 seconds) renders it unable to escape the Saltstone waste form and migrate to the land surface via air diffusion before it is transformed by radioactive decay.

5.1 Methodology

In this analysis radon is assumed to be released through the ground surface from decay of a number of radionuclides disposed in Saltstone, namely U-238, Pu-238, U-234, Th-230, and Ra-226. Radionuclides that create Rn-222 are illustrated in Figure 5-1. The diagram shows the specific decay chains that lead to the formation of Rn-222, as well as the half-lives for each nuclide. The extremely long half-life of U-238 (4.5 billion years) causes the other radioisotopes higher up in the chain of parents to be of little concern with regard to their potential to contribute significantly to the Rn-222 flux at the land surface over the period of interest.

A realistic conceptual model of radon transport was developed, as described in detail in Appendix D. The analysis incorporates a radon emanation coefficient and waste zone layering and properties (e.g., porosity) consistent with the current closure plan.

5.2 Results

Table 5-1 presents the peak flux rates and the Vault 4 disposal limits resulting from the radon analysis.

Table 5-1. Simulated Peak Instantaneous Rn-222 Flux Over 10,125 Years at the Land Surface and Associated Disposal Limits for Parent Radionuclides

Parent Radionuclide	Peak Instantaneous Rn-222 Flux at Land Surface (pCi/m^2/sec)	Disposal Limit per Unit Area (Ci/m^2)	Vault 4 Disposal Limit (Ci)
Ra-226	1.95E-07	1.03E+08	1.14E+12

This limit for the radon pathway is compared with limits derived for the other pathways and with the projected Vault 4 inventory in Section 7. The projected Vault 4 inventory of ^{226}Ra is an insignificant fraction of the radon limit.

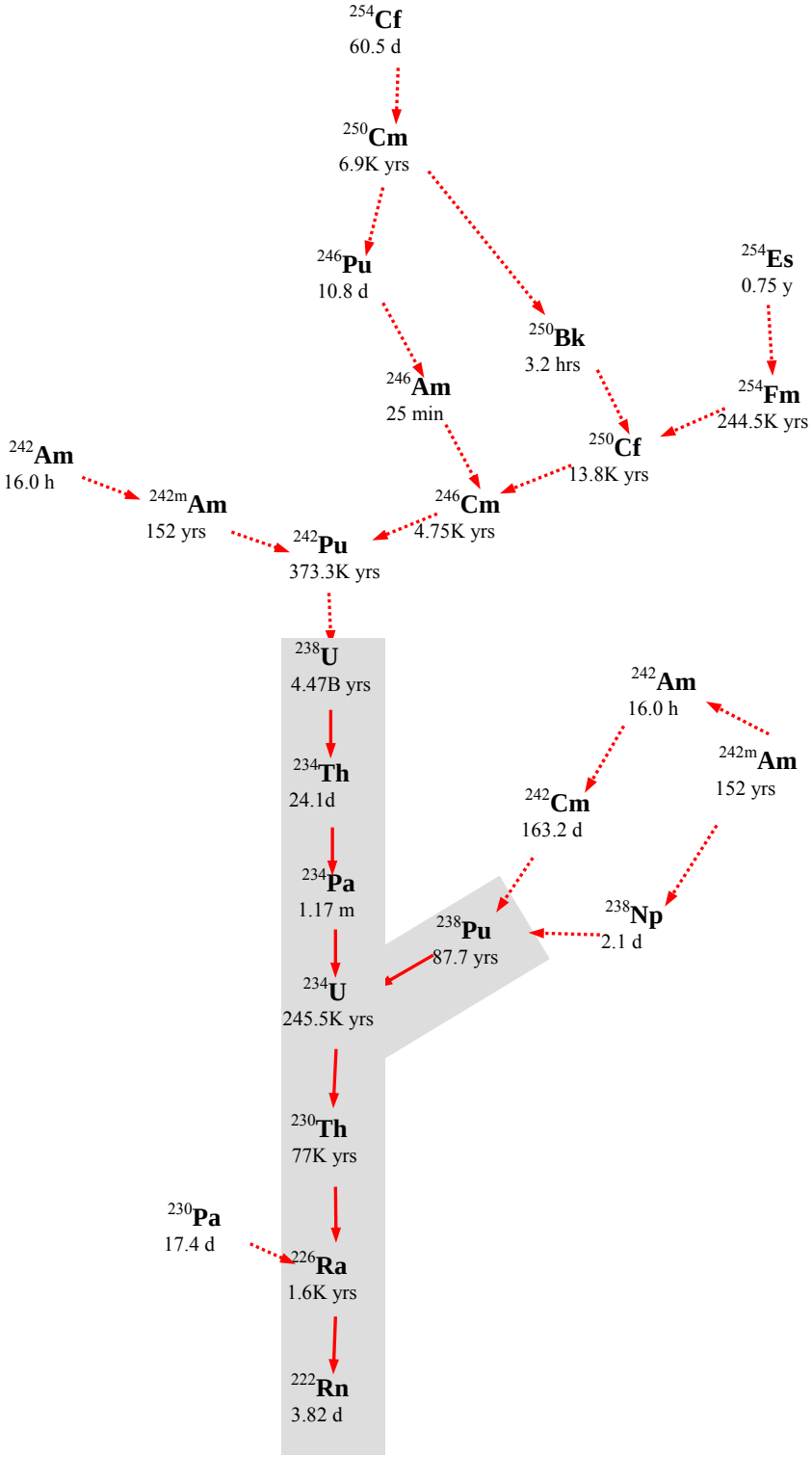

Figure 5-1. Radioactive Decay Chains Leading to Rn-222

6.0 ALL-PATHWAYS ANALYSIS

One of the USDOE performance objectives is DOE 435.1.IV.P (1) (a):

Dose to representative members of the public shall not exceed 25 mrem (0.25 mSv) in a year total effective dose equivalent from all exposure pathways, excluding the dose from radon and its progeny in air.

In this SA, exposures from all pathways are calculated using the peak groundwater concentrations derived in the groundwater analysis (Section 2) and the peak air doses derived in the air analysis (Section 4).

6.1 Methodology

For radionuclides transported by the groundwater, the maximum groundwater concentration of each radionuclide within the time frame of interest (i.e., 1,000 years or 10,000 years) calculated in Section 2 is input to the LADTAP XL© program (Jannik 2005), which is the model used at SRS for demonstrating water pathway dose compliance (Simpkins 2004). The maximum groundwater concentrations are calculated for a unit curie inventory of each radionuclide.

It is conservatively assumed that a future resident farmer uses the contaminated groundwater at the 100-meter well as a source of 1) drinking water, 2) pond water (in which fish are raised and recreational activities occur), and 3) irrigation water used for raising vegetables, meat, and milk.

LADTAP XL© contains two worksheets: LADTAP and IRRIDOSE. The LADTAP worksheet estimates dose from environmental pathways including external exposure resulting from recreational activities (swimming, boating, and shoreline use) and from ingestion of water and fish. IRRIDOSE estimates dose from food crops irrigated with contaminated water. It is conservatively assumed that all of the food consumed by the resident farmer was irrigated with contaminated groundwater.

The air pathway doses calculated in Section 4 include not only direct radiation and inhalation from the airborne plume but also doses from consumption of vegetables, meat, and milk contaminated from the airborne plume. The air pathway dose is also calculated for a unit curie inventory of each radionuclide.

The all-pathways dose from the groundwater pathway and the all-pathways dose from the air pathway are summed to obtain the total all-pathways dose. The total all-pathways dose per curie is ratioed with the all-pathways performance objective of 25 mrem/year to obtain the all-pathways limit for each radionuclide.

6.2 Results

Table 6-1 presents the all-pathways limits for both the 1,000-year and 10,000-year time frames.

These limits for the all pathways are compared with limits derived for the other pathways and with the projected Vault 4 inventory in Section 7. For the projected Vault 4 inventory, none of the radionuclides produces a significantly large fraction of the all-pathways limit.

Table 6-1. All-Pathways Disposal Limits for Saltstone Disposal Vault 4

Radionuclide	1,000-Year Disposal Limit (Ci/Vault 4)	10,000-Year Disposal Limit (Ci/Vault 4)
H-3	1.30E+12	1.30E+12
C-14	1.10E+08	1.10E+08
Al-26	4.86E+18	2.31E+10
Cl-36	3.67E+19	5.15E+18
K-40	1.10E+09	1.31E+04
Ni-59		1.58E+19
Se-79	9.85E+06	1.02E+03
Rb-87		5.12E+09
Sr-90	1.42E+17	1.42E+17
Nb-93m	8.99E+08	1.46E+05
Nb-94		6.98E+17
Mo-93	3.46E+09	6.17E+05
Tc-99		1.07E+17
Pd-107		1.84E+17
Sn-126		2.92E+19
I-129	3.27E+08	4.03E+03
Ra-226		3.84E+16
Np-237		8.93E+18

7.0 INTEGRATION AND INTERPRETATION

This section uses the results for the individual pathways from the previous sections to develop performance-based disposal limits for Vault 4. A projected inventory for Vault 4 is presented and compared with the disposal limits. The projected impacts from Vault 4 are then compared with the NRC performance objectives stated in 10 CFR 61. The results of sensitivity studies and a discussion of uncertainty follow.

7.1 Vault 4 Disposal Limits

In previous sections, limits were developed for a number of pathways, groundwater, inadvertent intrusion by residential use, releases to the atmosphere, radon emanation and "all pathways". The overall disposal limit for each radionuclide is the result for the pathway having the lowest limit.

Tables 7-1 and 7-2 show the results for each radionuclide and pathway for 1,000-year and 10,000-year times of compliance, respectively. Only radionuclides with a most restrictive limit less than 1E+20 Ci are shown. Limits greater than 1E+20 Ci are equivalent to unlimited quantities of that radionuclide being acceptable for disposal.

Because the waste stream being processed into Saltstone contains a high concentration of nitrate salts, limits for nitrate disposal were developed for the groundwater pathway. The limits for 1,000 and 10,000 year times of compliance are shown in Table 7-3.

7.2 Projected Vault 4 Radionuclide Inventory

The total radionuclide inventory that could be disposed in Vault 4 is composed of the current inventory and the projected Saltstone to be produced from salt waste extracted from the HLW tanks. The current inventory in vault four was obtained from the SDF PA Annual Review (Crapse et al. 2004). The projected inventory was developed from the projected radionuclide concentrations in salt waste batches expected to be produced over the next several years (d'Entremont 2005). It was assumed that all of the unused space in Vault 4 would be filled to a depth of 24.75 feet with Saltstone produced from these salt waste batches.

The total projected inventory for Vault 4 is presented in Table 7-4.

7.3 Comparison of Vault 4 Limits with the Projected Inventory

The Vault 4 disposal limits based on a 1,000-year time of compliance are compared with the estimate of the final inventory of Vault 4 in Table 7-5. This table also shows the fraction of the inventory limit represented by the estimated inventory for each radionuclide of interest. A sum of the individual fraction which is less than one indicates that disposal of that inventory will meet all of the USDOE performance objectives and requirements. The sum-of-fractions in Table 7-5 is 0.21, almost all of which is due to Cs-137.

Table 7-6 shows the same information based on the limits derived using the 10,000-year time of compliance. Cs-137 is again the major contributor to the sum-of-fractions, comprising 0.21 of the total of 0.22.

The results shown in Tables 7-5 and 7-6 provide reasonable assurance that disposal of the waste streams planned for Vault 4 will meet the USDOE performance objectives and requirements. Table 7-7 compares the results of this SA with the one prepared in 2002 for key radionuclides.

Table 7-1. Disposal Limits for Vault 4 Based on 1,000-Year Time of Compliance, Ci

	Pathways					
Radionuclide	Groundwater	Resident Intruder	Atmospheric	Radon	All Pathways	Most Restrictive
Ac-227		8.8E+07				8.8E+07
Ag-108m		5.7E+03				5.7E+03
Al-26	1.4E+19	1.6E+02			4.9E+18	1.6E+02
Am-241		4.8E+08				4.8E+08
Am-242m		1.6E+07				1.6E+07
Am-243		3.0E+05				3.0E+05
Ba-133		1.2E+10				1.2E+10
Bk-249		4.9E+07				4.9E+07
C-14			4.4E+07		1.1E+08	4.4E+07
Cf-249		1.3E+05				1.3E+05
Cf-250		2.2E+17				2.2E+17
Cf-251		1.8E+06				1.8E+06
Cf-252		6.3E+13				6.3E+13
Cl-36			1.5E+19		3.7E+19	1.5E+19
Cm-242		1.2E+11				1.2E+11
Cm-243		7.0E+09				7.0E+09
Cm-244		8.6E+16				8.6E+16
Cm-245		8.4E+06				8.4E+06
Cm-246		5.8E+14				5.8E+14
Cm-247		2.6E+04				2.6E+04
Cm-248		4.6E+08				4.6E+08
Co-60		5.8E+09				5.8E+09
Cs-134		4.1E+19				4.1E+19
Cs-137		6.0E+06				6.0E+06
Eu-152		6.4E+06				6.4E+06
Eu-154		1.2E+08				1.2E+08
Eu-155		1.1E+19				1.1E+19
H-3	1.8E+12		5.5E+11		1.3E+12	5.5E+11
I-129	1.8E+07		1.7E+14		3.3E+08	1.8E+07
K-40	1.1E+10	3.2E+03			1.1E+09	3.2E+03
Kr-85		2.7E+11				2.7E+11
Mo-93	7.9E+09				3.5E+09	3.5E+09
Na-22		7.8E+15				7.8E+15
Nb-93m					9.0E+08	9.0E+08
Nb-94		1.0E+03				1.0E+03
Np-237		7.7E+04				7.7E+04
Pa-231		2.2E+04				2.2E+04
Pb-210		3.9E+11				3.9E+11
Pu-238		6.2E+08				6.2E+08

Table 7-1. Disposal Limits for Vault 4 Based on 1,000-Year Time of Compliance, Ci

	Pathways					
Radionuclide	Groundwater	Resident Intruder	Atmospheric	Radon	All Pathways	Most Restrictive
Pu-239		3.0E+10				3.0E+10
Pu-240		2.3E+14				2.3E+14
Pu-241		1.5E+10				1.5E+10
Pu-242		5.2E+11				5.2E+11
Pu-244		3.7E+03				3.7E+03
Ra-226		4.2E+02		1.1E+12		4.2E+02
Ra-228		3.7E+08				3.7E+08
Sb-125		1.4E+17				1.4E+17
Se-79	2.0E+09		4.8E+06		9.9E+06	4.8E+06
Sn-126		1.2E+03				1.2E+03
Sr-90	2.4E+16				1.4E+17	2.4E+16
Tc-99		3.7E+13				3.7E+13
Th-228		1.9E+19				1.9E+19
Th-229		8.6E+03				8.6E+03
Th-230		8.7E+02				8.7E+02
Th-232		1.6E+02				1.6E+02
U-232		9.0E+03				9.0E+03
U-233		8.9E+04				8.9E+04
U-234		1.8E+05				1.8E+05
U-235		5.8E+05				5.8E+05
U-236		3.2E+09				3.2E+09
U-238		8.0E+04				8.0E+04

Table 7-2. Disposal Limits for Vault 4 Based on 10,000-Year Time of Compliance, Ci

	Pathway					
Radionuclide	Groundwater	Resident Intruder	Atmospheric	Radon	All Pathways	Most Restrictive
Ac-227		8.8E+07				8.8E+07
Ag-108m		5.7E+03				5.7E+03
Al-26	6.5E+10	1.6E+02			2.3E+10	1.6E+02
Am-241		3.4E+08				3.4E+08
Am-242m		9.8E+06				9.8E+06
Am-243		3.0E+05				3.0E+05
Ba-133		1.2E+10				1.2E+10
Bi-207		3.1E+05				3.1E+05
Bk-249		4.9E+07				4.9E+07
C-14			4.4E+07		1.1E+08	4.4E+07
Cf-249		1.3E+05				1.3E+05
Cf-250		3.1E+15				3.1E+15
Cf-251		1.8E+06				1.8E+06
Cf-252		6.3E+12				6.3E+12
Cl-36			1.5E+19		5.2E+18	5.2E+18
Cm-242		2.5E+09				2.5E+09
Cm-243		7.0E+09				7.0E+09
Cm-244		1.1E+15				1.1E+15
Cm-245		8.4E+06				8.4E+06
Cm-246		8.3E+12				8.3E+12
Cm-247		2.5E+04				2.5E+04
Cm-248		4.6E+07				4.6E+07
Co-60		5.8E+09				5.8E+09
Cs-134		4.1E+19				4.1E+19
Cs-135	8.1E+13					8.1E+13
Cs-137		6.0E+06				6.0E+06
Eu-152		6.4E+06				6.4E+06
Eu-154		1.2E+08				1.2E+08
Eu-155		1.1E+19				1.1E+19
H-3	1.8E+12		5.5E+11		1.3E+12	5.5E+11
I-129	2.2E+02		1.7E+14		4.0E+03	2.2E+02
K-40	1.3E+05	3.2E+03			1.3E+04	3.2E+03
Kr-85		2.7E+11				2.7E+11
Mo-93	1.4E+06				6.2E+05	6.2E+05
Na-22		7.8E+15				7.8E+15
Nb-93m					1.5E+05	1.5E+05
Nb-94	8.6E+19	1.0E+03			7.0E+17	1.0E+03
Ni-59	2.5E+17				1.6E+19	2.5E+17
Np-237	6.6E+19	6.7E+04			8.9E+18	6.7E+04

Table 7-2. Disposal Limits for Vault 4 Based on 10,000-Year Time of Compliance, Ci

	Pathway					
Radionuclide	Groundwater	Resident Intruder	Atmospheric	Radon	All Pathways	Most Restrictive
Pa-231		2.2E+04				2.2E+04
Pb-210		3.9E+11				3.9E+11
Pd-107	4.4E+16				1.8E+17	4.4E+16
Pu-238		1.3E+07				1.3E+07
Pu-239		1.4E+10				1.4E+10
Pu-240		3.0E+12				3.0E+12
Pu-241		1.0E+10				1.0E+10
Pu-242		4.9E+10				4.9E+10
Pu-244		3.7E+03				3.7E+03
Ra-226	4.8E+16	4.2E+02		1.1E+12	3.8E+16	4.2E+02
Ra-228		3.7E+08				3.7E+08
Rb-87	1.7E+13				5.1E+09	5.1E+09
Sb-125		1.4E+17	3.0E+47			1.4E+17
Se-79	3.8E+04		4.8E+06		1.0E+03	1.0E+03
Sn-126		1.2E+03	6.4E+62		2.9E+19	1.2E+03
Sr-90	2.4E+16				1.4E+17	2.4E+16
Tc-99	4.5E+17	3.7E+13			1.1E+17	3.7E+13
Th-228		1.9E+19				1.9E+19
Th-229		8.6E+03				8.6E+03
Th-230	1.1E+16	3.3E+02				3.3E+02
Th-232		1.6E+02				1.6E+02
U-232		9.0E+03				9.0E+03
U-233		1.4E+04				1.4E+04
U-234	1.5E+18	4.5E+03				4.5E+03
U-235		1.0E+05				1.0E+05
U-236		3.2E+08				3.2E+08
U-238		6.6E+04				6.6E+04

Table 7-3. Disposal Limits for Nitrate in Vault 4

Compliance Time, years	Peak Concentration, ppb/Kg	Peak Time, Years	Inventory Limit, Kg as Nitrogen
1000	3.46E-05	1.00E+03	2.89E+08
10,000	2.80E-03	9.80E+03	3.57E+06

Table 7-4. Total Projected Vault 4 Radionuclide Inventory

Radionuclide	Curies	Radionuclide	Curies
Am-241	4.93E+02	Pm-147	3.86E+03
Am-242m	3.31E+02	Pr-144	2.61E+00
Am-243	1.30E-03	Pu-238	3.33E+03
C-14	4.44E+00	Pu-239	4.20E+01
Ce-141	8.85E-06	Pu-240	7.74E+01
Ce-144	2.67E+00	Pu-241	1.55E+03
Cf-251	2.47E-01	Pu-242	1.56E-01
Cm-243	8.06E-02	Ru-103	2.70E-05
Cm-244	4.19E+02	Ru-106	6.48E+00
Cm-245	7.91E-02	Sb-124	2.39E-02
Co-60	3.90E+02	Sb-125	1.87E+02
Cs-134	7.35E+00	Se-79	1.99E+00
Cs-135	2.29E-02	Sm-151	9.29E-04
Cs-137	1.25E+06	Sn-126	2.65E+00
Eu-152	5.14E-03	Sr-90	1.24E+05
Eu-154	1.08E+03	Tc-99	9.82E+01
Eu-155	1.58E-03	Th-232	3.62E-03
H-3	1.96E+02	U-232	9.46E+00
I-129	8.09E-01	U-233	1.46E+01
Nb-94	9.91E-04	U-234	6.53E+00
Ni-59	3.35E+00	U-235	7.91E-02
Ni-63	4.23E+00	U-236	1.85E-01
Np-237	7.23E-01	U-238	3.61E-01
Pm-144	7.45E-03		
Pm-146	1.97E-04		

Table 7-5. Comparison of 1,000-Year Limits with Projected Inventory

Radionuclide	Limit, Ci	Estimated Inventory, Ci	Fraction of Limit
Am-241	4.8E+08	4.9E+02	1.0E-06
Am-242m	1.6E+07	3.3E+02	2.1E-05
Am-243	3.0E+05	1.3E-03	4.3E-09
C-14	4.4E+07	4.4E+00	1.0E-07
Cf-251	1.8E+06	2.5E-01	1.4E-07
Cm-243	7.0E+09	8.1E-02	1.2E-11
Cm-244	8.6E+16	4.2E+02	4.9E-15
Cm-245	8.4E+06	7.9E-02	9.4E-09
Co-60	5.8E+09	3.9E+02	6.7E-08
Cs-134	4.1E+19	7.4E+00	1.8E-19
Cs-137	6.0E+06	1.3E+06	2.1E-01
Eu-152	6.4E+06	5.1E-03	8.0E-10
Eu-154	1.2E+08	1.1E+03	9.0E-06
Eu-155	1.1E+19	1.6E-03	1.4E-22
H-3	5.5E+11	2.0E+02	3.6E-10
I-129	1.8E+07	8.1E-01	4.5E-08
Nb-94	1.0E+03	9.9E-04	9.9E-07
Np-237	7.7E+04	7.2E-01	9.4E-06
Pu-238	6.2E+08	3.3E+03	5.4E-06
Pu-239	3.0E+10	4.2E+01	1.4E-09
Pu-240	2.3E+14	7.7E+01	3.4E-13
Pu-241	1.5E+10	1.5E+03	1.0E-07
Pu-242	5.2E+11	1.6E-01	3.0E-13
Sb-125	1.4E+17	1.9E+02	1.3E-15
Se-79	4.8E+06	2.0E+00	4.1E-07
Sn-126	1.2E+03	2.7E+00	2.2E-03
Sr-90	2.4E+16	1.2E+05	5.2E-12
Tc-99	3.7E+13	9.8E+01	2.7E-12
Th-232	1.6E+02	3.6E-03	2.3E-05
U-232	9.0E+03	9.5E+00	1.1E-03
U-233	8.9E+04	1.5E+01	1.6E-04
U-234	1.8E+05	6.5E+00	3.6E-05
U-235	5.8E+05	7.9E-02	1.4E-07
U-236	3.2E+09	1.9E-01	5.8E-11
U-238	8.0E+04	3.6E-01	4.5E-06
	Sum-of-Fractions		2.1E-01

Table 7-6. Comparison of 10,000-Year Limits with Projected Inventory

Radionuclide	Limit, Ci	Estimated Inventory, Ci	Fraction of Limit
Am-241	3.4E+08	4.9E+02	1.5E-06
Am-242m	9.8E+06	3.3E+02	3.4E-05
Am-243	3.0E+05	1.3E-03	4.3E-09
C-14	4.4E+07	4.4E+00	1.0E-07
Cf-251	1.8E+06	2.5E-01	1.4E-07
Cm-243	7.0E+09	8.1E-02	1.2E-11
Cm-244	1.1E+15	4.2E+02	3.8E-13
Cm-245	8.4E+06	7.9E-02	9.4E-09
Co-60	5.8E+09	3.9E+02	6.7E-08
Cs-134	4.1E+19	7.4E+00	1.8E-19
Cs-135	8.1E+13	2.3E-02	2.8E-16
Cs-137	6.0E+06	1.3E+06	2.1E-01
Eu-152	6.4E+06	5.1E-03	8.0E-10
Eu-154	1.2E+08	1.1E+03	9.0E-06
Eu-155	1.1E+19	1.6E-03	1.4E-22
H-3	5.5E+11	2.0E+02	3.6E-10
I-129	2.2E+02	8.1E-01	3.7E-03
Nb-94	1.0E+03	9.9E-04	9.9E-07
Ni-59	2.5E+17	3.3E+00	1.3E-17
Np-237	6.7E+04	7.2E-01	1.1E-05
Pu-238	1.3E+07	3.3E+03	2.6E-04
Pu-239	1.4E+10	4.2E+01	3.0E-09
Pu-240	3.0E+12	7.7E+01	2.6E-11
Pu-241	1.0E+10	1.5E+03	1.5E-07
Pu-242	4.9E+10	1.6E-01	3.2E-12
Sb-125	1.4E+17	1.9E+02	1.3E-15
Se-79	1.0E+03	2.0E+00	2.0E-03
Sn-126	1.2E+03	2.7E+00	2.2E-03
Sr-90	2.4E+16	1.2E+05	5.2E-12
Tc-99	3.7E+13	9.8E+01	2.7E-12
Th-232	1.6E+02	3.6E-03	2.3E-05
U-232	9.0E+03	9.5E+00	1.1E-03
U-233	1.4E+04	1.5E+01	1.0E-03
U-234	4.5E+03	6.5E+00	1.5E-03
U-235	1.0E+05	7.9E-02	7.9E-07
U-236	3.2E+08	1.9E-01	5.8E-10
U-238	6.6E+04	3.6E-01	5.5E-06
		Sum of Fractions	2.2E-01

Table 7-7. Comparison of 10,000-Year Limits from This Analysis and 2002 SA

Radionuclide	New SA Limit, Ci	2002 SA Limit, Ci/Vault[a]	Estimated Inventory, Ci
C-14	4.4E+07	1.2E+04[b]	4.4E+00
Cs-137	6.0E+06	1.0E+09	1.3E+06
I-129	2.2E+02	1.4E+00	8.1E-01
Np-237	6.7E+04	6.9E+03	7.2E-01
Se-79	1.0E+03	2.7E+02	2.0E+00
Sn-126	1.2E+03	1.0E+03	2.7E+00
Sr-90	2.4E+16	No Limit	1.2E+05
Tc-99	3.7E+13	2.8E+04	9.8E+01

[a] From Table 8-1 of Cook et al. 2002. Groundwater limits have been converted from total Ci to Ci/vault by dividing by 14.5.

[b] Cook and Kaplan 2003.

7.4 Projected Vault 4 Impacts Compared to 10 CFR 61 Performance Objectives

Section 3116 of the Ronald W. Reagan NDAA for Fiscal Year 2005 (U.S. Congress 2004) requires, in part, that certain USDOE High Level Wastes that are shown to not need the degree of isolation provided by a geological repository be managed to comply with the performance objectives of 10 CFR 61 (CFR 2004). This section will compare estimated impacts from the disposal of Saltstone in Vault 4 with two of these performance objectives.

There are five performance objectives stated in 10 CFR 61. Only two, protection of the general population from release of radioactivity (i.e., 10 CFR 61.41) and protection of individuals from inadvertent intrusion (i.e., 10 CFR 61.42) are pertinent for comparison with results of a performance assessment calculation such as those presented in this SA.

7.4.1 10 CFR 61 Performance Objectives

Two of the four performance objectives in 10 CFR 61 are pertinent to this discussion. They are 10 CFR 61.41 and 10 CFR 61.42.

10 CFR 61.41 states:

Concentrations of radioactive material which may be released to the general environment in ground water, surface water, air, soil, plants, or animals must not result in an annual dose exceeding an equivalent of 25 millirems to the whole body, 75 millirems to the thyroid, and 25 millirems to any other organ of any member of the public. Reasonable effort should be made to maintain releases of radioactivity in effluents to the general environment as low as is reasonably achievable.

10 CFR 61.42 states:

Design, operation, and closure of the land disposal facility must ensure protection of any individual inadvertently intruding into the disposal site and occupying the site or contacting the waste at any time after active institutional controls over the disposal site are removed.

The dose calculations in this SA use newer dose methodology than that stated in the performance objective for protection of the public. However, the NRC has stated: "The dose methodology used

in 10 CFR 61 Subpart C is different from that used in the newer 10 CFR 20 Subpart E. However, the resulting allowable doses are comparable and NRC expects USDOE to use the newer methodology in 10 CFR 20 Subpart E. Part 61 is based on International Commission on Radiological Protection Publication 2 (ICRP 2) and Part 20 is based on ICRP 26" (USNRC 2002). The methodology defined in ICRP 26 calculates dose in TEDE versus the organ doses of the earlier methodology. Radiological doses are calculated in TEDE in this SA in accordance with the newer methodology.

7.4.2 Projected Doses

Doses to a member of the public and the inadvertent intruder from Vault 4 are estimated from the all-pathways and inadvertent intruder disposal limits presented in Sections 6 and 3, respectively, and the projected inventory for Vault 4, presented in Section 7.2. For each radionuclide, the all-pathways and intruder disposal limits were determined by calculating the maximum dose that would result from disposal of one curie (i.e., mrem/year per curie). Then, the performance measure (e.g., 25 mrem/year) was divided by the dose per curie to give the disposal limit in curies. To estimate the dose that would result from disposal of the projected Vault 4 inventory (i.e., that shown in Table 7-4), the inventory for each radionuclide was divided by its all-pathways and resident intruder 10,000-year limit to obtain an inventory fraction of the limit. The fraction of the limits were then multiplied by the respective performance measure (i.e., 25 mrem/year for all-pathways and 100 mrem/year for the resident intruder) to give the dose for each radionuclide. The doses were summed to give the total all-pathways and resident intruder doses. The 10,000-year limits were used because the NRC staff has suggested that 10,000 years is the appropriate compliance time for LLW PA (USNRC 2000). This method is quite conservative because it presumes that the doses from all radionuclides are coincident in time.

The resulting doses are presented in Table 7-8.

Table 7-8. Projected Dose from Vault 4 Compared with 10 CFR 61 Performance Objectives

Receptor	Projected Dose[a]	10 CFR 61 Dose Objective
Member of the Public	0.05 mrem/year effective whole body	25 mrem/year
	0.19 mrem/year thyroid	75 mrem/year
	0.12 mrem/year any other organ	25 mrem/year
Intruder Resident Scenario	21.5 mrem/year	500 mrem/year

a. Since the NRC performance objective for the member of the public is stated in terms of doses to particular organs, the Total Effective Dose Equivalent doses calculated in this SA were used to estimate organ doses by ratio with the organ dose conversion factors in Eckerman et al 1988.

The projected doses from disposal of salt waste in Saltstone Vault 4 are very low. The dose to the member of the public is 0.05 mrem/year, which is 0.2% of the performance objective. The dose to the inadvertent intruder from the resident scenario, which is the only credible scenario within the 10,000-year time frame, is 21.5 mrem/year, which is 4% of the NRC performance objective of 500 mrem/year (USNRC 1982). Therefore, disposal in Vault 4 will comply with the 10 CFR 61 performance objectives.

7.5 Sensitivity

7.5.1 Vault 1 and 4 Plume Interaction Sensitivity

Vault 1 is an existing vault with waste located approximately 580 feet upgradient of Vault 4. During the design check of the saturated (aquifer) portion of this special analysis, it was shown that there was potential plume interaction from Vault 1 based on stream traces (particle tracking).

Figures 7-1 and 7-2 show stream traces from Vault 1 and Vault 4 source nodes with 10-year timing markers, respectively. Stream traces from Vault 1 source nodes indicate advective transport times between 5 and 10 years to reach beneath Vault 4. Therefore, there is potential for plume interaction depending on the depth of each plume downgradient of Vault 4 from Vault 1 and 4. To quantify plume interaction from Vault 1, a conservative nonabsorbent tracer, nitrate, was chosen.

The nitrate SDF Vault 4 vadose zone model was used to compute the transient fractional release of nitrate from Vault 4 to the water table over the time period of 0 to 10,000 years. The fractional release of nitrate to the water table was normalized by the initial inventory of 1E+6 moles and has units of mole/yr/mole. Given the short time to complete this study and schedule constraints, the nitrate SDF Vault 1 vadose zone was not explicitly modeled using actual waste inventory. The transient fractional release of nitrate from the SDF Vault 4 vadose zone was independently applied to both Vault 1 and Vault 4 aquifer source nodes. For each set of aquifer source nodes, the transient fractional release was partitioned to each aquifer source node by cell volume.

Two nitrate aquifer transport simulations were modeled: one case with only Vault 4 aquifer source nodes (base case), another with both Vault 1 and 4 aquifer source nodes active. The simulation time was from 0 to 10,000 years. During each simulation the STAT command was executed to capture the transient maximum concentration beyond the 100-ft point of assessment and a 100-m perimeter. Figure 7-3 shows an aerial view of the 100-ft point of assessment wells (blue) and the 100-m Vault 4 wells (red). In addition, polygons extruded from the bottom to the top of the model domain were used to exclude source nodes, nodes between the vaults, and to establish 100-ft and 100-m perimeters about the respective vaults. A separate set of STAT commands were used to record maximum nitrate concentrations based on these extruded polygons. This was done to compare the maximum nitrate concentrations based on base case well selections to the polygon-based selection method. The well selections in general recorded higher concentrations than the polygon-based selection due to closer proximity to the Vault 4 footprint.

The Vault 4 only aquifer transport simulation results are shown in Figures 7-4 to 7-9. Figures 7-4 and 7-5 show the maximum nitrate concentration beyond the 100-ft point of assessment for time periods 0 to 1,000 years and 0 to 10,000 years, respectively. The difference between the well node and polygon curves is explained by the well locations shown in Figure 7-6. The peak nitrate concentrations for Figures 7-4 and 7-5 are 3.46E-5 (1,000 years) and 2.80E-3 (9,800 years) ppb/kg, respectively. Figures 7-7 and 7-8 show the maximum nitrate concentration beyond the 100-m perimeter of Vault 4 for time periods 0 to 1,000 years and 0 to 10,000 years, respectively. The difference between the well node and polygon curves is smaller and the well locations are shown in Figure 7-9. The peak nitrate concentrations for Figures 7-7 and 7-8 are 1.44E-5 (1,000 years) and 1.17E-3 (9,800 years) ppb/kg, respectively.

The Vault 1 and 4 aquifer transport simulation results are shown in Figures 7-10 to 7-15. Figures 7-10 and 7-11 show the maximum nitrate concentration beyond the 100-ft point of assessment for time periods 0 to 1,000 years and 0 to 10,000 years, respectively. The difference between the well nodes and polygons curves is explained by the well locations shown in Figure 7-12. The peak nitrate concentrations for Figures 7-10 and 7-11 are 3.46E-5 (1,000 years) and 2.80E-3 (9,800 years) ppb/kg, respectively. Figures 7-13 and 7-14 show the maximum nitrate concentration beyond the 100-m perimeter of Vault 4 for time periods 0 to 1,000 years and 0 to 10,000 years, respectively. There is no difference between the well node and polygon curves because the well locations are identical and are shown in Figure 7-15. The peak nitrate concentrations for Figures 7-13 and 7-14 are 1.78E-5 (1,000 years) and 1.45E-3 (9,800 years) ppb/kg, respectively.

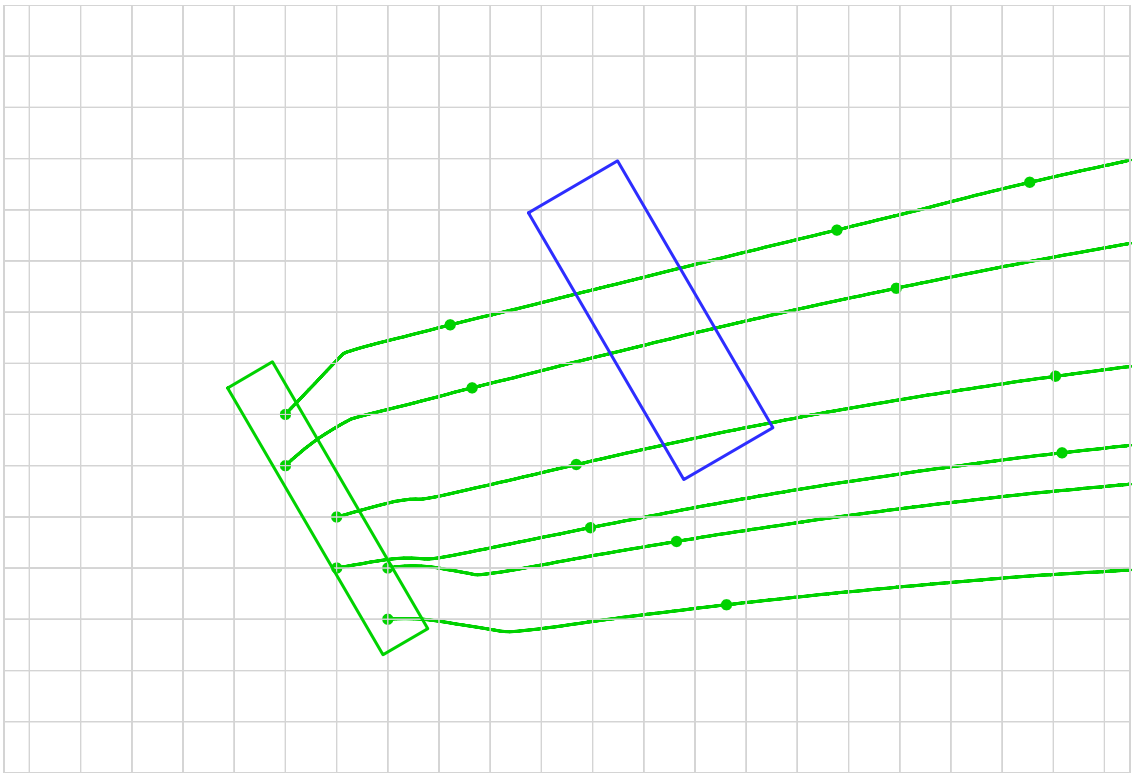

Figure 7-1. Vault 1 Stream Traces from Source Nodes with 10-year Timing Markers

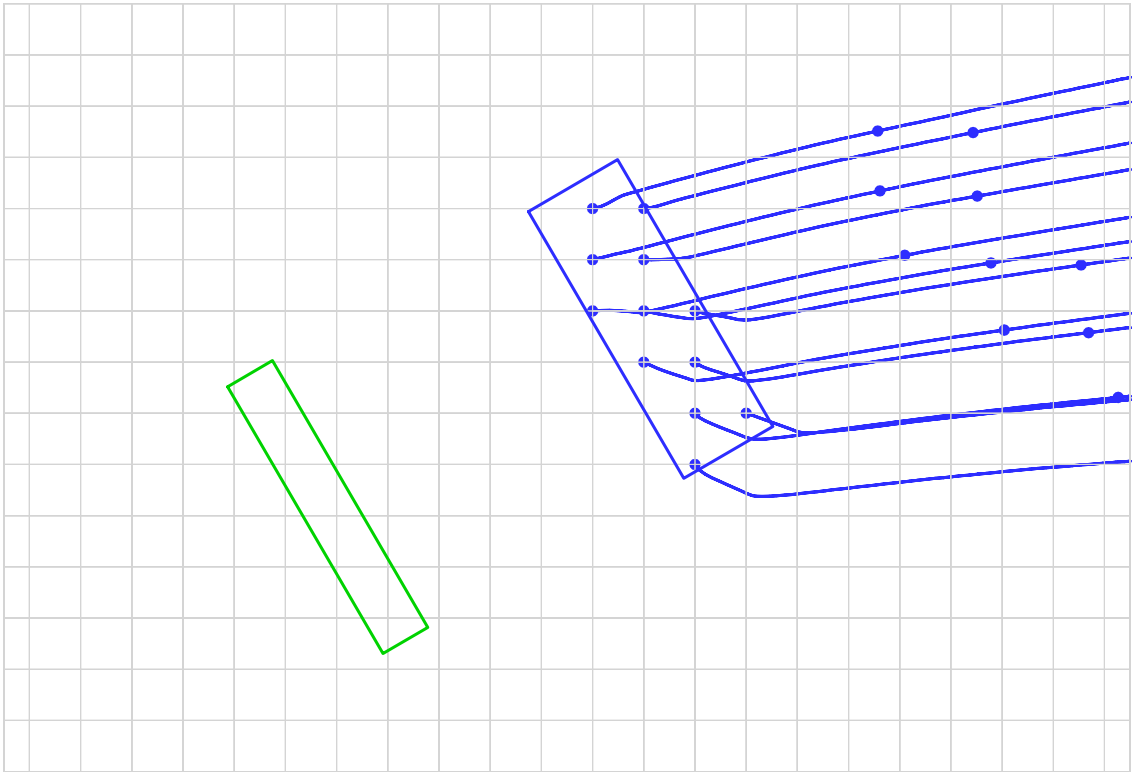

Figure 7-2. Vault 4 Stream Traces from Source Nodes with 10-year Timing Markers

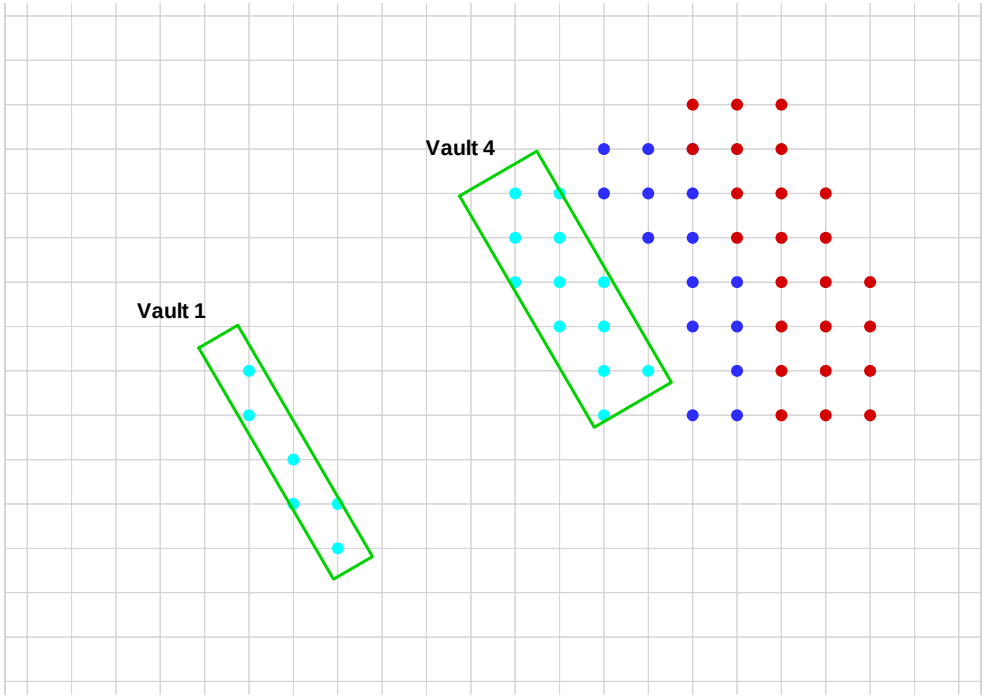

Figure 7-3. Aerial View of Vault 1 and 4 Source Nodes, 100-ft Point of Assessment Wells and 100-m Vault 4 Wells.

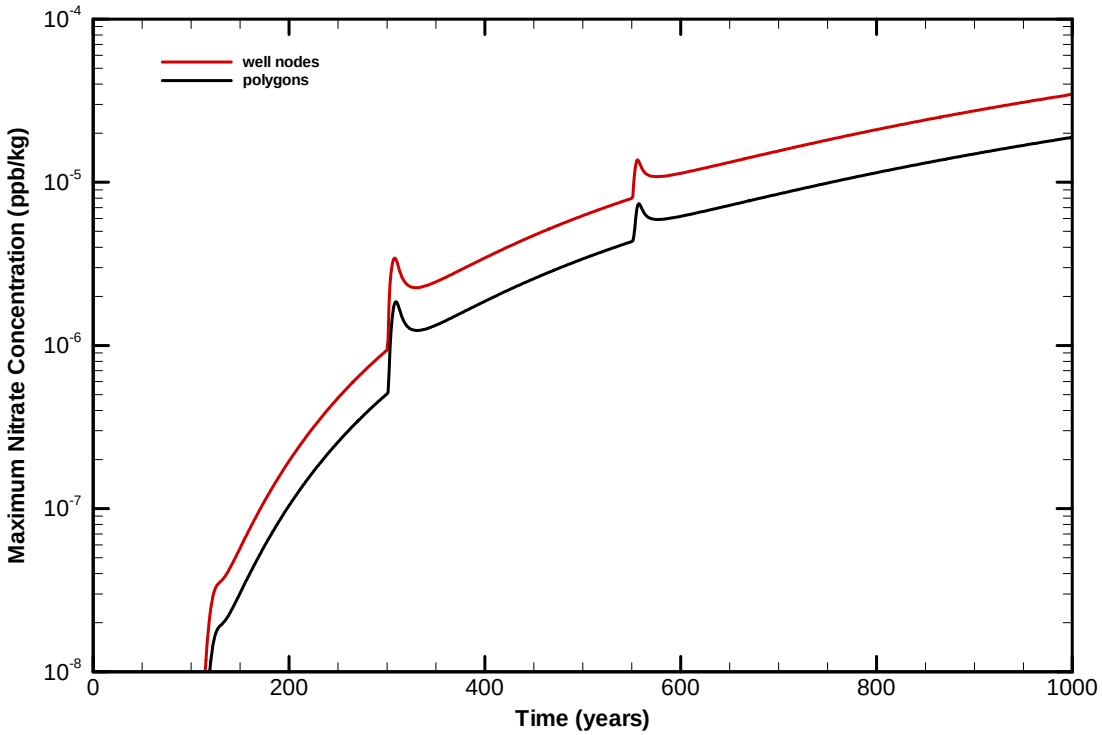

Figure 7-4. Maximum Nitrate Concentration Beyond 100-ft Point of Assessment (Vault 1:off, Vault 4:on, 0 to 1,000 yr)

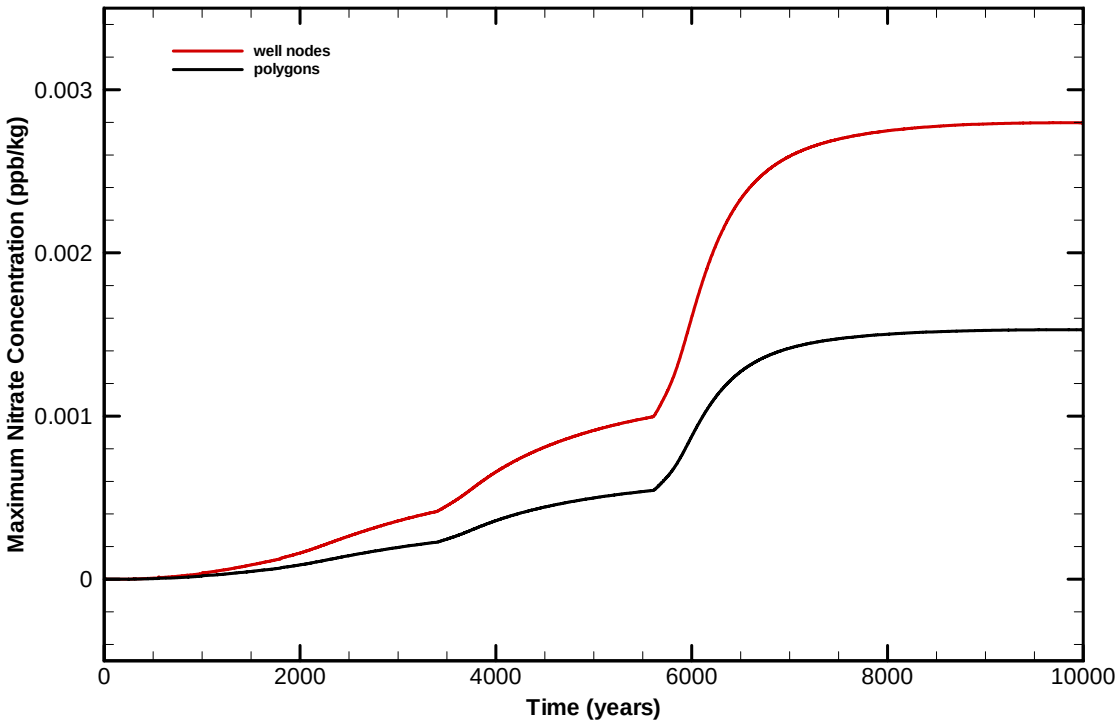

Figure 7-5. Maximum Nitrate Concentration Beyond 100-ft Point of Assessment (Vault 1:off, Vault 4:on, 0 to 10,000 yr)

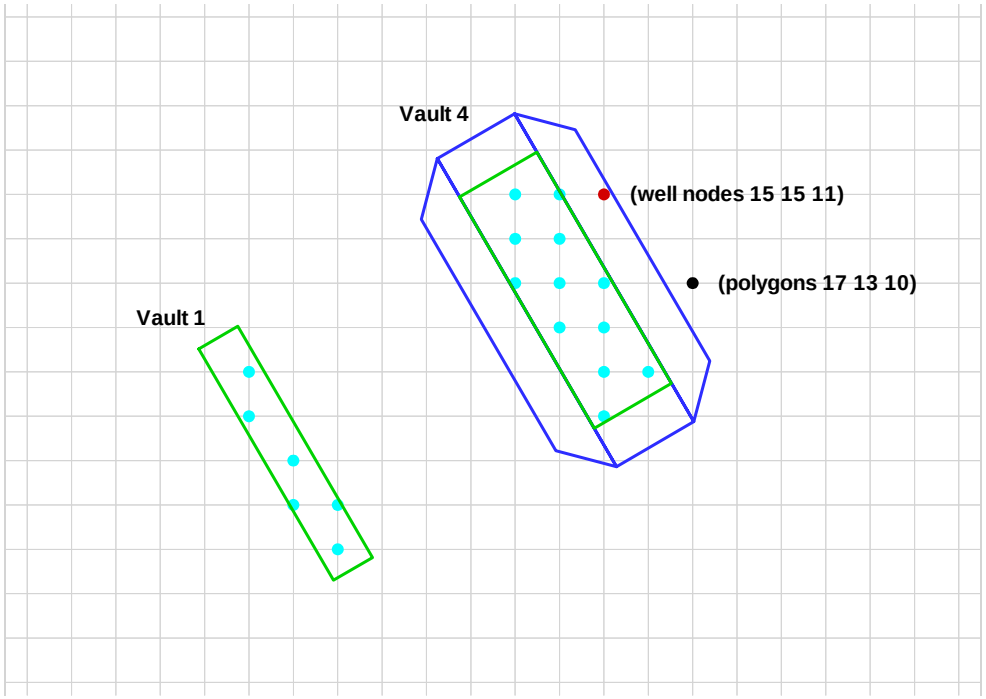

Figure 7-6. Well Locations of Maximum Nitrate Concentration Beyond 100-ft Point of Assessment (Vault 1:off, Vault 4:on)

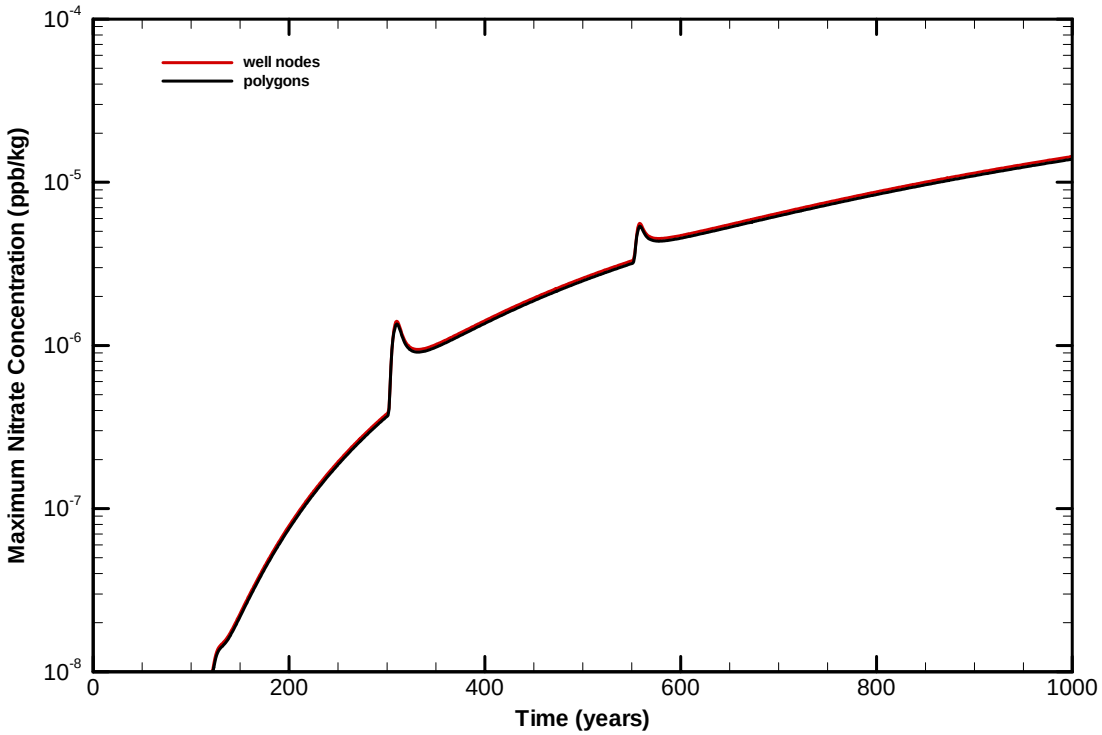

Figure 7-7. Maximum Nitrate Concentration Beyond 100-m Perimeter of Vault 4 (Vault 1:off, Vault 4:on, 0 to 1,000 yr)

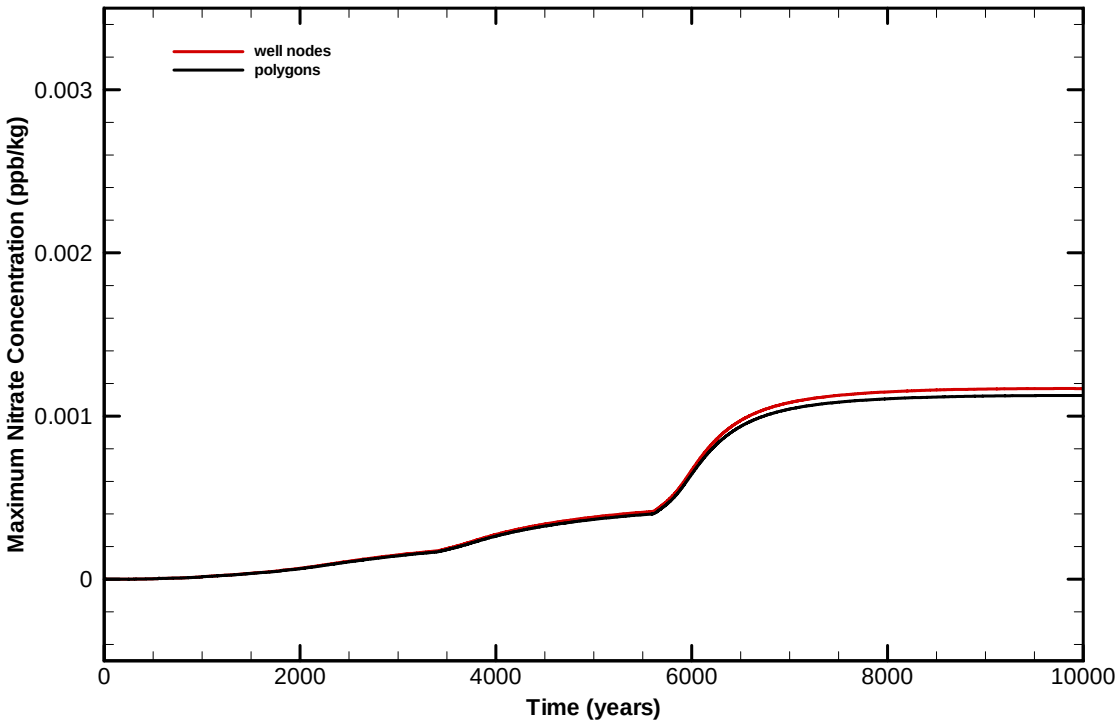

Figure 7-8. Maximum Nitrate Concentration Beyond 100-m Perimeter of Vault 4 (Vault 1:off, Vault 4:on, 0 to 10,000 yr)

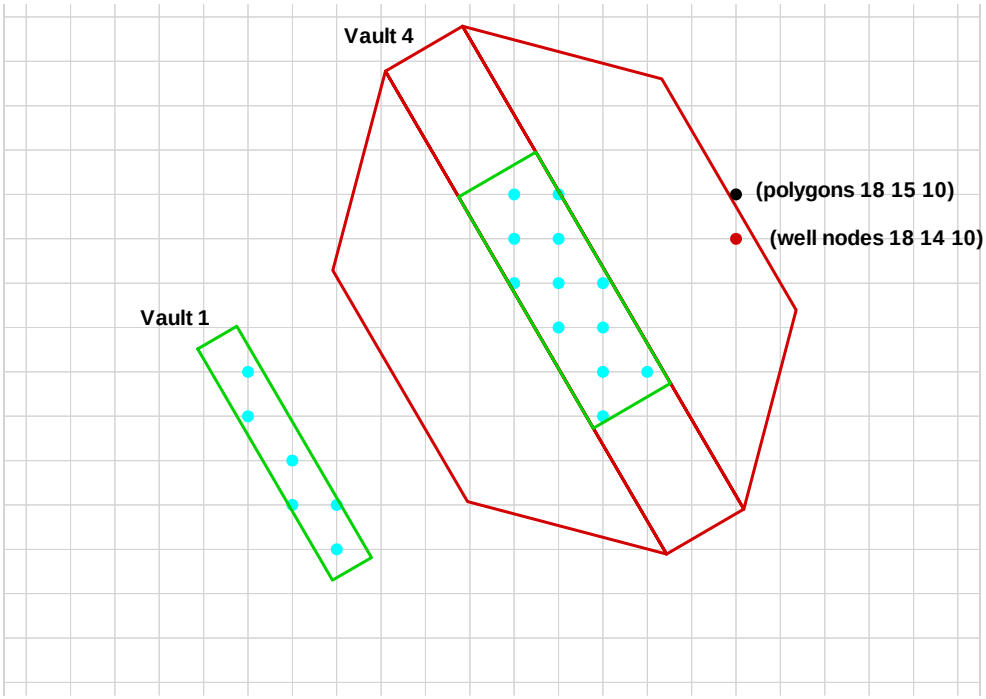

Figure 7-9. Well Locations of Maximum Nitrate Concentration Beyond 100-m Perimeter of Vault 4 (Vault 1:off, Vault 4:on)

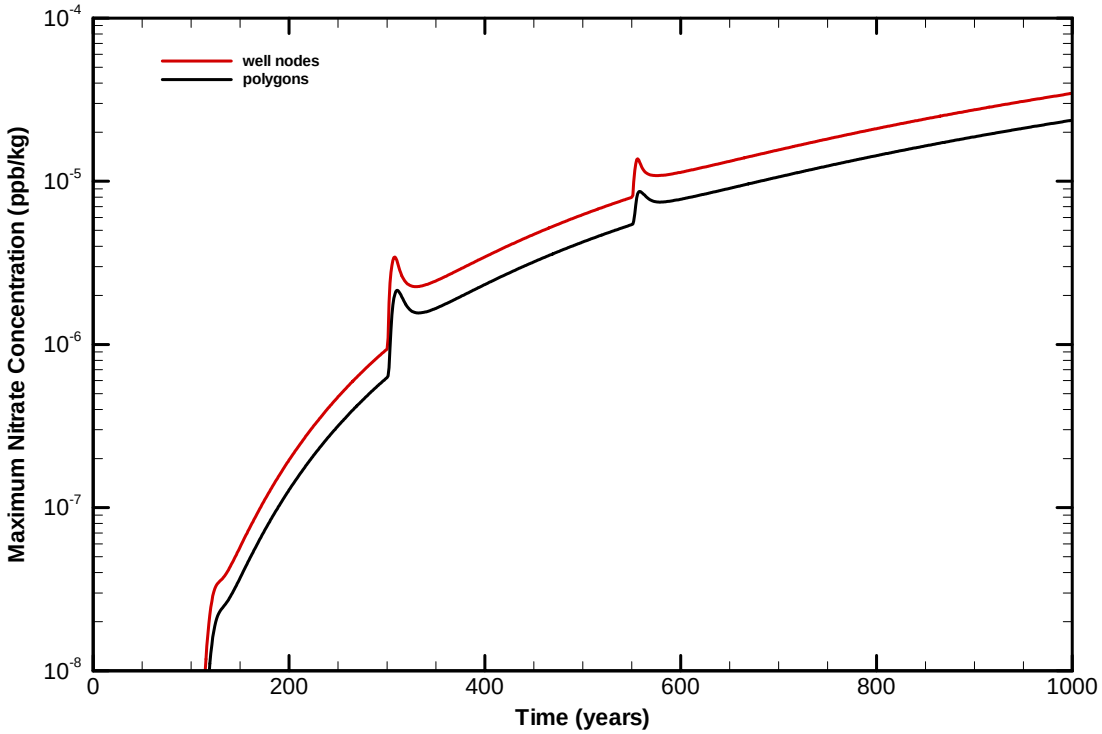

Figure 7-10. Maximum Nitrate Concentration Beyond 100-ft Point of Assessment (Vault 1:on, Vault 4:on, 0 to 1,000 yr)

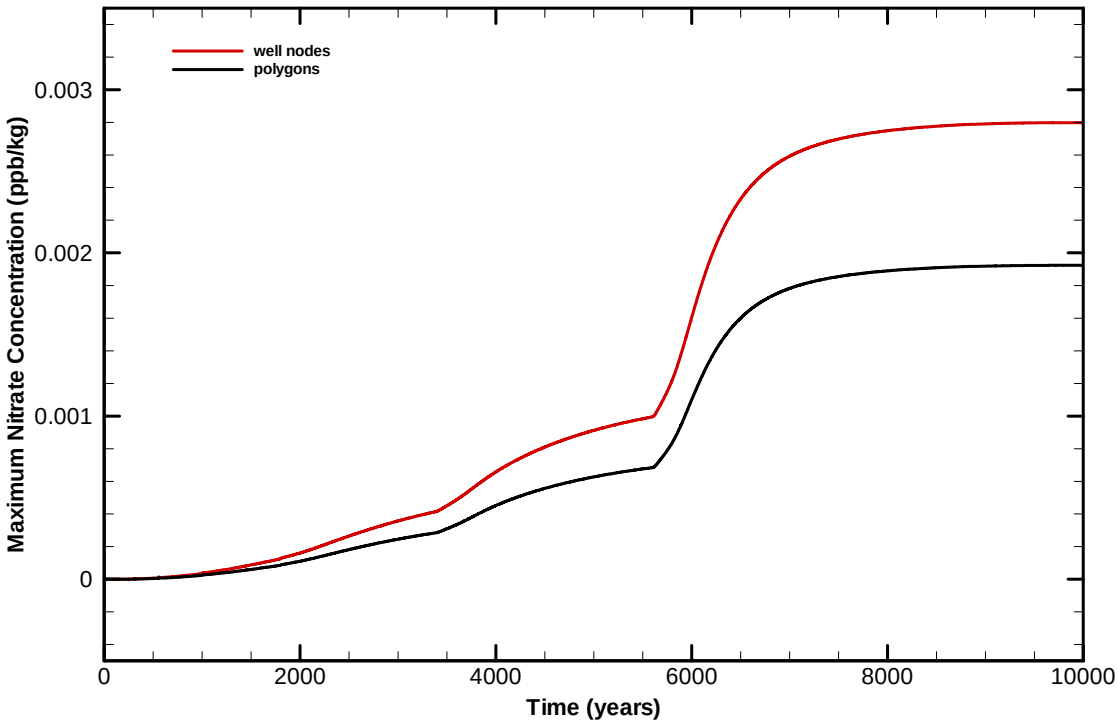

Figure 7-11. Maximum Nitrate Concentration Beyond 100-ft Point of Assessment (Vault 1:on, Vault 4:on, 0 to 10,000 yr)

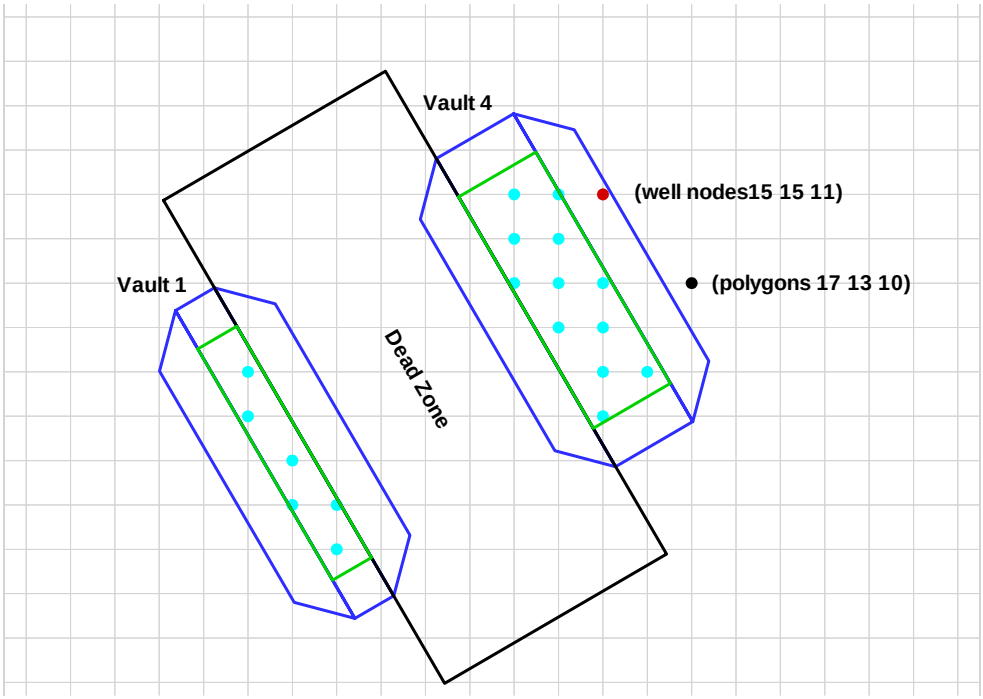

Figure 7-12. Well Locations of Maximum Nitrate Concentration Beyond 100-ft Point of Assessment (Vault 1:on, Vault 4:on)

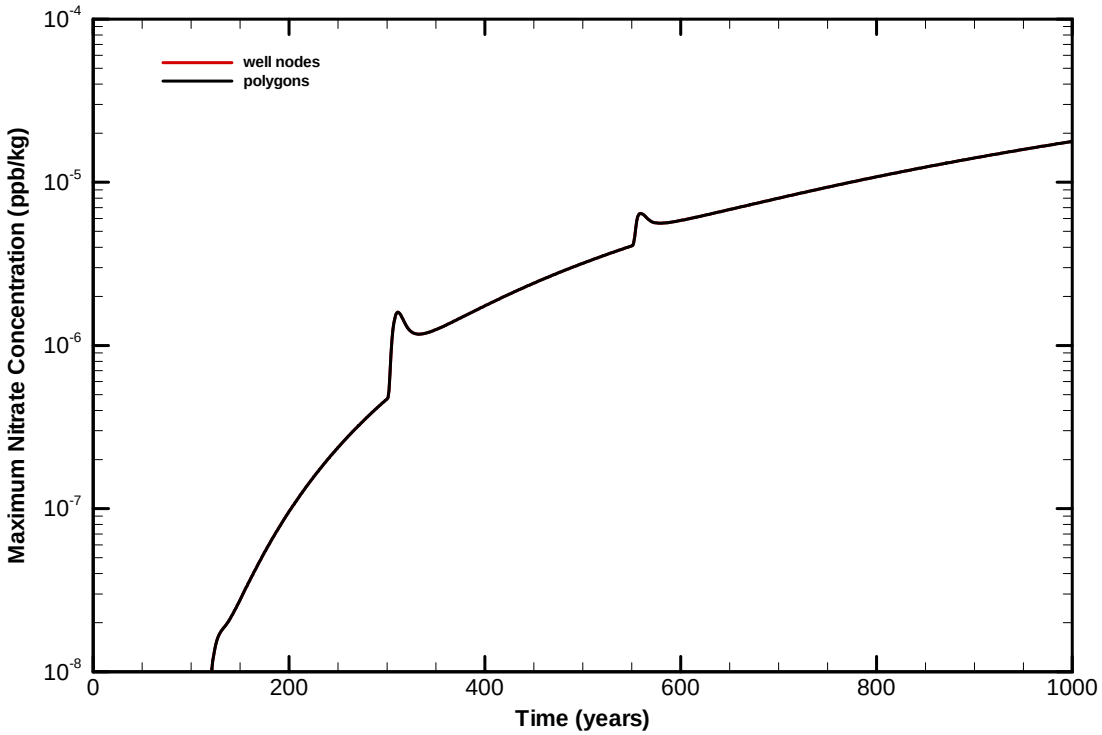

Figure 7-13. Maximum Nitrate Concentration Beyond 100-m Vault 4 Perimeter (Vault 1:on, Vault 4:on, 0 to 1,000 yr)

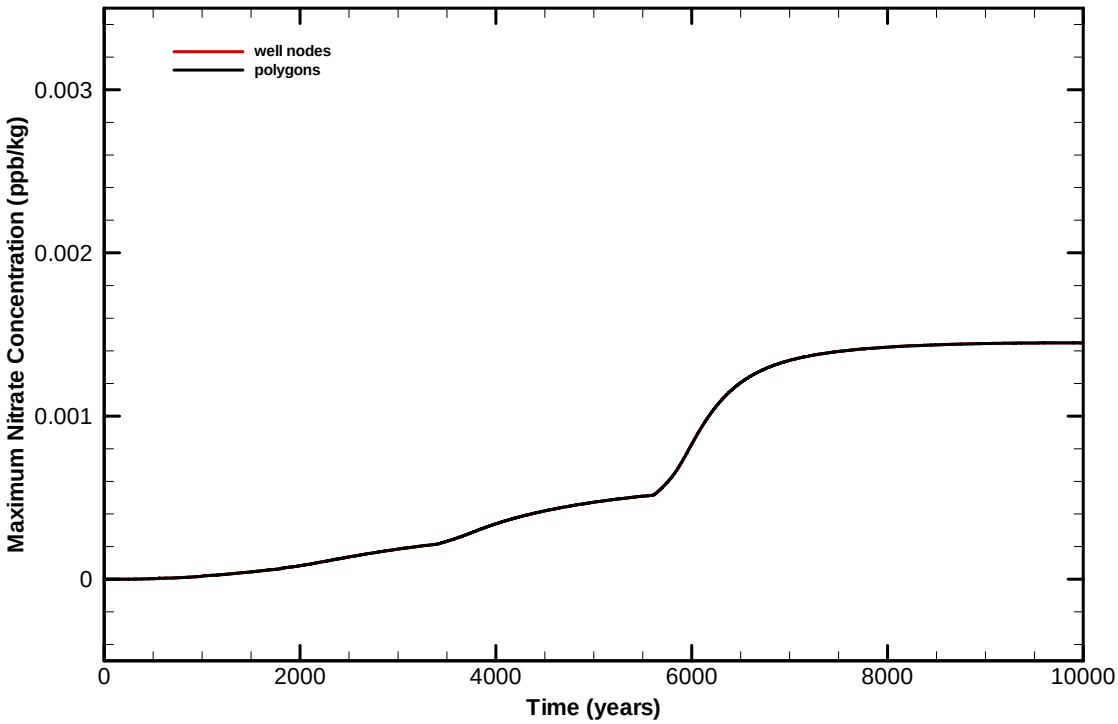

Figure 7-14. Maximum Nitrate Concentration Beyond 100-m Perimeter of Vault 4 (Vault 1:on, Vault 4:on, 0 to 10,000 yr)

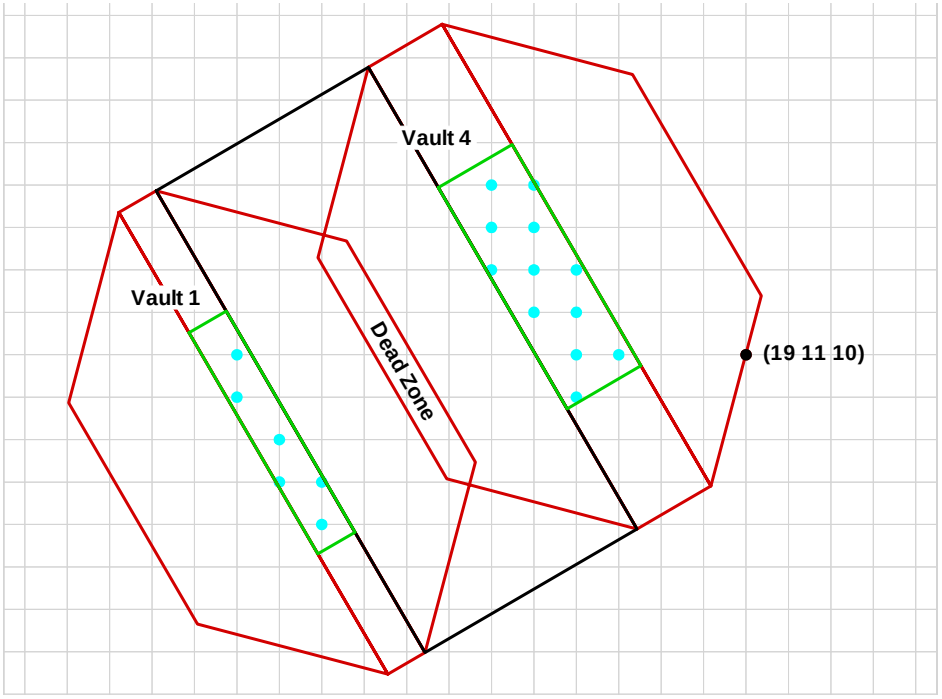

Figure 7-15. Well Locations of Maximum Nitrate Concentration Beyond 100-m Perimeter of Vault 4 (Vault 1:on, Vault 4:on)

The conclusion of this quick study is that there is no impact of plume interaction from Vault 1 for nitrate beyond the 100-ft point of assessment and the 1,000-year time of assessment. There appears to be an impact beyond the 100-m perimeter of Vault 4. However, the interaction only increases nitrate concentrations by about 25%. The Sum-of-Fractions of the 10,000-year groundwater limits is only 0.004. Applying a 25% reduction factor to all 10,000-year groundwater limits would only increase the Sum-of-Fractions to 0.005. The potential for plume interaction will be quantified in the upcoming Saltstone PA revision and will be included, as appropriate, in limits determined therein.

7.5.2 Peak Fractional Contaminant Flux of I-129 to the Water Table

The fractional contaminant flux of I-129 to the water table at 10,000 years is 1.29E-07 mole/yr/mole as shown in Table A-11. The flux is predominantly the diffusive component of the total flux and quickly rising beyond 10,000 years (Figure 7-16). To capture the peak of the flux, the simulation run time was extended to 70,000 years. As shown in Figure 7-17, the flux curve has an inflection point before 30,000 years and approaches a peak at 70,000 years. The peak fractional contaminant flux of I-129 to the water table at 70,000 years is 3.83E-06 mole/yr/mole which is a factor of 30 greater than the value at 10,000 years. This result is helpful in understanding the behavior of the SDF over extremely long times but results calculated over such time frames are not appropriate for establishing disposal limits. However, even if the 10,000-year disposal limit for ^{129}I based on the groundwater pathway were decreased by a factor of 30 (i.e., to 7.3 Ci), the projected Vault 4 inventory of ^{129}I would be only about 10% of that limit.

7.5.3 Inadvertent Intruder Post-Drilling Scenario

In the inadvertent intruder analysis, which is presented in Section 3 and Appendix B, the long-term durability of the Saltstone waste form and the concrete vault are assumed to prevent drilling a well through a disposal vault. To explore the sensitivity of the analysis results to this assumption, an alternate scenario, termed the post-drilling scenario, was assessed.

The post-drilling scenario is based on the assumption that a person could drill a well through a disposal vault. For this sensitivity analysis, the assumption is that drilling through a vault first becomes credible at 1,000 years after closure. The post-drilling scenario is assessed from 1,000 years after closure to 10,000 years after closure. In the post-drilling scenario, the subsurface material exhumed during drilling includes some of the Saltstone waste. This material is assumed to be mixed with soil in a garden and the intruder is exposed to the waste through a variety of pathways (e.g. direct radiation, ingesting food stuffs grown in the garden). The limits derived from the post-drilling analysis are presented in Table B-5.

The post-drilling limits are generally smaller (i.e., more restrictive) than the resident limits, which are presented in Table 3-2. If the post-drilling scenario were to be considered credible, the sum-of-fractions of the 10,000-year limits would increase from 0.22 to 0.31.

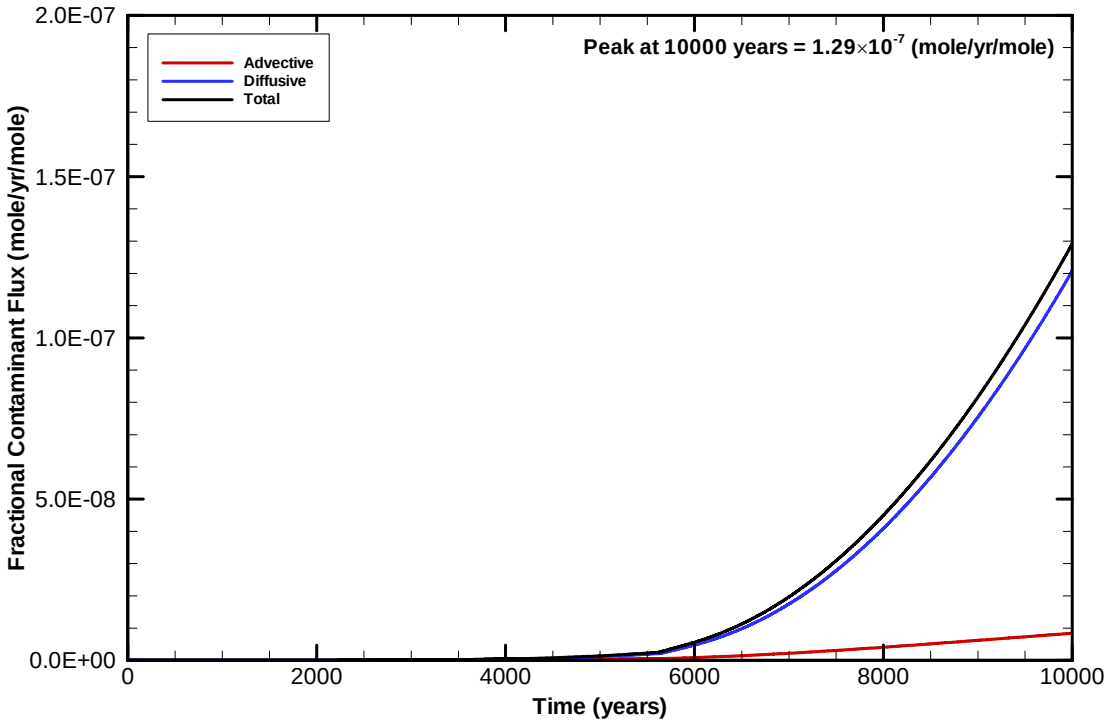

Figure 7-16. Instantaneous I-129 Fractional Contaminant Flux to the Water Table (0 to 10,000 yrs)

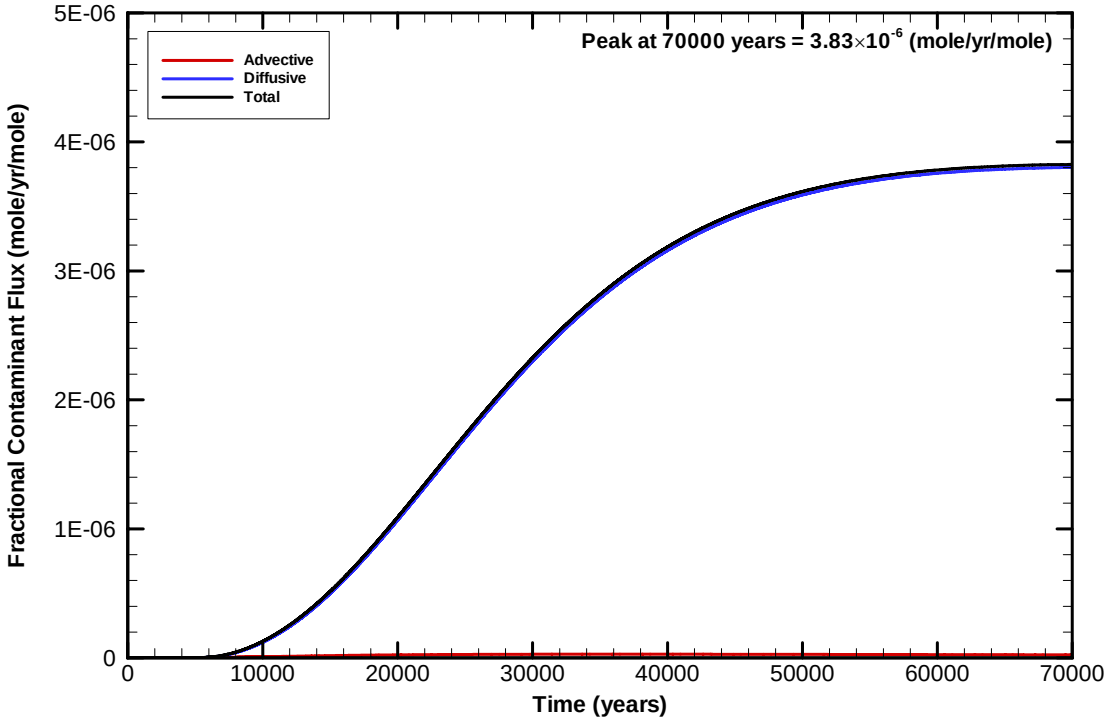

Figure 7-17. Instantaneous I-129 Fractional Contaminant Flux to the Water Table (0 to 70,000 yrs)

7.5.4 Agricultural Scenario Following Failure of Erosion Barrier

In the inadvertent intruder analysis, which is presented in Section 3 and Appendix B, the long-term persistence of the erosion barrier is assumed to preclude the Agricultural Scenario by maintaining a distance greater than that required to excavate a basement (10 ft.). To explore the sensitivity of the analysis results to this assumption, an alternate scenario in which the erosion barrier was assumed to erode at the same rate as the other cover material was assessed. The disposal limits derived from this study for a 10,000-year assessment period are shown in Table 7-9. Table 7-10 shows a comparison of these limits with the projected Vault 4 inventory.

The Sum-of-Fractions for these limits is 1.49, which, if the scenario were considered credible, would indicate non-compliance with the intruder performance measure. However, the erosion barrier is constructed of material sized to remain in place during a rainfall event with a 10,000-year recurrence interval calculated using an extreme-value distribution (i.e., 3.3 inches of rain in a 15 minute time span, [Weber 1998]). Thus, the scenario is not credible.

Table 7-9. Intruder-Based Radionuclide Disposal Limits for Vault 4 – Agriculture Scenario Following Failure of Erosion Barrier with Transient Calculation for 100 – 10,000 Years

Radionuclide	Time of Limit (Years)	Concentration Limit (uCi/m3)	Inventory Limit (Ci/Unit)
C-14	3275	1.64E+04	1.30E+03
Al-26	3275	4.37E+01	3.44E+00
Cl-36	3275	1.43E+02	1.13E+01
Ar-39	1132	1.63E+07	1.29E+06
K-40	3275	5.84E+02	4.60E+01
Ca-41	3275	6.90E+04	5.44E+03
Ni-59	3275	2.43E+06	1.91E+05
Ni-63	1280	8.72E+10	6.87E+09
Se-79	3275	1.33E+05	1.05E+04
Rb-87	3275	8.50E+04	6.70E+03
Sr-90	1132	2.11E+16	1.66E+15
Zr-93	3275	2.61E+06	2.06E+05
Nb-94	1132	8.18E+01	6.45E+00
Mo-93	1720	1.31E+06	1.03E+05
Tc-99	3275	1.39E+04	1.09E+03
Pd-107	3275	4.89E+06	3.85E+05
Ag-108m	1132	5.17E+02	4.07E+01
Sn-121m	1132	5.67E+11	4.47E+10
Sn-126	1132	6.48E+01	5.11E+00
I-129	3275	2.07E+03	1.63E+02
Cs-135	3275	1.37E+05	1.08E+04
Cs-137	1132	4.82E+13	3.79E+12
Sm-151	1132	9.51E+11	7.50E+10
Eu-152	3275	4.12E+17	3.25E+16
Pb-210	1150	---	9.56E+18
Bi-207	1132	5.15E+12	4.06E+11

Table 7-9. Intruder-Based Radionuclide Disposal Limits for Vault 4 – Agriculture Scenario Following Failure of Erosion Barrier with Transient Calculation for 100 – 10,000 Years

Radionuclide	Time of Limit (Years)	Concentration Limit (uCi/m3)	Inventory Limit (Ci/Unit)
Ra-226	1132	1.11E+02	8.76E+00
Ac-227	1132	1.18E+18	9.32E+16
Th-229	1132	4.51E+02	3.55E+01
Th-230	9080	6.25E+01	4.92E+00
Th-232	3275	4.39E+01	3.46E+00
Pa-231	3275	1.87E+02	1.48E+01
U-232	1132	6.34E+06	5.00E+05
U-233	10000	5.70E+02	4.49E+01
U-234	10000	8.03E+02	6.33E+01
U-235	10000	4.64E+02	3.66E+01
U-236	3275	1.50E+04	1.18E+03
U-238	10000	4.01E+03	3.16E+02
Np-237	10000	3.13E+02	2.47E+01
Pu-238	10000	2.28E+06	1.80E+05
Pu-239	3275	5.65E+03	4.45E+02
Pu-240	3275	7.28E+03	5.73E+02
Pu-241	1132	1.33E+06	1.05E+05
Pu-242	3275	5.44E+03	4.28E+02
Pu-244	10000	3.37E+02	2.65E+01
Am-241	1132	4.55E+04	3.58E+03
Am-242m	1132	8.32E+05	6.56E+04
Am-243	1132	8.88E+02	7.00E+01
Cm-242	10000	4.49E+08	3.53E+07
Cm-243	3275	4.48E+06	3.53E+05
Cm-244	3275	2.63E+06	2.07E+05
Cm-245	3275	1.37E+03	1.08E+02
Cm-246	3275	8.01E+03	6.31E+02
Cm-247	10000	2.85E+02	2.24E+01
Cm-248	3275	1.37E+03	1.08E+02
Bk-249	1132	1.33E+06	1.05E+05
Cf-249	1132	3.43E+03	2.70E+02
Cf-250	3275	2.91E+06	2.29E+05
Cf-251	1132	3.02E+03	2.38E+02
Cf-252	3275	1.87E+08	1.47E+07

Table 7-10. Comparison of 10,000-Year Agriculture Scenario Limits with Projected Inventory

Radionuclide	Limit, Ci	Estimated Inventory, Ci	Fraction of Limit
Am-241	3.58E+03	4.93E+02	1.38E-01
Am-242m	6.56E+04	3.31E+02	5.05E-03
Am-243	7.00E+01	1.30E-03	1.86E-05
C-14	1.30E+03	4.44E+00	3.43E-03
Cf-251	2.38E+02	2.47E-01	1.04E-03
Cm-243	3.53E+05	8.06E-02	2.28E-07
Cm-244	2.07E+05	4.19E+02	2.02E-03
Cm-245	1.08E+02	7.91E-02	7.33E-04
Cs-135	1.08E+04	2.29E-02	2.12E-06
Cs-137	3.79E+12	1.25E+06	3.29E-07
Eu-152	3.25E+16	5.14E-03	1.58E-19
I-129	1.63E+02	8.09E-01	4.96E-03
Nb-94	6.45E+00	9.91E-04	1.54E-04
Ni-59	1.91E+05	3.35E+00	1.75E-05
Ni-63	6.87E+09	4.23E+00	6.15E-10
Np-237	2.47E+01	7.23E-01	2.93E-02
Pu-238	1.80E+05	3.33E+03	1.85E-02
Pu-239	4.45E+02	4.20E+01	9.43E-02
Pu-240	5.73E+02	7.74E+01	1.35E-01
Pu-241	1.05E+05	1.55E+03	1.48E-02
Pu-242	4.28E+02	1.56E-01	3.64E-04
Se-79	1.05E+04	1.99E+00	1.89E-04
Sm-151	7.50E+10	9.29E-04	1.24E-14
Sn-126	5.11E+00	2.65E+00	5.19E-01
Sr-90	1.66E+15	1.24E+05	7.47E-11
Tc-99	1.09E+03	9.82E+01	8.98E-02
Th-232	3.46E+00	3.62E-03	1.05E-03
U-232	5.00E+05	9.46E+00	1.89E-05
U-233	4.49E+01	1.46E+01	3.25E-01
U-234	6.33E+01	6.53E+00	1.03E-01
U-235	3.66E+01	7.91E-02	2.16E-03
U-236	1.18E+03	1.85E-01	1.57E-04
U-238	3.16E+02	3.61E-01	1.14E-03
		Sum-of-Fractions	1.49E+00

7.5.5 Impact of Cover and Vault Degradation Beyond 10,000 Years

The fractional flux of I-129 at the water table at 10,000 years is 1.29E-07 mole/yr/mole and rising as shown in Table A-11 and Figure 7-16. To capture the peak of the flux transient, assuming hydrologic conditions at 10,000 years persist indefinitely, the simulation run time was extended to 70,000 years as shown in Figure 7-17 and discussed in Section 7.5.2. Additional simulations were performed considering continued degradation of the cover system, vault, and Saltstone contents beyond 10,000 years, with and without consideration of large-scale cracks in Saltstone due to differential settlement and earthquakes. Table 7-11 summarizes the assumed changes in hydraulic conductivities and infiltration between 10,000 and 100,000 years for these sensitivity runs.

From 10,000 to about 12,000 years, the gravel drainage layer overlying the vault roof is predicted to completely silt up with fines (Phifer 2004b), producing a significantly lower hydraulic conductivity. The lower hydraulic conductivity estimate is conservatively assumed to apply over the entire 10,000 to 25,000 year period in model simulations. Compared to the 5600 to 10,000 year period, the horizontal conductivity for this layer and time period abruptly decreases approximately 2.5 orders of magnitude, as indicated by Tables A-4 and 7-11. The change drastically reduces the ability of the layer to drain water off the top of the vault. Without macroscopic cracks in Saltstone, water ponds over the vault roof from 10,000 to 50,000 years in PORFLOW flow simulations. The increased hydraulic head gradient driving flow through Saltstone, coupled with moderately increased Saltstone and concrete conductivities compared to earlier times, produces a higher fractional flux shown in Figure 7-18 (No Crack curve) due to post-10,000 year degradation. Flux peaks occur shortly after 10,000 and 25,000 years in response to step changes in the modeled properties for Saltstone and concrete.

However, under ponded water or positive pressure conditions, large-scale cracks are expected to preferentially transmit water compared to the surrounding matrix, as discussed in section A-4. The additional effect of cracks on flow and water table flux was considered in a second sensitivity run. The physical cracks are predicted to occur at a 30 ft spacing within the plane of the 2D PORFLOW vadose zone model, which is a typical cross-section of the long axis of the vault. To approximately estimate the impact of transverse physical cracks, three longitudinal cracks at a nominal 30 ft spacing were placed in the half-width 2D model as surrogates (Figure 7-19), and assigned the properties of the vertical drain. Each crack was assigned to one column of grids with a width of 2 feet and given a porosity of 0.08 to represent the flow properties of a crack with a width of 2 inches. The presence of cracks in the model prevents water from ponding on the vault roof, but provides sudden pathways for water to infiltrate the core of the Saltstone waste. The resulting flux transient for I-129 is shown in Figure 7-18 (Crack curve). A very sharp peak in flux is observed immediately following 10,000 years, when the cracks suddenly become active in the simulations. The flux is diffusion-limited, and stabilizes to a much lower value after I-129 is leached from Saltstone near the crack faces. A second peak occurs at 25,000 years in response to increased Saltstone conductivity, similar to the no-crack sensitivity run. At 50,000 years, the conductivity of Saltstone is assumed to increase by 2 orders of magnitude, and the remaining inventory flushes from the vault by advection.

To a large extent, the abrupt changes in flux observed in the simulations including cracks are an artifact of simulating transport using a sequence of steady-state flow fields. In reality, the flow conditions would change gradually over time, and the flux transient would be much smoother than depicted in Figure 7-18. In particular, flux peaks are expected to be lower in peak magnitude, but broader in duration.

This study demonstrates the importance of the drainage layer at the top of the vault. The time over which the layer continues to function could be increased by making the layer thicker.

Table 7-11. Material Properties and Infiltration Beyond 10,000 Years.

Hydraulic Conductivity and Infiltration (cm/yr)	TI09 10,000 to 25,000 years	TI10 25,000 to 50,000 years	TI11 50,000 to 100,000 years
Horizontal conductivity			
Native and backfilled soil	3.15E+03	3.15E+03	3.15E+03
Drain, bottom	1.77E+06	3.15E+03	3.15E+03
Drain, vertical	3.15E+06	1.06E+06	1.81E+04
Drain, top	3.15E+03	3.15E+03	3.15E+03
Concrete	9.46E-02	3.15E-01	3.15E+01
Saltstone	9.46E-02	3.15E-01	3.15E+01
Vertical conductivity			
Drain, bottom	7.16E+03	3.15E+03	3.15E+03
Drain, top	3.15E+03	3.15E+03	3.15E+03
Infiltration	35.81	35.81	40.93

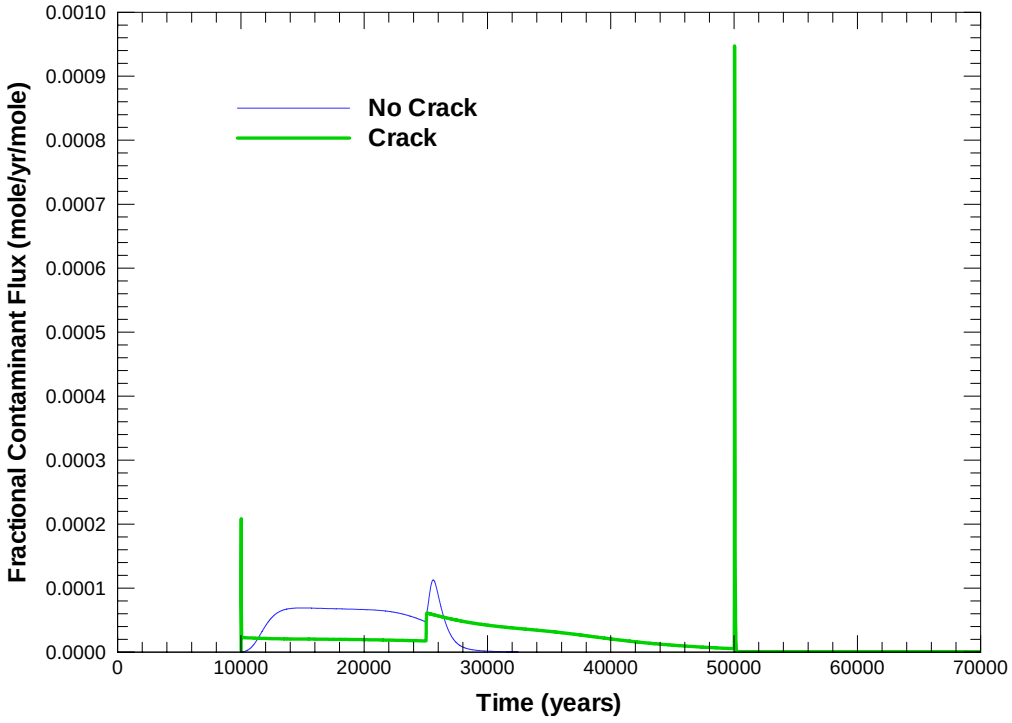

Figure 7-18. Instantaneous I-129 Fractional Contaminant Flux to the Water Table (10,000 to 70,000 yrs) Assuming Cover and Vault Degradation, With and Without Cracks.

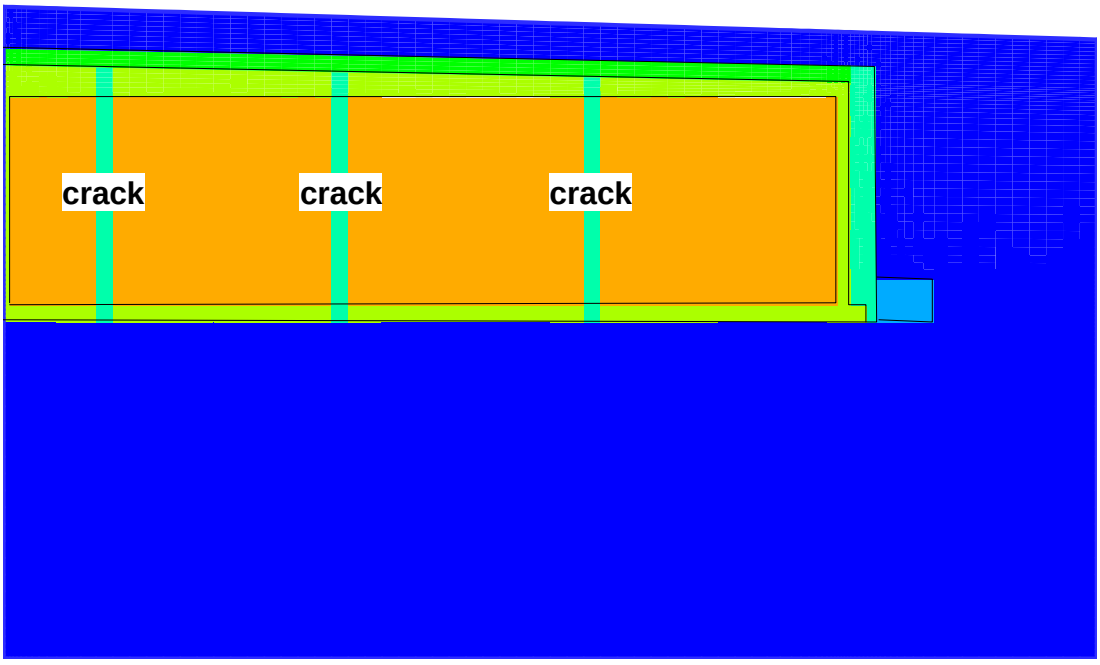

Figure 7-19. Surrogate Longitudinal Cracks in Two-Dimensional PORFLOW Model Representing Transverse Physical Cracks.

7.6 Uncertainty

The projected impacts from Saltstone disposal are very low. The disposal limits presented in Table 7-1 for those pathways involving protection of public health and the environment (i.e., groundwater, air, and all-pathways) are very large in comparison with the projected Vault 4 inventory shown in Table 7-4. The sum-of-fractions for the groundwater pathway is 4.6E-08, the sum-of-fractions for the atmospheric pathway is 5.2E-07, and that for all pathways is 2.4E-07.

In the 1992 Saltstone PA (MMES 1992), analyses of the sensitivity of model results to parameter changes and of uncertainty were performed for the groundwater pathway. These analyses investigated the fluxes to the water table from intact and degraded vaults. The most sensitive parameters for intact vaults were: 1) the saturated hydraulic conductivity of Saltstone, 2) the diffusivity of nitrate in the Saltstone, 3) the saturated hydraulic conductivity of concrete; and 4) the diffusivity of nitrate in the concrete. For degraded vaults, the sensitivity analysis considered depth of perched water on top of the vaults, crack spacing, crack aperture, and distribution coefficient, K_d. A sensitivity analysis for the groundwater flow and transport model used in the PA was also conducted. The most sensitive parameter was the saturated hydraulic conductivity of the hydrologic units considered in the model. Latin Hypercube Sampling techniques were applied to the parameter distributions studied to estimate uncertainty in the nitrate concentration in the groundwater at the 100-meter point of assessment.

Although a quantitative analysis of uncertainty has not been done for this SA, it is clear from the very low sums-of-fractions that the calculated disposal limits would have to decrease by several orders of magnitude for the impacts from Saltstone disposal in the SDF to approach an appreciable fraction of one of the performance objectives. For example, in the all pathways analysis, the sum-of-fractions of the limits is 2.4×10^{-7}. If each of these disposal limits decreased by four orders of magnitude (i.e., by a factor of 10,000), the sum-of-fractions would still be only 0.0024, which would represent a dose of only 0.06 mrem/year.

In evaluating uncertainties in doses to future members of the public, projected over long time-frames, the most important consideration may be the definitions of the exposure scenarios. In this SA, as in the PA, it was assumed that a future member of the public would have access to the land within 100 meters of the disposed waste. However, the SRS Land Use Plan (DOE 2000) requires Federal ownership and control of the site well beyond 100 years after closure of SDF. DOE 5400.5 precludes release of the area unless the radiological hazard meets the requirements of DOE 5400.5 Chapter 4, which requires virtual perpetual DOE control. No unrestricted use of the land or groundwater will be permitted for the central portion of the site, which includes SDF. Thus, a member of the public could not contact the groundwater in the vicinity of SDF. Due to the restrictions in the SRS Land Use Plan, a member of the public could only contact potentially contaminated surface water off-site, approximately six miles from the facility at the mouth of Upper Three Runs. Furthermore, concentrations of SDF radionuclides in that surface water will be much less than that assessed in the SA at 100 meters from SDF due to decay and other natural processes.

7.7 As Low As Reasonably Achievable (ALARA)

One of the DOE 435.1 PA requirements is that Performance assessments shall include a demonstration that projected releases of radionuclides to the environment shall be maintained as low as reasonably achievable (ALARA). The disposal limits presented in Table 7-1 for those pathways involving release of radionuclides to the environment (i.e., groundwater, air, and radon) are very large in comparison with the projected vault 4 inventory shown in Table 7-4. The sum-of-fractions for each of the release pathways represents the fraction of the pathway limit that

would result from disposal of the estimated inventory. The sum-of-fractions for the groundwater pathway is 4.6E-08, the sum-of-fractions for the atmospheric pathway is 5.2E-07, and that for the radon pathway is 1.1E-30. The solidified Saltstone waste form and the SDF vault design work together to reduce releases from SDF to the environment to very low levels, as demonstrated by the very low sums-of-fractions.

8.0 CONCLUSIONS

8.1 Conclusions

This SA has analyzed the long-term performance of Saltstone Vault 4 in terms of releases and exposures by way of a number of pathways. Disposal limits have been determined for each radionuclide analyzed using the DOE performance measures as stated in DOE 435.1 (USDOE 1999).

This study shows that the operation and closure of Vault 4 will result in groundwater concentrations that do not exceed the Safe Drinking Water Act Maximum Contaminant Levels. Because these concentration limits are lower and measured much closer to the disposal unit than the performance objective for the Composite Analysis, the conclusions of the Composite Analysis will not be altered by the results of this SA.

The disposal limits have been compared with the estimated final inventory of Vault 4. The sum-of-fractions of the disposal limits is less than one, which indicates that none of the DOE performance measures will be exceeded. This SA has not altered the conceptual model (i.e., migration of radionuclides from the Saltstone waste form and Vault 4 to the environment via the processes of diffusion and advection) of the Saltstone PA (MMES 1992) nor has it altered the conclusions of the PA (i.e., disposal of the proposed waste in the SDF will meet DOE performance measures). Thus a PA revision is not required and this SA serves to update the disposal limits for Vault 4.

Doses have been calculated for the estimated final inventory of Vault 4. These have been compared to the pertinent NRC performance objectives. The conclusion is that the operation and closure of Vault 4 will comply with the performance objectives of 10 CFR 61 for protection of the general population and the inadvertent intruder.

THIS PAGE INTENTIONALLY LEFT BLANK

9.0 LIST OF PREPARERS

CHANDLER, TIMOTHY E., WSRC/Waste Solidification

B.S. Hazardous Materials Management - University of Maryland

Experience: Mr. Chandler has over 25 years of experience in the Naval Nuclear, Commercial Nuclear, and USDOE High-level Waste fields. Mr. Chandler has 12 years of experience at the Savannah River Site, directly involved in the storage, treatment, and disposal of both high-level and low-level radioactive waste. He serves as the Saltstone Facility representative on the Special Analysis team.

Contributions: Technical reviewer for the WSRC Saltstone Facility Performance Assessment team.

COOK, JAMES R., WSRC/SRNL, Geology, Geochemistry

M.S. Geochemistry - State University of New York at Binghamton

B.S. Geology - University of Arizona

Experience: Mr. Cook has 25 years of experience at the Savannah River Site, 23 of which have been in various aspects of low-level waste research. Research topics have included site selection, site characterization, site closure, and performance assessment. Mr. Cook served on the revision team for Chapter 3 of DOE Order 5820.2A and was a member of the Performance Assessment Task Team. He serves as the technical lead on the Special Analysis team.

Contributions: WSRC Technical Leader Performance Assessment team, air pathway analysis, intruder analysis.

FLACH, GREGORY P., WSRC/SRNL, Hydrology

Ph.D., Mechanical Engineering - North Carolina State University

Master of Mechanical Engineering - North Carolina State University

B.S., Mechanical Engineering - University of Kentucky

Experience: Dr. Flach has 16 years of experience at SRNL in applying mathematical analysis and numerical simulation to nuclear and environmental engineering topics, including multiphase multicomponent reactor thermal-hydraulics, groundwater flow and contaminant transport, and high-level waste processing. He has contributed to E-Area and Z-Area performance assessment and high level waste tank closures for more than 10 years, primarily through groundwater pathway analysis.

Contributions: Crack analysis.

GOLDSTON, W. T. (SONNY), BNFL, Regulatory Issues

B.S. Chemical Engineering, University of South Carolina

Masters in Business Administration, University of South Carolina.

Experience: Mr. Goldston has 30 years of experience with both the Department of Energy and Westinghouse. He has worked with LLW, HLW and TRU issues with both organizations. He has developed and implemented strategies for Public Involvement concerning Solid Waste activities and Environmental Management Integration.

Contributions: Regulatory issues interface

HIERGESELL, ROBERT A., WSRC/SRNL, Groundwater Hydrology

M.S. Hydrogeology - Univ. of Nebraska-Lincoln

B.S. Geology - Virginia Polytechnic Institute and State University

Mr. Hiergesell has over 30 years experience in a wide variety of subsurface hydrology projects, with primary emphasis on supporting the SRS low-level radioactive waste disposal and environmental remediation programs. Specific assignments have related to analysis of subsurface hydrology using analytical and numerical models, characterization of aquifer and vadose zone parameters through field-scale testing and groundwater monitoring. Recent assignments have focused on several aspects of implementing DOE Order 435.1, Radioactive Waste Management, with respect to the low-level waste facilities at SRS.

Contributions: Atmospheric release modeling

JANNIK, G. TIMOTHY, WSRC/SRNL, Environmental Dosimetry, Environmental Health Physics

M.S. Health Physics – Georgia Institute of Technology

B.S. Mechanical Engineering – Villanova University

Experience: Mr. Jannik is the SRNL subject matter expert in the fields of environmental dosimetry, human health risk analysis, radiological source term evaluations, and environmental pathway analysis. He has over 25 years of experience in fields of environmental dose/risk assessments and effluent and environmental monitoring. He serves as the technical lead for the SRNL Environmental Dosimetry Group and is the technical advisor to the WSRC Environmental Monitoring Section.

Contributions: Assessment of Potential Groundwater Doses

LEE, PATRICIA l., WSRC/SRNL, Health Physics, Environmental Dosimetry

Ph.D. Nuclear Engineering/Health Physics – Georgia Institute of Technology

M.S. Physics - Clark Atlanta University

B.S. Physics – Lincoln University

Experience: Dr. Lee has 13 years of experience in Environmental Health Physics with expertise in dose and risk assessment for radiological and chemical exposures. Her 5 years of experience at the Savannah River Site include modeling doses to offsite individuals from accidents or routine operations at SRS; performing dose and risk assessments in support of facility decommissioning, performance assessments and environmental remediation; and providing technical support for compliance with state and federal regulations.

Contributions: Intruder analysis.

PEREGOY, WILLIAM l., BSRI, Civil/Structural

M.S. Structural Engineering, University of California, Berkeley

B.S. Civil Engineering, University of California, Berkeley

Experience: Mr. Peregoy has 29 years experience in the nuclear industry, including 18 years at a commercial nuclear plant and 11 years at USDOE complex sites including Rocky Flats and SRS. He served as lead engineer for the Seismic Hazard Study at Rocky Flats and has worked on a wide variety of structural issues for both sites, primarily in the area of earthquake engineering. Mr. Peregoy has performed complex structural analyses in support of safe storage of nuclear materials.

Contributions: Support Performance Assessment by probabilistic analysis of structural behavior of disposal units over very long time periods.

PHIFER, MARK A., WSRC/SRNL, Civil Engineering (Environmental and Geotechnical)

M.S. Civil Engineering (Environmental and Geotechnical) – University of Tennessee, 1993

B.S. Civil Engineering – Tennessee Tech, 1981

Professional South Carolina Registered Professional Engineer (No. 12310)

Experience: Mr. Phifer has 21 years of environmental and geotechnical experience at the Savannah River Site. The first 10 years included environmental regulatory compliance, civil/environmental design, project engineering (closure of a mixed waste landfill and basins covering a total of 80 acres), and management (environmental remediation technology). The subsequent 11 years have been at the Savannah River National Laboratory developing, deploying, and evaluating waste site closure, groundwater remediation, and radioactive waste disposal technologies. These technologies include horizontal and vertical barrier systems, diffusion barriers, closure caps (including their degradation), waste subsidence, low-level radioactive waste disposal facilities, Saltstone, permeable reactive barriers, GeoSiphon / GeoFlow groundwater treatment systems, sulfate reduction remediation, reductive dechlorination, and vadose zone and aquifer characterization and testing.

Contributions: Closure cap configuration and degradation, infiltration estimates, and Performance Assessment team member.

SIMPKINS, ALI A., WSRC/SRNL, Dose Modeling

M.S. Nuclear Engineering, University of Missouri-Rolla

B.S. Nuclear Engineering, University of Missouri-Rolla

Experience: Ms. Simpkins has 13 years of experience at the Savannah River Site in various aspects of Environmental Dose Modeling. Research topics have included atmospheric dose modeling, code development, environmental impact statements, uncertainty/sensitivity analysis, and risk assessments in support of decommissioning of facilities. Ms. Simpkins performed atmospheric dose modeling for the Performance Assessment.

Contributions: atmospheric dose modeling

VARGO, MICHAEL S., WSRC/SRNL, Schedule Management

MBA Business - University Of Baltimore

B.S. Business – University Of Baltimore

Certification Primavera P3 Training

Certification Configuration Management – Arizona State

Experience: Mr. Vargo has 15 years of experience at the Savannah River Site of which 10 years with Savannah River National Lab (SRNL) have been to work mainly with all aspects of SRNL Program Controls Management (PCM) such as; program planning, activities scheduling, budget formulation, program cost controls (labor, materials, spending), other department's financial liaison and participating in Plan of the Week (POW) meetings.

Contribution: Saltstone Vault 4 Performance Assessment role as a team member has been to work closely with the program leads with maintaining the P3 status of activities on the Saltstone Vault 4 Special Analysis schedule and to verify the program budget and weekly spending.

WILHITE, ELMER L., WSRC/SRNL, Chemistry

M.S. Inorganic Chemistry – Washington University, St. Louis, MO

B.S. Chemistry – University of Missouri

Experience: Mr. Wilhite has 35 years experience at the Savannah River Site. His assignments include environmental research, high-level and low-level waste research, and supervision of environmental monitoring and analytical chemistry groups. He served as a consultant to DOE Headquarters on low-level waste management for 18 years. He was the chairman of the former DOE Peer Review Panel and the technical lead for DOE for the radiological assessment section of the response to the DNFSB recommendation 94-2.

Contribution: PA team member; Integration and Interpretation

YOUNG, KAREN E., Exploration Resources, Principal Scientist/Project Manager

B.S. Environmental Resource Management, The Pennsylvania State University

Experience: Ms. Young has over 14 years of experience as an environmental scientist with expertise in regulatory compliance. She is an expert in Resource Conservation and Recovery Act (RCRA) compliance and has assisted the U.S. Environmental Protection Agency (USEPA) in developing RCRA regulations. Other regulatory experience includes CERCLA, NEPA, and compliance with USDOE Orders.

Contributions: Document preparation.

YU, ANDREW D., ALARA Environmental Analysis, Inc., Partner

Ph.D. Chemical Engineering - University of Wisconsin

B.S. Chemical Engineering - National Taiwan University

Experience: Dr. Yu has 28 years of experience in subsurface flow and transport modeling. He worked 12 years in simulating enhanced oil recovery processes in the oil industry, 9 years in groundwater modeling with Savannah River Technology Center, and 7 years as a consultant with Applied Geotech, Inc. His current interests are in performance assessment, groundwater modeling and waste disposal technology.

Contributions: Performed subsurface flow and transport modeling.

10.0 REFERENCES

Beres, D.A. 1990. *The Clean Air Act Assessment package-1988 (CAP-88) A dose and Risk Assessment Methodology for Radionuclide Emissions to Air*. U.S. Environmental Protection Agency Contract No. 68-D9-0170, Washington, DC.

CFR 2004. *Code of Federal Regulation 10 CFR 61, Licensing Requirements for Land Disposal of Radioactive Waste*, US Nuclear Regulatory Commission, 1-1-04 Edition.

Cook, J. R. 1983. *Estimation of High Water Table Levels at the Saltstone Disposal Site (Z-Area)*, DPST-83-607, Savannah River Laboratory, E.I. du Pont de Nemours & Company, Inc., Aiken, SC.

Cook, J. R. 2000. *Special Analysis: Updated Analysis of the Effect of Wood Products on Trench Disposal Limits at the E-Area Low-Level Waste Facility*, WSRC-RP-2000-00523, Revision 0, Westinghouse Savannah River Company, Aiken, South Carolina.

Cook, J. R. 2002. *Special Analysis: Effect of New Plutonium Chemistry on SRS Trench Disposal Limits*, WSRC-TR-2002-00154, Revision 0, Westinghouse Savannah River Company, Aiken, South Carolina.

Cook, J. R., and S. K. Salvo 1992. *Final Vegetative Cover for Closed Waste Sites.* WSRC-RP-92-1361. Westinghouse Savannah River Company, Savannah River Site, Aiken, SC.

Cook, J. R., Kocher, D. C. McDowell-Boyer, L., and Wilhite, E. L. 2002. *Special Analysis: Reevaluation of the Inadvertent Intruder, Groundwater, Air and Radon Analyses for the Saltstone Disposal Facility,* Westinghouse Savannah River Company, Aiken, South Carolina.

Cook, J. R. and Kaplan, D. I. 2003. *Special Analysis: Revised ^{14}C Disposal Limits for the Saltstone Disposal Facility*. WSRC-TR-2003-00417, Revision 0. Westinghouse Savannah River Company, Aiken, South Carolina.

Cook, J. R., and Wilhite, E.L. 2004, *Special Analysis: Radionuclide Screening Analysis for E Area*, WSRC-TR-2004-00294, Revision 0, Westinghouse Savannah River Company, Aiken, South Carolina.

Crapse, K. P., Chandler, T. E. and Cook, J. R. 2004. *FY 2004 Annual Review – Saltstone Disposal Facility (Z-Area) (Covering the Performance Period FY 1999-2004)*. Westinghouse Savannah River Company, Savannah River Site, Aiken, SC.

Crapse, K. P., and Cook, J. R. 2004. *Atmospheric Pathway Screening Analysis for Saltstone Disposal Facility Vault 4*, WSRC-TR-2004-00555, Westinghouse Savannah River Company, Aiken, South Carolina.

d'Entremont, P.D.2005. *Radionuclide Concentrations in Saltstone*, CBU-PIT-2005-00013, Rev. 2, February 24, 2005.

Eckerman, K.F., Wolbarst, A.B., and Richardson, A.C.B. 1988. *Limiting Values of Radionuclide Intake and Air Concentration and Dose Conversion Factors for Inhalation, Submersion*, and Ingestion Federal Guidance Report No. 11, USEPA 520/1-88-020, U.S. Environmental Protection Agency, Washington, DC.

Flach, G. P. 2004. *Groundwater Flow Model of the General Separations Area Using PORFLOW*, WSRC-TR-2004-00106, Revision 0, Westinghouse Savannah River Company, Aiken, South Carolina.

Jannik, G. T. 2005. *Potential Radiological Doses from Groundwater Contaminated by the Saltstone Disposal Facility*. WSRC-TR-2005-00084. Westinghouse Savannah River Company, Aiken, South Carolina. February 2005.

Kaplan, D. I., 2004, *Recommended Geochemical Input Values for the Special Analysis of the Slit/Engineered Trenches and Intermediate Level Vault*, WSRC-RP-2004-00267, Revision 0, Westinghouse Savannah River Company, Aiken, South Carolina.

Koffman, L. D. 2004. *An Automated Inadvertent Intruder Analysis Application*, WSRC-TR-2004-00293, Revision 0, Westinghouse Savannah River Company, Aiken, South Carolina.

Langton, C. A. 1986. *Slag Substituted Concrete for Saltstone Vault Construction.* DPST-86-830. E. I. du Pont de Nemours & Company, Inc., Savannah River Laboratory, Aiken, SC.

Lee, Patricia L. 2004. *Inadvertent Intruder Analysis Input for Radiological Performance Assessments*. WSRC-TR-2004-00295. Westinghouse Savannah River Company, Savannah River Site, Aiken, SC.

MMES 1992. *Radiological Performance Assessment for the Z-Area Saltstone Disposal Facility*, WSRC-RP-92-1360, Martin Marietta Energy Systems, Inc., EG&G Idaho, Westinghouse Hanford Company and Westinghouse Savannah River Company, 1992, Westinghouse Savannah River Company, Aiken, South Carolina..

NCRP 1996. National Council on Radiation Protection and Measurements, *Screening Models for Releases of Radionuclides to Atmosphere, Surface Water, and Ground*, NCRP Report No. 123, Volumes I and II, January, 1996.

Peregoy, W. 2003. *Saltstone Vault Structural Degradation Prediction*, T-CLC-Z-00006, July 2003. Westinghouse Savannah River Company, Aiken, South Carolina.

Phifer, Mark A. and Nelson, Eric A. 2003. *Saltstone Disposal Facility Closure Cap Configuration and Degradation Base Case: Institutional Control to Pine Forest*. WSRC-TR-2003-00436. Westinghouse Savannah River Company, Savannah River Site, Aiken, SC.

Phifer, M. A. 2004. Interoffice Memorandum to J. R. Cook, et al, *Vault 4 Infiltration and Hydraulic Conductivity Input for the Vadose Zone PORFLOW Modeling*, SRT-EST-2004-00068, February 26, 2004. Westinghouse Savannah River Company, Aiken, South Carolina.

Phifer, M. A. 2004b. Interoffice Memorandum to J. R. Cook, et al, *Vault #4 Closure Cap Estimated Infiltration for Years 50,000 to 1,000,000*, SRT-EST-2004-00103, December 17, 2004. Westinghouse Savannah River Company, Aiken, South Carolina.

Simpkins, A. A. 2004. *Modeling of Releases from the Saltstone Disposal Facility for NESHAP Compliance Considering an Area Source,* SRNL-EST-2004-00071, Westinghouse Savannah River Company, Aiken, South Carolina. December 2, 2004.

Tuli, J. K. 2000. *Nuclear Wallet Cards*, sixth edition. Brookhaven National Laboratory, Upton, NY.

U.S. Congress 2004. *Ronald W. Reagan National Defense Authorization Act for FY 2005,* Public Law108-375, Section 3116, October 28, 2004.

USDOE 1993, *Radiation Protection of the Public and the Environment*, U.S. Department of Energy, Washington, DC.

USDOE 1999. "Low-Level Waste Requirements," Chapter IV in *Radioactive Waste Management Manual,* USDOE Manual 435.1-1. U.S Department of Energy, Washington, DC.

USDOE 2000, *SRS Long Range Comprehensive Plan*, December 2000.

USEPA 1992. 40 CFR 268. Code of Federal Regulations, Title 40, *Protection of the Environment*, Part 268 "Land Disposal Restrictions". U. S. Environmental Protection Agency, Washington DC. May 8, 1992.

USEPA 1994a. *The Hydrologic Evaluation of Landfill Performance (HELP) Model User's Guide for Version 3*, EPA/600/R-94/168a, Office of Research and Development, United States Environmental Protection Agency, Washington, DC. September 1994.

USEPA 1994b. *The Hydrologic Evaluation of Landfill Performance (HELP) Engineering Documentation for Version 3*, EPA/600/R-94/168b, Office of Research and Development, United States Environmental Protection Agency, Washington, DC. September 1994.

USEPA 2004. *National Primary Drinking Water Regulations*, 40 CFR Part 141, 8-27-04 Edition.

USNRC 1982. *Final Environmental Impact Statement on 10 CFR Part 61 Licensing Requirements for Land Disposal of Radioactive Waste*, NUREG-0945, November 1982.

USNRC 2000. *A Performance Assessment Methodology for Low-Level Radioactive Waste Disposal Facilities: Recommendations of NRC's Performance Assessment Working Group, NUREG-1573*, June 2000.

USNRC 2002. *Decommissioning Criteria for the West Valley Demonstration Project (M-32) at the West Valley Site; Final Policy Statement*, February 2002.

Weber, A. H. 1998. *Tornado, Maximum Wind Gust and Extreme Rainfall Event Recurrence Frequencies at the Savannah River Site*, WSRC-TR-98-00329. Westinghouse Savannah River Company, Aiken SC.

Wilhite, E. L. 1985. *Estimated Composition of Decontaminated Salt Solution Feed to Saltstone.* E. I. du Pont de Nemours & Co., Inc., Savannah River Laboratory, Aiken, SC.

Wilhite, E. L. 1986. *Evaluation of Potential Disposal Alternatives for Low-Level Salt Solution.* Internal report DPST-86-698. E. I. du Pont de Nemours & Company, Inc., Savannah River Laboratory, Aiken, SC.

Wolf, H. C. 1984. Technical Data Summary: *Decontaminated Salt Disposal as Saltstone in an Engineered Landfill,* DPSTD-82-65, Rev. 2. E. I. du Pont de Nemours & Company, Inc., Savannah River Laboratory, Aiken, SC.

WSRC 1992. *Safety Analysis Report - 200-Z Area, Savannah River Site, Saltstone Disposal Facility,* WSRC-SA-3, draft in review by Department of Energy. Savannah River Laboratory, Westinghouse Savannah River Company, P.O. Box 616, Aiken, South Carolina 29802.

THIS PAGE INTENTIONALLY LEFT BLANK

APPENDIX A
ADDITIONAL INFORMATION ON GROUNDWATER ANALYSIS

THIS PAGE INTENTIONALLY LEFT BLANK

A.1 INTRODUCTION

Saltstone Vault No. 4 is an existing disposal unit at the SDF. It is approximately 200 feet wide, 600 feet long and 25 feet tall. Grouted wastes have been poured into this unit for permanent disposal. A radiological PA is required to calculate the inventory limit for specific contaminant species in all credible pathways. This study simulates fluid flow and contaminant transport in the unsaturated zone and the saturated zone that will be used to calculate the inventory limits for the groundwater pathway. A complete list of the 46 contaminants modeled with respective decay daughters is shown in Table A-1. The radionuclides modeled were selected from Cook and Wilhite, 2004.

In 1992, a PA was conducted for Saltstone Vault No. 1 (MMES 1992). Vault No. 1 is approximately 100 feet wide, 600 feet long and 25 feet tall. In the original PA, an unsaturated-zone numerical simulation was performed for the intact scenario only, for which the Saltstone vault and closure were assumed to have the properties of the new facility for the entire period of analysis.

In order to facilitate the Z-Area (i.e., Saltstone) waste management programs at the SRS, it is necessary to revise the Saltstone groundwater analysis because of the following reasons:

- Vaults of different designs have been built or proposed.
- The closure concept has been improved. The impact of these design changes on the PA needs to be assessed.
- The time of compliance has been changed to 1,000 years. Because the SDF conceptual design is based on controlled contaminant release, a change in the time of compliance will have a significant impact on inventory limits.
- The PORFLOW code and modeling methodology have been improved in the last decade (ACRI 2004).
- The capacity, speed and versatility of computers have improved. This allows construction of more sophisticated models and implementation of modeling work in a shorter time frame.
- PA results are used to demonstrate compliance and are an important tool in development of future waste management strategies.

The PORFLOW computer program employed in this analysis has been used in all other SRS performance assessments. The earlier analyses were accepted after extensive external peer review during the approval process.

The groundwater modeling work performed by ALARA Environmental Analysis, Inc. has incorporated the most recent available data and improved methodology. WSRC personnel have also performed a detailed design check prior to the production run process. This initial coordination on development of assumptions, input parameters, data to be used and continuous coordination throughout the process has proven to be a very successful strategy to conduct this type of complex modeling work.

Table A-1. List of Modeled Contaminants and Decay Daughters

NO3
Al-26
Am-243
Np-239
Pu-239
Pu5-239
Bi-210
Po-210
C-14
Cf-249
Cm-245
Pu-241
Pu5-241
Am-241
Np-237
Cl-36
Cm-245
Pu-241
Pu5-241
Am-241
Np-237
Cm-246
Cm-247
Am-243
Np-239
Pu-239
Pu5-239
Cm-248
Pu-244
Pu5-244
Cs-135
Cs-137
H-3
I-129
K-40
Mo-93
Nb-93m
Nb-94
Nb-95m
Nb-95
Ni-59
Np-237
Pd-107
*Pu-238
*Pu5-238
U-234
*Pu-239
*Pu5-239
U-235
*Pu-240
*Pu5-240
U-236
*Pu-241
*Pu5-241

Table A-1. List of Modeled Contaminants and Decay Daughters

Am-241
Np-237
***Pu-242**
***Pu5-242**
U-238
***Pu-244**
***Pu5-244**
Ra-226
Rb-87
Se-79
Sn-126
Sr-90
Tc-99
Th-228
Ra-224
Th-229
Ra-225
Ac-225
Th-230
Ra-226
Pb-210
Po-210
Th-232
Ra-228
Th-228
Ra-224
U-232
Th-228
Ra-224
U-233
Th-229
Ra-225
U-234
Th-230
Ra-226
Pb-210
Po-210
U-235
Pa-231
Ac-227
Th-227
Ra-223
U-236
U-238
Th-234
U-234
Zr-93
Nb-93m
Zr-95
Nb-95

* To indicate the plutonium oxidation states that were considered, Pu- represents the III,IV oxidation states and Pu5- represents the V,VI oxidation states

.

A.2 SALTSTONE VAULT NUMBER 4 UNSATURATED ZONE GROUNDWATER MODELING

A.2.1 Conceptual Model and Modeling Grid

The conceptual model describes the materials, layout, and dimensions of the SDF. Figure A-1 depicts the conceptual model used for the Vault No. 4. The Saltstone monolith is approximately 200×600×25 ft^3. Only half of a vault in the short dimension is modeled, taking advantage of symmetry. The top of the modeling domain is the bottom of the upper geosynthetic clay liner (GCL) layer. Infiltration through this layer as a function of time is calculated by the HELP code (USEPA 1994a, 1994b). The constant infiltration rate is used as a flow boundary condition at the top of the modeling domain. The bottom of the modeling domain is the water table. Capillary pressure at the water table is set to zero to simulate 100% water saturation. The vertical boundary through the center of the vault at the left side of the figure is modeled as a no-flow boundary due to symmetry. The right boundary is also assumed to be a no-flow boundary because it is sufficiently far away from the vault and the predominant contaminant transport mechanism is downward convection.

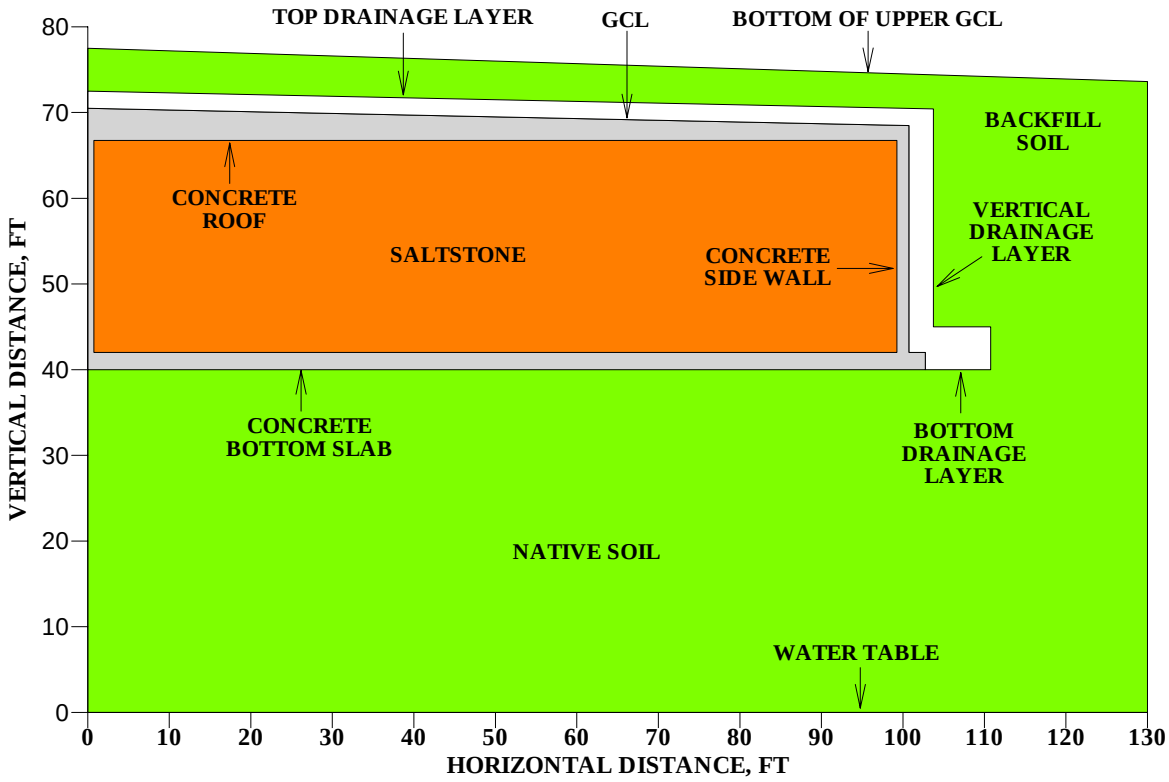

Figure A-1. Conceptual Model for the Saltstone Vault No. 4

The dimensions of the vault and lower portion of the closure are summarized in Table A-2. The "concrete" zone above the Saltstone pour level (at 66.75 ft) includes the top portion of the center and exterior walls and the concrete roof. The drainage layer is a gravel/sand mixture. It is used to reduce water perching above the vault. Test modeling results indicate that perching water can increase water flow rate through the vault, which results in a higher contaminant leaching rate.

The drainage layer is divided into three sections: top, vertical and bottom. The initial hydraulic conductivities in these sections are the same. However, these conductivities degrade at different rates (Phifer 2004) as will be described later. Because the backfill is largely soil excavated during vault construction, it is assumed that the backfill soil has the same properties as the native soil. There is a GCL above the vault roof. Since the conductivity of the Saltstone and the vault is less than or equal to the conductivity of the GCL (10^{-9} cm/sec), this GCL is ignored in the simulation.

Table A-2. Dimensions of Saltstone Vault No. 4

Component	Dimensions of Vertical Distances		
	From (ft)	To (ft)	Thickness (ft)
Native Soil	0.00	40.00	40.00
Bottom Concrete Slab	40.00	42.00	2.00
Saltstone	42.00	66.75	24.75
Concrete at Center[1]	66.75	70.50	3.75
Drainage Layer[2]	70.50	72.50	2.00
Drainage Layer at the Vault Base	40.00	45.00	5.00
Backfill above Drainage Layer[3]	72.50	77.50	5.00
	Dimensions of Horizontal Distances		
Center Slab[4]	0.00	0.75	0.75
Saltstone	0.75	99.25	98.50
Side Slab	99.25	100.75	1.50
Drainage Layer	100.75	103.75	3.00
Drainage Layer at the Vault Base	100.75	110.75	10.00

[1] Concrete includes tip of vault wall, concrete pour and concrete roof.

[2] Slope = 2.0%

[3] Slope = 3.0% at the upper boundary

[4] Actual center slab thickness = 1.50 ft.

The potential impact of cracks on the performance of Vault 4 is discussed in Section A.4. Over 10,000 years, the suction head is great enough that flow through cracks, whether through-wall or not, can be neglected.

The modeling grid used for PORFLOW simulation is shown in Figure A-2. Trapezoidal grid blocks are used for the concrete roof and the backfill to mimic the facility geometry.

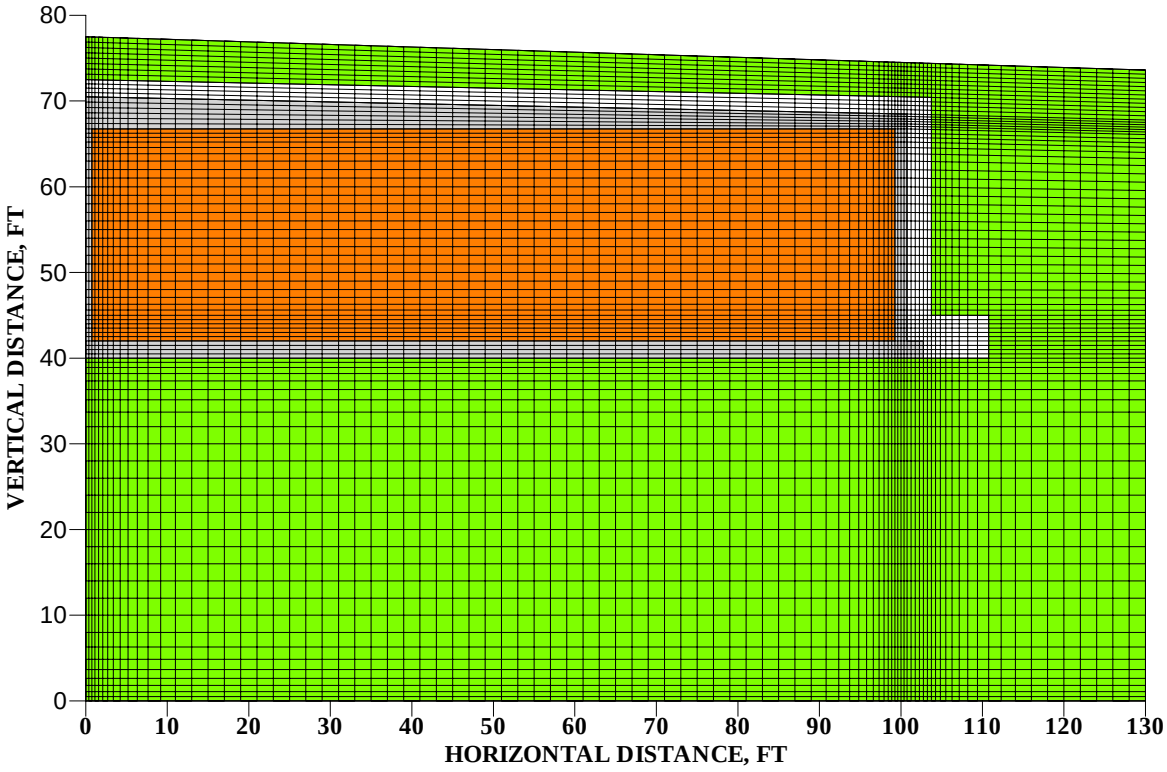

Figure A-2. Modeling Grid

A.2.2 Time of Compliance and Simulation Time Intervals

The DOE time of compliance is 1,000 years (Wilhite 2003). However, the total time used for groundwater modeling is extended to 10,000 years to assess the impact of a longer period of compliance. The eight time intervals (Phifer 2004) used for groundwater modeling are shown in Table A-3.

Table A-3. Simulation Time Intervals

INTERVAL	TIME (YEARS)		
TI01	0	to	100
TI02	100	to	300
TI03	300	to	550
TI04	550	to	1,000
TI05	1,000	to	1,800
TI06	1,800	to	3,400
TI07	3,400	to	5,600
TI08	5,600	to	10,000

A.2.3 Flow Modeling

A.2.3.1 Flow Properties

The fundamental concept of the SDF (wasteform and facility features) is controlled contaminant release. Due to the low hydraulic conductivity and low molecular diffusion in cementitious materials, contaminant leaching from the SDF is very slow. This makes transformation into Saltstone an effective method for liquid waste disposal. Among all the factors affecting the SDF performance, the most important factor is hydraulic conductivity. The saturated hydraulic conductivities of the engineered porous media (Saltstone, concrete and gravel drain layers) were measured by Core Lab as described in 1993 (Yu 1993). These intact values are used for the first 100 years of simulation under the column heading TI01 in Table A-4.

Table A-4. Saturated Hydraulic Conductivities (cm/sec)

	TI01	TI02	TI03	TI04	TI05	TI06	TI07	TI08
				Horizontal conductivity:				
Nati/Back	1.00E-04	1.00E-04	1.00E-04	1.00E-04	1.00E-04	1.00E-04	1.00E-04	1.00E-04
Drain Bot	1.00E-01	9.99E-02	9.97E-02	9.90E-02	9.71E-02	9.30E-02	8.63E-02	7.46E-02
Drain Ver	1.00E-01	1.00E-01	1.00E-01	1.00E-01	1.00E-01	1.00E-01	1.00E-01	1.00E-01
Drain Top	1.00E-01	9.99E-02	9.93E-02	9.75E-02	9.28E-02	8.25E-02	6.58E-02	3.66E-02
Concrete	1.00E-12	5.20E-12	1.29E-11	3.16E-11	7.64E-11	1.98E-10	4.19E-10	1.00E-09
Saltstone	1.00E-11	3.00E-11	5.50E-11	1.00E-10	1.80E-10	3.40E-10	5.60E-10	1.00E-09
				Vertical conductivity:				
Drain Bot	9.52E-02	6.45E-02	2.70E-02	8.94E-03	3.34E-03	1.41E-03	7.25E-04	3.93E-04
Drain Top	8.89E-02	4.21E-02	1.29E-02	3.78E-03	1.36E-03	5.69E-04	2.91E-04	1.57E-04

In this SA, it is assumed the hydraulic conductivities of Saltstone and concrete will increase as time proceeds. As a result, water percolation will gradually increase through the vault. It is also assumed that the conductivities of the top and bottom drains will decrease with time due to plugging in the lower part of these drains resulting in the engineered drains becoming less effective in shedding perched water above the concrete roof. It is assumed that the effective

vertical hydraulic conductivities decrease more rapidly than the horizontal conductivities. All of the saturated hydraulic conductivities used for the simulation are summarized in Table A-4. The data, equations, and rationale used to obtain these data are discussed below.

NATIVE AND BACKFILL SOIL

The saturated hydraulic conductivity of native and backfill soil is revised from 10^{-5} to 10^{-4} cm/sec to be consistent with the generally accepted value for the SRS General Separations Area. Since soil is a geological material, its conductivity is assumed to be constant.

SALTSTONE AND CONCRETE

In the time interval of 0 and 100 years, the hydraulic conductivities of Saltstone and concrete are 10^{-11} and 10^{-12} cm/sec, respectively. Both conductivities degrade to 10^{-9} cm/sec at 10,000 years. The degradation rate for concrete is faster because it is exposed to the environment and is more vulnerable to be attacked by sulfate, chloride and other chemical reactions. The decay rate is calculated by a log-log correlation:

$$\log_{10}(k/k_o) = \alpha \log_{10}(t/t_o) \quad \text{(A-1)}$$

where k = conductivity at time t, cm/sec

k_o = conductivity at t_o = 100 years, cm/sec

α = degradation rate constant (α =1.0 for Saltstone and 1.5 for concrete)

Calculated k values at the end of each time interval are used as PORFLOW input data to generate the steady-state flow field for the time interval. They are summarized in Table A-4.

GRAVEL DRAIN LAYERS

The initial hydraulic conductivity of the gravel drain layers is 10^{-1} cm/sec. As time goes on, soil particles carried by the percolation water will plug the drains from the bottom. The plugged-zone thickness will increase with increasing time. Calculated thickness (Phifer 2004) is shown in Table A-5.

Table A-5. Plugged-Zone Thickness as a Function of Time

TIME (YEARS)	PLUGGED-ZONE THICKNESS, FT
0	0
100	0.0005
300	0.005
550	0.022
1,000	0.08
1,800	0.21
3,400	0.49
5,600	0.88
10,000	1.66

Plugging results in reduction in effective hydraulic conductivity. Freeze and Cherry (Freeze 1979) suggested equations to calculate horizontal and vertical effective conductivities:

$$k_{h,eff} = [(H-h)k_g + hk_s]/H \quad \text{(A-2)}$$

$$k_{v,eff} = H/[(H-h)/k_g + h/k_s] \quad \text{(A-3)}$$

where H = total thickness (2 ft for top drainage layer and 5 ft for bottom drainage layer)

h = plugged-zone thickness, ft

k_g =conductivity of gravel (10^{-1} cm/sec)

k_s =conductivity of soil (10^{-4} cm/sec)

Calculated horizontal and vertical effective hydraulic conductivities for the top and the bottom drainage layers are summarized in Table A-4. The plugged zone thickness used for the calculation is the average for the time interval. For the vertical drainage layer, conductivity remains constant at 10^{-1} cm/sec.

These assumptions on the changes in hydraulic properties over time are based on professional judgment, since actual data over the time periods of interest do not exist. They were discussed during meetings of the performance assessment team and the team agreed to use these values in this analysis.

Because the SDF is constructed in the unsaturated zone, water saturation in the modeling domain is expected to be below 100%. Fluid flow is affected by the capillary pressure (or suction pressure) and relative permeability (or conductivity). Capillary pressure decreases with increasing water saturation, whereas relative permeability increases with increasing water saturation. Saturation dependence of these two parameters is often depicted as characteristic curves. The characteristic curves for Saltstone are illustrated in Figure A-3. Figures A-4 through A-6 show the same curves for the other porous media. In the unsaturated-zone flow model, the capillary pressure and relative permeability are entered as table input.

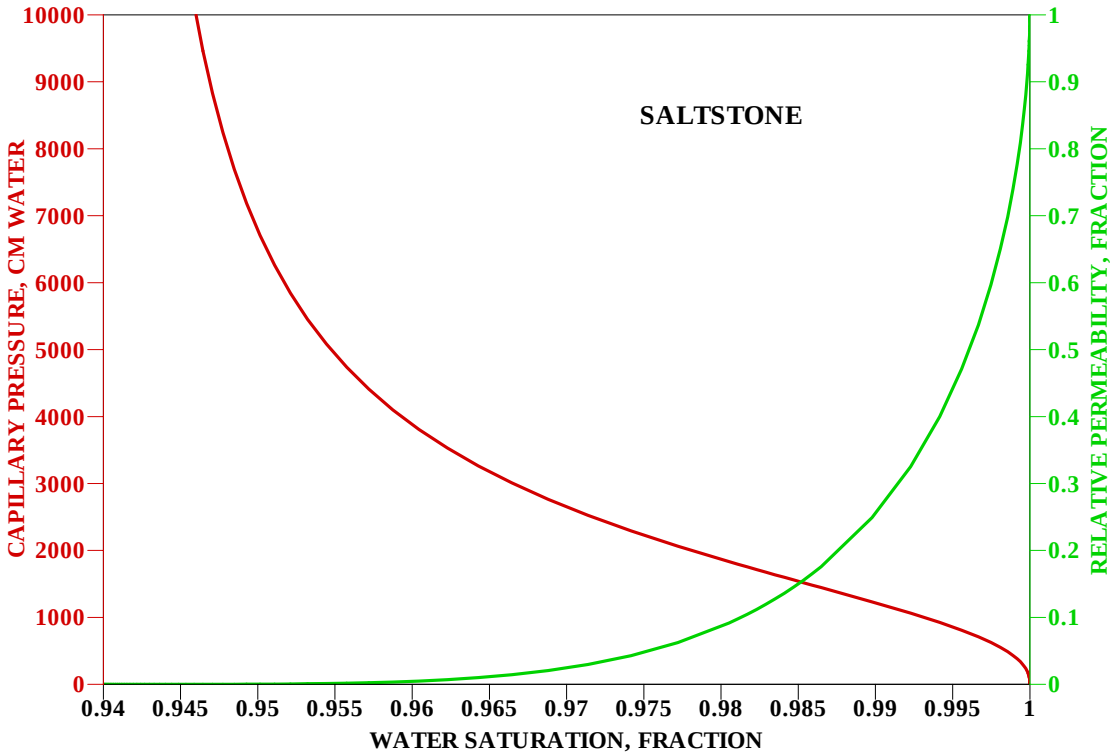

Figure A-3. Characteristic Curves for Saltstone

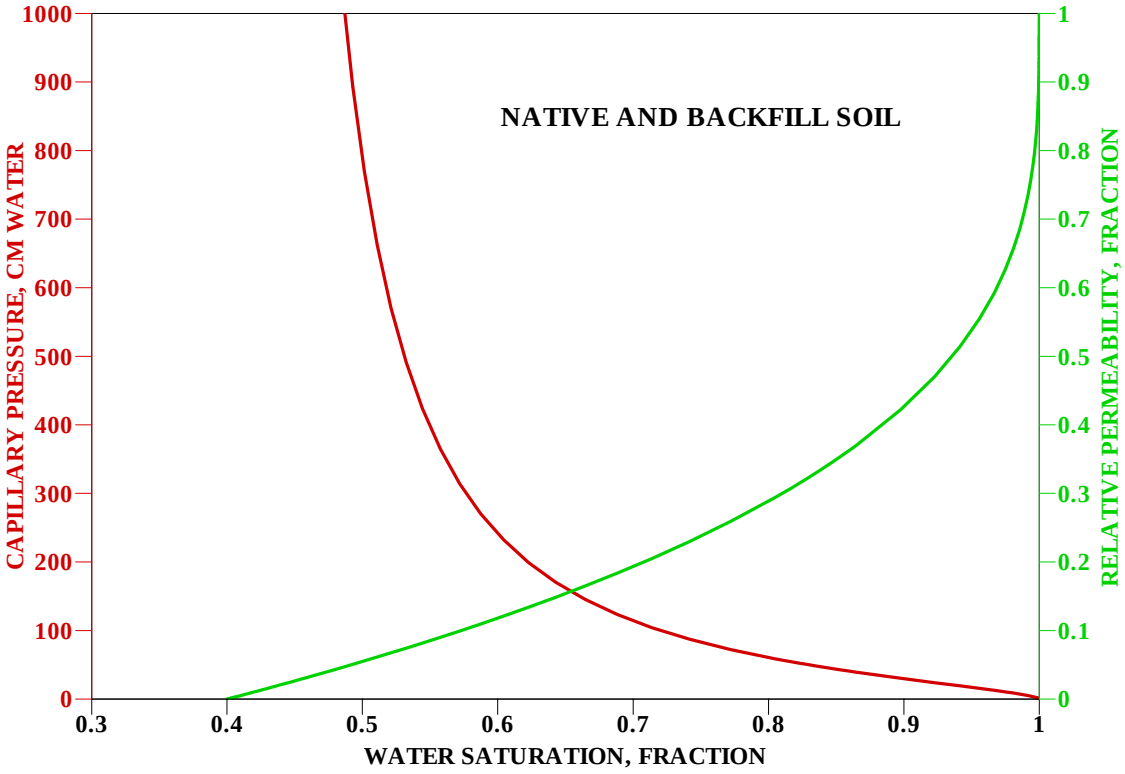

Figure A-4. Characteristic Curves for Native and Backfill Soil

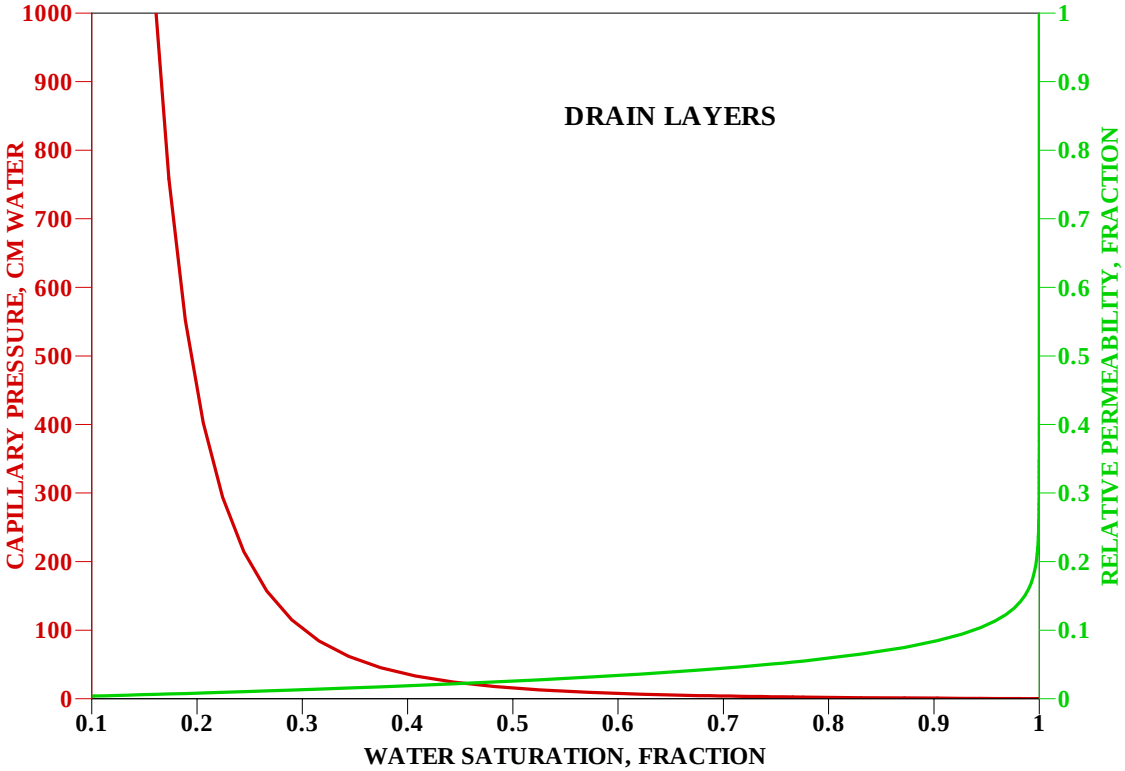

Figure A-5. Characteristic Curves for Drain Layers

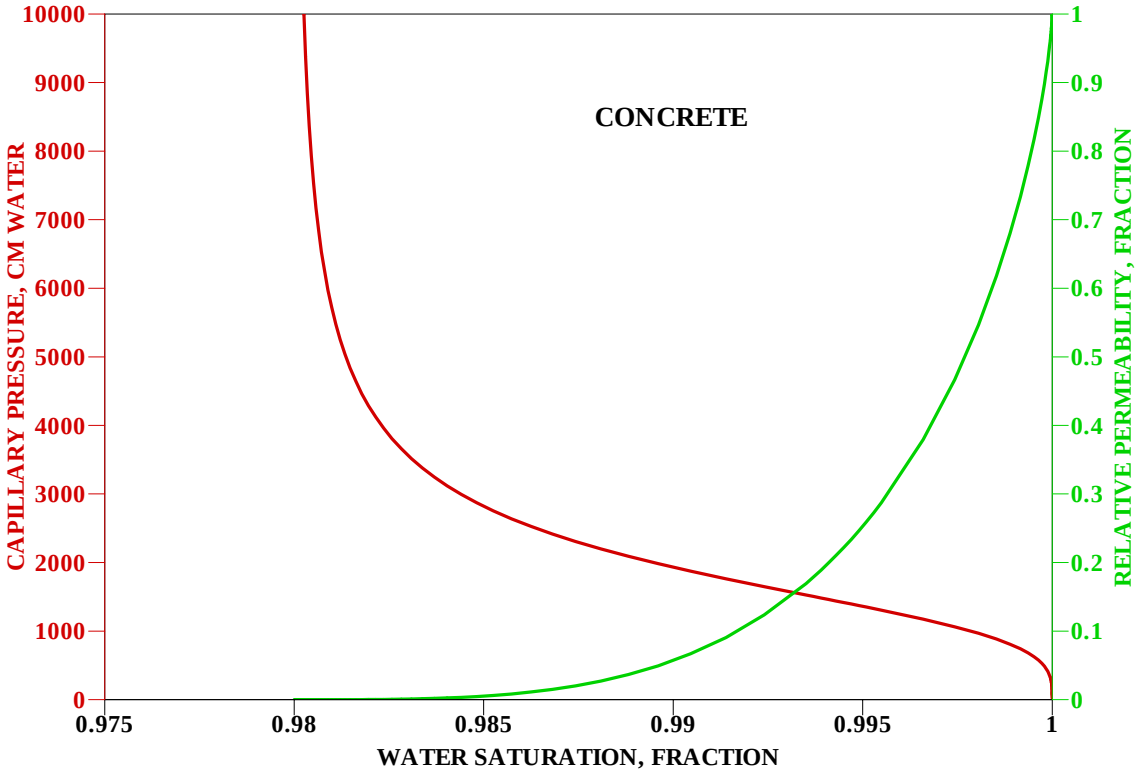

Figure A-6. Characteristic Curves for Concrete

A.2.3.2 Infiltration Rates

The infiltration rates (in inches/year) through the lower GCL (Phifer 2004) used for this study are summarized in Table A-6 and shown in Figure A-7.

Table A-6. Infiltration Rates Used as Upper Boundary Conditions

Time Interval	Infiltration Rate (in/yr)
0 to 100	0.39
100 to 300	1.73
300 to 550	5.48
550 to 1,000	9.97
1,000 to 1,800	12.90
1,800 to 3,400	13.90
3,400 to 5,600	14.06
5,600 to 10,000	14.09

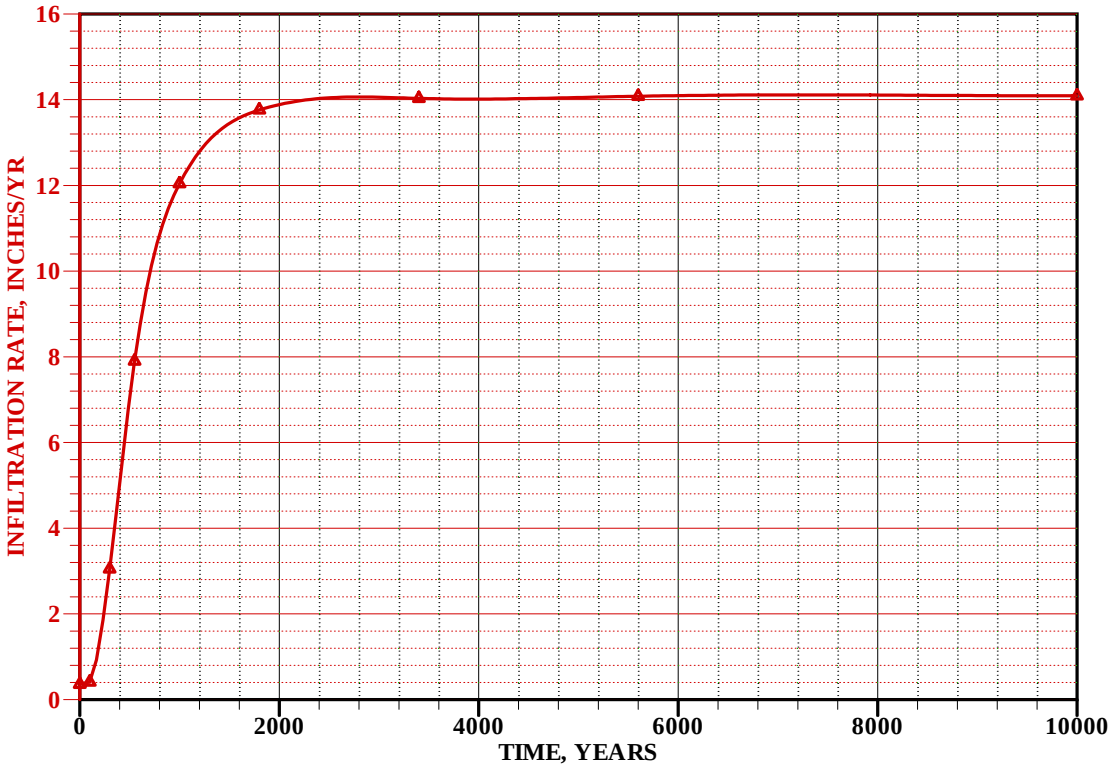

Figure A-7. Infiltration Rate Through the Lower GCL

A.2.3.3 PORFLOW Input Files

For each of the time intervals, a steady-state flow field is obtained by solving the flow equations for a very long simulation time so that pressure, saturation, and water velocity vectors at each of the nodes remains unchanged with respect to time. These flow fields form the steady–state flow field for the subsequent transient-state transport simulations. PORFLOW input files incorporate geometry, properties of the fluids and porous media, initial and boundary conditions, and numerical solution schemes.

A.2.3.4 Predicted Pressure, Saturation, and Flow Vectors

For each of the time intervals, an initial saturation is assigned to each of the nodes in the domain. The choice of initial saturation is based on the flow properties of the porous media. For a given saturation, the capillary pressure is also fixed. Under the initial and boundary conditions, the two-phase (water-air) flow equations are solved numerically. The time-steps used for the solution are very small in the beginning and gradually increase with simulation time.

Post-processing capabilities were developed to plot predicted pressure contours, saturation contours and velocity vectors throughout the domain. These tools provide a means to interpret and assess the predicted flow fields. Plots are provided for TI04 (550 to 1,000 years) in Figures A-8 through A-11.

The pressure profile for TI04 is depicted in Figure A-8. In this time interval, the infiltration rate is 9.97 inches/year (25 cm/year). The saturation profile is shown in Figure A-9. Water saturations in Saltstone and the concrete vault are near 100%. This is mainly due to the high capillary pressure of cementitious materials. Water saturations in the top, vertical and bottom drainage layers remain low. This indicates that the drain layers are still effective. Water saturation for native soil is 1.0 (100%) at the water table, and decreases with increasing elevation. These observations are consistent with the properties of the porous media and the conceptual model.

The velocity profile for the entire modeling domain is shown in Figure A-10. As indicated, most of the infiltration water flows around the vault. The drain layers facilitate the removal of perched water from above the vault. Water velocities in Saltstone and vault are very low and they are depicted in Figure A-11. The velocity vectors are generally downward and in the order of 1×10^{-4} cm/yr, or about 3×10^{-12} cm/sec, which is lower than the T104 saturated hydraulic conductivity of Saltstone (1×10^{-10} cm/sec) and higher than that of concrete (1×10^{-11} cm/sec).

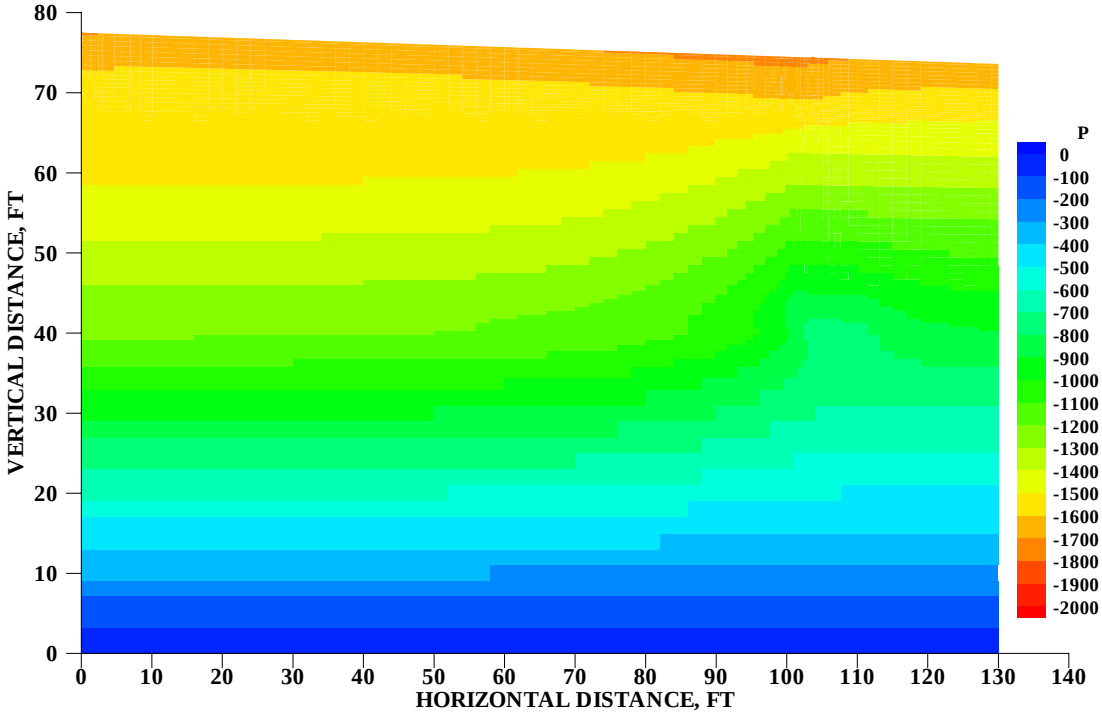

Figure A-8. Pressure Profile for TI04

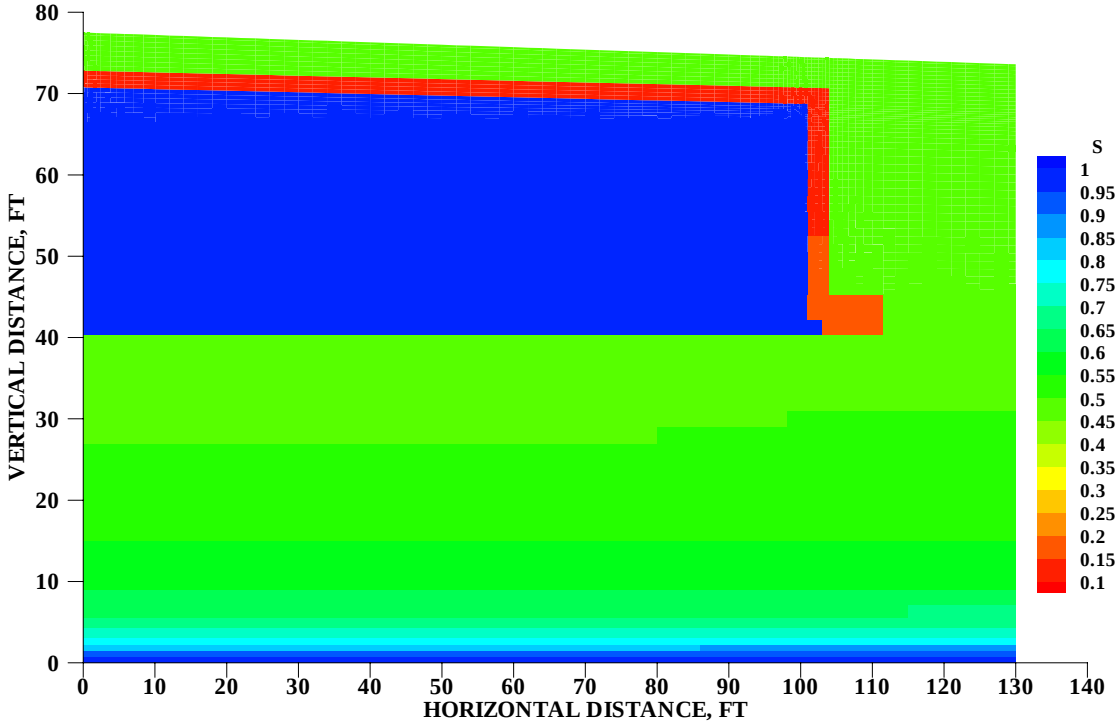

Figure A-9. Saturation Profile for TI04

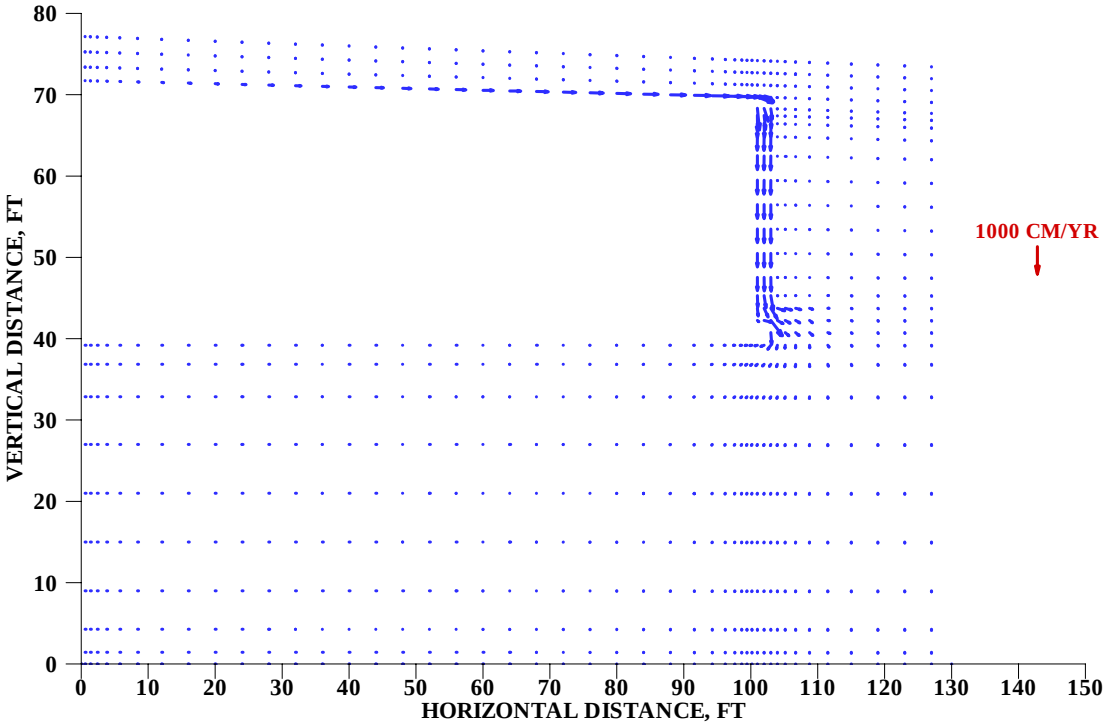

Figure A-10. Velocity Profile in Modeling Domain for TI04

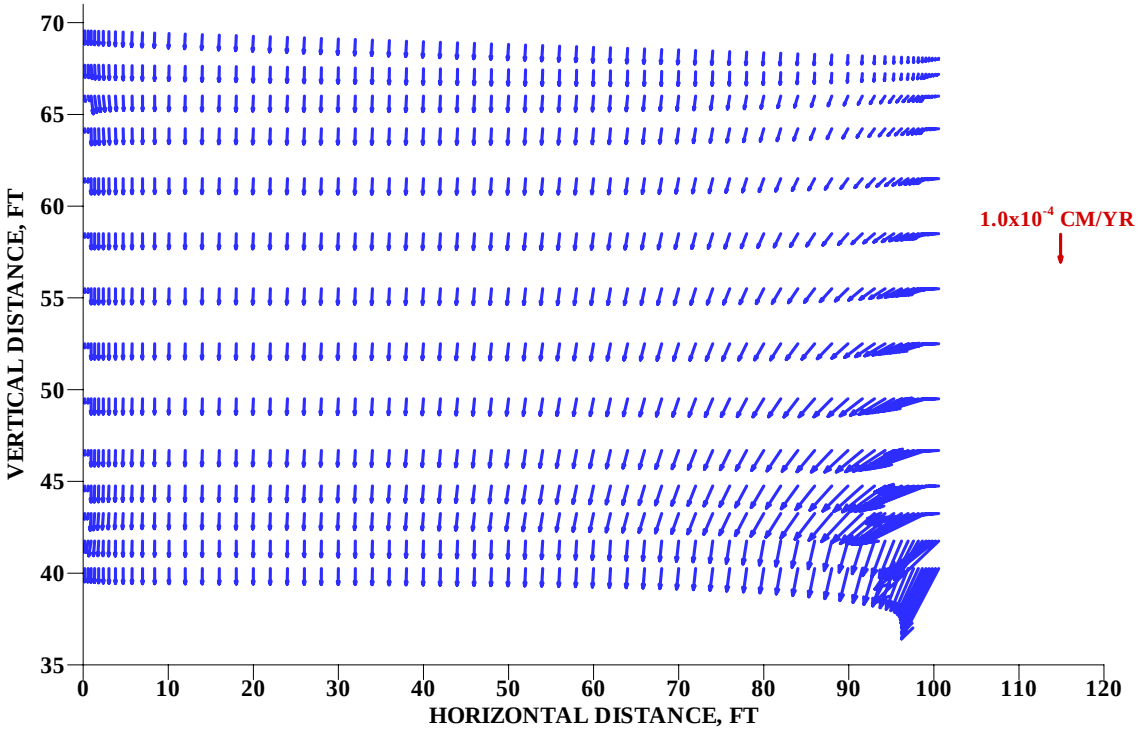

Figure A-11. Velocity Profile in Saltstone and Vault for TI04

A.2.4 Contaminant Transport Modeling

A.2.4.1 Contaminants Selected for Modeling

In this study, 46 contaminants were modeled (Table A-1). Except for nitrate (NO_3), all other contaminants are radionuclides. Some of the radionuclides also have decay daughters. Nitrate is not only one of the most important contaminants of concern (very mobile, low regulatory standard, high concentrations in the SDF) but also a conservative tracer because nitrate does not adsorb or decay. Compared to other long-lived contaminants, nitrate should have the highest predicted peak flux to the water table per unit inventory.

A.2.4.2 Plutonium Speciation Modeling

Because plutonium isotopes of different oxidation states have significantly different adsorption behaviors in soil, the drain and clay, it is necessary to model the speciation and account for the retardation of different species in the transport modeling (Kaplan 2004).

The plutonium speciation is represented by equilibrium between two pseudo components, Pu (III, IV) and Pu (V,VI). The plutonium isotopes may also be parents or daughters, or both, in a decay chain, as shown in Figure A-12.

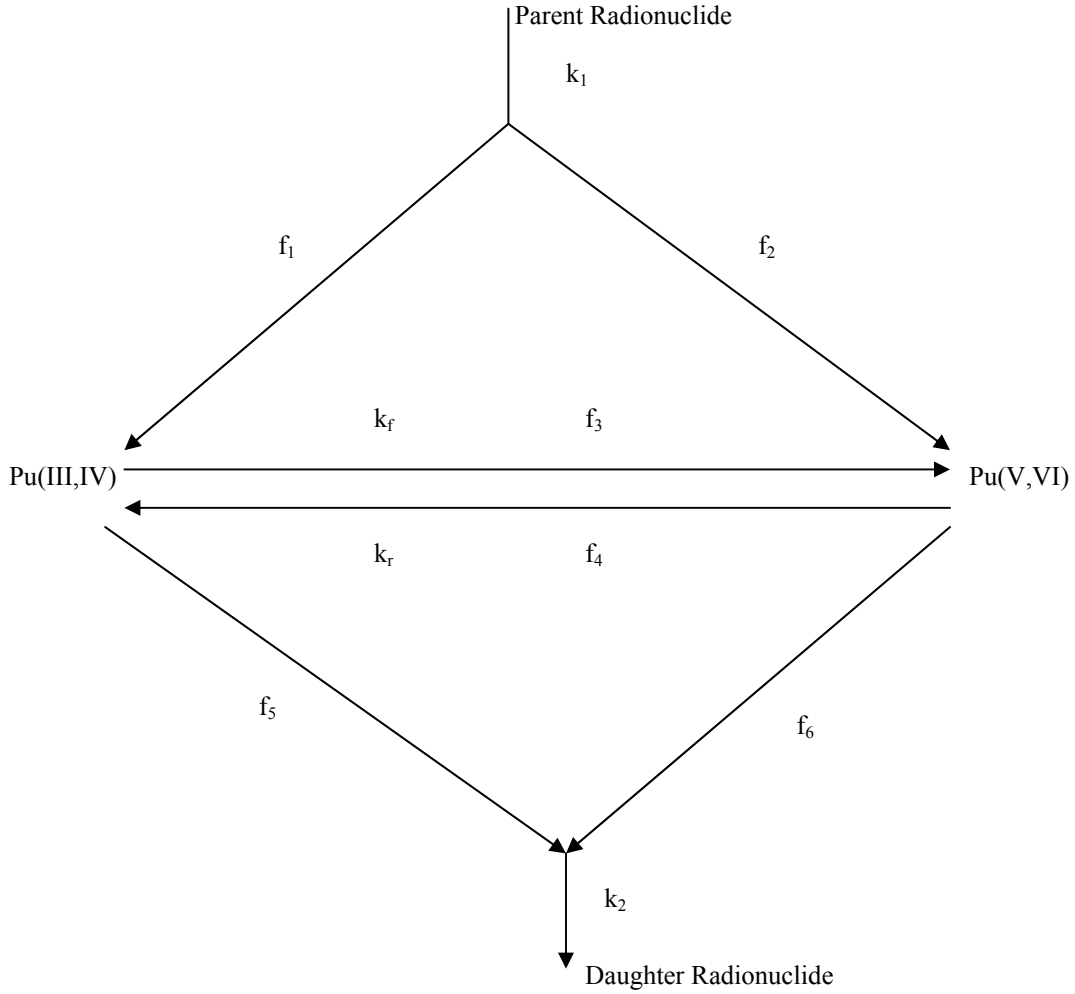

Figure A-12. Decay and Chemical Reactions Involving Plutonium of Two Oxidation States

In Figure A-12, the parent radionuclide (P) decays into Pu (III, IV) and Pu (V,VI) simultaneously, with a first-order rate constant k_1, and

$$k_1 = \ln(2) / t_{½,P} \quad \text{(A-4)}$$

Where $t_{½,P}$ is the half-life of P. When one mole of P is decayed, f_1 mole of Pu (III, IV) and f_2 mole of Pu (V,VI) are formed. Obviously, $f_1 + f_2 = 1$. Pu (III, IV) and Pu (V,VI) are in equilibrium at all times. The forward reaction rate constant (k_f) is 1.31×10^{-4} yr^{-1}. The reverse reaction rate constant (k_r) is 8.76 yr^{-1}. The "regeneration fractions" f_1 and f_2 are calculated as

$$f_1 = k_r / (k_f + k_r) \quad \text{(A-5)}$$

$$f_2 = k_f / (k_f + k_r) \quad \text{(A-6)}$$

in order to maintain equilibrium between Pu (III, IV) and Pu (V,VI).

Both Pu (III, IV) and Pu (V,VI) decay to the daughter isotope D at the same rate k_2 and

$$k_2 = \ln (2) / t_{½,Pu} \quad \text{(A-7)}$$

The over-all reaction rate constant for Pu (III, IV) is equal to $k_f + k_2$ and

$$f_3 = k_f / (k_f + k_2) \quad \text{(A-8)}$$

$$f_5 = k_2 / (k_f + k_2) \quad \text{(A-9)}$$

Similarly, the over-all reaction rate constant for Pu (V,VI) is equal to $k_r + k_2$ and

$$f_4 = k_r / (k_r + k_2) \quad \text{(A-10)}$$

$$f_6 = k_2 / (k_r + k_2) \quad \text{(A-11)}$$

A.2.4.3 Contaminant and other transport properties

The most important properties of radionuclides are atomic weight, half-life, specific activity, distribution coefficient (K_d), and the molecular diffusion coefficients. The atomic weights, half-lives and specific activities for all simulated contaminants (including decay daughters) are summarized in Table A-7. Density of the solid matrix was assumed to be 2.65 g/cm^3 for all the porous materials.

Table A-7. Atomic Weight, Half-life and Specific Activity

Nuclide	Atomic Wt. g/mol	Half-life year	Specific Activity Ci/g
NO3	6.20E+01	1.00E+20	5.77E-17
Al-26	2.60E+01	7.17E+05	1.92E-02
Am-243	2.43E+02	7.37E+03	2.00E-01
Np-239	2.39E+02	6.45E-03	2.32E+05
Pu-239	2.39E+02	2.41E+04	6.21E-02
Pu5-239	2.39E+02	2.41E+04	6.21E-02
Bi-210	2.10E+02	1.37E-02	1.24E+05
Po-210	2.10E+02	3.79E-01	4.49E+03
C-14	1.40E+01	5.73E+03	4.46E+00
Cf-249	2.49E+02	3.51E+02	4.09E+00
Cm-245	2.45E+02	8.50E+03	1.72E-01
Pu-241	2.41E+02	1.43E+01	1.04E+02
Pu5-241	2.41E+02	1.43E+01	1.04E+02
Am-241	2.41E+02	4.32E+02	3.43E+00
Np-237	2.37E+02	2.14E+06	7.05E-04
Cl-36	3.60E+01	3.01E+05	3.30E-02
Cm-245	2.45E+02	8.50E+03	1.72E-01
Pu-241	2.41E+02	1.43E+01	1.04E+02
Pu5-241	2.41E+02	1.43E+01	1.04E+02
Am-241	2.41E+02	4.32E+02	3.43E+00
Np-237	2.37E+02	2.14E+06	7.05E-04
Cm-246	2.46E+02	4.76E+03	3.05E-01
Cm-247	2.47E+02	1.56E+07	9.28E-05
Am-243	2.43E+02	7.37E+03	2.00E-01
Np-239	2.39E+02	6.45E-03	2.32E+05
Pu-239	2.39E+02	2.41E+04	6.21E-02
Pu5-239	2.39E+02	2.41E+04	6.21E-02
Cm-248	2.48E+02	3.48E+05	4.14E-03
Pu-244	2.44E+02	8.00E+07	1.83E-05
Pu5-244	2.44E+02	8.00E+07	1.83E-05
Cs-135	1.35E+02	2.30E+06	1.15E-03
Cs-137	1.37E+02	3.01E+01	8.67E+01
H-3	3.02E+00	1.23E+01	9.62E+03
I-129	1.29E+02	1.57E+07	1.77E-04
K-40	4.00E+01	1.28E+09	6.99E-06
Mo-93	9.30E+01	4.00E+03	9.61E-01
Nb-93m	9.29E+01	1.61E+01	2.39E+02
Nb-94	9.39E+01	2.03E+04	1.88E-01
Nb-95m	9.49E+01	9.88E-03	3.81E+05
Nb-95	9.49E+01	9.58E-02	3.93E+04
Ni-59	5.89E+01	7.60E+04	7.98E-02
Np-237	2.37E+02	2.14E+06	7.05E-04
Pd-107	1.07E+02	6.50E+06	5.14E-04
Pu-238	2.38E+02	8.77E+01	1.71E+01
Pu5-238	2.38E+02	8.77E+01	1.71E+01
U-234	2.34E+02	2.46E+05	6.21E-03
Pu-239	2.39E+02	2.41E+04	6.21E-02
Pu5-239	2.39E+02	2.41E+04	6.21E-02
U-235	2.35E+02	7.04E+08	2.16E-06

Pu-240	2.40E+02	6.56E+03	2.27E-01
Pu5-240	2.40E+02	6.56E+03	2.27E-01
U-236	2.36E+02	2.34E+07	6.47E-05
Pu-241	2.41E+02	1.43E+01	1.04E+02
Pu5-241	2.41E+02	1.43E+01	1.04E+02
Am-241	2.41E+02	4.32E+02	3.43E+00
Np-237	2.37E+02	2.14E+06	7.05E-04
Pu-242	2.42E+02	3.73E+05	3.96E-03
Pu5-242	2.42E+02	3.73E+05	3.96E-03
U-238	2.38E+02	4.47E+09	3.36E-07
Pu-244	2.44E+02	8.00E+07	1.83E-05
Pu5-244	2.44E+02	8.00E+07	1.83E-05
Ra-226	2.26E+02	1.60E+03	9.88E-01
Rb-87	8.70E+01	4.75E+10	8.65E-08
Se-79	7.89E+01	1.10E+06	4.12E-03
Sn-126	1.26E+02	1.00E+05	2.84E-02
Sr-90	8.99E+01	2.88E+01	1.38E+02
Tc-99	9.89E+01	2.11E+05	1.71E-02
Th-228	2.28E+02	1.91E+00	8.21E+02
Ra-224	2.24E+02	1.00E-02	1.60E+05
Th-229	2.29E+02	7.34E+03	2.13E-01
Ra-225	2.25E+02	4.08E-02	3.89E+04
Ac-225	2.25E+02	2.74E-02	5.80E+04
Th-230	2.30E+02	7.54E+04	2.06E-02
Ra-226	2.26E+02	1.60E+03	9.88E-01
Pb-210	2.10E+02	2.23E+01	7.63E+01
Po-210	2.10E+02	3.79E-01	4.49E+03
Th-232	2.32E+02	1.41E+10	1.09E-07
Ra-228	2.28E+02	5.75E+00	2.73E+02
Th-228	2.28E+02	1.91E+00	8.21E+02
Ra-224	2.24E+02	1.00E-02	1.60E+05
U-232	2.32E+02	6.89E+01	2.24E+01
Th-228	2.28E+02	1.91E+00	8.21E+02
Ra-224	2.24E+02	1.00E-02	1.60E+05
U-233	2.33E+02	1.59E+05	9.65E-03
Th-229	2.29E+02	7.34E+03	2.13E-01
Ra-225	2.25E+02	4.08E-02	3.89E+04
U-234	2.34E+02	2.46E+05	6.21E-03
Th-230	2.30E+02	7.54E+04	2.06E-02
Ra-226	2.26E+02	1.60E+03	9.88E-01
Pb-210	2.10E+02	2.23E+01	7.63E+01
Po-210	2.10E+02	3.79E-01	4.49E+03
U-235	2.35E+02	7.04E+08	2.16E-06
Pa-231	2.31E+02	3.28E+04	4.72E-02
Ac-227	2.27E+02	2.18E+01	7.22E+01
Th-227	2.27E+02	5.13E-02	3.07E+04
Ra-223	2.23E+02	3.13E-02	5.12E+04
U-236	2.36E+02	2.34E+07	6.47E-05
U-238	2.38E+02	4.47E+09	3.36E-07
Th-234	2.34E+02	6.60E-02	2.31E+04
U-234	2.34E+02	2.46E+05	6.21E-03
Zr-93	9.29E+01	1.53E+06	2.51E-03
Nb-93m	9.29E+01	1.61E+01	2.39E+02
Zr-95	9.49E+01	1.75E-01	2.15E+04
Nb-95	9.49E+01	9.58E-02	3.93E+04

A.2.5 Distribution Coefficient

The distribution coefficients (K_d) of all contaminants and daughters used for this study are summarized in Table A-8. The values for clay are used for the saturated-zone models. Various plutonium isotopes of different oxidation states are lumped into two pseudo components: Pu- for Pu (III, IV) and Pu5- for Pu (V,VI). For soil, drain and clay, K_d in Pu (III, IV) is significantly higher than Pu (V,VI).

Table A-8. Distribution Coefficients (K_d in cm^3/g)

Nuclides	Soil	Drain	Clay	Saltstone	Concrete
NO3	0.00E+00	0.00E+00	0.00E+00	0.00E+00	0.00E+00
Al-26	4.00E+01	4.00E+01	0.00E+00	2.00E+01	2.00E+01
Am-243	1.90E+03	1.90E+03	8.40E+03	5.00E+03	5.00E+03
Np-239	5.00E+00	5.00E+00	5.50E+01	5.00E+03	5.00E+03
Pu-239	3.70E+02	3.70E+02	6.50E+03	5.00E+03	5.00E+03
Pu5-239	1.50E+01	1.50E+01	5.00E+01	5.00E+03	5.00E+03
Bi-210	4.50E+02	4.50E+02	1.20E+04	5.00E+03	5.00E+03
Po-210	1.50E+02	1.50E+02	3.00E+03	5.00E+02	5.00E+02
C-14	2.00E+00	2.00E+00	1.00E+00	5.00E+03	5.00E+03
Cf-249	5.10E+02	5.10E+02	8.40E+03	5.00E+03	5.00E+03
Cm-245	4.00E+03	4.00E+03	6.00E+03	5.00E+03	5.00E+03
Pu-241	3.70E+02	3.70E+02	6.50E+03	5.00E+03	5.00E+03
Pu5-241	1.50E+01	1.50E+01	5.00E+01	5.00E+03	5.00E+03
Am-241	1.90E+03	1.90E+03	8.40E+03	5.00E+03	5.00E+03
Np-237	5.00E+00	5.00E+00	5.50E+01	5.00E+03	5.00E+03
Cl-36	0.00E+00	0.00E+00	0.00E+00	5.00E+03	5.00E+03
Cm-245	4.00E+03	4.00E+03	6.00E+03	5.00E+03	5.00E+03
Pu-241	3.70E+02	3.70E+02	6.50E+03	5.00E+03	5.00E+03
Pu5-241	1.50E+01	1.50E+01	5.00E+01	5.00E+03	5.00E+03
Am-241	1.90E+03	1.90E+03	8.40E+03	5.00E+03	5.00E+03
Np-237	5.00E+00	5.00E+00	5.50E+01	5.00E+03	5.00E+03
Cm-246	4.00E+03	4.00E+03	6.00E+03	5.00E+03	5.00E+03
Cm-247	4.00E+03	4.00E+03	6.00E+03	5.00E+03	5.00E+03
Am-243	1.90E+03	1.90E+03	8.40E+03	5.00E+03	5.00E+03
Np-239	5.00E+00	5.00E+00	5.50E+01	5.00E+03	5.00E+03
Pu-239	3.70E+02	3.70E+02	6.50E+03	5.00E+03	5.00E+03
Pu5-239	1.50E+01	1.50E+01	5.00E+01	5.00E+03	5.00E+03
Cm-248	4.00E+03	4.00E+03	6.00E+03	5.00E+03	5.00E+03
Pu-244	3.70E+02	3.70E+02	6.50E+03	5.00E+03	5.00E+03
Pu5-244	1.50E+01	1.50E+01	5.00E+01	5.00E+03	5.00E+03
Cs-135	3.30E+02	3.30E+02	1.90E+03	2.00E+01	2.00E+01
Cs-137	3.30E+02	3.30E+02	1.90E+03	2.00E+01	2.00E+01
H-3	0.00E+00	0.00E+00	0.00E+00	0.00E+00	0.00E+00
I-129	6.00E-01	6.00E-01	1.00E+00	2.00E+00	2.00E+00
K-40	3.00E+00	3.00E+00	5.00E+00	2.00E+00	2.00E+00
Mo-93	3.00E+00	3.00E+00	1.30E+01	1.00E+00	1.00E+00
Nb-93m	1.60E+02	1.60E+02	9.00E+02	5.00E+02	5.00E+02
Nb-94	1.60E+02	1.60E+02	9.00E+02	5.00E+02	5.00E+02
Nb-95m	1.60E+02	1.60E+02	9.00E+02	5.00E+02	5.00E+02
Nb-95	1.60E+02	1.60E+02	9.00E+02	5.00E+02	5.00E+02
Ni-59	4.00E+02	4.00E+02	6.50E+02	1.00E+02	1.00E+02
Np-237	5.00E+00	5.00E+00	5.50E+01	5.00E+03	5.00E+03
Pd-107	5.50E+01	5.50E+01	2.70E+02	1.00E+02	1.00E+02
Pu-238	3.70E+02	3.70E+02	6.50E+03	5.00E+03	5.00E+03
Pu5-238	1.50E+01	1.50E+01	5.00E+01	5.00E+03	5.00E+03
U-234	8.00E+02	8.00E+02	1.60E+03	2.00E+03	2.00E+03
Pu-239	3.70E+02	3.70E+02	6.50E+03	5.00E+03	5.00E+03
Pu5-239	1.50E+01	1.50E+01	5.00E+01	5.00E+03	5.00E+03
U-235	8.00E+02	8.00E+02	1.60E+03	2.00E+03	2.00E+03
Pu-240	3.70E+02	3.70E+02	6.50E+03	5.00E+03	5.00E+03
Pu5-240	1.50E+01	1.50E+01	5.00E+01	5.00E+03	5.00E+03
U-236	8.00E+02	8.00E+02	1.60E+03	2.00E+03	2.00E+03
Pu-241	3.70E+02	3.70E+02	6.50E+03	5.00E+03	5.00E+03
Pu5-241	1.50E+01	1.50E+01	5.00E+01	5.00E+03	5.00E+03
Am-241	1.90E+03	1.90E+03	8.40E+03	5.00E+03	5.00E+03
Np-237	5.00E+00	5.00E+00	5.50E+01	5.00E+03	5.00E+03
Pu-242	3.70E+02	3.70E+02	6.50E+03	5.00E+03	5.00E+03

Pu5-242	1.50E+01	1.50E+01	5.00E+01	5.00E+03	5.00E+03
U-238	8.00E+02	8.00E+02	1.60E+03	2.00E+03	2.00E+03
Pu-244	3.70E+02	3.70E+02	6.50E+03	5.00E+03	5.00E+03
Pu5-244	1.50E+01	1.50E+01	5.00E+01	5.00E+03	5.00E+03
Ra-226	5.00E+02	5.00E+02	9.10E+03	5.00E+01	5.00E+01
Rb-87	5.50E+01	5.50E+01	2.70E+02	5.50E+01	5.50E+01
Se-79	3.60E+01	3.60E+01	7.60E+01	1.00E-01	1.00E-01
Sn-126	1.30E+02	1.30E+02	6.70E+02	1.00E+03	1.00E+03
Sr-90	1.00E+01	1.00E+01	1.10E+02	1.00E+00	1.00E+00
Tc-99	1.00E-01	1.00E-01	1.00E-01	1.00E+03	1.00E+03
Th-228	3.20E+03	3.20E+03	5.80E+03	5.00E+03	5.00E+03
Ra-224	5.00E+02	5.00E+02	9.10E+03	5.00E+01	5.00E+01
Th-229	3.20E+03	3.20E+03	5.80E+03	5.00E+03	5.00E+03
Ra-225	5.00E+02	5.00E+02	9.10E+03	5.00E+01	5.00E+01
Ac-225	4.50E+02	4.50E+02	2.40E+03	5.00E+03	5.00E+03
Th-230	3.20E+03	3.20E+03	5.80E+03	5.00E+03	5.00E+03
Ra-226	5.00E+02	5.00E+02	9.10E+03	5.00E+01	5.00E+01
Pb-210	2.70E+02	2.70E+02	5.50E+02	5.00E+02	5.00E+02
Po-210	1.50E+02	1.50E+02	3.00E+03	5.00E+02	5.00E+02
Th-232	3.20E+03	3.20E+03	5.80E+03	5.00E+03	5.00E+03
Ra-228	5.00E+02	5.00E+02	9.10E+03	5.00E+01	5.00E+01
Th-228	3.20E+03	3.20E+03	5.80E+03	5.00E+03	5.00E+03
Ra-224	5.00E+02	5.00E+02	9.10E+03	5.00E+01	5.00E+01
U-232	8.00E+02	8.00E+02	1.60E+03	2.00E+03	2.00E+03
Th-228	3.20E+03	3.20E+03	5.80E+03	5.00E+03	5.00E+03
Ra-224	5.00E+02	5.00E+02	9.10E+03	5.00E+01	5.00E+01
U-233	8.00E+02	8.00E+02	1.60E+03	2.00E+03	2.00E+03
Th-229	3.20E+03	3.20E+03	5.80E+03	5.00E+03	5.00E+03
Ra-225	5.00E+02	5.00E+02	9.10E+03	5.00E+01	5.00E+01
U-234	8.00E+02	8.00E+02	1.60E+03	2.00E+03	2.00E+03
Th-230	3.20E+03	3.20E+03	5.80E+03	5.00E+03	5.00E+03
Ra-226	5.00E+02	5.00E+02	9.10E+03	5.00E+01	5.00E+01
Pb-210	2.70E+02	2.70E+02	5.50E+02	5.00E+02	5.00E+02
Po-210	1.50E+02	1.50E+02	3.00E+03	5.00E+02	5.00E+02
U-235	8.00E+02	8.00E+02	1.60E+03	2.00E+03	2.00E+03
Pa-231	5.50E+02	5.50E+02	2.70E+03	5.00E+03	5.00E+03
Ac-227	4.50E+02	4.50E+02	2.40E+03	5.00E+03	5.00E+03
Th-227	3.20E+03	3.20E+03	5.80E+03	5.00E+03	5.00E+03
Ra-223	5.00E+02	5.00E+02	9.10E+03	5.00E+01	5.00E+01
U-236	8.00E+02	8.00E+02	1.60E+03	2.00E+03	2.00E+03
U-238	8.00E+02	8.00E+02	1.60E+03	2.00E+03	2.00E+03
Th-234	3.20E+03	3.20E+03	5.80E+03	5.00E+03	5.00E+03
U-234	8.00E+02	8.00E+02	1.60E+03	2.00E+03	2.00E+03
Zr-93	6.00E+02	6.00E+02	3.30E+03	5.00E+03	5.00E+03
Nb-93m	1.60E+02	1.60E+02	9.00E+02	5.00E+02	5.00E+02
Zr-95	6.00E+02	6.00E+02	3.30E+03	5.00E+03	5.00E+03
Nb-95	1.60E+02	1.60E+02	9.00E+02	5.00E+02	5.00E+02

A.2.6 Molecular Diffusion

The molecular diffusion coefficients selected for use in this investigation were established by material type, and are listed below in Table A-9. These values are not expected to vary significantly as the material hydraulic properties in some zones and no attempt was made to re-define them as such changes occurred. The selected values are consistent within the range of diffusion coefficients reported for ionic solutes in porous media (Domenico and Schwartz, 1990). The values selected for Saltstone and concrete are near the lower end of this range, as one would expect.

Table A-9. Molecular Diffusion Coefficients

	Molecular Diffusion Coefficients	
Porous Media	cm^2/sec	$cm^2/year$
Native/Backfill Soil	5.E-05	1.58E+02
Drainage Layer	5.E-05	1.58E+02
Saltstone	5.E-09	1.58E-01
Concrete	1.E-08	3.15E-01

A.2.7 Initial and Boundary Conditions

For the first time period (0 to 100 years), an initial amount of 1,000,000 moles of the parent radionuclide is placed in the Saltstone, from NX = 4 to 64 (0.75 to 99.25 ft) and NY = 33 to 61 (42.0 to 65.75 ft). The height from 65.75 to 66.75 ft is clean pour (i.e., concrete containing no waste). The thickness of the third dimension is 1.0 cm. The porosity of Saltstone is 0.42. PORFLOW sets the initial concentration in the pore water at every node of the "waste" zone to be equal. From PORFLOW output, this concentration for nitrate is 1.1138 mol/cm^3. Since $Q = C \times V \times \phi \times S = 10^6$ moles and $V = 98.5 \times 23.75 \times 30.48^2 = 2.1734 \times 10^6$ cm^3, then S = 0.9836. This is in good agreement with the average Saltstone saturation predicted by the TI01 steady-state flow field.

No-flux boundary conditions for contaminant transport are assumed for the top and both sides of the modeling domain. No boundary condition is specified for the bottom of the modeling domain. PORFLOW 5.97.0 has a default algorithm to calculate convective and diffusive fluxes to the water table.

A.2.8 PORFLOW Transport Runs

Under the initial and boundary conditions, contaminant transport is simulated for the first time interval (0 to 100 years). The steady-state flow field is used for the transient-state transport simulations. Contaminant migration is generally in a downward direction from Saltstone to the water table. The time-history of the contaminant release to the water table is saved for post processing. In the post-processing program, the predicted quantity of contaminant release in mole/yr is divided by the initial amount of 1,000,000 moles to get a fractional release rate (unit = mole/year/mole parent).

For the second time interval (100 to 300 years), the flow field is represented by a new set of saturations and velocities. Because the infiltration rate is higher, the saturation at each of the

nodes also tends to be higher. In order to conserve mass, the contaminant concentration in every modeling cell must be recalculated The equations used to convert the concentrations are:

$$C_S = K_d C_L \tag{A-12}$$

$$m = S_W \left[C_S (1-\phi)\rho_S + C_L \phi \right] \tag{A-13}$$

where C_S = concentration in solid, mol/g,

C_L = concentration in liquid, mol/g, or mol/cm^3,

m = total moles of contaminant,

ρ_S = density of waste matrix = 2.65 g/cm^3, and

ϕ = porosity = 0.42.

The above equations are used by PORFLOW to define distribution coefficient and mass conservation. Substituting equation (A-12) into (A-13), then:

$$\frac{m}{K_d (1-\phi)\rho_S + \phi} = S_w C_L \tag{A-14}$$

Because the left-hand side of equation (A-14) is constant, C_L can be converted from the end of one time period (C_{L1}) to the beginning of the next (C_{L2}) by equation (A-15):

$$C_{L2} = S_{w1} C_{L1} / S_{w2} \tag{A-15}$$

The converted concentrations are used as the initial conditions for the transport run under the steady-state flow field of the next time interval. This concentration conversion and subsequent transport simulation is repeated until the end of the simulation period. In PORFLOW 5.97.0, the concentration conversions are calculated automatically and a single run can execute transport through all eight flow fields

A.2.9 Predicted Contaminant Fluxes to the Water Table

Predicted flux and cumulative release history for nitrate up to 1,000 years are depicted in Figure A-13. The peak flux is 4.03×10^{-7} year^{-1}. The "blips" at 300 and 500 years result from abrupt changes in flow velocities between time intervals. Only about 1.2×10^{-4} of the initial amount of nitrate is released to the water table in 1,000 years. The same plots for all contaminants listed in Table A-10 with a peak great than 1E-30 are depicted in Figures A-14 through A-26.

In discussions of the flux results the term "peak flux" will be used. In actuality what is being referred to is the peak annual fractional flux, since we used a unit initial inventory and calculate the flux on an annual basis. Peak annual fractional flux is a unitless quantity and we will use "peak flux "to represent this unitless quantity.

Predicted peak fluxes for the contaminants modeled from 0 to 1,000 years are summarized in Table A-10. In this table, values smaller than 1.0×10^{-99} have been set to 0. Except for some radionuclides with short half-lives, the peak times all occur at 1,000 years. Using multiple time intervals to simulate gradual degradation of the facility removes unnecessary conservatism and results in lower peak fluxes. The peak flux for nitrate is 4.03E-07 at year 1,000.

Table A-10. Predicted Peak Annual Fractional Fluxes Over 1,000 Years

Nuclide	Peak Annual Fractional Flux	Peak Time years
NO3	4.03E-07	1.00E+03
Al-26	4.21E-19	1.00E+03
Am-243	1.51E-67	1.00E+03
Np-239	5.70E-71	1.00E+03
Pu-239	1.19E-48	1.00E+03
Pu5-239	4.85E-52	1.00E+03
Bi-210	0.00E+00	
Po-210	0.00E+00	
C-14	2.05E-29	1.00E+03
Cf-249	1.03E-51	1.00E+03
Cm-245	6.86E-54	1.00E+03
Pu-241	2.04E-55	1.00E+03
Pu5-241	8.82E-59	1.00E+03
Am-241	5.76E-56	1.00E+03
Np-237	3.25E-31	1.00E+03
Cl-36	3.49E-29	1.00E+03
Cm-245	6.78E-78	1.00E+03
Pu-241	1.68E-60	1.00E+03
Pu5-241	7.35E-64	1.00E+03
Am-241	1.57E-60	1.00E+03
Np-237	6.87E-31	1.00E+03
Cm-246	6.35E-78	1.00E+03
Cm-247	7.37E-78	1.00E+03
Am-243	2.52E-72	1.00E+03
Np-239	9.55E-76	1.00E+03
Pu-239	1.02E-53	1.00E+03
Pu5-239	4.16E-57	1.00E+03
Cm-248	7.36E-78	1.00E+03
Pu-244	2.57E-50	1.00E+03
Pu5-244	1.05E-53	1.00E+03
Cs-135	6.05E-34	1.00E+03
Cs-137	4.54E-44	1.00E+03
H-3	4.03E-13	1.20E+02
I-129	1.75E-12	1.00E+03
K-40	1.26E-12	1.00E+03
Mo-93	2.21E-11	1.00E+03
Nb-93m	1.67E-15	1.00E+03
Nb-94	7.51E-34	1.00E+03
Nb-95m	0.00E+00	
Nb-95	0.00E+00	
Ni-59	1.48E-39	1.00E+03
Np-237	1.64E-29	1.00E+03
Pd-107	1.42E-23	1.00E+03
Pu-238	1.16E-50	1.00E+03
Pu5-238	4.74E-54	1.00E+03
U-234	2.68E-51	1.00E+03
Pu-239	3.50E-47	1.00E+03
Pu5-239	1.43E-50	1.00E+03
U-235	2.01E-50	1.00E+03
Pu-240	3.24E-47	1.00E+03
Pu5-240	1.32E-50	1.00E+03
U-236	6.86E-50	1.00E+03

Pu-241	2.92E-68	9.37E+02
Pu5-241	1.21E-71	9.35E+02
Am-241	2.26E-67	1.00E+03
Np-237	1.34E-29	1.00E+03
Pu-242	3.60E-47	1.00E+03
Pu5-242	1.47E-50	1.00E+03
U-238	1.33E-51	1.00E+03
Pu-244	3.61E-47	1.00E+03
Pu5-244	1.47E-50	1.00E+03
Ra-226	8.35E-41	1.00E+03
Rb-87	2.81E-22	1.00E+03
Se-79	2.07E-09	1.00E+03
Sn-126	1.23E-33	1.00E+03
Sr-90	4.32E-19	5.62E+02
Tc-99	1.03E-25	1.00E+03
Th-228	0.00E+00	
Ra-224	0.00E+00	
Th-229	9.84E-75	1.00E+03
Ra-225	3.56E-79	1.00E+03
Ac-225	2.69E-79	1.00E+03
Th-230	1.07E-74	1.00E+03
Ra-226	4.58E-44	1.00E+03
Pb-210	2.10E-44	1.00E+03
Po-210	6.71E-46	1.00E+03
Th-232	1.08E-74	1.00E+03
Ra-228	6.35E-78	1.00E+03
Th-228	3.40E-79	1.00E+03
Ra-224	1.14E-80	1.00E+03
U-232	9.50E-59	1.00E+03
Th-228	6.16E-61	1.00E+03
Ra-224	2.07E-62	1.00E+03
U-233	2.67E-54	1.00E+03
Th-229	8.11E-59	1.00E+03
Ra-225	2.89E-63	1.00E+03
U-234	2.67E-54	1.00E+03
Th-230	5.26E-59	1.00E+03
Ra-226	6.99E-48	1.00E+03
Pb-210	3.64E-48	1.00E+03
Po-210	1.16E-49	1.00E+03
U-235	2.68E-54	1.00E+03
Pa-231	1.68E-56	1.00E+03
Ac-227	1.98E-59	1.00E+03
Th-227	6.52E-63	1.00E+03
Ra-223	2.55E-62	1.00E+03
U-236	2.68E-54	1.00E+03
U-238	2.68E-54	1.00E+03
Th-234	9.87E-66	1.00E+03
U-234	4.23E-61	1.00E+03
Zr-93	9.05E-53	1.00E+03
Nb-93m	1.17E-51	1.00E+03
Zr-95	0.00E+00	
Nb-95	0.00E+00	

Predicted flux and cumulative release history for contaminants listed in Table A-10 having a predicted peak flux greater than 1E-30 are depicted in Figures A-13 through A-25. The units mol/yr/mol that are specified on the figures are equivalent to Ci/yr/Ci for radionuclides.

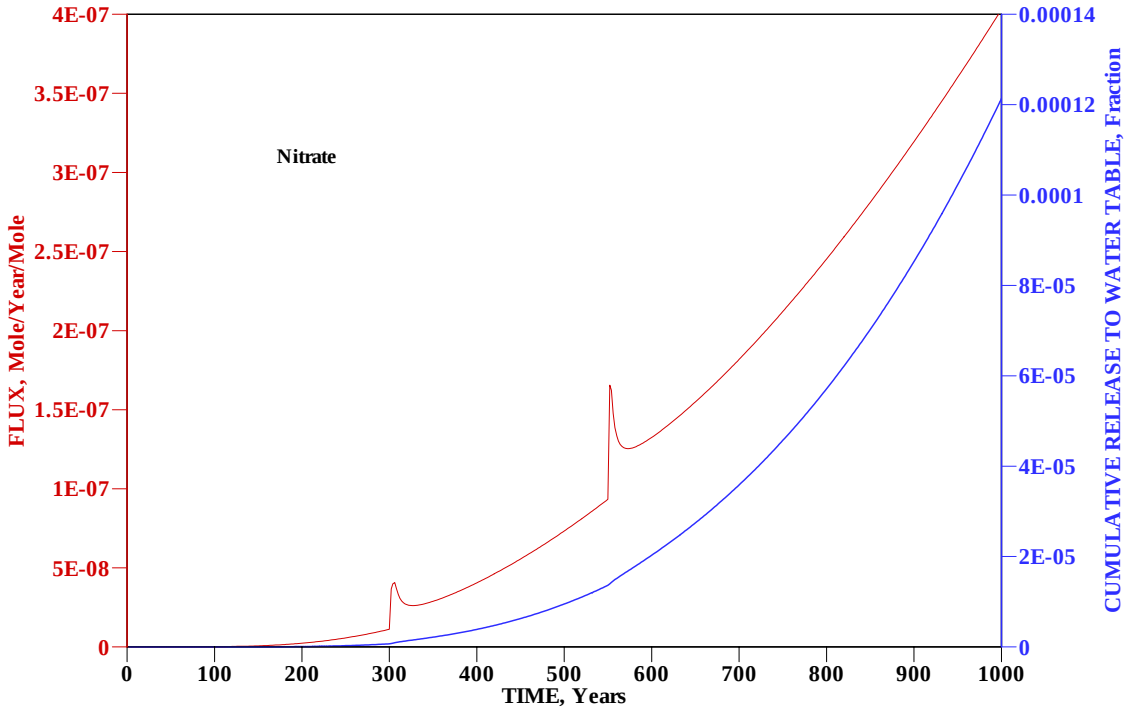

Figure A-13. Predicted Peak Nitrate Flux and Cumulative Release in 1000 Years

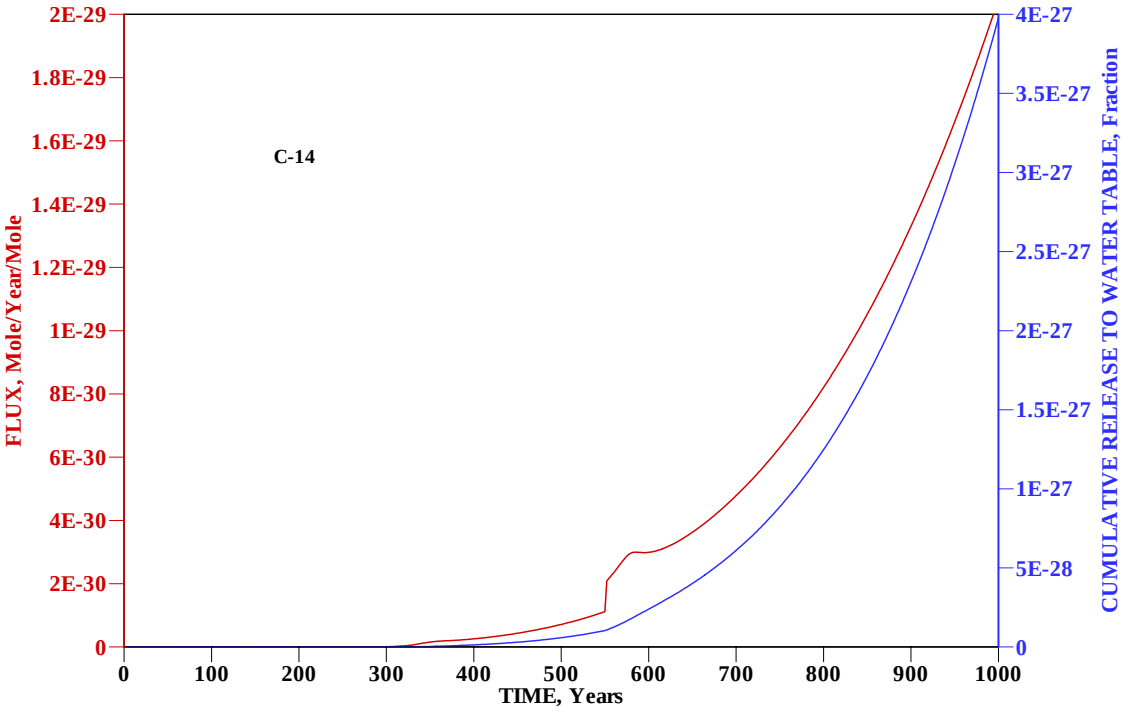

Figure A-14. Predicted Peak C-14 Flux and Cumulative Release in 1000 Years

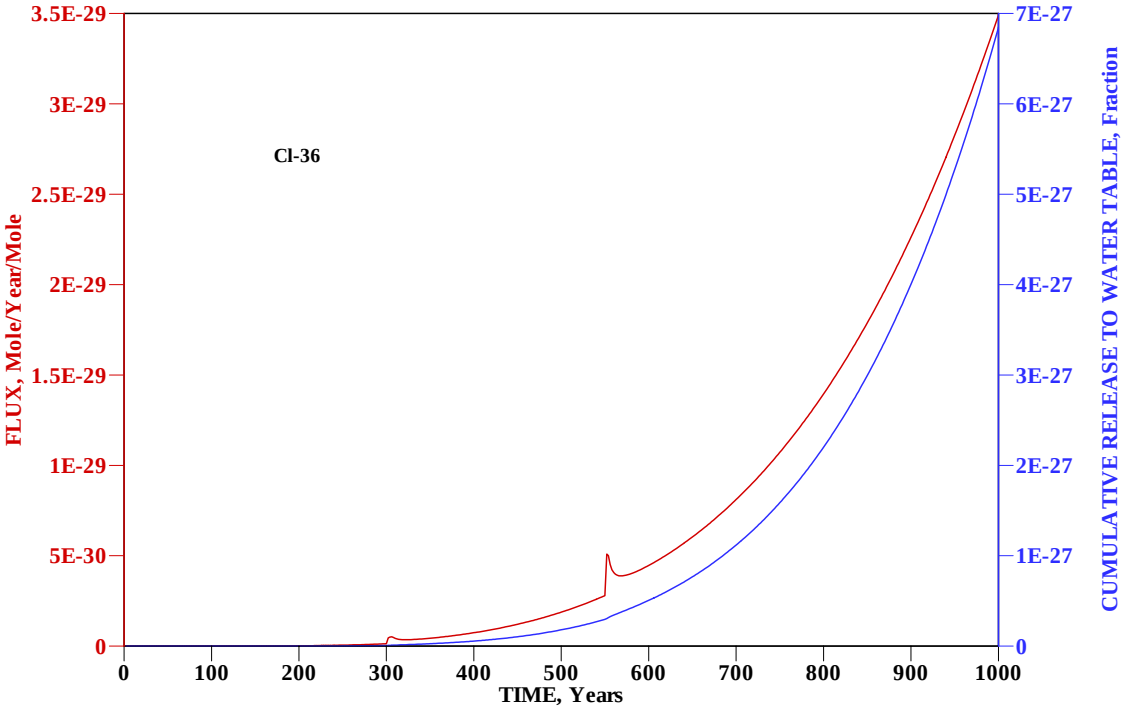

Figure A-15. Predicted Peak Cl-36 Flux and Cumulative Release in 1000 Years

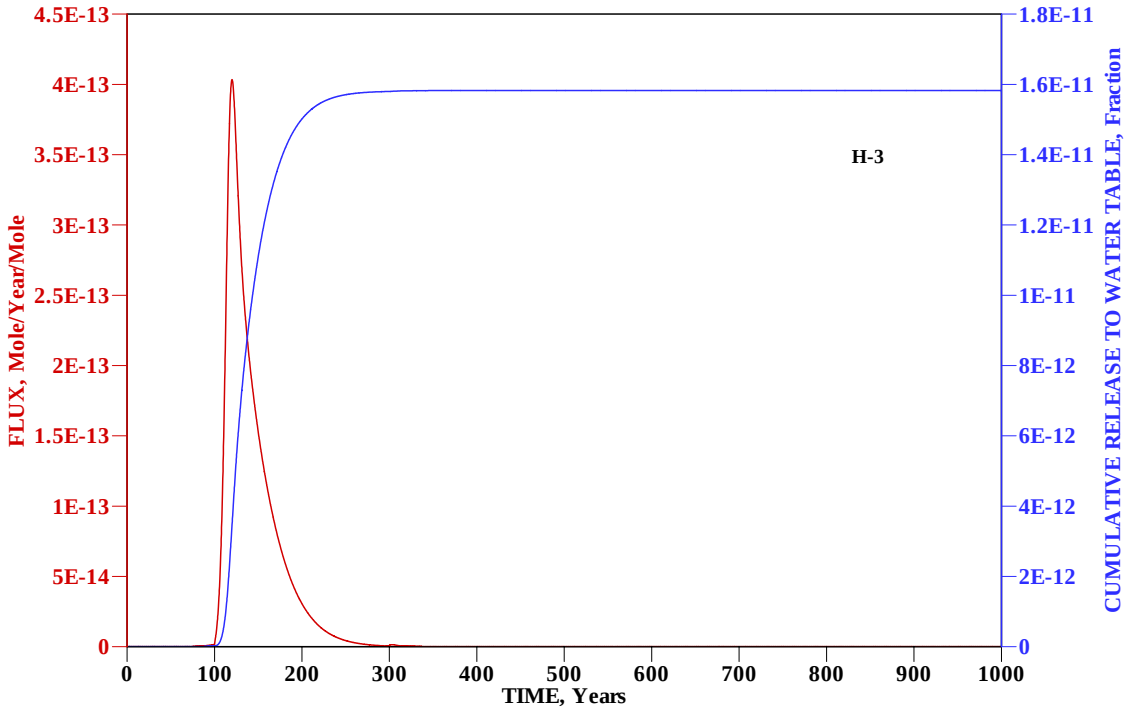

Figure A-16. Predicted Peak H-3 Flux and Cumulative Release in 1000 Years

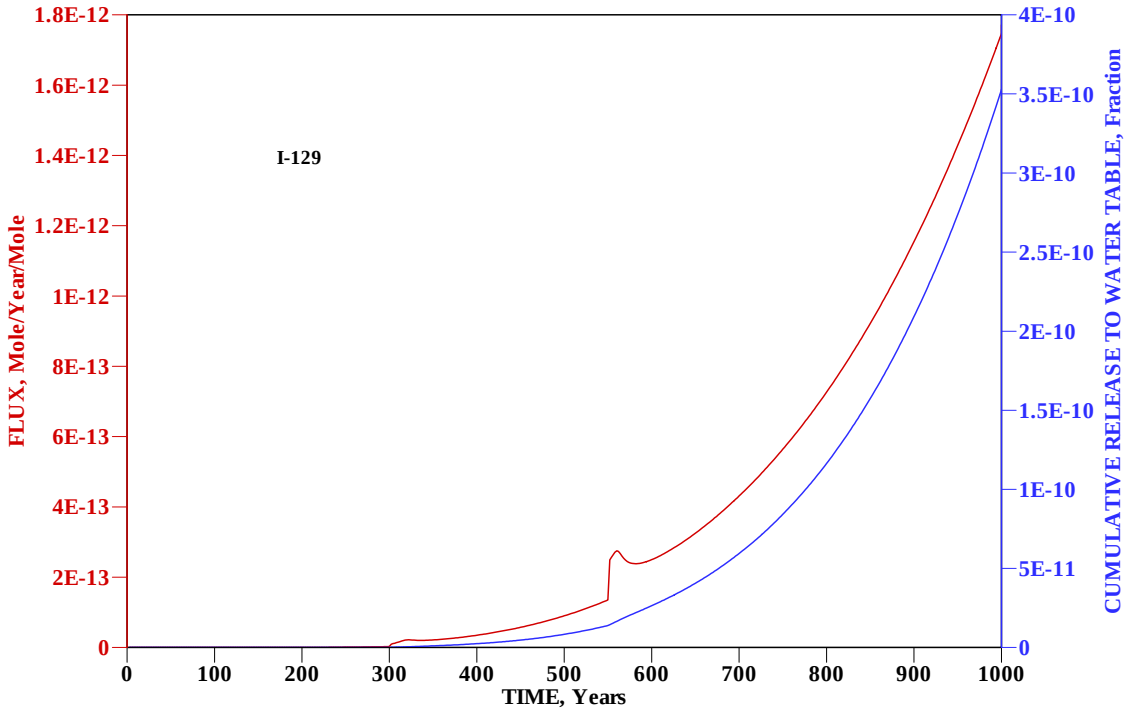

Figure A-17. Predicted Peak I-129 Flux and Cumulative Release in 1000 Years

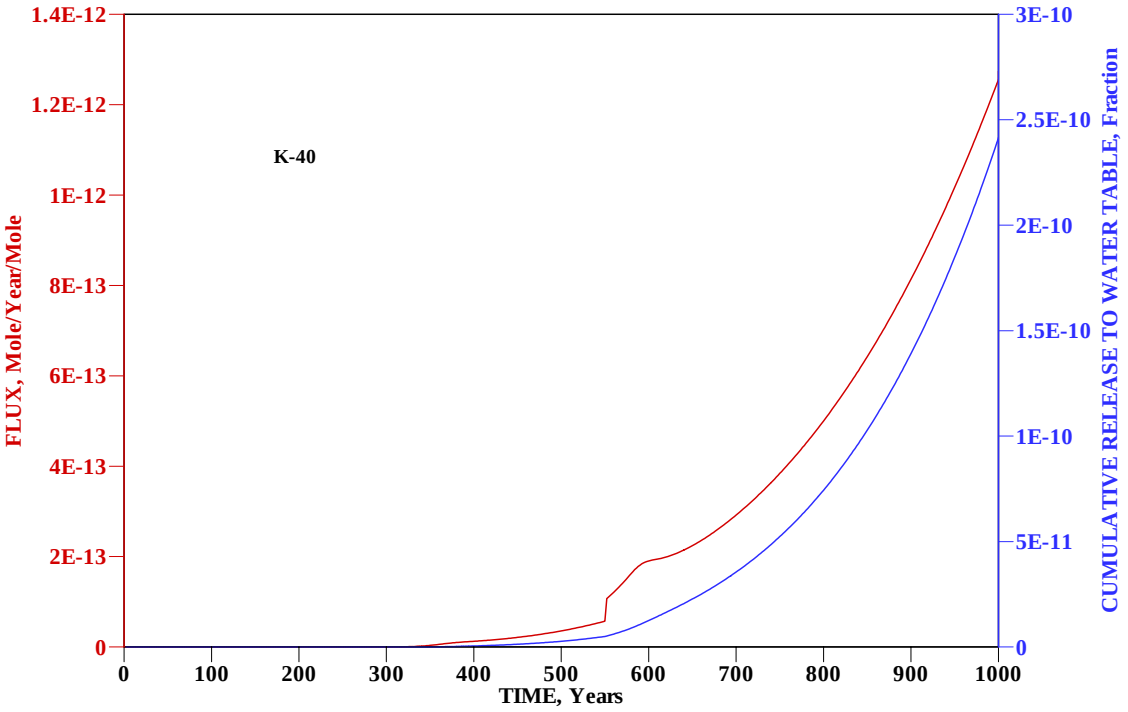

Figure A-18. Predicted Peak K-40 Flux and Cumulative Release in 1000 Years

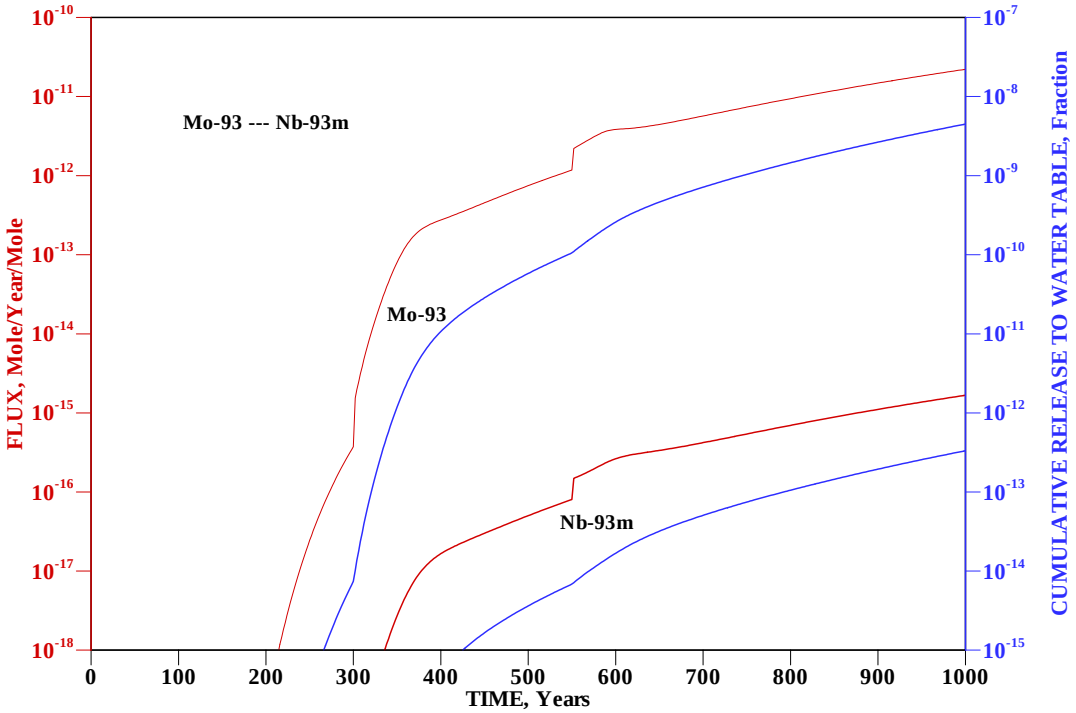

Figure A-19. Predicted Peak Mo-93-Nb93m Flux and Cumulative Release in 1000 Years

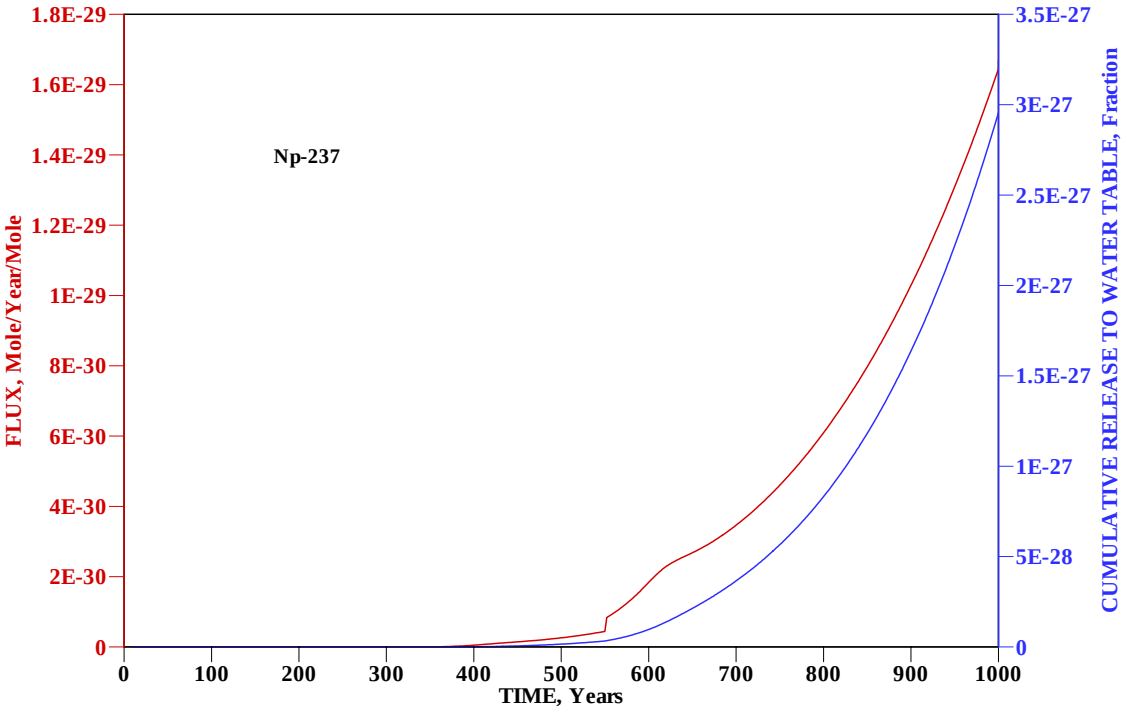

Figure A-20. Predicted Peak Np-237 Flux and Cumulative Release in 1000 Years

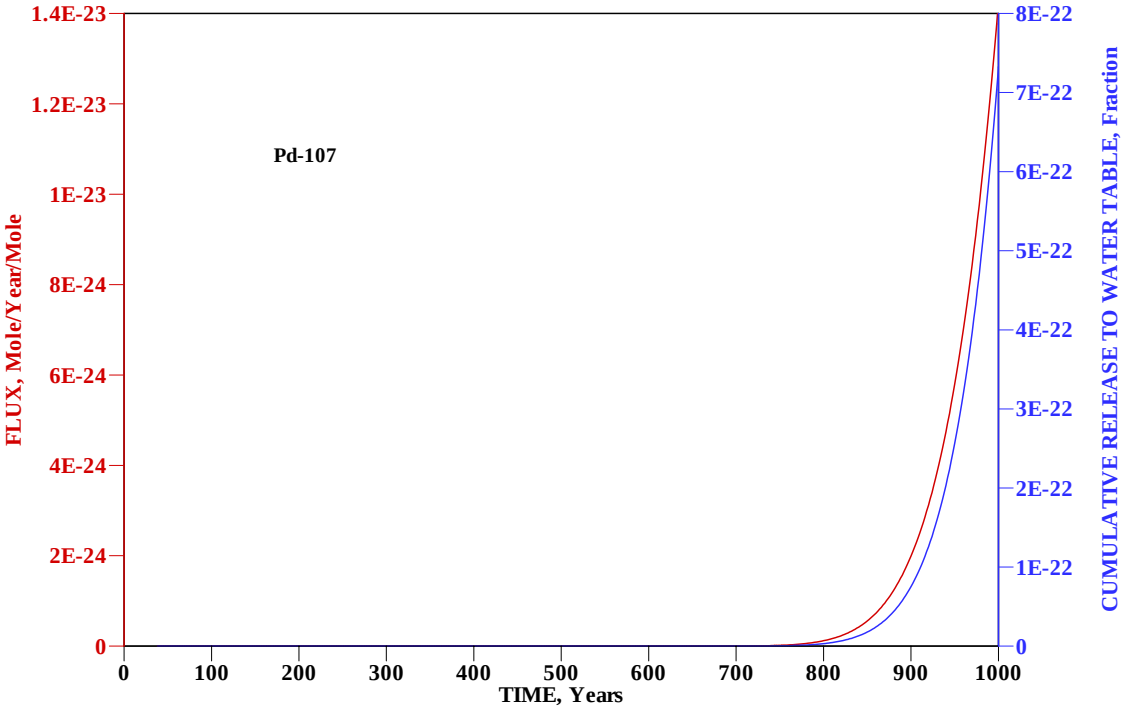

Figure A-21. Predicted Peak Pd-107 Flux and Cumulative Release in 1000 Years

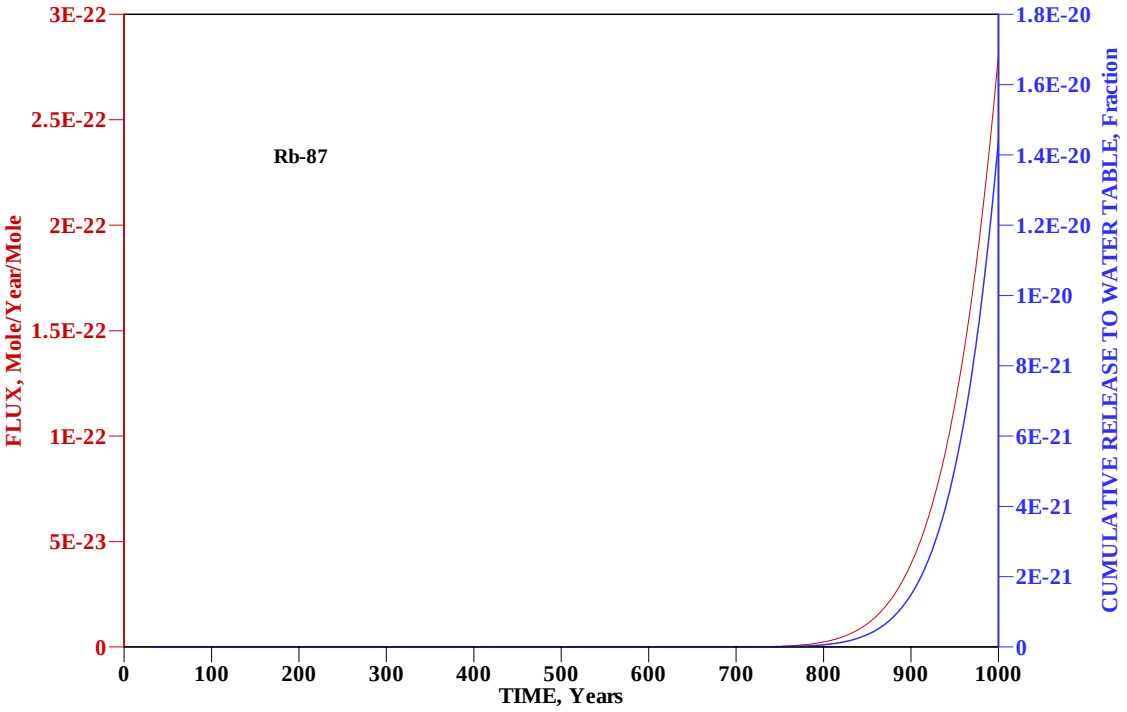

Figure A-22. Predicted Peak Rb-87 Flux and Cumulative Release in 1000 Years

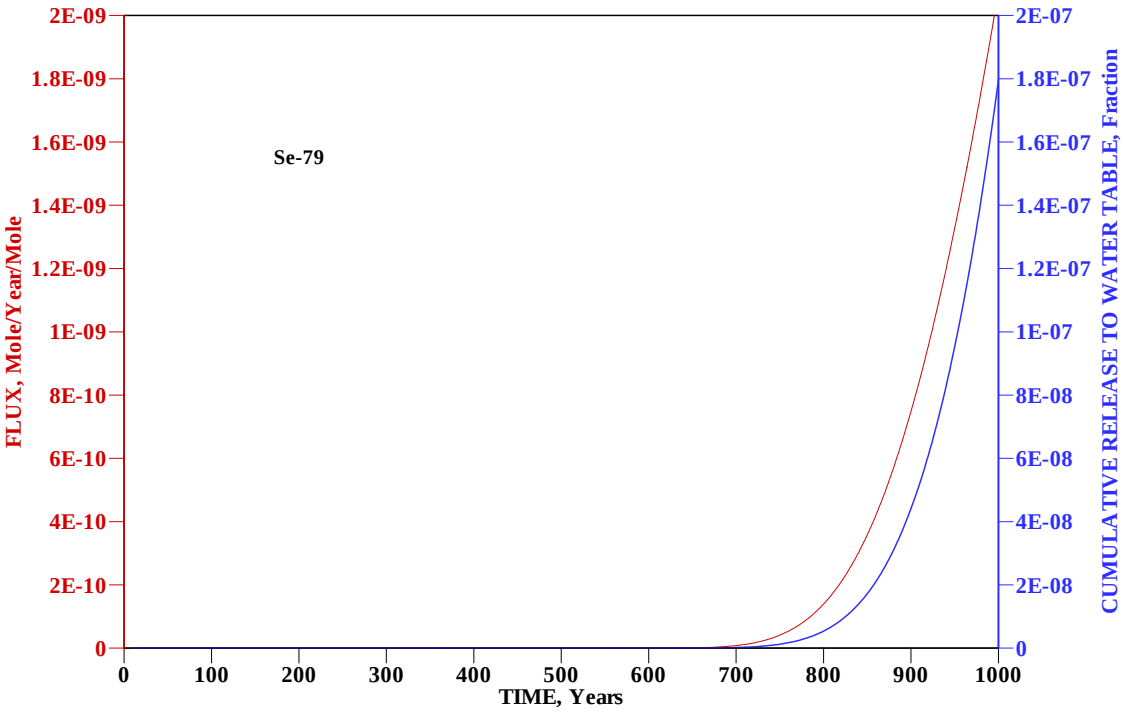

Figure A-23. Predicted Peak Se-79 Flux and Cumulative Release in 1000 Years

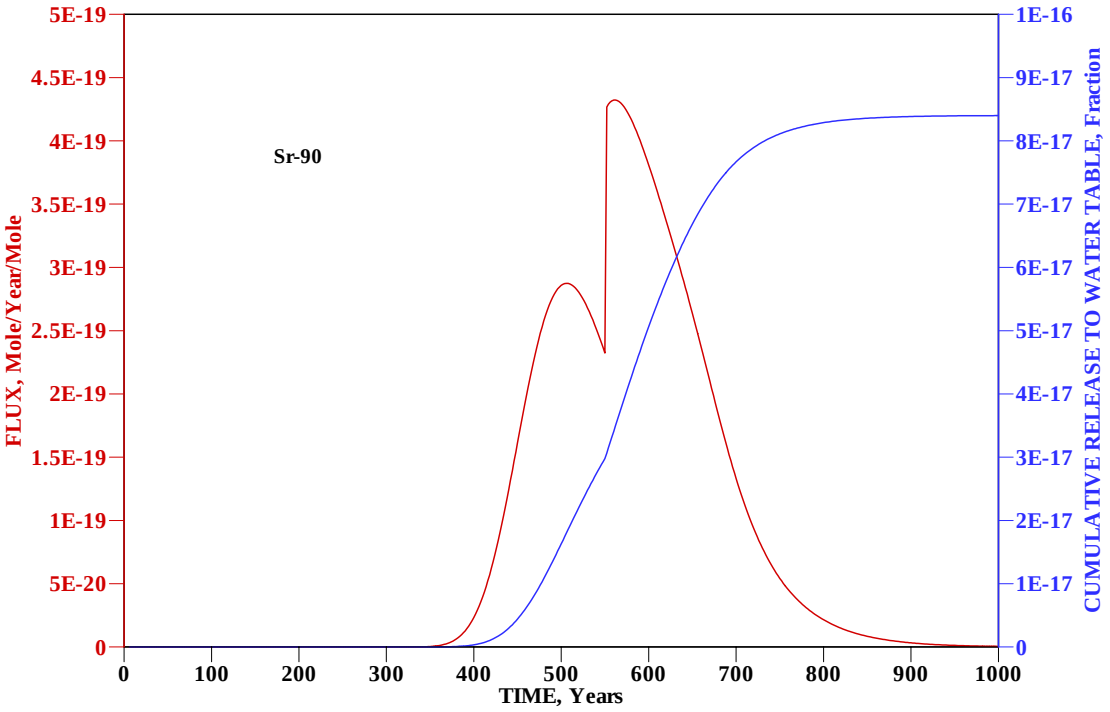

Figure A-24. Predicted Peak Sr-90 Flux and Cumulative Release in 1000 Years

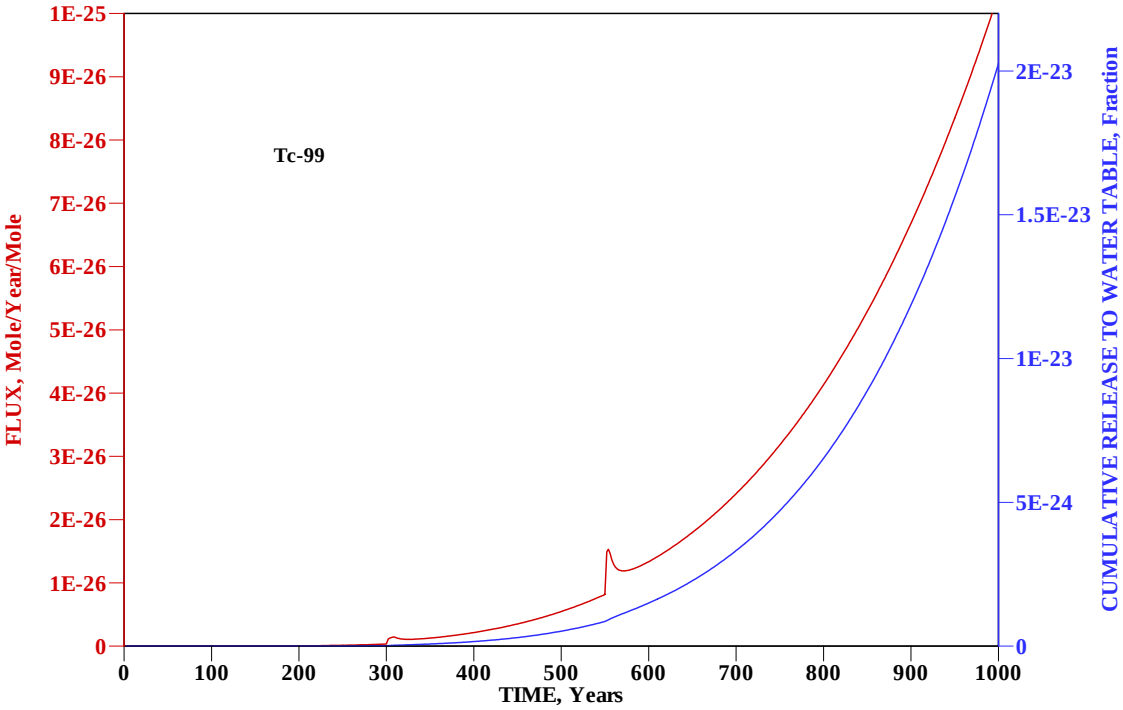

Figure A-25. Predicted Peak Tc-99 Flux and Cumulative Release in 1000 Years

Unsaturated zone flow and transport modeling for the four time intervals TI05 through TI08 (1,000 through 10,000 years) are also performed. Predicted peak fluxes from 0 to 10,000 years are shown in Table A-11. The peak fractional flux for nitrate is 3.2410^{-5} at year 9,800. Since nitrate is a conservative tracer, all of the long-lived contaminants should have lower peak fluxes and longer peak times, as shown in Table A-11.

Table A-11. Predicted Peak Fluxes over 10,000 Years

Nuclides	Peak Flux mol/yr/mol	Peak Time years
NO3	3.24E-05	9.80E+03
Al-26	5.49E-13	1.00E+04
Am-243	1.43E-32	1.00E+04
Np-239	4.53E-36	1.00E+04
Pu-239	4.53E-27	1.00E+04
Pu5-239	1.65E-30	1.00E+04
Bi-210	0.00E+00	
Po-210	0.00E+00	
C-14	3.44E-24	1.00E+04
Cf-249	3.71E-34	5.76E+03
Cm-245	7.17E-34	1.00E+04
Pu-241	1.38E-35	1.00E+04
Pu5-241	5.06E-39	1.00E+04
Am-241	1.07E-34	1.00E+04
Np-237	3.82E-24	1.00E+04
Cl-36	1.88E-23	1.00E+04
Cm-245	1.24E-38	1.00E+04
Pu-241	4.48E-40	1.00E+04
Pu5-241	1.75E-43	1.00E+04
Am-241	2.32E-37	1.00E+04
Np-237	3.96E-24	1.00E+04
Cm-246	6.54E-39	1.00E+04
Cm-247	2.82E-38	1.00E+04
Am-243	2.40E-36	1.00E+04
Np-239	7.62E-40	1.00E+04
Pu-239	9.20E-31	1.00E+04
Pu5-239	3.34E-34	1.00E+04
Cm-248	2.76E-38	1.00E+04
Pu-244	1.58E-28	1.00E+04
Pu5-244	5.76E-32	1.00E+04
Cs-135	1.10E-14	1.00E+04
Cs-137	1.42E-41	1.46E+03
H-3	4.03E-13	1.20E+02
I-129	1.29E-07	1.00E+04
K-40	6.97E-08	1.00E+04
Mo-93	8.21E-08	1.00E+04
Nb-93m	6.72E-12	1.00E+04
Nb-94	3.33E-21	1.00E+04
Nb-95m	0.00E+00	
Nb-95	0.00E+00	
Ni-59	2.37E-18	1.00E+04
Np-237	7.25E-24	1.00E+04
Pd-107	1.25E-16	1.00E+04
Pu-238	5.59E-42	2.60E+03
Pu5-238	2.07E-45	2.60E+03
U-234	4.13E-26	1.00E+04
Pu-239	7.75E-27	1.00E+04
Pu5-239	2.81E-30	1.00E+04
U-235	1.83E-27	1.00E+04
Pu-240	3.59E-27	1.00E+04
Pu5-240	1.30E-30	1.00E+04

U-236	5.85E-27	1.00E+04
Pu-241	3.93E-68	1.06E+03
Pu5-241	1.64E-71	1.06E+03
Am-241	4.00E-39	1.00E+04
Np-237	7.25E-24	1.00E+04
Pu-242	1.01E-26	1.00E+04
Pu5-242	3.68E-30	1.00E+04
U-238	1.26E-28	1.00E+04
Pu-244	1.03E-26	1.00E+04
Pu5-244	3.75E-30	1.00E+04
Ra-226	5.55E-19	1.00E+04
Rb-87	2.38E-15	1.00E+04
Se-79	7.11E-07	1.00E+04
Sn-126	2.03E-22	1.00E+04
Sr-90	4.32E-19	5.62E+02
Tc-99	5.61E-20	1.00E+04
Th-228	0.00E+00	
Ra-224	0.00E+00	
Th-229	1.21E-36	1.00E+04
Ra-225	4.32E-41	1.00E+04
Ac-225	3.23E-41	1.00E+04
Th-230	2.85E-36	1.00E+04
Ra-226	8.04E-21	1.00E+04
Pb-210	2.16E-22	1.00E+04
Po-210	6.60E-24	1.00E+04
Th-232	3.13E-36	1.00E+04
Ra-228	9.13E-45	1.00E+04
Th-228	4.74E-46	1.00E+04
Ra-224	1.59E-47	1.00E+04
U-232	2.38E-48	2.79E+03
Th-228	1.66E-50	2.80E+03
Ra-224	5.58E-52	2.80E+03
U-233	4.45E-26	1.00E+04
Th-229	5.04E-29	1.00E+04
Ra-225	1.79E-33	1.00E+04
U-234	4.52E-26	1.00E+04
Th-230	3.58E-29	1.00E+04
Ra-226	2.86E-23	1.00E+04
Pb-210	7.72E-25	1.00E+04
Po-210	2.36E-26	1.00E+04
U-235	4.65E-26	1.00E+04
Pa-231	1.09E-30	1.00E+04
Ac-227	8.86E-34	1.00E+04
Th-227	2.93E-37	1.00E+04
Ra-223	1.15E-36	1.00E+04
U-236	4.65E-26	1.00E+04
U-238	4.65E-26	1.00E+04
Th-234	1.72E-37	1.00E+04
U-234	7.12E-32	1.00E+04
Zr-93	2.22E-27	1.00E+04
Nb-93m	9.19E-32	1.00E+04
Zr-95	0.00E+00	
Nb-95	0.00E+00	

The curves showing fractional rates (or fluxes in mole/year/mole) and cumulative release (in mole/mole) for the entire 10,000 years are depicted in Figures A-26 through A-38. The peak flux for nitrate (Figure A-26) is 3.24×10^{-5} year^{-1}. About 16% of the initial amount of nitrate is released to the water table in 10,000 years. In the following figures, the red curves are fluxes. The blue curves are cumulative releases. Contaminant names are shown in each of the respective plots.

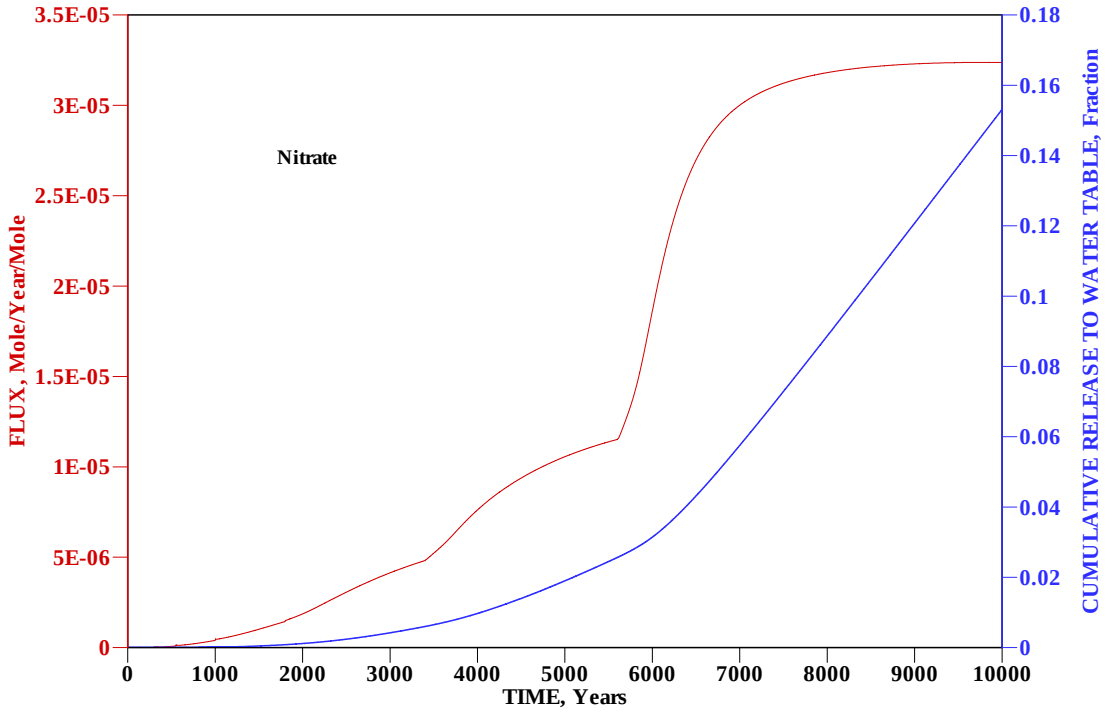

Figure A-26. Predicted Peak Flux and Cumulative Release for Nitrate in 10,000 Years

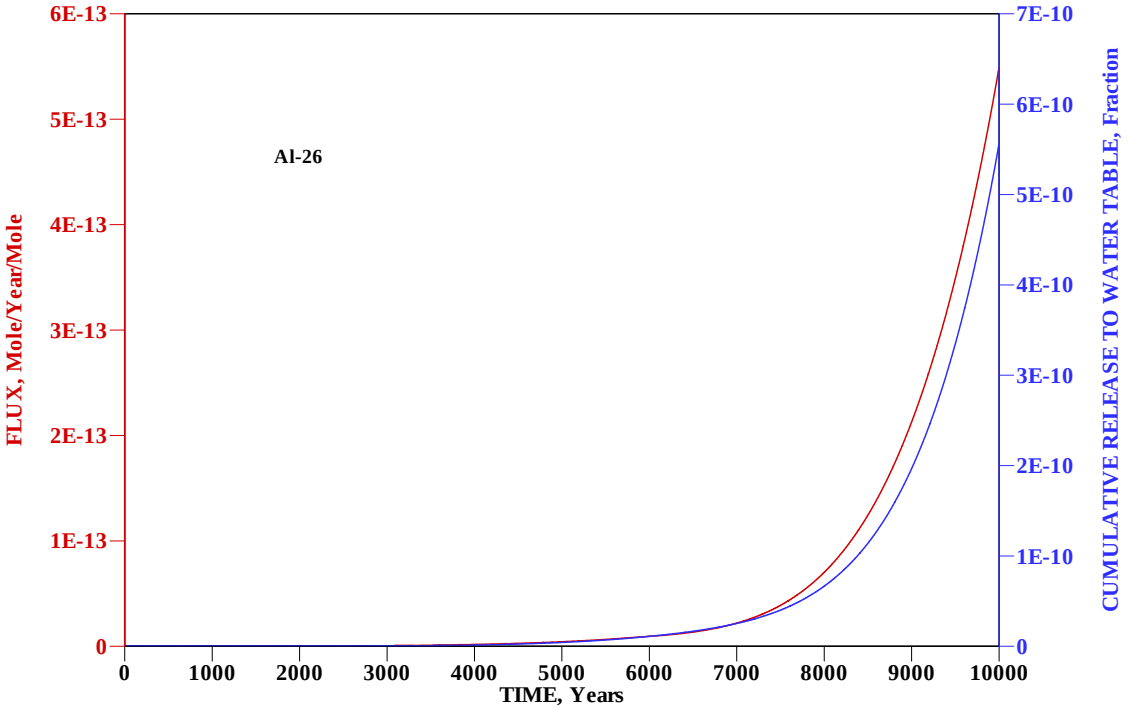

Figure A-27. Predicted Peak Flux and Cumulative Release for Al-26 in 10,000 Years

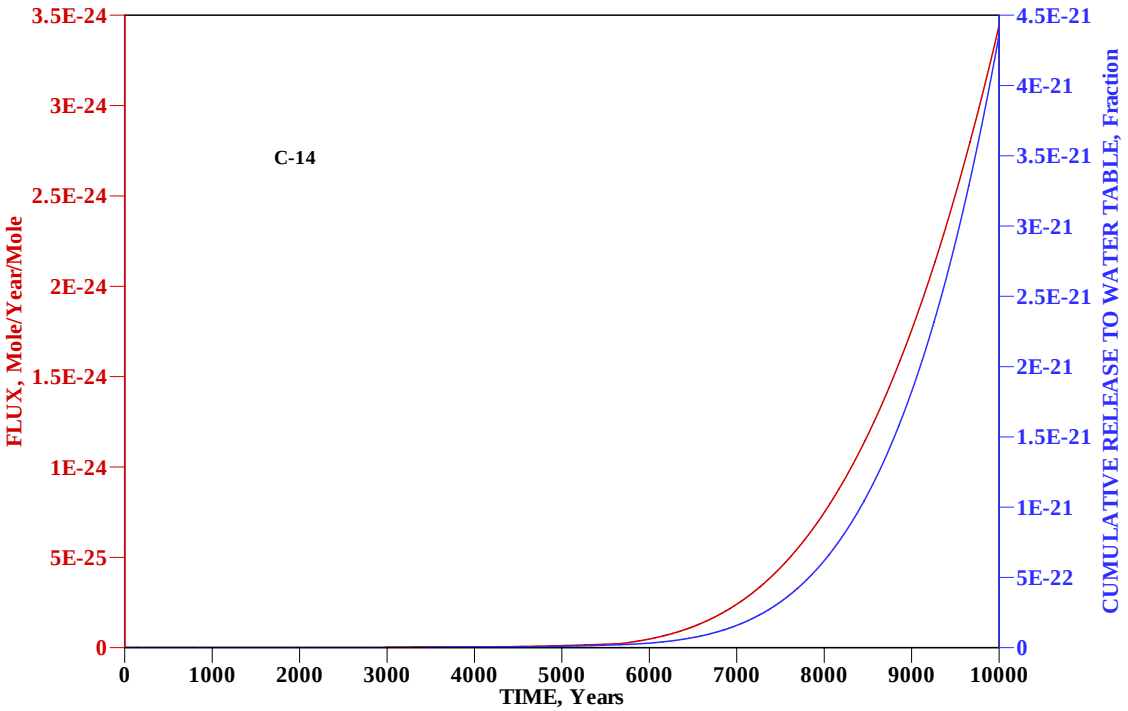

Figure A-28. Predicted Peak Flux and Cumulative Release for C-14 in 10,000 Years

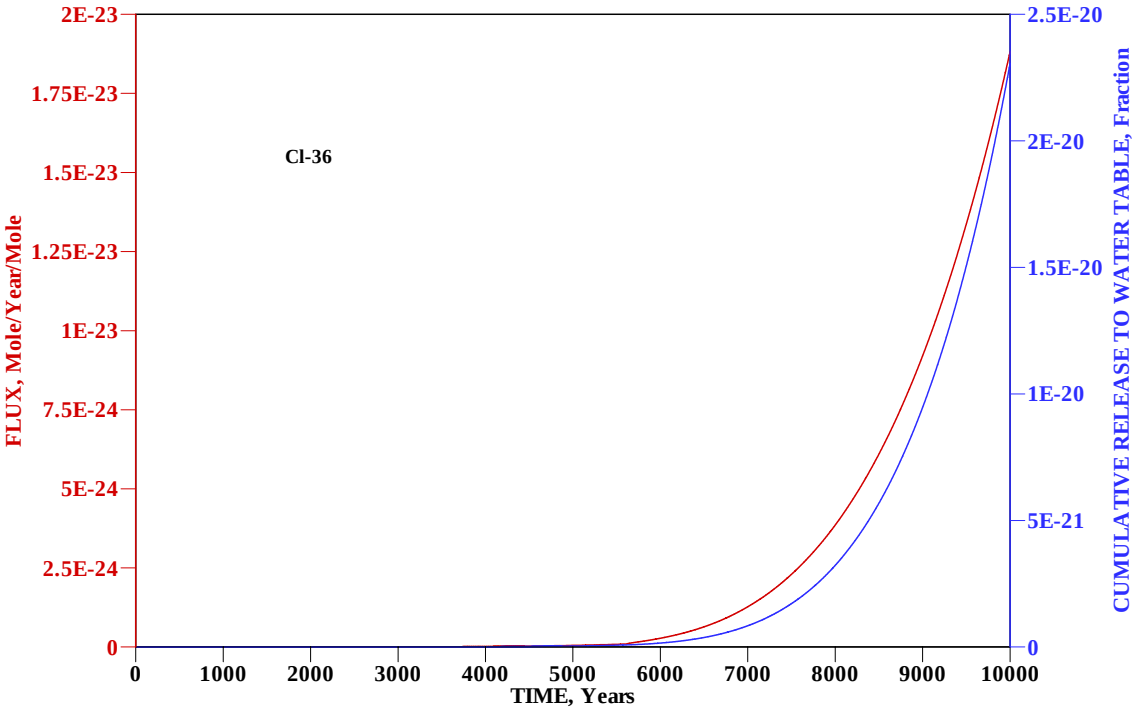

Figure A-29. Predicted Peak Flux and Cumulative Release for Cl-36 in 10,000 Years

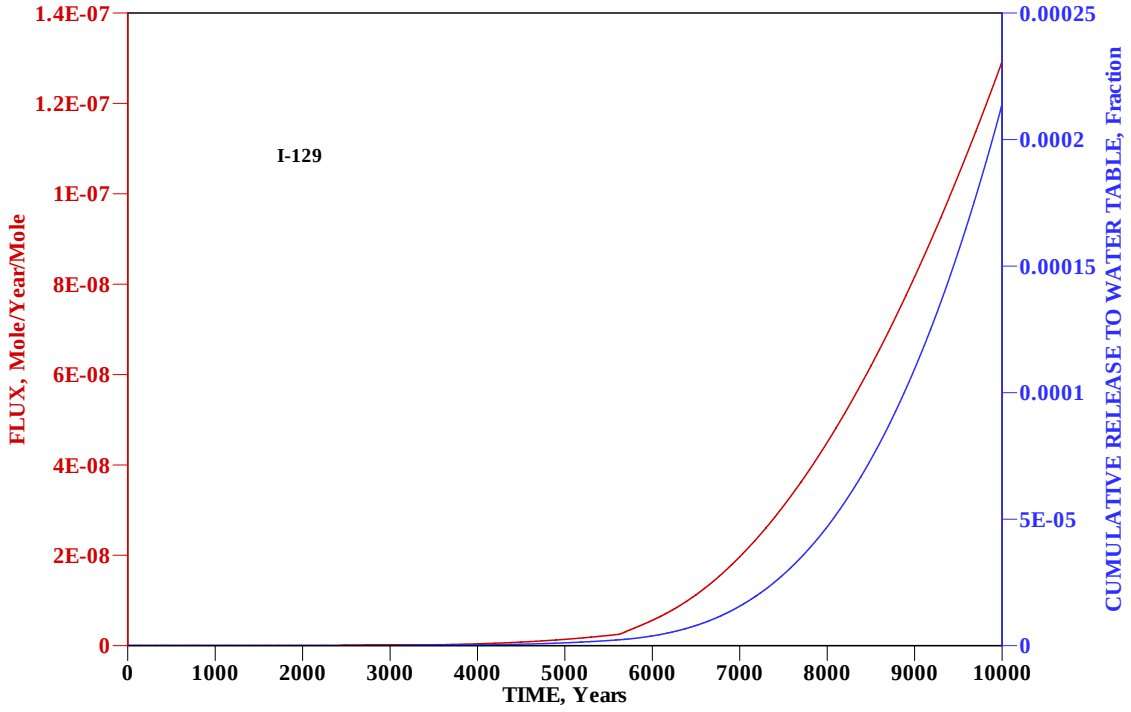

Figure A-30. Predicted Peak Flux and Cumulative Release for I-129 in 10,000 Years

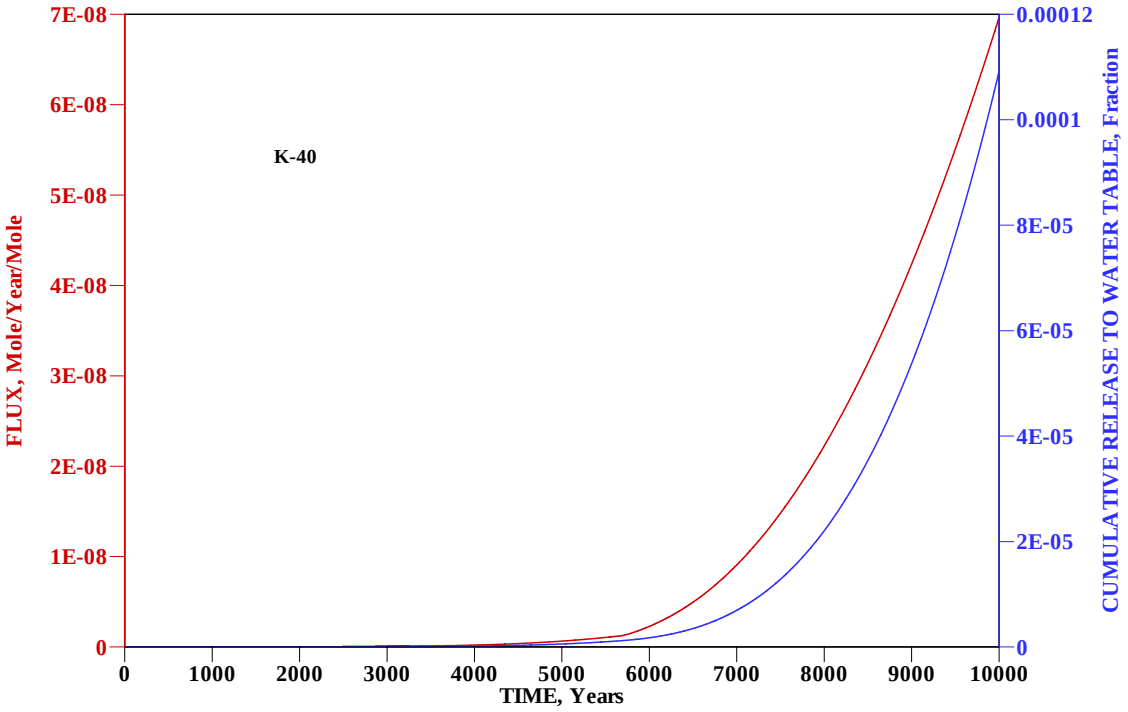

Figure A-31. Predicted Peak Flux and Cumulative Release for K-40 in 10,000 Years

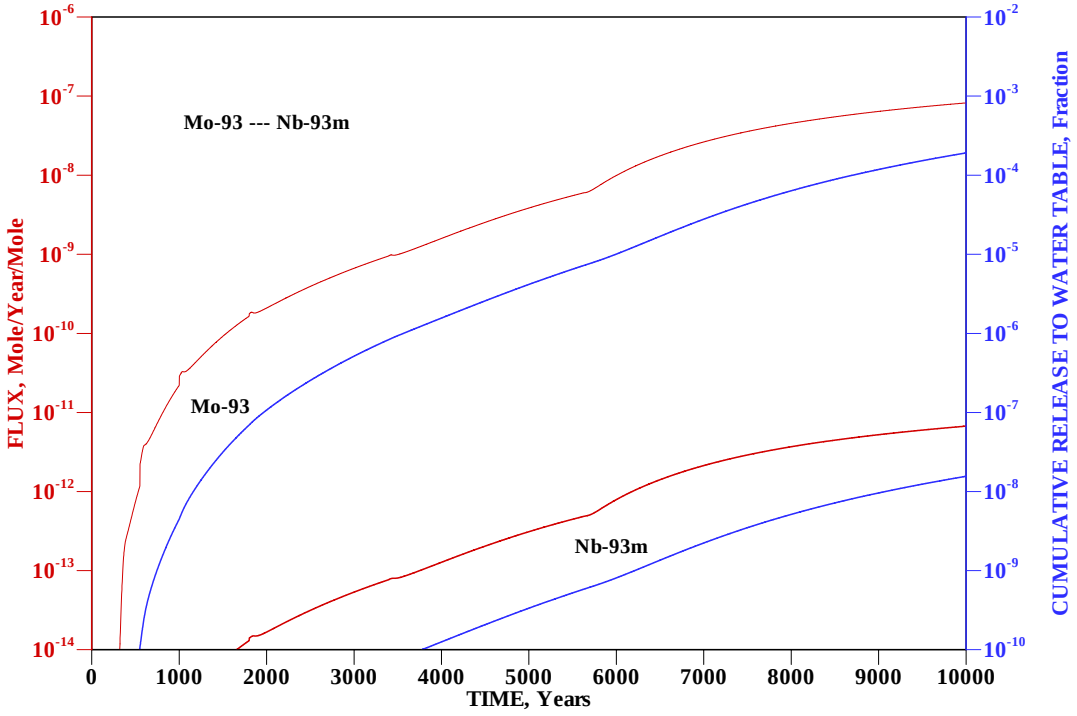

Figure A-32. Predicted Peak Flux and Cumulative Release for Mo-93-Nb-93m in 10,000 Years

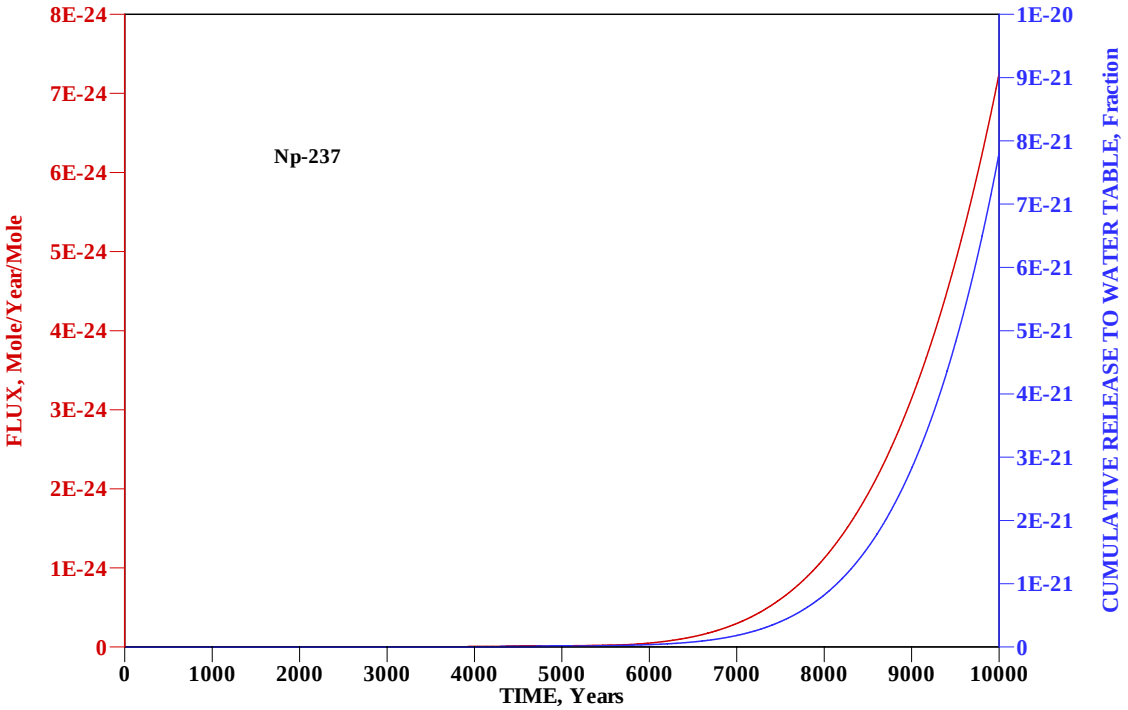

Figure A-33. Predicted Peak Flux and Cumulative Release for Np-237 in 10,000 Years

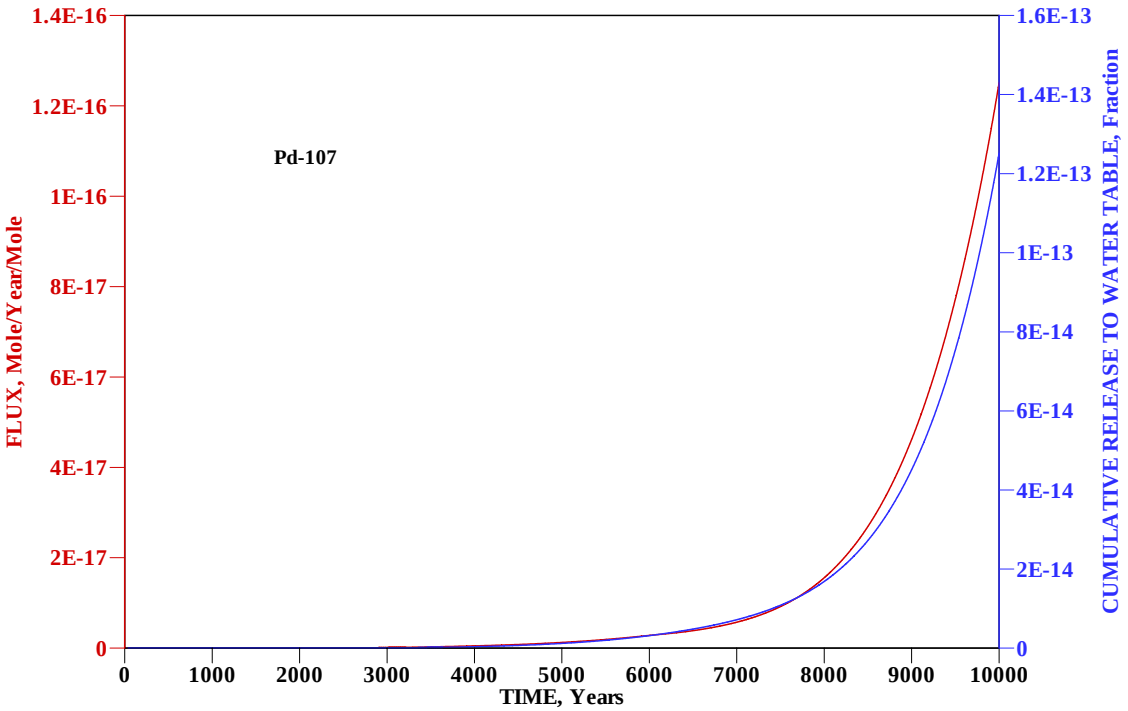

Figure A-34. Predicted Peak Flux and Cumulative Release for Pd-107 in 10,000 Years

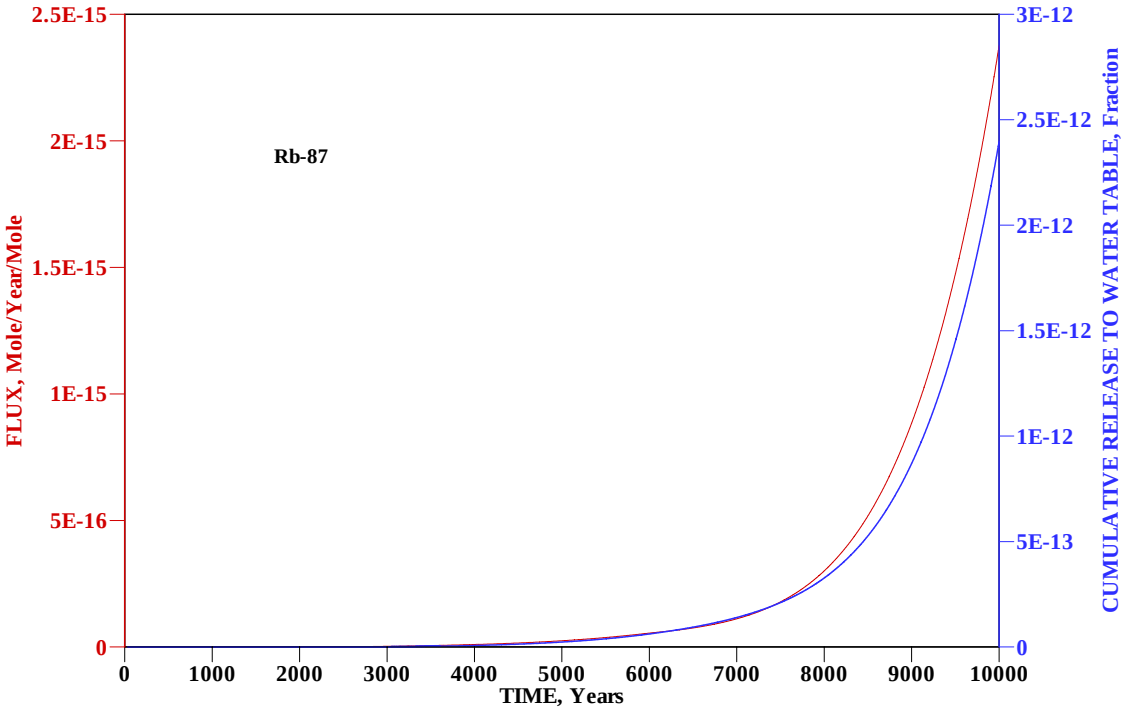

Figure A-35. Predicted Peak Flux and Cumulative Release for Rb-87 in 10,000 Years

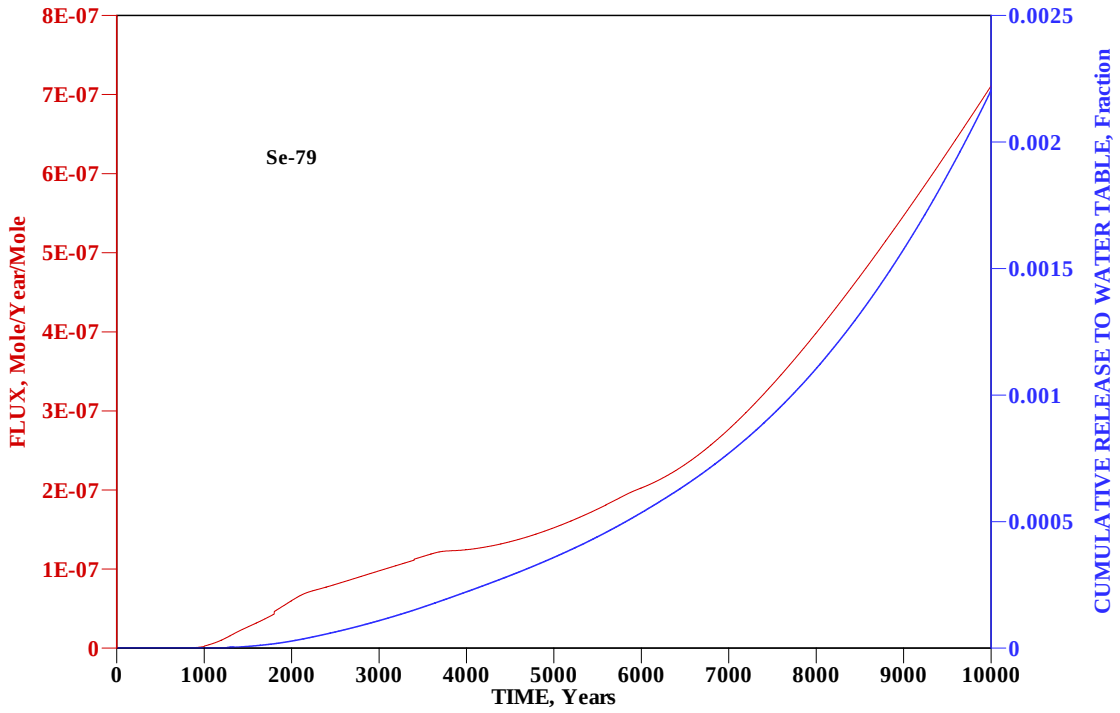

Figure A-36. Predicted Peak Flux and Cumulative Release for Se-79 in 10,000 Years

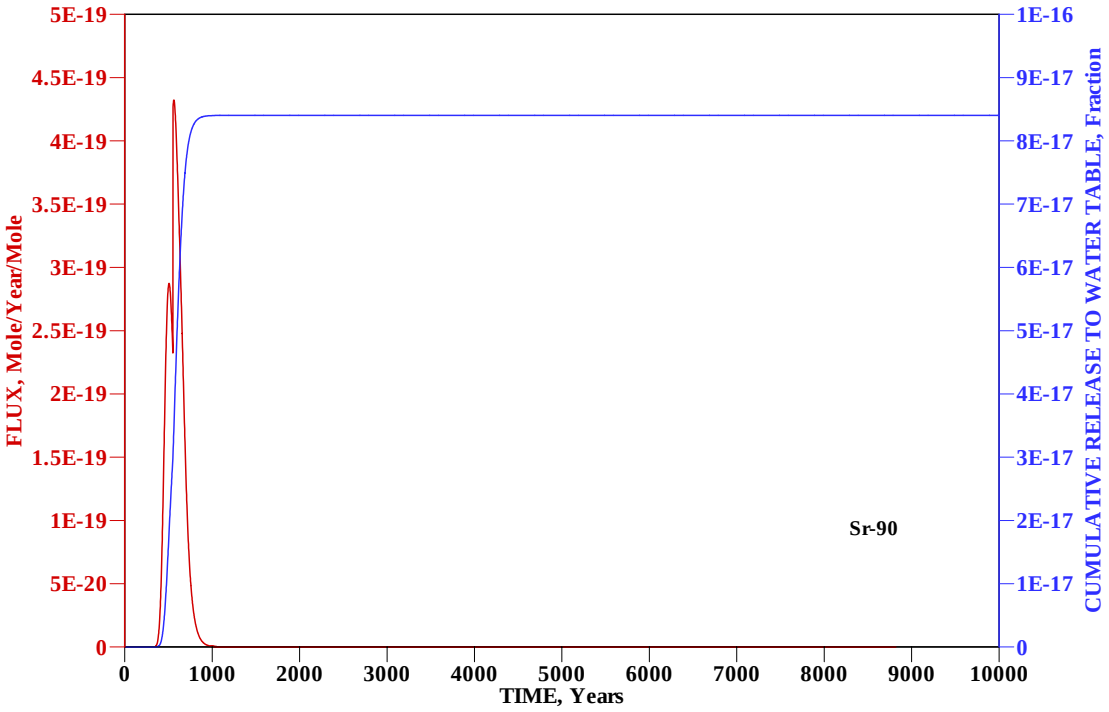

Figure A-37. Predicted Peak Flux and Cumulative Release for Sr-90 in 10,000 Years

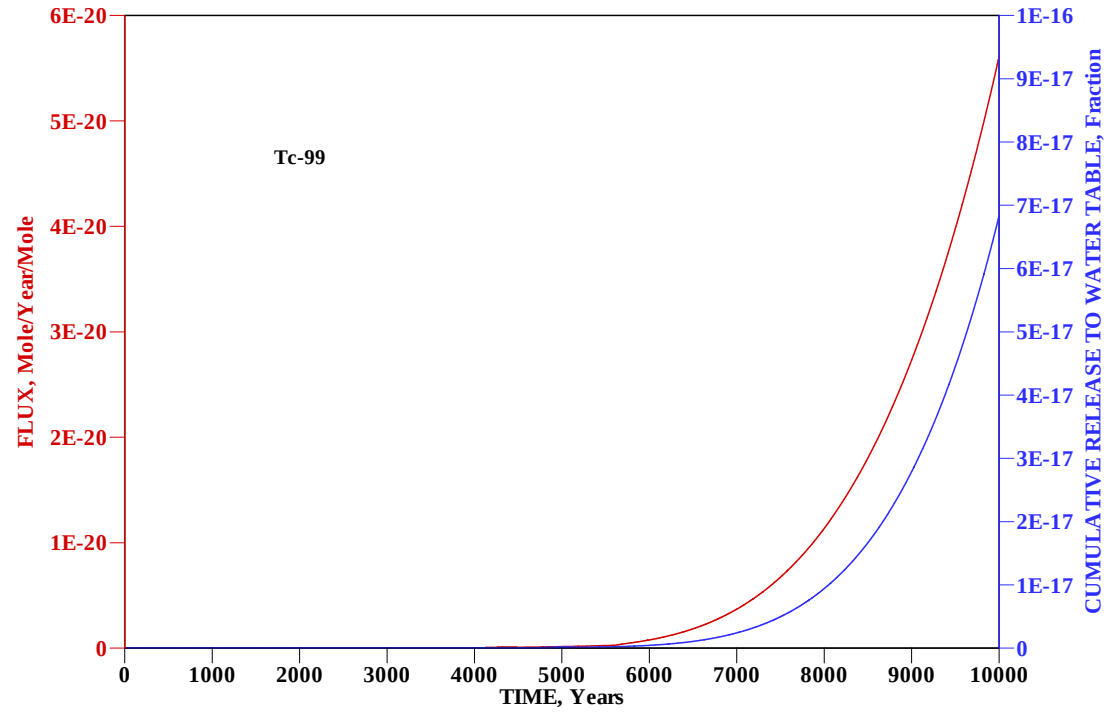

Figure A-38. Predicted Peak Flux and Cumulative Release for Tc-99 in 10,000 Years

A.2.10 Contaminant Migration Mechanisms

The basic concept of the SDF is controlled release of contaminants. Due to the low hydraulic conductivity of Saltstone and concrete, convective transport is well under control. The drain layer removes perched water above the vault. This is a key design feature to reduce water infiltration through the Saltstone monolith. When the facility is intact, the predominant contaminant release mechanism is diffusion. As time goes on, the closure cap, the drain layer and the Saltstone flow properties degrade to cause more water percolating through the closure cap and Saltstone monolith. Convective transport becomes increasingly important as indicated by the increasing water velocity through the Saltstone. Due to these contaminant transport mechanisms, it is necessary to use multiple time intervals to simulate the progressive degradation of the SDF in order to obtain accurate and yet still conservative contaminant release rates.

Most of the radionuclides are adsorbed within the Saltstone, concrete and soil zones. Retardation due to K_d accounts for the extremely slow release rates for most of the radionuclides under investigation. As a result, Saltstone Vault No. 4 should have relatively high disposal limits for all radionuclides.

Some of the contaminants are relatively short lived. These contaminants would decay into insignificant amounts before reaching the water table. However, due to their higher radioactivity, they may be of more significance in the intruder scenarios rather than groundwater concerns.

The contaminant transport mechanisms can be illustrated by the concentration contour plots. For example, the normalized nitrate concentration profile at 1,000 years is shown in Figure A-39. From these "snap shots", the progressive migration of nitrate from Saltstone to the water table can be visualized.

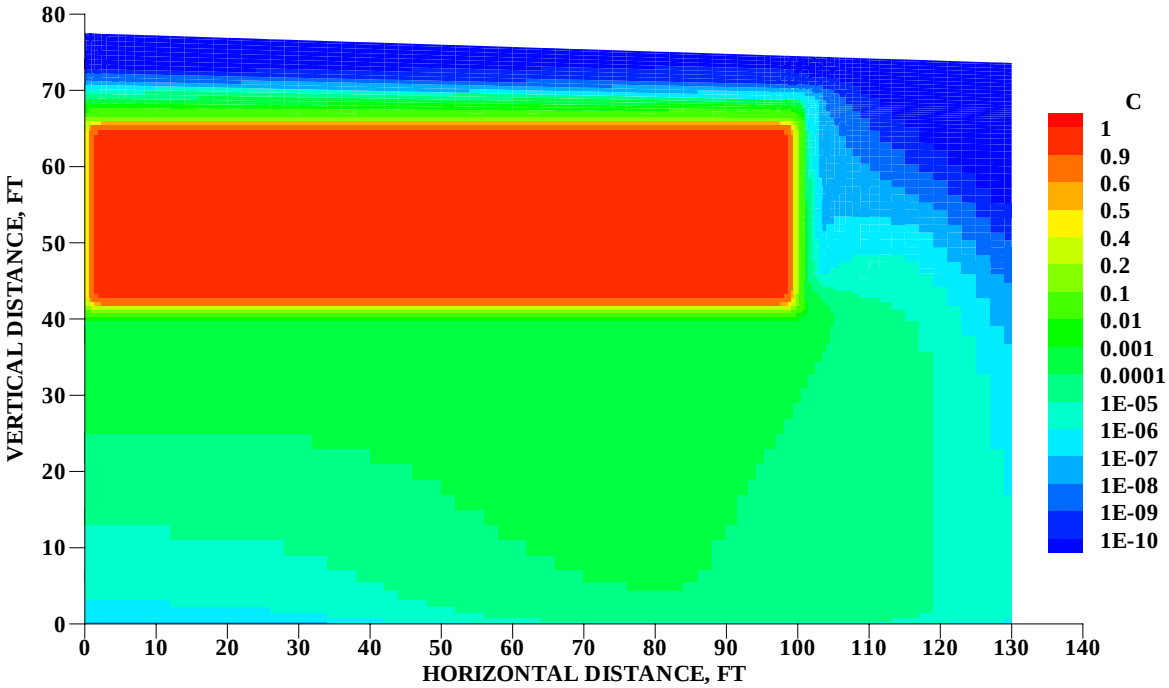

Figure A-39. Predicted Nitrate Concentration Profile at 1,000 Years

A.3 SALTSTONE VAULT NUMBER 4 SATURATED ZONE GROUNDWATER MODELING

A.3.1 Conceptual Model and Modeling Grid

A saturated-zone flow model of the GSA at SRS has been developed using the PORFLOW code (Flach, 2004). The flow model incorporated detailed site-specific hydrogeologic data. In order to cut down computer run time, a grid system of reduced x- y- and z-dimensions is used to simulate contaminant transport in the Z-area. An aerial view of the reduced modeling domain is depicted in Figure A-40.

Figure A-40 depicts the gridding of the model area. The grid lines are the faces of the finite element cells. There are 22, 20, and 14 cell blocks in the x-, y- and z- directions, respectively. According to PORFLOW notation, the center of each cubic cell is a node point. However, the first node is lower boundary and the last node is at the higher boundary. These two nodes are 'inactive nodes' because the flow vectors in these nodes do not affect contaminant transport rates. Using this notation, the x- y- and z-dimensions have 24, 22 and 16 nodes, respectively. Among these nodes, only 22 (2 to 22) in x-direction, 20 (2 to 21) in y-direction, and 14 (2 to 15) in z-direction are active.

In Figure A-40, the small red rectangle is the footprint of the Saltstone No. 1 Vault. The large red rectangle is that of the No. 4 Vault. A plan view of the contaminant migration paths from the corners of the disposal units are shown in the same figure. These particle-tracking results indicate groundwater flow direction is largely to the east and slightly to the north, based on modeling coordinates.

The vertical grid points are selected to trace the geological settings of the aquifer/aquitard units at the GSA. Figure A-41 depicts the selected vertical layers and their corresponding geological units.

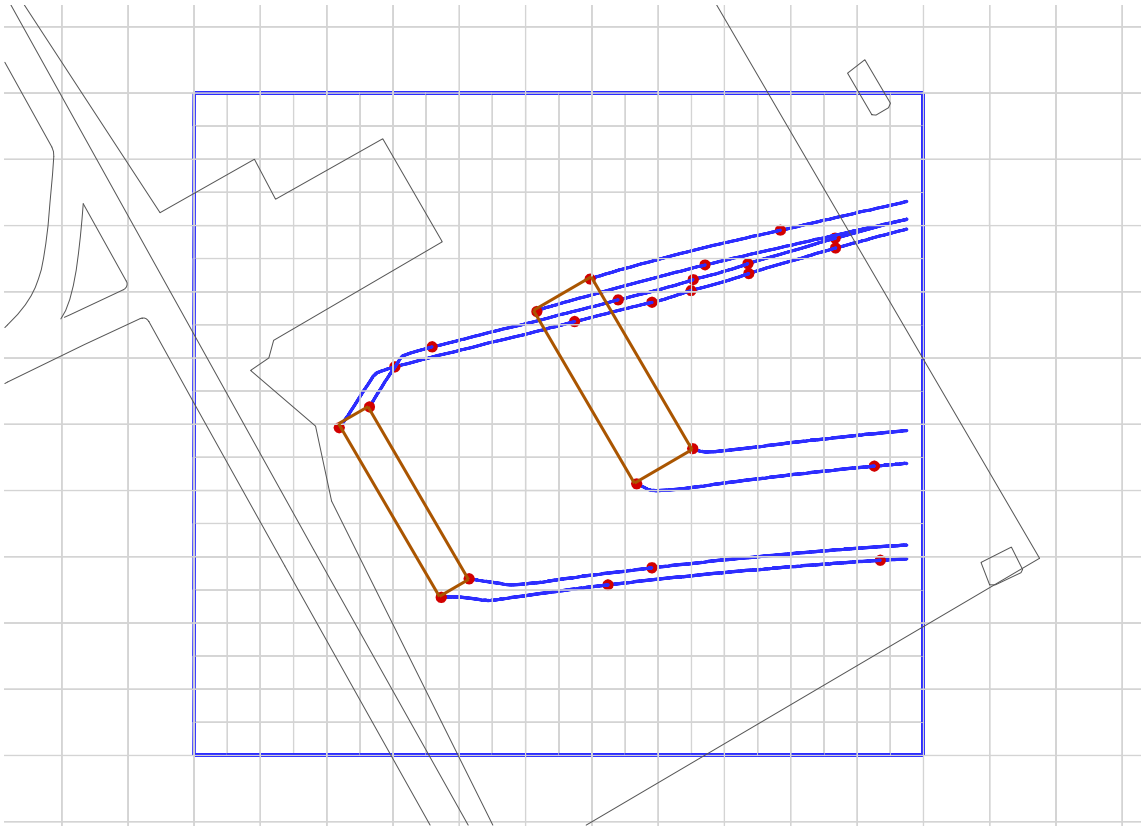

Figure A-40. PORFLOW Model Horizontal Grids and Particle Tracking

Figure A-41. Schematic of the Aquifer/Aquitard System for the Reduced Model

As indicated in Figure A-41, the active nodes in the vertical direction are from 2 to 15. Nodes 2 and 3 are the Gordon Aquifer. Nodes 4 and 5 are the Gordon Confining Unit. Nodes 6 through 10 are the Lower (Upper Three Runs) Aquifer. Nodes 11 and 12 are the Tan Clay. Nodes 13, 14, and 15 are the Upper Aquifer. There are six more layers above node 16 in the Upper Aquifer. These layers represent the unsaturated zone and therefore are not represented in the reduced model. Since contaminants enter the water table below these layers and flow in these layers is predominantly downward, truncating them does not affect the contaminant migration simulations.

A.3.1.1 Locations of Source Nodes and Observation Nodes

The source nodes extend beneath the footprint of Vault No. 4. The water table at these locations is mostly at K-node number 14. We set all source nodes at this elevation, as shown in Table A-12. There are 12 source nodes covering the footprint of Saltstone No. 4 Vault. Since the horizontal cell dimension is 100 ft × 100 ft, the total area covered by the 12 cells is 120,000 square feet. The vault footprint is also 120,000 square feet (200 ft × 600 ft).

Table A-12
Node Indices for Locations of the Source Nodes

I	J	K
13	13	14
13	14	14
13	15	14
14	12	14
14	13	14
14	14	14
14	15	14
15	10	14
15	11	14
15	12	14
15	13	14
16	11	14

In the saturated-zone modeling, we selected two groups of nodes as observation nodes. The first group is selected to capture the peak groundwater concentration for radionuclides at their point of compliance and within the time of compliance. The point of compliance is anywhere 100 meters beyond the edge of the disposal unit. The time of compliance is 1,000 years. These criteria are established in DOE Order 435.1.

For chemicals, such as nitrate, the point of compliance is anywhere 100 feet beyond the edge of the disposal unit. Due to the difference in point of compliance, another group of observation nodes was added.

The aerial locations of the source nodes and observation nodes are depicted in Figure A-42, along with the horizontal flow vectors for k=14. The red triangles are the source nodes. The orange squares are the group-one observation nodes for radionuclides. The blue circles are group-two observation nodes for nitrate compliance.

A.3.2 Flow Model

The horizontal component of groundwater flow at K = 14 (Figure A-42) is relatively slow, especially in the area represented by the Vault No. 4 footprint and the observation nodes. All four

figures indicate groundwater flow direction is toward the east in the three units comprising the Upper Three Runs Aquifer.

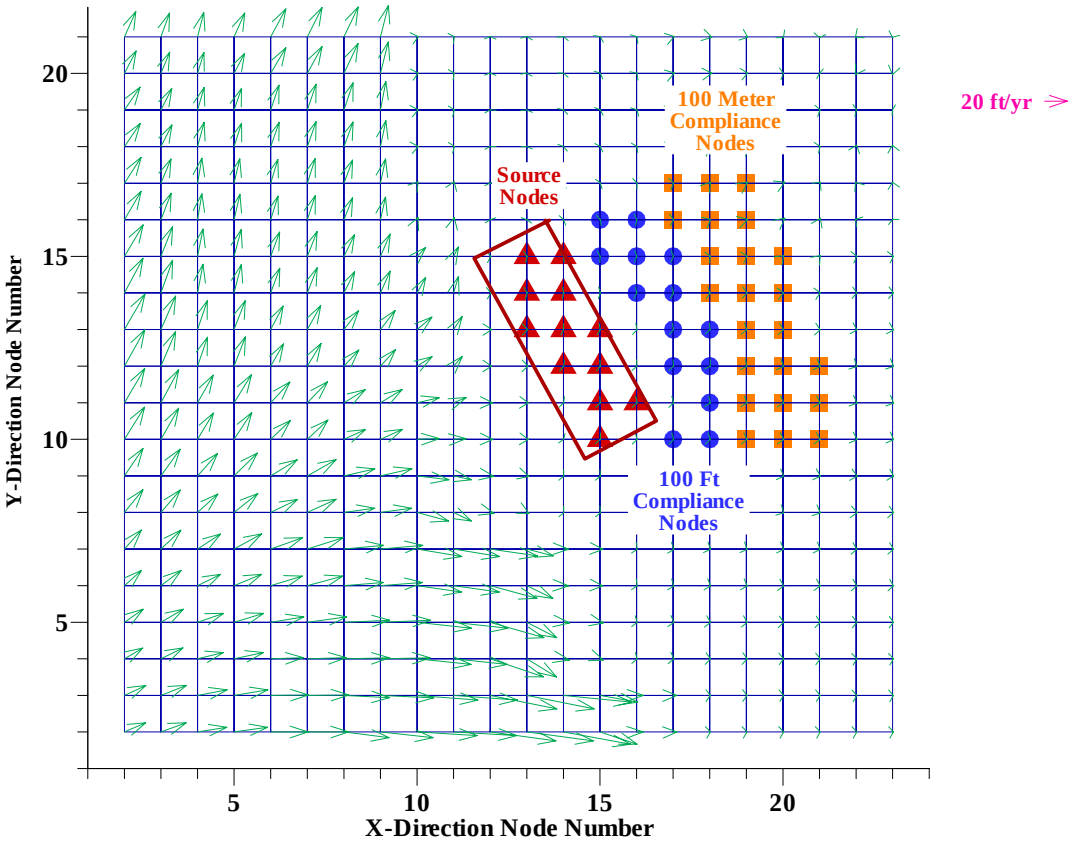

Figure A-42. Locations of Source Nodes and Observation Nodes.

The above analyses confirm the flow direction to be towards the east. As a result, selecting observations at the downstream positions is valid. Another concern is: "How many layers should the observation nodes cover in order to catch the peak concentration?" The side view of the particle tracking in Figure A-43 provides some clue for this concern.

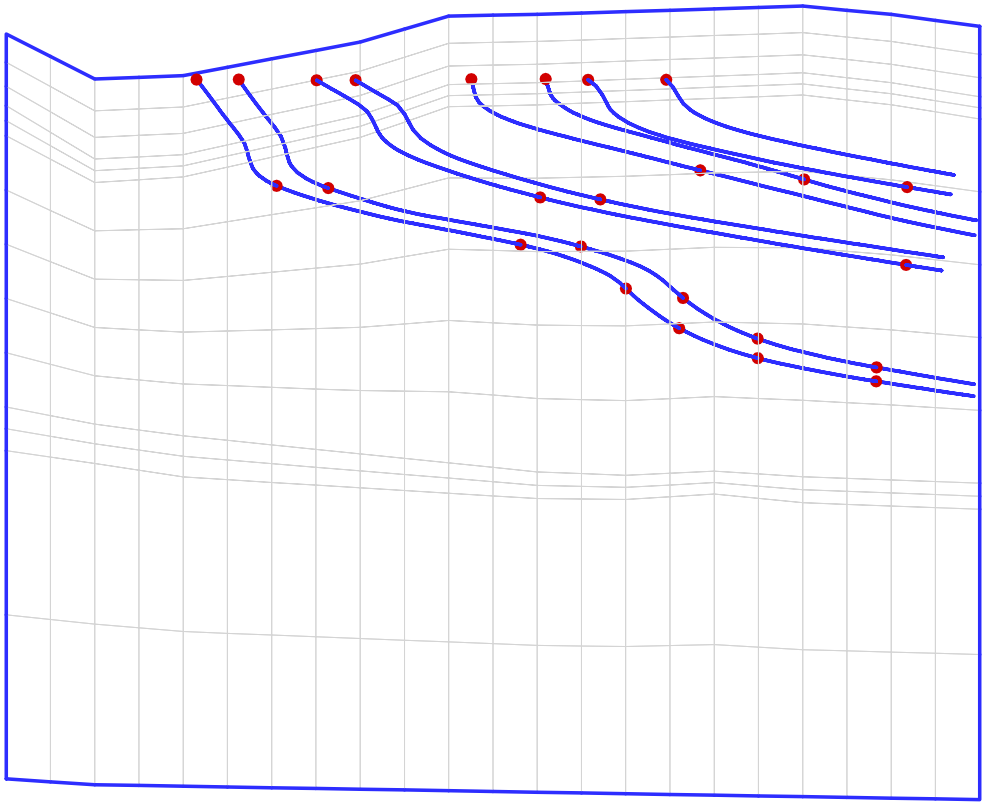

Figure A-43. PORFLOW Model X-Z Plane Nodes and Particle Tracking

In Figure A-43, a particle travels from an upper position at the water table to the lower aquifer/aquitard system. The four upper left points correspond to the four corners of Vault No. 1. The four upper right points correspond to the four corners of Vault No. 4. The elevation of the upper points is at K = 14. The particle tracking shows contaminants would go down from the source nodes and travel to the east and downward. They would penetrate the Tan Clay and into the Lower Aquifer. Very little would reach the Gordon Confining Unit and the Gordon Aquifer at the bottom of the modeling domain. The peak concentration would not show up in these lowest units.

The velocity vectors shown in Figure A-44, at an X-Z plane with J = 14, lend additional support to the above argument. The vertical nodes are from 2 to 15. The horizontal nodes are from 2 to 23. Vectors are vertically downward at z = 15 because it is in the unsaturated zone. Water penetrates the Tan Clay and into the lower aquifer. Water velocities are highest at layers 8 and 9. The velocity increases as more infiltration water joins the streams in these two layers. Because the Gordon Confining Unit is a very effective aquitard, water penetration through this unit is minimal. The flows in the two aquifers above and below Gordon Confining Unit are even in opposite directions.

Similar observations are made for the cross-sectional slices at J = 10, 12, and 16. All of the plots appear to be similar.

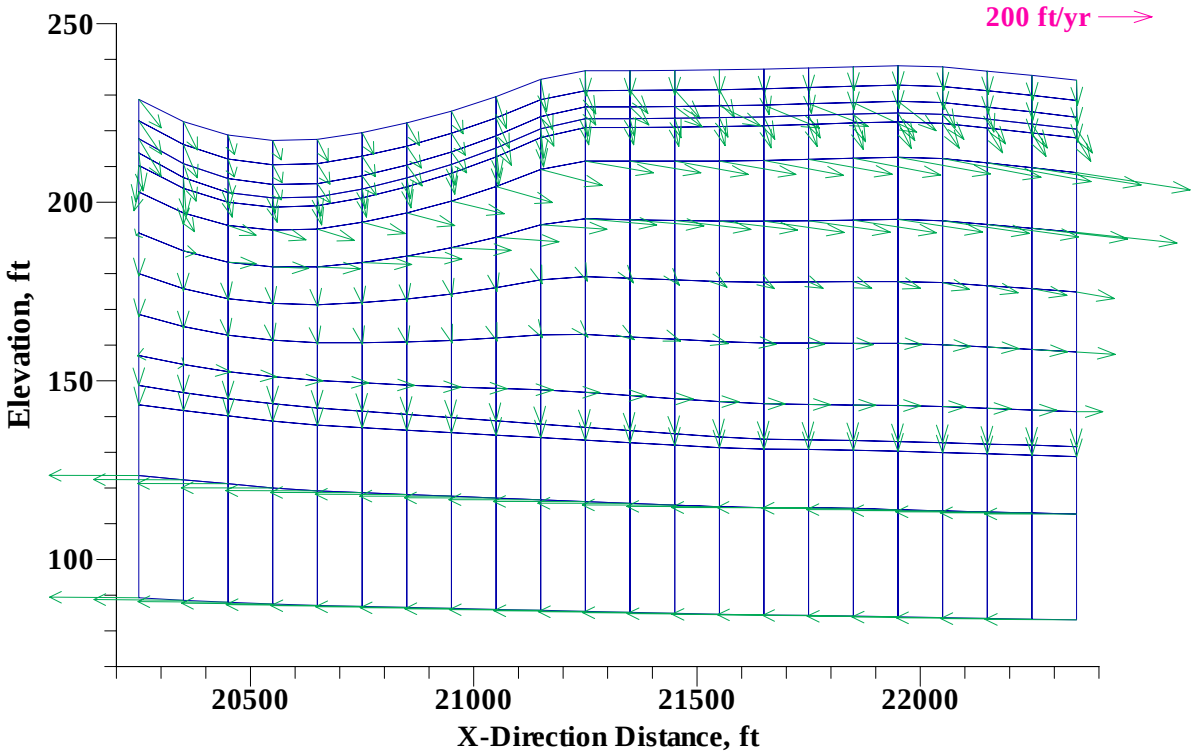

Figure A-44. Velocity Vectors in the X-Z Plane at J = 14

Both particle tracking and velocity vectors indicate minimal contaminants would reach the Gordon Confining Unit. Based on these observations, we select k-nodes from 5 to 14, inclusive, for each of the I-j locations as observation nodes. Based on this selection, there are 10 observation nodes for each of the i-j locations depicted in Figure A-42. As a result, there are 230 Group-1 (approximately 100 meters and beyond) observation nodes for all radionuclides and nitrate. For nitrate, 140 additional observation nodes are selected to cover the Group-2 (approximately 100 feet to 100 meters) i-j locations.

A.3.3 Transport Model

A.3.3.1 Source Terms

For each of the contaminants and all daughters, the source terms are expressed as the fractional release to the water table calculated by the unsaturated-zone modeling. The fractional release has the unit of mole/year/mole of parent. The time history of each component is used as the source term. The amount released is assumed to be evenly distributed to the total volume of the 12 source cells listed in Table A-12. Based on the grid coordinates, the volumes of all these cells are calculated (Table A-13). The total volume is 6.1215×10^5 ft^3.

Table A-13
Source Node Locations and Volumes

I	J	K	XC	YC	ZC	VOL
13	13	14	21350.0	11750.0	230.110	5.1200E+04
13	14	14	21350.0	11850.0	230.650	5.0900E+04
13	15	14	21350.0	11950.0	231.306	5.0525E+04
14	12	14	21450.0	11650.0	229.997	5.1250E+04
14	13	14	21450.0	11750.0	230.353	5.1100E+04
14	14	14	21450.0	11850.0	230.822	5.0850E+04
14	15	14	21450.0	11950.0	231.405	5.0500E+04
15	10	14	21550.0	11450.0	229.486	5.1525E+04
15	11	14	21550.0	11550.0	229.935	5.1250E+04
15	12	14	21550.0	11650.0	230.340	5.1050E+04
15	13	14	21550.0	11750.0	230.699	5.0925E+04
16	11	14	21650.0	11550.0	230.306	5.1075E+04
					---	---
					TOTAL	6.1215E+05

The fractional release is divided by the total volume to obtain the concentration increments in the source nodes in mole/ ft^3/mole parent. However, because fractional release is often a very small number, within PORFLOW we multiply it by $10^{12}/6.1215\times10^5$ ft^3 = 1.6336×10^6. The concentration unit in PORFLOW saturated-zone computation is, therefore, pico-mole/ft^3/mole parent. This multiplication factor is the same for every contaminant. PORFLOW has a "SCALE" command so that users can apply it to each fractional release time history. In PORFLOW 5.97.0, the scaling is performed by the code if a user enters "TOTAl VOLUme" in the SOURce command. The source terms are read by a PORFLOW input file.

The flux terms exiting the bottom of the unsaturated zone model was processed using a Fortran program to truncate the fluxes less than 10^{-20} times the peak flux such that only the significant part of the output flux profile was utilized to generate the input source terms for the saturated zone model.

A.3.3.2 Saturated-Zone PORFLOW Modeling

In the saturated zone model, the simulation is controlled by a main input file that calls other input files that describe the domain geometry, material properties of the porous media, transport properties of contaminants, initial and boundary conditions, source locations and their time histories, the solution methods, and output specifications. The main simulation strategy is to utilize a steady-state flow field to perform transient transport simulations for the full period of interest.

For each time step, an amount of each contaminant is added to the source nodes according to its fractional release curve. Migration of contaminants in the reduced-extent groundwater model is calculated. The migration mechanisms are convection and diffusion. Convection is determined by the steady-state flow vectors. Diffusion is governed by the molecular diffusion within the porous matrix material, and influenced by porosity and tortuosity. Because the velocity vectors are large, the dominant transport mechanism in the aquifer/aquitard system is convection.

The flow field of the groundwater transport model has excellent material balance. The excellent mass balance permits the use of relatively large time-steps for the transport modeling without causing convergence difficulties.

The concentration changes at each of the observation nodes are saved in a "HISTory" file at every 10 years. A post-processing FORTRAN program reads the HIST file and produces the peak concentration, peak time and peak node among all Group-1 nodes for all contaminants and in addition, for nitrate, among the Group-2 nodes. To check the validity of the peak-picking algorithm, we used another PORFLOW option. This option is triggered by a "STATistic" command, which output the maximum concentration among a selected group of observation wells and the corresponding node. The HIST and STAT results are always in perfect agreement.

A.3.3.3 Saturated-Zone Model Results

Nitrate

Except for Bi-210, Nb-95m, Th-228 and Zr-95, all 42 of the 46 contaminants used for the unsaturated-zone modeling are modeled for transport in the saturated zone. No runs are made for these four radionuclides because of the extremely low ($<10^{-99}$) fractional release to the water table. For nitrate, predicted peak concentration, peak time and peak node are depicted in Table A-14.

Table A-14
Predicted Peak Concentrations, Peak Times, and Peak Nodes for Nitrate

Contaminant	Peak Conc. pMol/L/mol	Peak Time Years	Peak Node
NO3	3.46E-02	1.00E+03	15,15,11
NO3	2.80E+00	9.80E+03	15,15,11

Among all 140 Group-2 observation nodes, the peak nitrate concentration occurs at 1,000 years and 10,000 years in the cell of node 15,15,11. This node is one of the closest observation nodes to the facility boundary (Figure A-42) and is in the bottom layer of the Tan Clay. The nitrate concentration history curves at node 15,15,11 in 1,000 and 10,000 years are shown in Figures A-45 and A-46, respectively.

Radionuclides

Predicted peak concentration, peak time and peak node for all of the radionuclides modeled in the first 1,000 years are summarized in Tables A-15. To comply with DOE guidelines (USDOE 1999) the peak nodes in Table A-15 are all Group-1 observation nodes. They are at 100 meters and beyond the waste disposal facility boundary. In Table A-15, the peak concentrations are in the unit of pico Curies per liter per Curie of parent. They are converted from the molar concentration of picomoles/L/mole parent by:

$$C_{Ci} = C_{mol} \times \lambda_d / \lambda_p \qquad \text{(A-16)}$$

where λ_d and λ_p are the specific activity of the daughter and parent radionuclides, respectively. The concentration histories for the key radionuclides are shown in Figures A-47 through A-59.

Predicted peak concentration, peak times and peak nodes for all of the radionuclides modeled over 10,000 years are summarized in Tables A-16. As was the case for the 1,000-year results, concentrations were evaluated at 100 meters and at points beyond the waste disposal facility boundary. The concentration histories for the key radionuclides are shown in Figures A-60 through A-76.

For a relatively mobile radionuclide, or a radionuclide with small k_d, the peak node is at simulation node 3801. The i-, j-, k-indexes of this node are (18,14,10). Horizontally, this is the node closest to the edge of Vault 4 (Figure A-42). Vertically, it is in the Lower Aquifer and the first layer underneath the Tan Clay. For a highly adsorbed radionuclide with large k_d, the peak node is 5056, or (19,11,13), located one node beneath the water table and adjacent to Vault 4. Due to the high k_d, there is little penetration into the Tan Clay. The peak concentrations observed for highly adsorbed radionuclides are so low that they are not of concern.

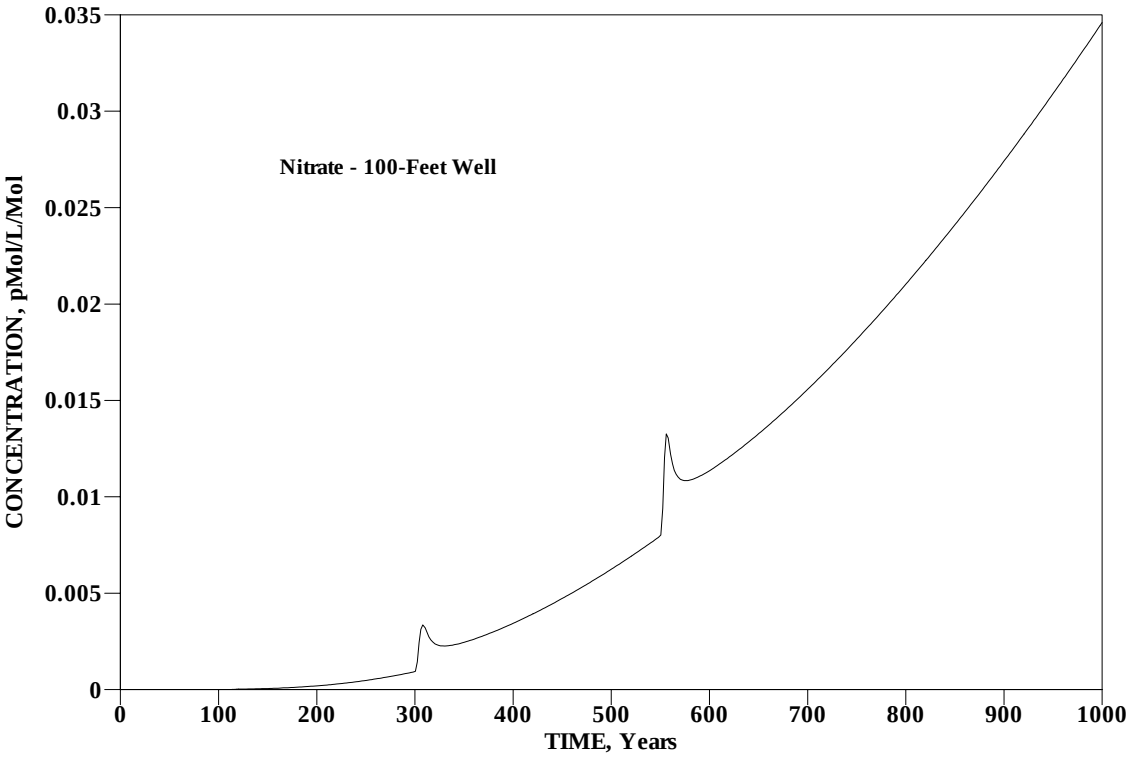

Figure A-45. Nitrate concentration history at node 15,15,11 in the first 1,000 years.

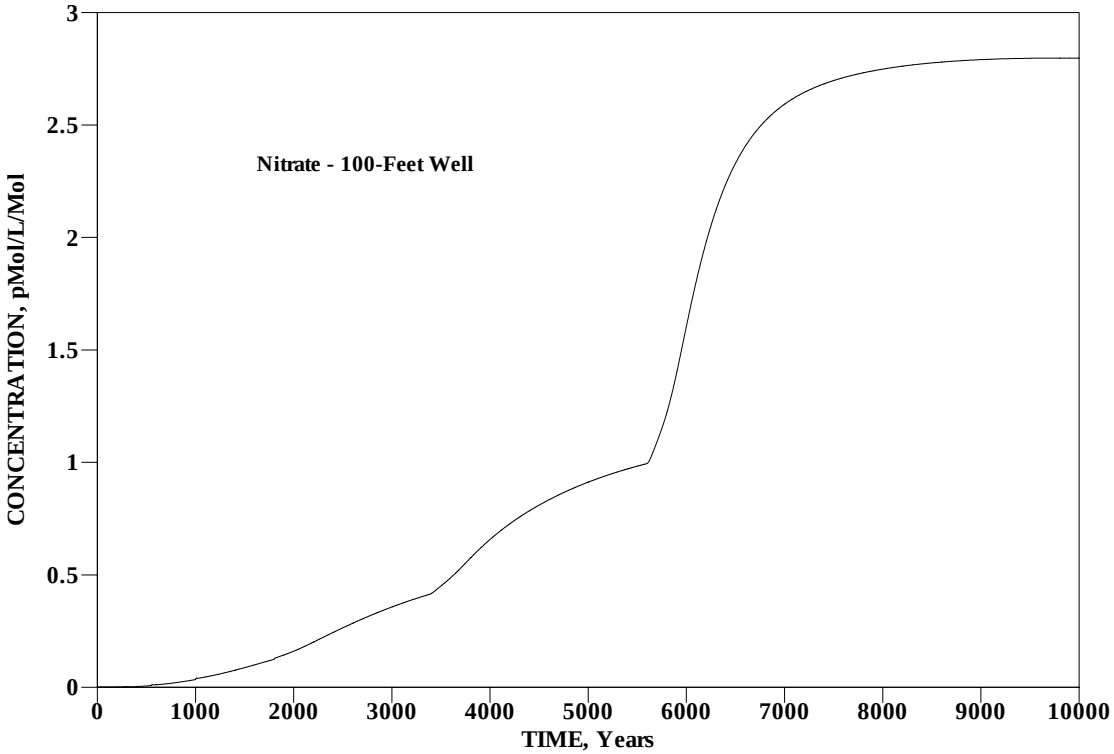

Figure A-46. Nitrate concentration history at node 15,15,11 in 10,000 years.

Table A-15

Peak Concentrations, Peak Times, and Peak Nodes in the first 1,000 Years for Radionuclides

Nuclides	Peak Conc. pCi/L/Ci	Peak Time Years	Peak Node
Al-26	2.94E-17	1.00E+03	19,11,13
Am-243	1.70E-75	1.00E+03	19,11,13
Np-239	7.94E-73	1.00E+03	19,11,13
Pu-239	2.73E-53	1.00E+03	19,11,13
Pu5-239	1.14E-56	1.00E+03	19,11,13
Bi-210	0.00E+00		
Po-210	0.00E+00		
C-14	5.34E-25	1.00E+03	18,14,10
Cf-249	1.41E-56	1.00E+03	19,11,13
Cm-245	3.73E-60	1.00E+03	19,11,13
Pu-241	7.07E-59	1.00E+03	19,11,13
Pu5-241	3.14E-62	1.00E+03	19,11,13
Am-241	6.17E-61	1.00E+03	19,11,13
Np-237	6.54E-31	1.00E+03	19,11,10
Cl-36	1.24E-24	1.00E+03	18,14,10
Cm-245	1.60E-87	1.00E+03	19,11,13
Pu-241	9.43E-63	1.00E+03	19,11,13
Pu5-241	4.25E-66	1.00E+03	19,11,13
Am-241	2.10E-64	1.00E+03	19,11,13
Np-237	3.61E-29	1.00E+03	19,11,10
Cm-246	1.13E-87	1.00E+03	19,11,13
Cm-247	1.53E-87	1.00E+03	19,11,13
Am-243	5.72E-77	1.00E+03	19,11,13
Np-239	2.69E-74	1.00E+03	19,11,13
Pu-239	4.64E-55	1.00E+03	19,11,13
Pu5-239	1.95E-58	1.00E+03	19,11,13
Cm-248	1.57E-87	1.00E+03	19,11,13
Pu-244	8.38E-57	1.00E+03	19,11,13
Pu5-244	3.51E-60	1.00E+03	19,11,13
Cs-135	9.24E-38	1.00E+03	19,11,13
Cs-137	5.08E-48	1.00E+03	19,11,13
H-3	1.10E-08	1.25E+02	18,14,10
I-129	5.69E-08	1.00E+03	18,14,10
K-40	2.83E-08	1.00E+03	18,14,10
Mo-93	5.07E-07	1.00E+03	18,14,10
Nb-93m	9.01E-09	1.00E+03	18,14,10
Nb-94	7.93E-36	1.00E+03	19,11,13
Nb-95m	0.00E+00		
Nb-95	0.00E+00		
Ni-59	7.66E-44	1.00E+03	19,11,13
Np-237	2.65E-25	1.00E+03	19,11,10
Pd-107	1.22E-22	1.00E+03	19,11,13
Pu-238	8.12E-55	1.00E+03	19,11,13
Pu5-238	3.40E-58	1.00E+03	19,11,13
U-234	5.85E-59	1.00E+03	19,11,13
Pu-239	2.75E-51	1.00E+03	19,11,13
Pu5-239	1.15E-54	1.00E+03	19,11,13
U-235	5.06E-59	1.00E+03	19,11,13

Pu-240	2.54E-51	1.00E+03	19,11,13
Pu5-240	1.06E-54	1.00E+03	19,11,13
U-236	1.41E-57	1.00E+03	19,11,13
Pu-241	1.21E-72	1.00E+03	19,11,13
Pu5-241	5.15E-76	1.00E+03	19,11,13
Am-241	1.02E-73	1.00E+03	19,11,13
Np-237	1.38E-30	1.00E+03	19,11,10
Pu-242	2.83E-51	1.00E+03	19,11,13
Pu5-242	1.18E-54	1.00E+03	19,11,13
U-238	8.18E-60	1.00E+03	19,11,13
Pu-244	2.83E-51	1.00E+03	19,11,13
Pu5-244	1.18E-54	1.00E+03	19,11,13
Ra-226	1.24E-45	1.00E+03	19,11,13
Rb-87	2.42E-21	1.00E+03	19,11,13
Se-79	3.50E-07	1.00E+03	19,11,13
Sn-126	4.64E-35	1.00E+03	19,11,13
Sr-90	3.35E-16	6.57E+02	19,11,13
Tc-99	3.59E-21	1.00E+03	18,14,10
Th-228	0.00E+00		
Ra-224	0.00E+00		
Th-229	5.93E-84	1.00E+03	19,11,13
Ra-225	3.99E-83	1.00E+03	19,11,13
Ac-225	4.50E-83	1.00E+03	19,11,13
Th-230	7.78E-84	1.00E+03	19,11,13
Ra-226	3.15E-47	1.00E+03	19,11,13
Pb-210	4.38E-45	1.00E+03	19,11,13
Po-210	8.26E-45	1.00E+03	19,11,13
Th-232	6.99E-84	1.00E+03	19,11,13
Ra-228	1.51E-75	1.00E+03	19,11,13
Th-228	2.46E-76	1.00E+03	19,11,13
Ra-224	1.63E-75	1.00E+03	19,11,13
U-232	9.25E-65	1.00E+03	19,11,13
Th-228	2.21E-65	1.00E+03	19,11,13
Ra-224	1.46E-64	1.00E+03	19,11,13
U-233	2.99E-60	1.00E+03	19,11,13
Th-229	1.88E-63	1.00E+03	19,11,13
Ra-225	1.25E-62	1.00E+03	19,11,13
U-234	3.12E-60	1.00E+03	19,11,13
Th-230	1.93E-64	1.00E+03	19,11,13
Ra-226	1.50E-50	1.00E+03	19,11,13
Pb-210	2.44E-48	1.00E+03	19,11,13
Po-210	4.61E-48	1.00E+03	19,11,13
U-235	3.00E-60	1.00E+03	19,11,13
Pa-231	2.94E-57	1.00E+03	19,11,13
Ac-227	5.69E-57	1.00E+03	19,11,13
Th-227	7.98E-58	1.00E+03	19,11,13
Ra-223	5.29E-57	1.00E+03	19,11,13
U-236	3.00E-60	1.00E+03	19,11,13
U-238	3.00E-60	1.00E+03	19,11,13
Th-234	7.72E-61	1.00E+03	19,11,13
U-234	9.04E-63	1.00E+03	19,11,13
Zr-93	5.05E-58	1.00E+03	19,11,13
Nb-93m	1.17E-49	1.00E+03	19,11,13
Zr-95	0.00E+00		
Nb-95	0.00E+00		

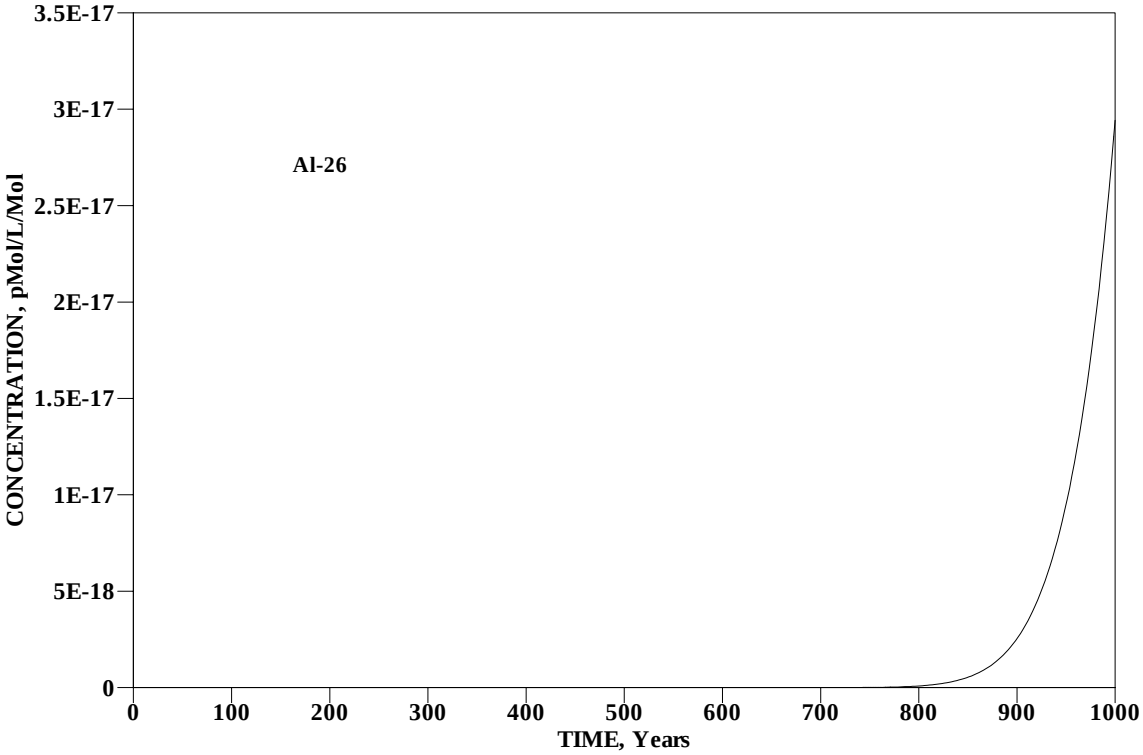

Figure A-47. Concentration of Al-26 vs Time for 1,000 Years

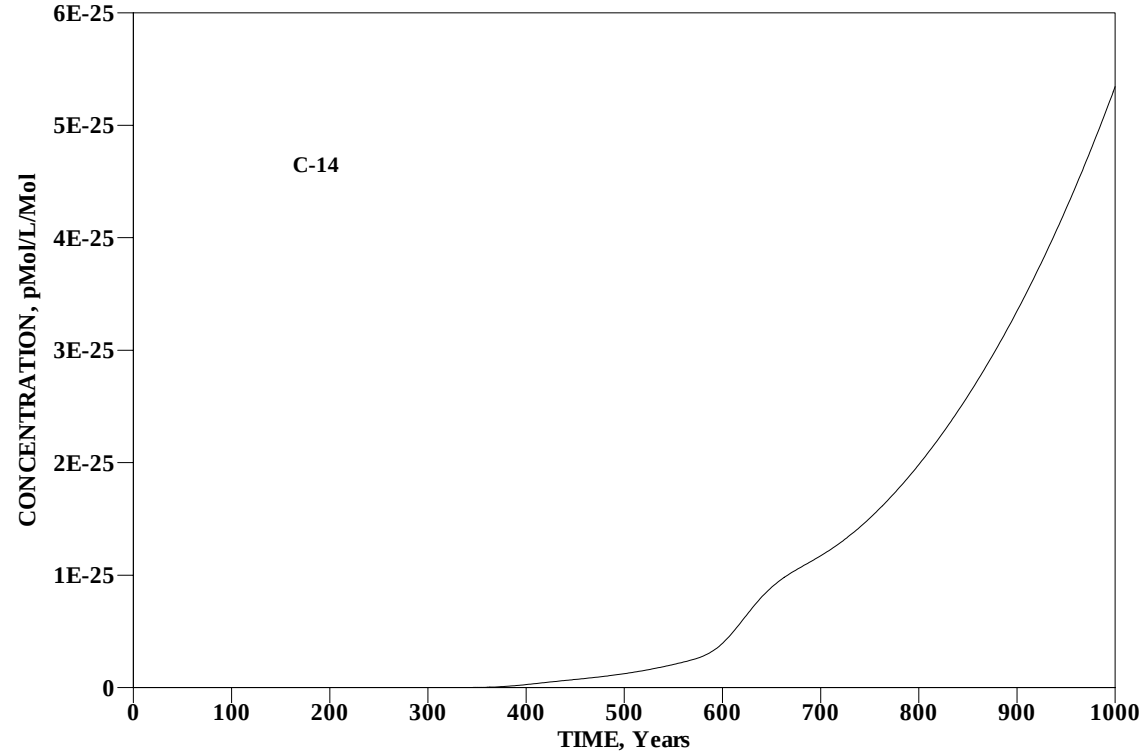

Figure A-48. Concentration of C-14 vs Time for 1,000 Years

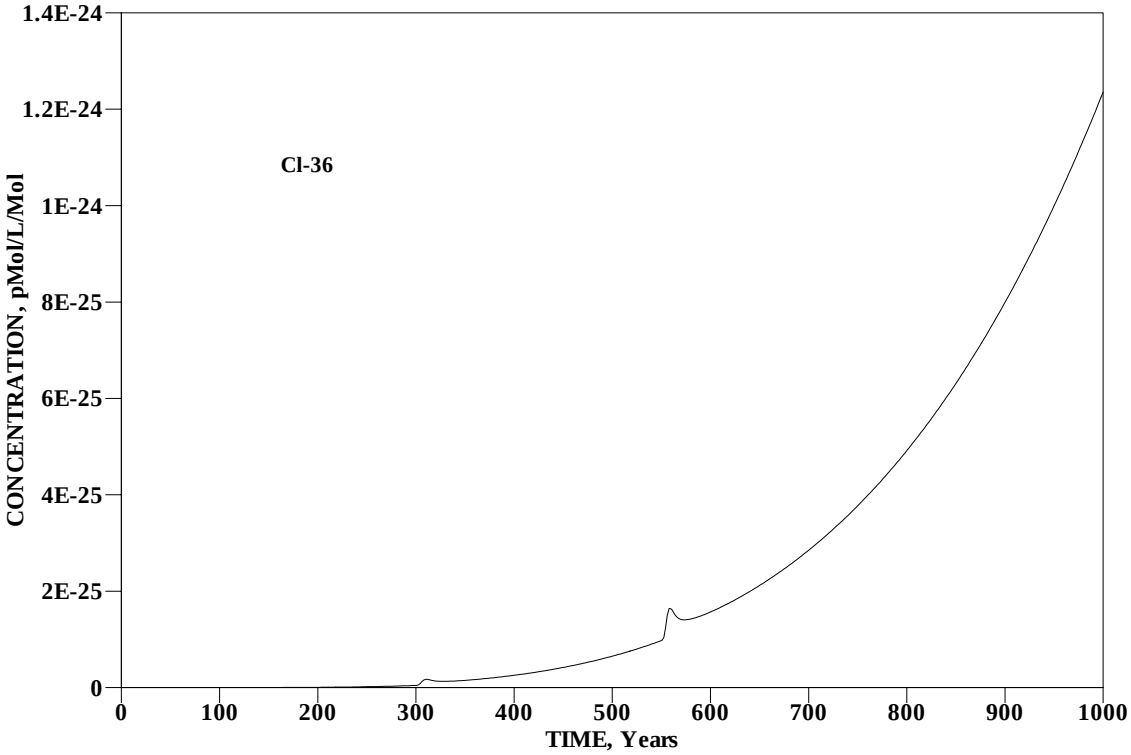

Figure A-49. Concentration of Cl-36 vs Time for 1,000 Years

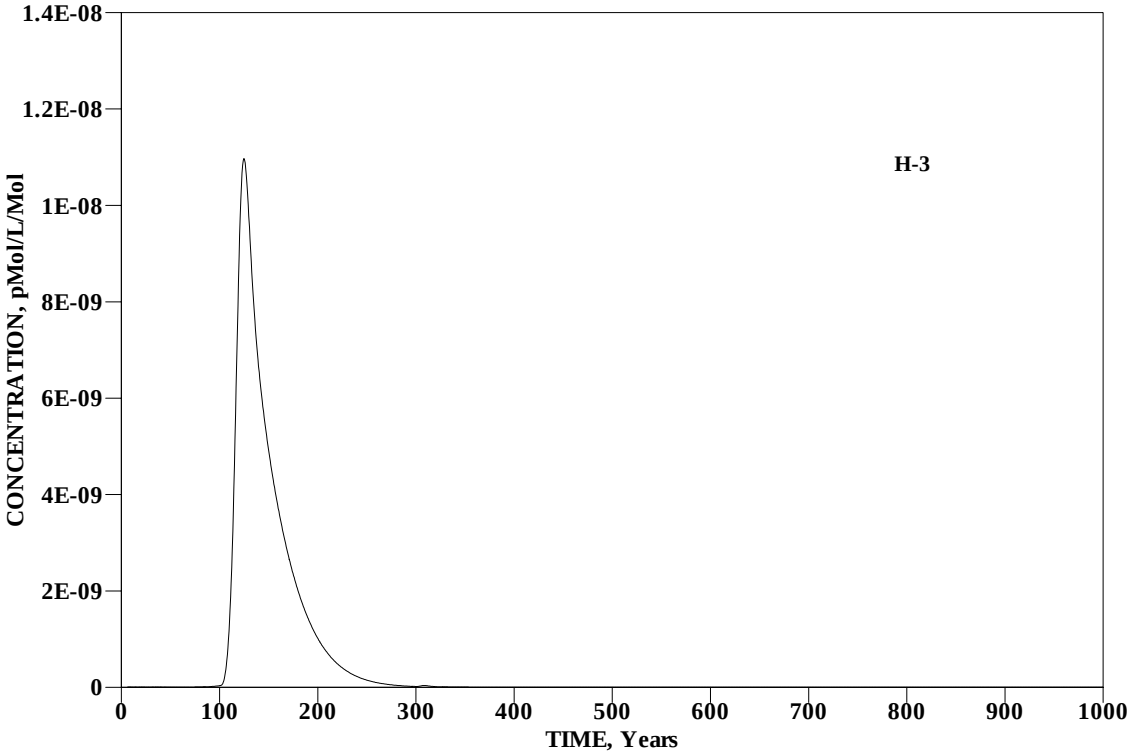

Figure A-50. Concentration of H-3 vs Time for 1,000 Years

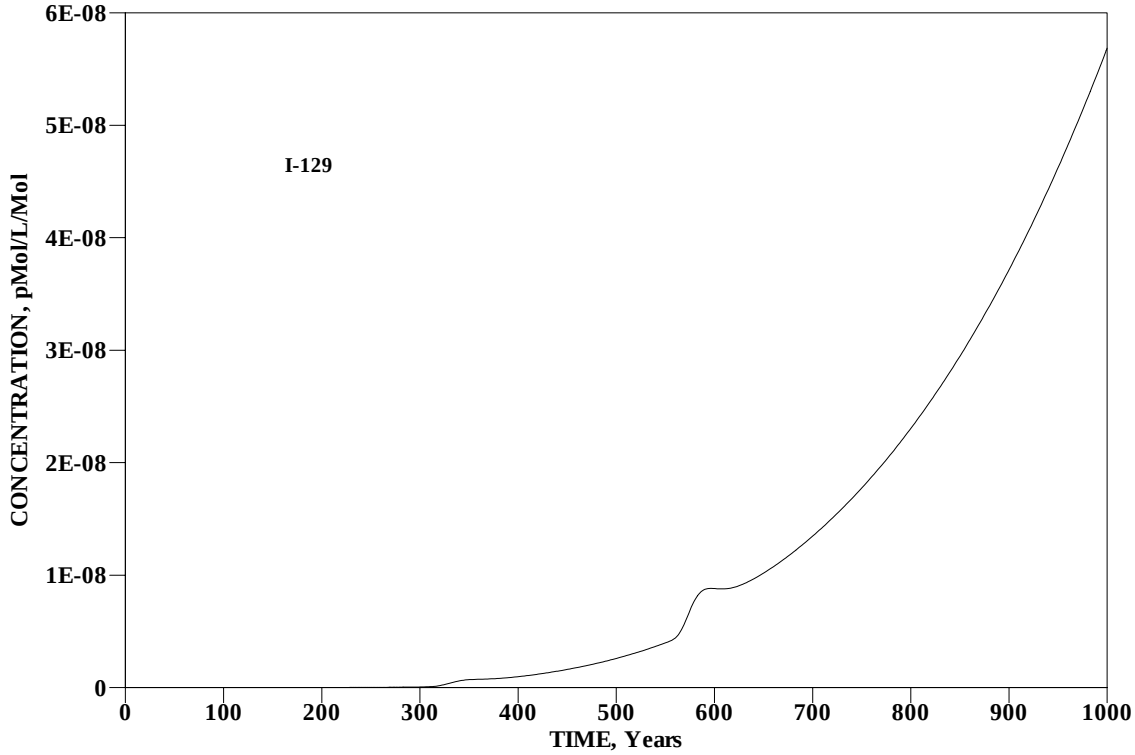

Figure A-51. Concentration of I-129 vs Time for 1,000 Years

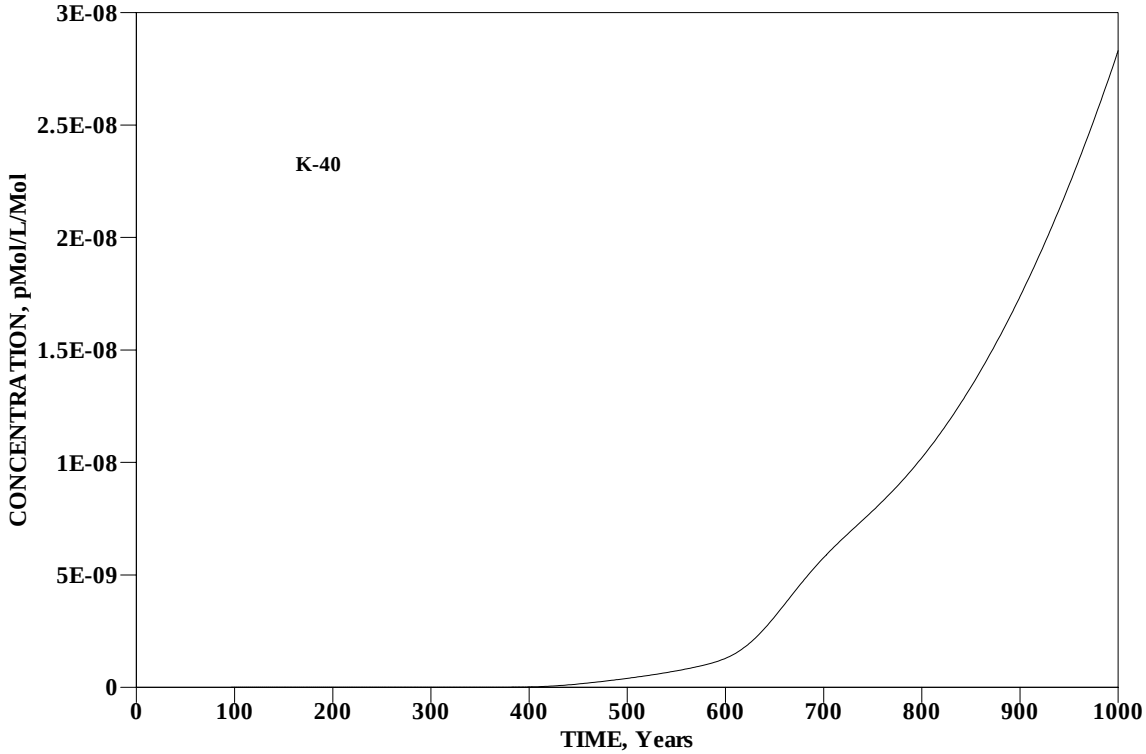

Figure A-52. Concentration of K-40 vs Time for 1,000 Years

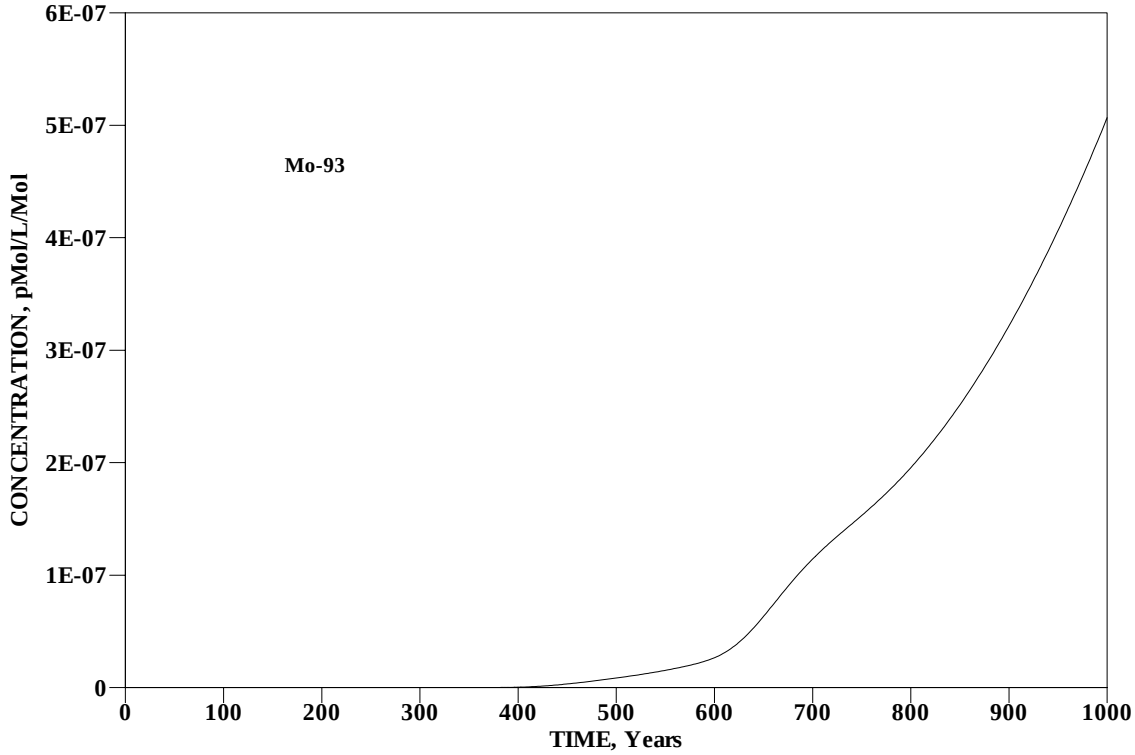

Figure A-53. Concentration of Mo-93 vs Time for 1,000 Years

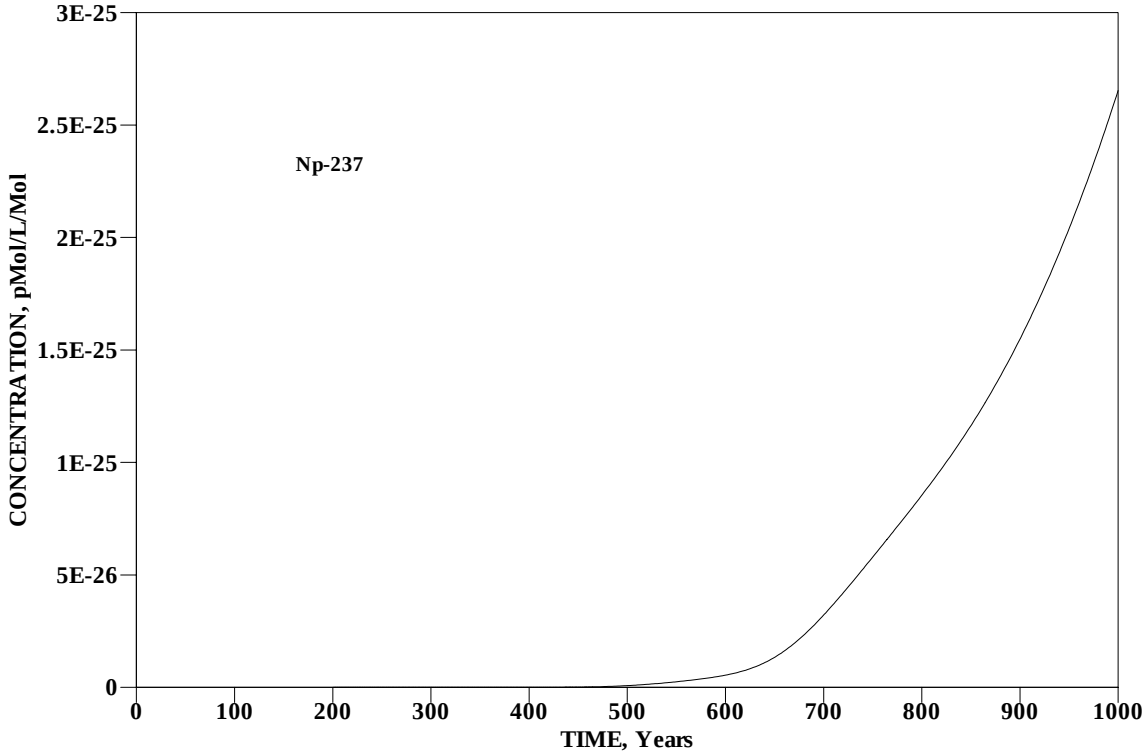

Figure A-54. Concentration of Np-237 vs Time for 1,000 Years

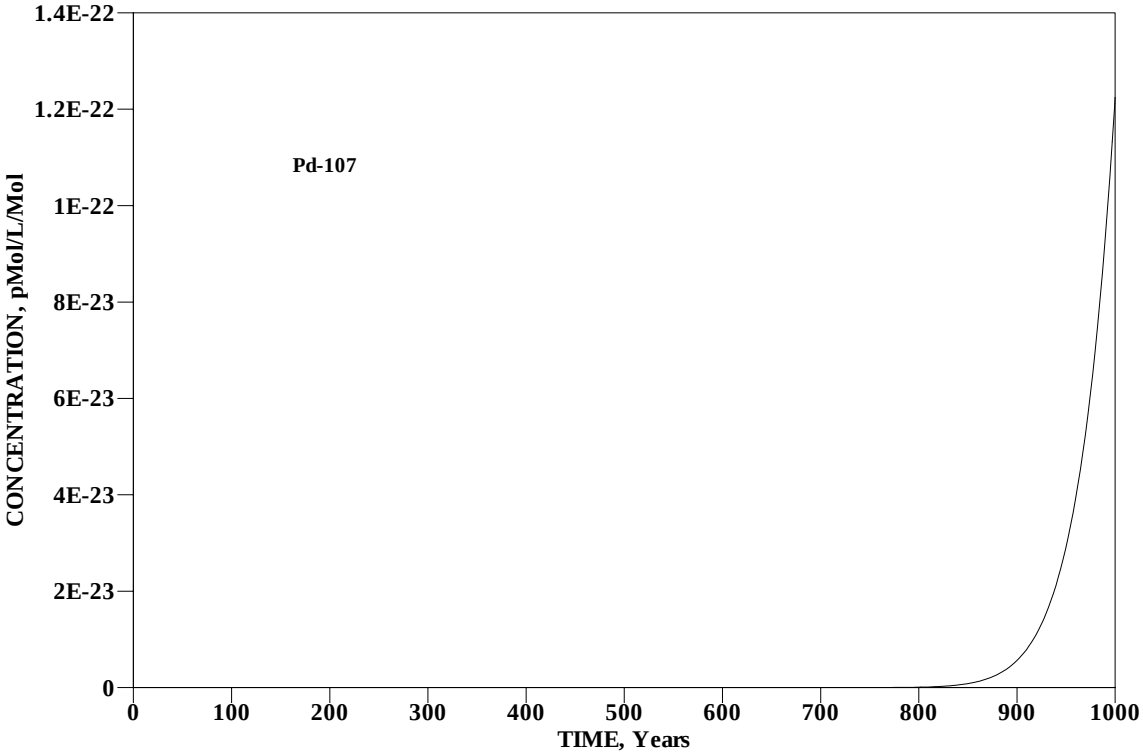

Figure A-55. Concentration of Pd-107 vs Time for 1,000 Years

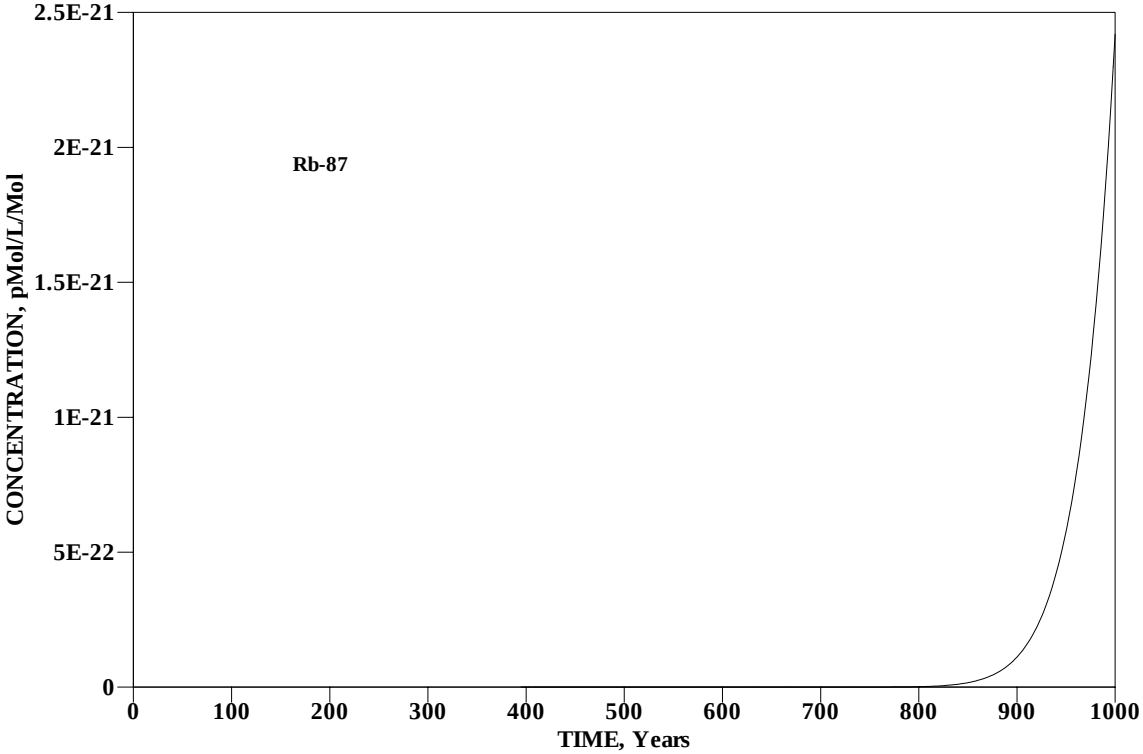

Figure A-56. Concentration of Rb-87 vs Time for 1,000 Years

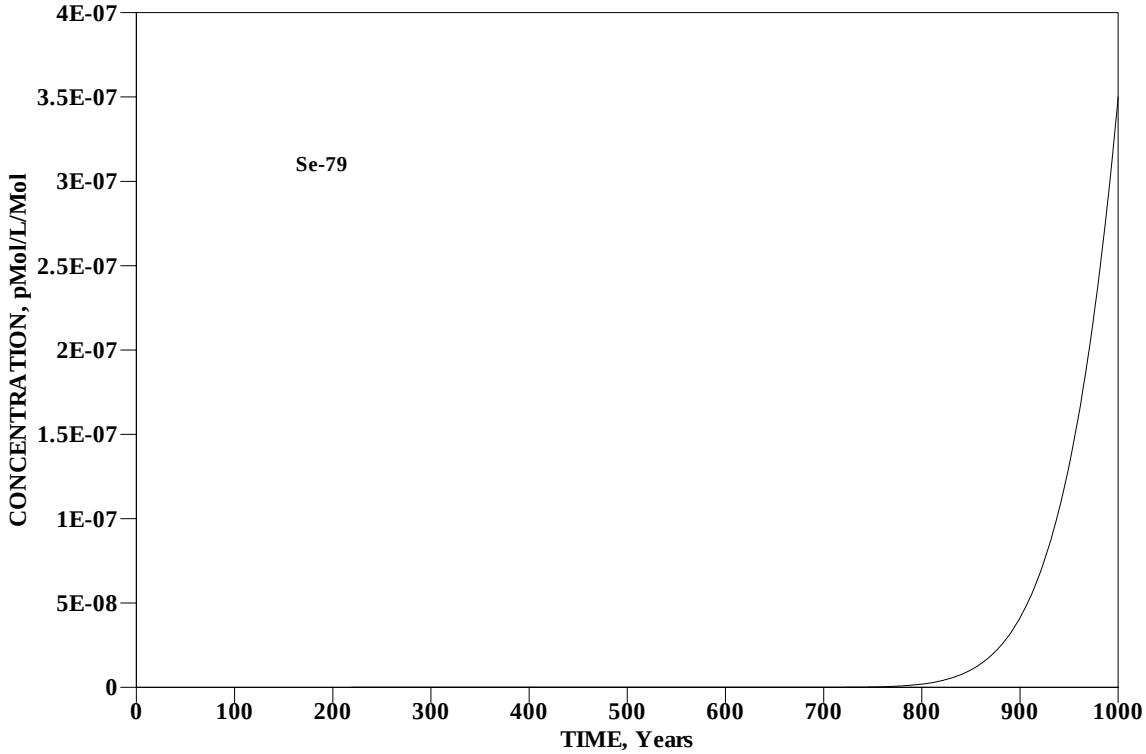

Figure A-57. Concentration of Se-79 vs Time for 1,000 Years

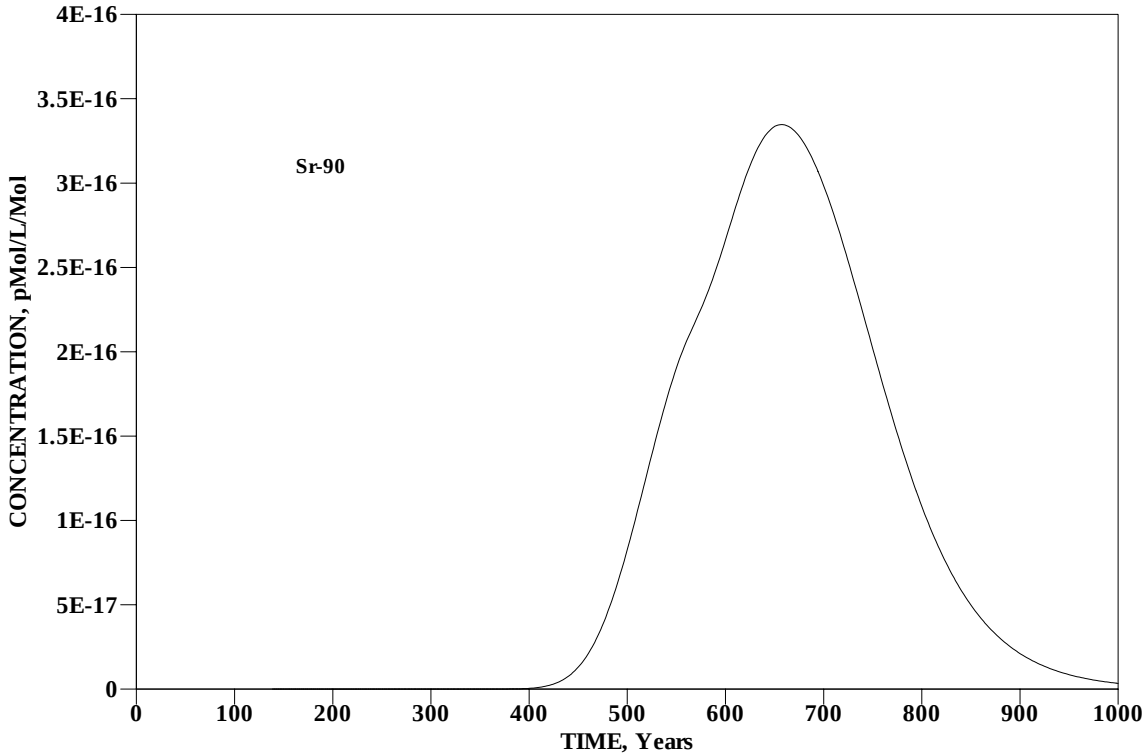

Figure A-58. Concentration of Sr-90 vs Time for 1,000 Years

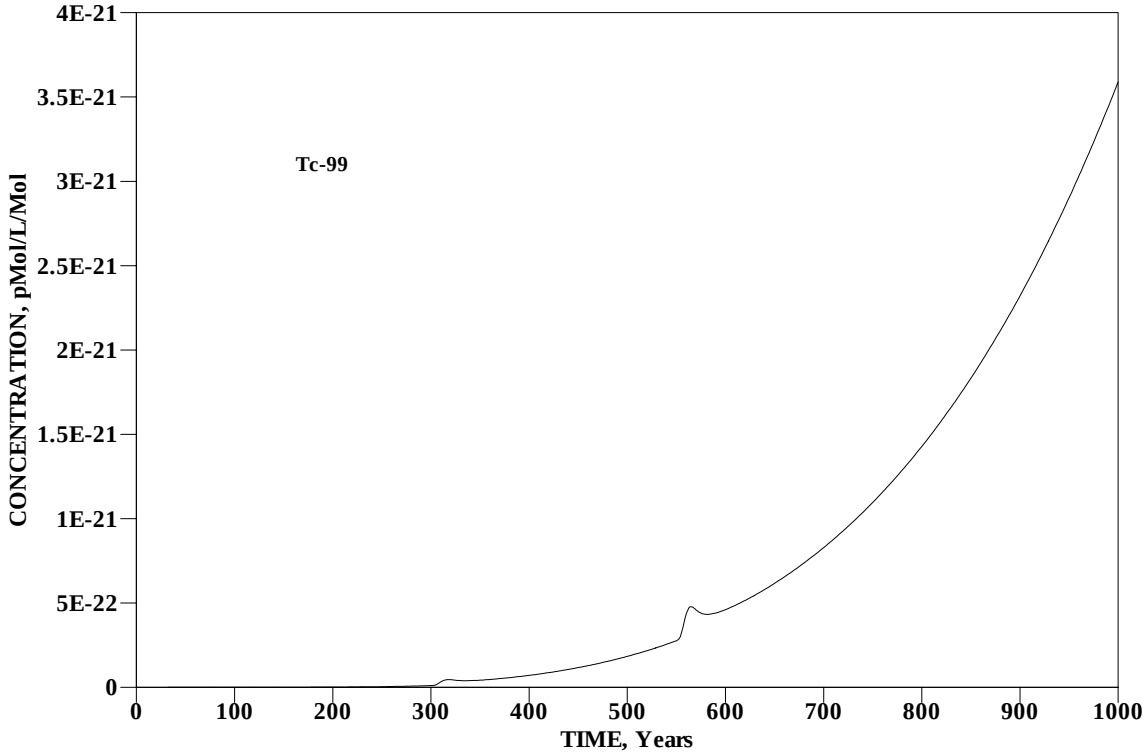

Figure A-59. Concentration of Tc-99 vs Time for 1,000 Years

Table A-16. Peak Concentrations, Peak Times, and Peak Nodes in 10,000 Years for Radionuclides

Nuclides	Peak Conc. pCi/L/Ci	Peak Time Years	Peak Node
Al-26	6.19E-09	1.00E+04	19,11,10
Am-243	5.78E-34	1.00E+04	19,11,13
Np-239	2.23E-31	1.00E+04	19,11,13
Pu-239	6.70E-25	1.00E+04	19,11,13
Pu5-239	2.46E-28	1.00E+04	19,11,13
Bi-210	0.00E+00		
Po-210	0.00E+00		
C-14	1.18E-19	1.00E+04	18,14,10
Cf-249	5.47E-33	7.58E+03	19,11,13
Cm-245	3.67E-34	1.00E+04	19,11,13
Pu-241	4.35E-33	1.00E+04	19,11,13
Pu5-241	1.61E-36	1.00E+04	19,11,13
Am-241	1.04E-33	1.00E+04	19,11,13
Np-237	2.13E-23	1.00E+04	18,14,10
Cl-36	6.77E-19	1.00E+04	18,14,10
Cm-245	4.94E-42	1.00E+04	19,11,13
Pu-241	1.41E-40	1.00E+04	19,11,13
Pu5-241	5.63E-44	1.00E+04	19,11,13
Am-241	3.71E-38	1.00E+04	19,11,13
Np-237	5.18E-22	1.00E+04	18,14,10
Cm-246	2.60E-42	1.00E+04	19,11,13
Cm-247	1.12E-41	1.00E+04	19,11,13
Am-243	1.61E-34	1.00E+04	19,11,13
Np-239	6.22E-32	1.00E+04	19,11,13
Pu-239	1.96E-25	1.00E+04	19,11,13
Pu5-239	7.18E-29	1.00E+04	19,11,13
Cm-248	1.10E-41	1.00E+04	19,11,13
Pu-244	3.11E-28	1.00E+04	19,11,13
Pu5-244	1.14E-31	1.00E+04	19,11,13
Cs-135	1.11E-11	1.00E+04	19,11,13
Cs-137	3.85E-44	1.67E+03	19,11,13
H-3	1.10E-08	1.25E+02	18,14,10
I-129	4.62E-03	1.00E+04	18,14,10
K-40	2.39E-03	1.00E+04	18,14,10
Mo-93	2.84E-03	1.00E+04	18,14,10
Nb-93m	5.53E-05	1.00E+04	18,14,10
Nb-94	1.17E-17	1.00E+04	19,11,13
Nb-95m	0.00E+00		
Nb-95	0.00E+00		
Ni-59	1.19E-15	1.00E+04	19,11,13
Np-237	2.28E-19	1.00E+04	18,14,10
Pd-107	9.15E-13	1.00E+04	19,11,10
Pu-238	1.17E-42	3.16E+03	19,11,13
Pu5-238	4.37E-46	3.16E+03	19,11,13
U-234	1.86E-28	1.00E+04	19,11,13
Pu-239	5.12E-24	1.00E+04	19,11,13
Pu5-239	1.88E-27	1.00E+04	19,11,13
U-235	4.75E-30	1.00E+04	19,11,13
Pu-240	2.37E-24	1.00E+04	19,11,13
Pu5-240	8.70E-28	1.00E+04	19,11,13

U-236	8.08E-29	1.00E+04	19,11,13
Pu-241	1.76E-72	1.16E+03	19,11,13
Pu5-241	7.40E-76	1.16E+03	19,11,13
Am-241	5.22E-42	1.00E+04	19,11,13
Np-237	1.56E-24	1.00E+04	18,14,10
Pu-242	6.71E-24	1.00E+04	19,11,13
Pu5-242	2.46E-27	1.00E+04	19,11,13
U-238	9.23E-31	1.00E+04	19,11,13
Pu-244	6.83E-24	1.00E+04	19,11,13
Pu5-244	2.51E-27	1.00E+04	19,11,13
Ra-226	1.05E-16	1.00E+04	19,11,13
Rb-87	1.76E-11	1.00E+04	19,11,10
Se-79	1.83E-02	1.00E+04	18,14,10
Sn-126	8.01E-19	1.00E+04	19,11,13
Sr-90	3.35E-16	6.57E+02	19,11,13
Tc-99	2.01E-15	1.00E+04	18,14,10
Th-228	0.00E+00		
Ra-224	0.00E+00		
Th-229	1.85E-39	1.00E+04	19,11,13
Ra-225	1.22E-38	1.00E+04	19,11,13
Ac-225	1.36E-38	1.00E+04	19,11,13
Th-230	4.36E-39	1.00E+04	19,11,13
Ra-226	4.04E-17	1.00E+04	19,11,13
Pb-210	9.13E-17	1.00E+04	19,11,13
Po-210	1.65E-16	1.00E+04	19,11,13
Th-232	4.78E-39	1.00E+04	19,11,13
Ra-228	3.63E-38	1.00E+04	19,11,13
Th-228	5.67E-39	1.00E+04	19,11,13
Ra-224	3.75E-38	1.00E+04	19,11,13
U-232	4.99E-51	3.27E+03	19,11,13
Th-228	1.30E-51	3.27E+03	19,11,13
Ra-224	8.58E-51	3.27E+03	19,11,13
U-233	5.68E-25	1.00E+04	19,11,13
Th-229	9.66E-27	1.00E+04	19,11,13
Ra-225	6.39E-26	1.00E+04	19,11,13
U-234	5.77E-25	1.00E+04	19,11,13
Th-230	1.00E-27	1.00E+04	19,11,13
Ra-226	2.96E-19	1.00E+04	19,11,13
Pb-210	6.72E-19	1.00E+04	19,11,13
Po-210	1.21E-18	1.00E+04	19,11,13
U-235	5.94E-25	1.00E+04	19,11,13
Pa-231	1.87E-24	1.00E+04	19,11,13
Ac-227	2.39E-24	1.00E+04	19,11,13
Th-227	3.35E-25	1.00E+04	19,11,13
Ra-223	2.22E-24	1.00E+04	19,11,13
U-236	5.94E-25	1.00E+04	19,11,13
U-238	5.94E-25	1.00E+04	19,11,13
Th-234	1.53E-25	1.00E+04	19,11,13
U-234	1.71E-26	1.00E+04	19,11,13
Zr-93	1.61E-25	1.00E+04	19,11,13
Nb-93m	6.60E-25	1.00E+04	19,11,13
Zr-95	0.00E+00		
Nb-95	0.00E+00		

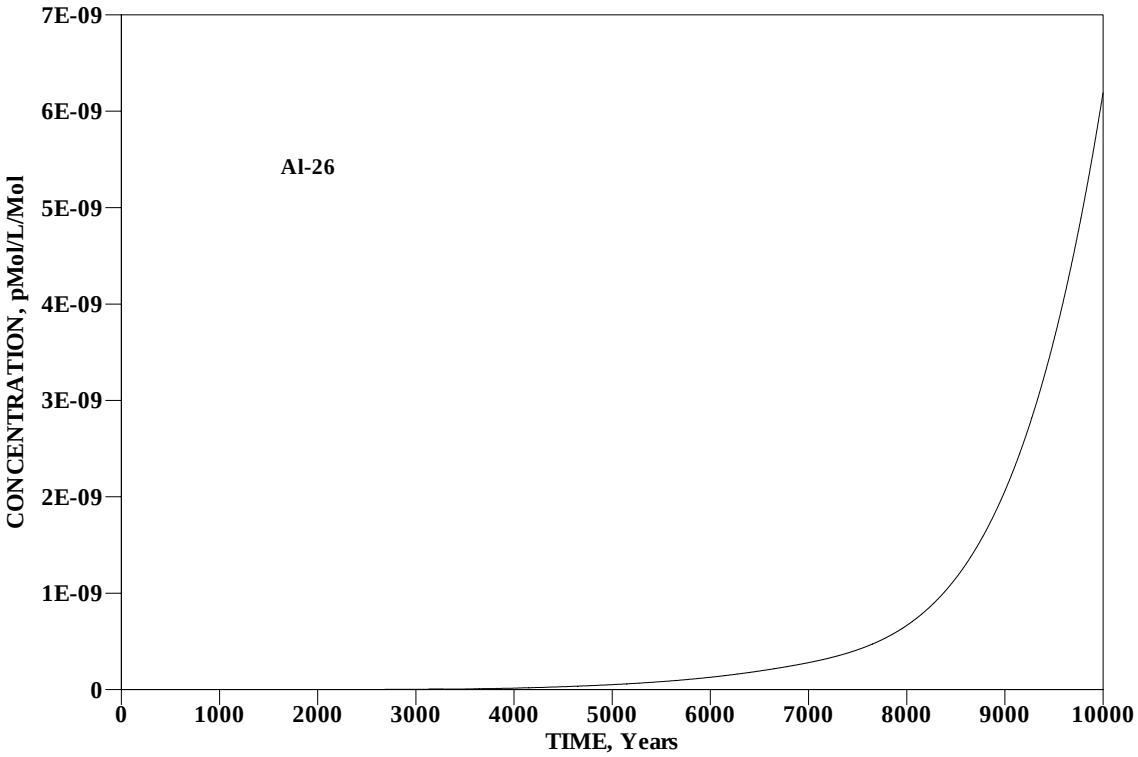

Figure A-60. Concentration of Al-26 vs Time for 10,000 Years

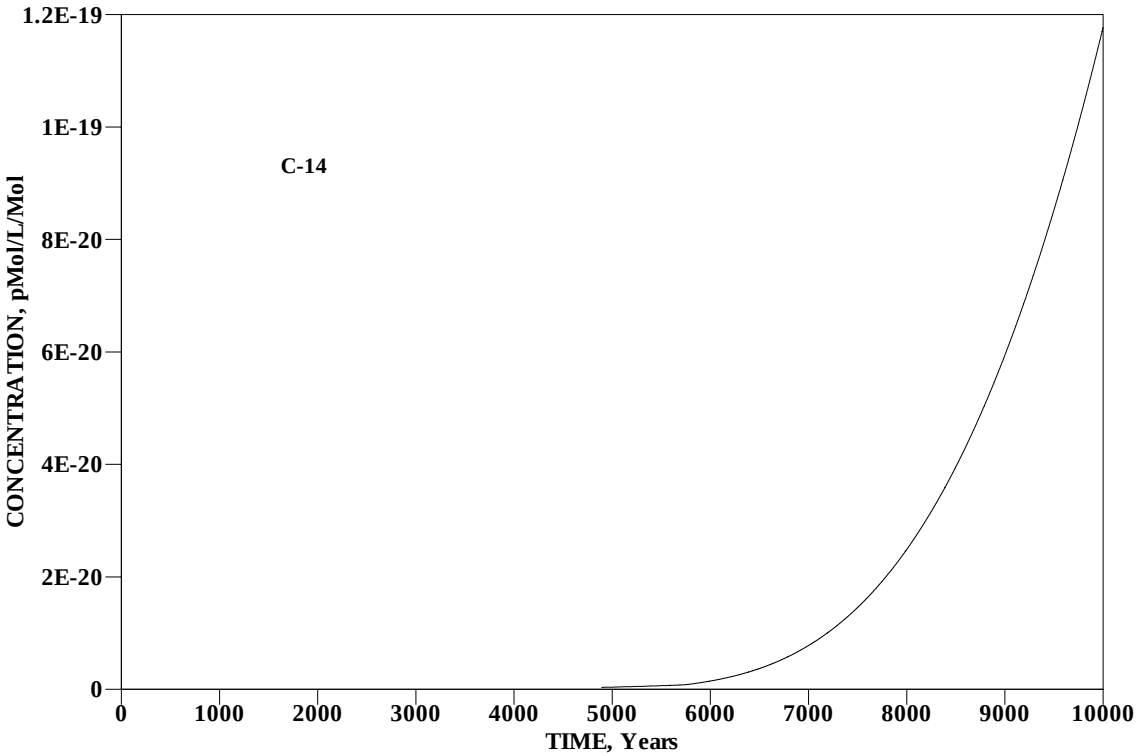

Figure A-61. Concentration of C-14 vs Time for 10,000 Years

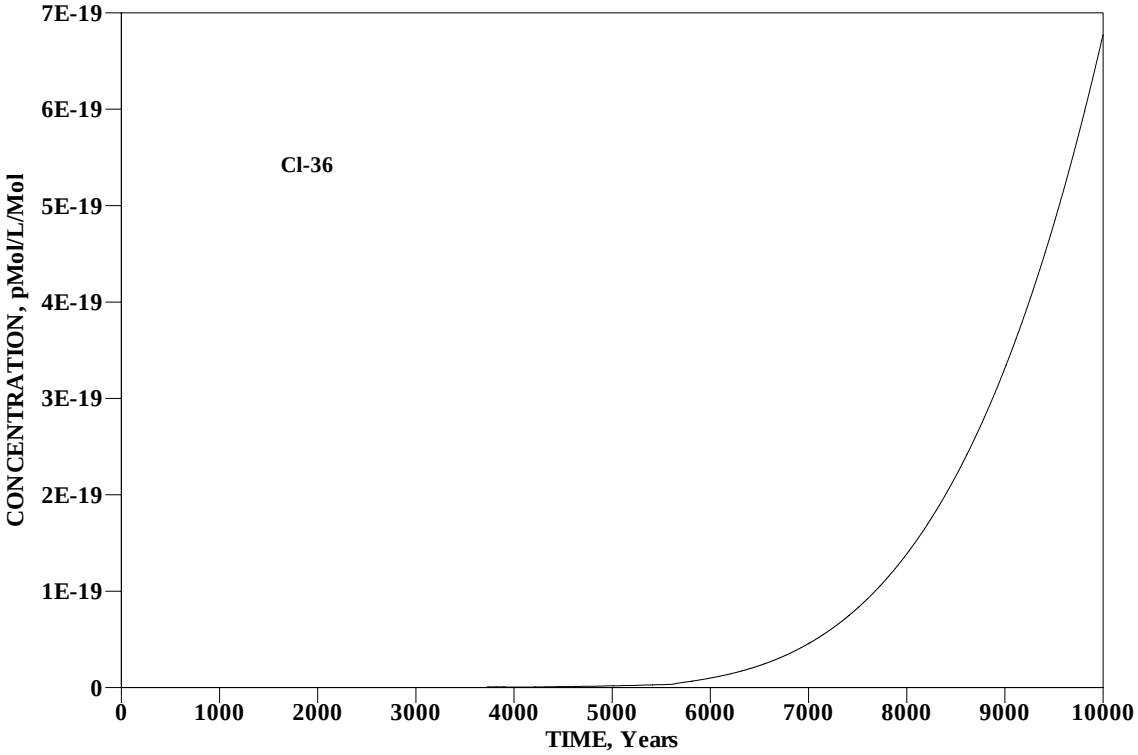

Figure A-62. Concentration of Cl-36 vs Time for 10,000 Years

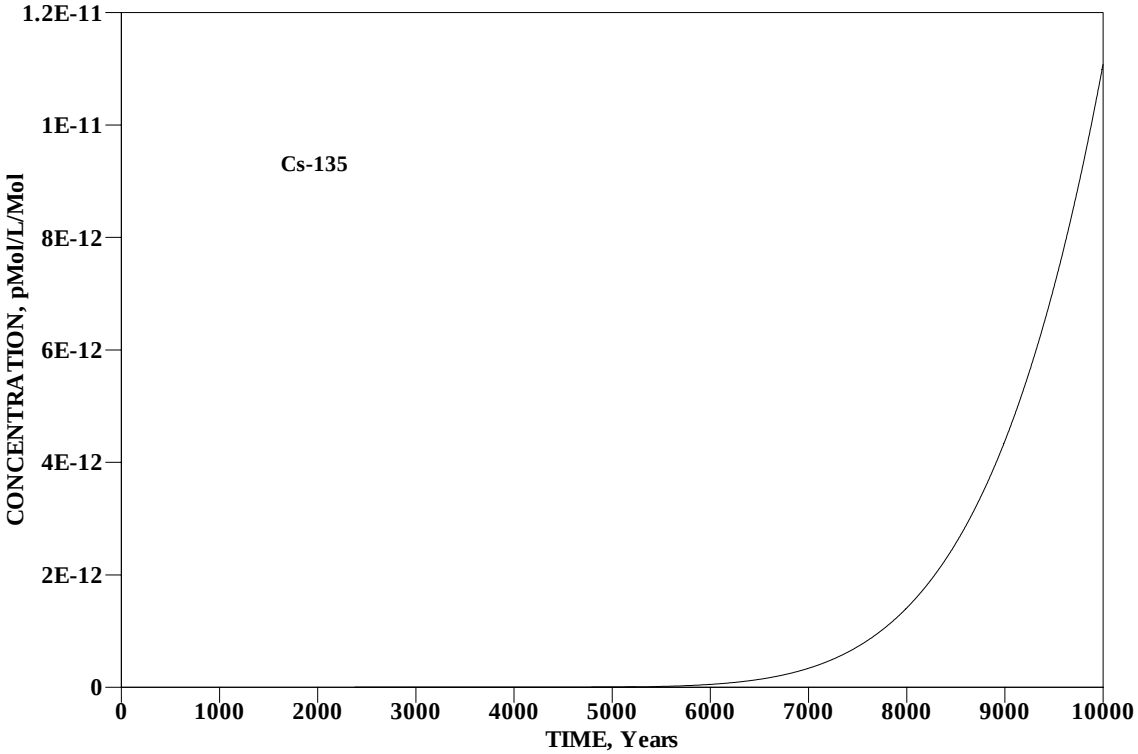

Figure A-63. Concentration of Cs-135 vs Time for 10,000 Years

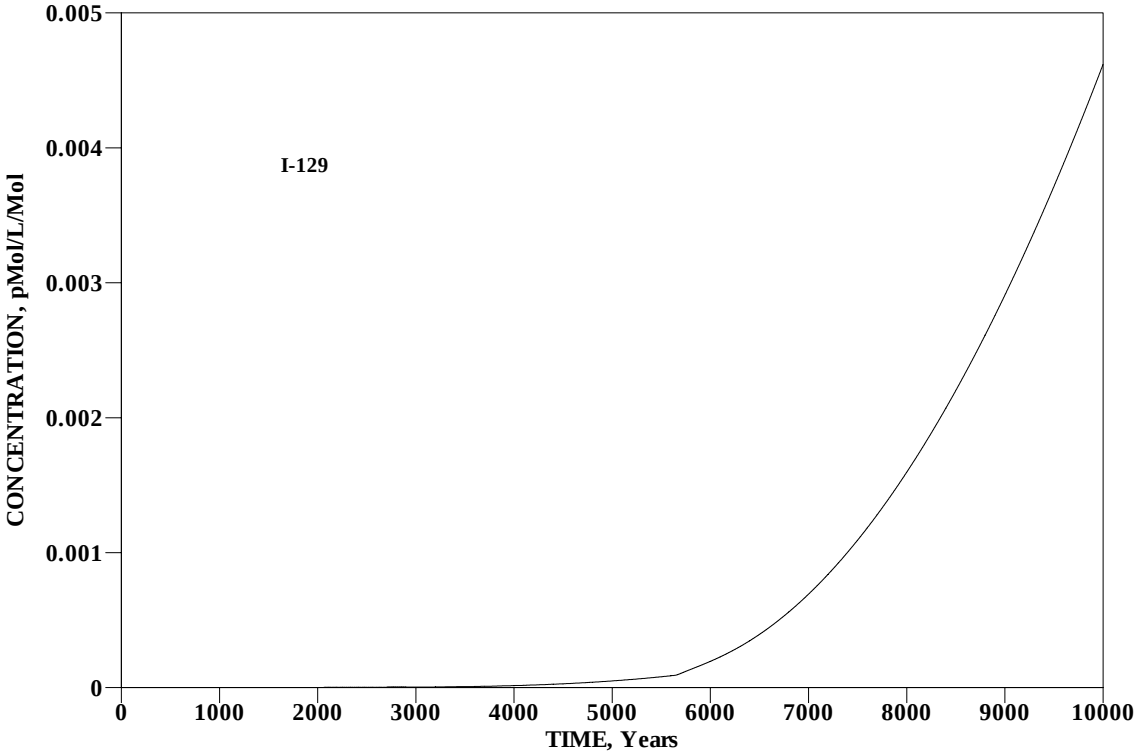

Figure A-64. Concentration of I-129 vs Time for 10,000 Years

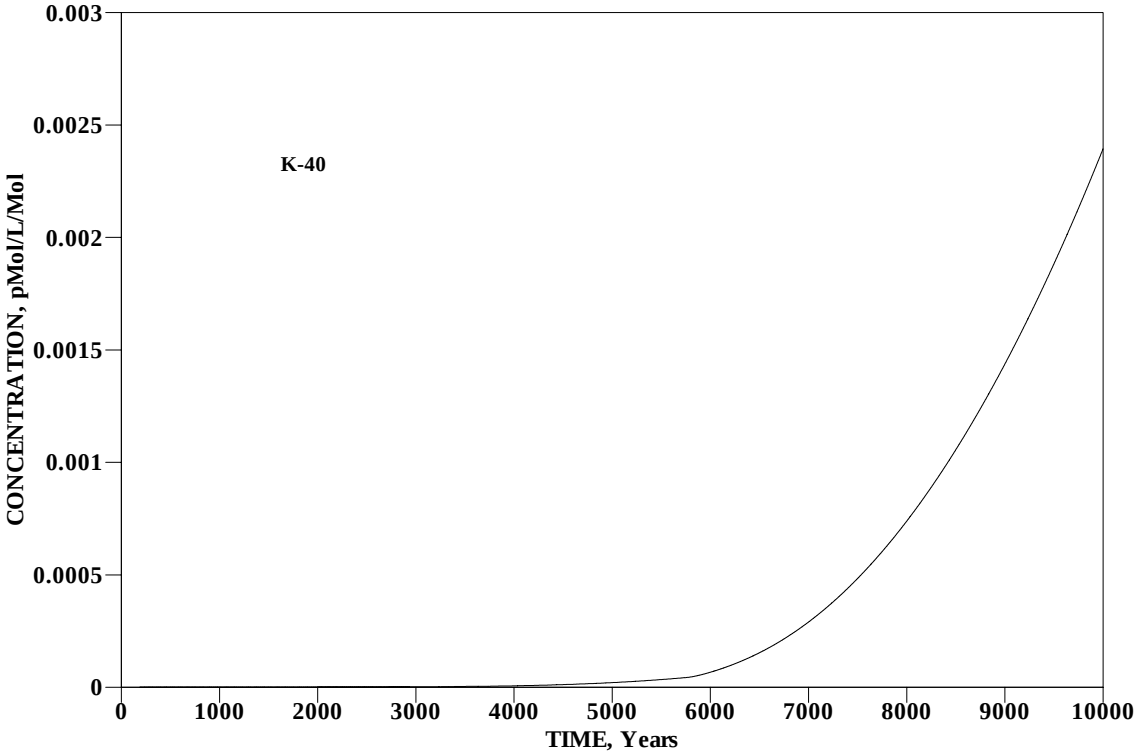

Figure A-65. Concentration of K-40 vs Time for 10,000 Years

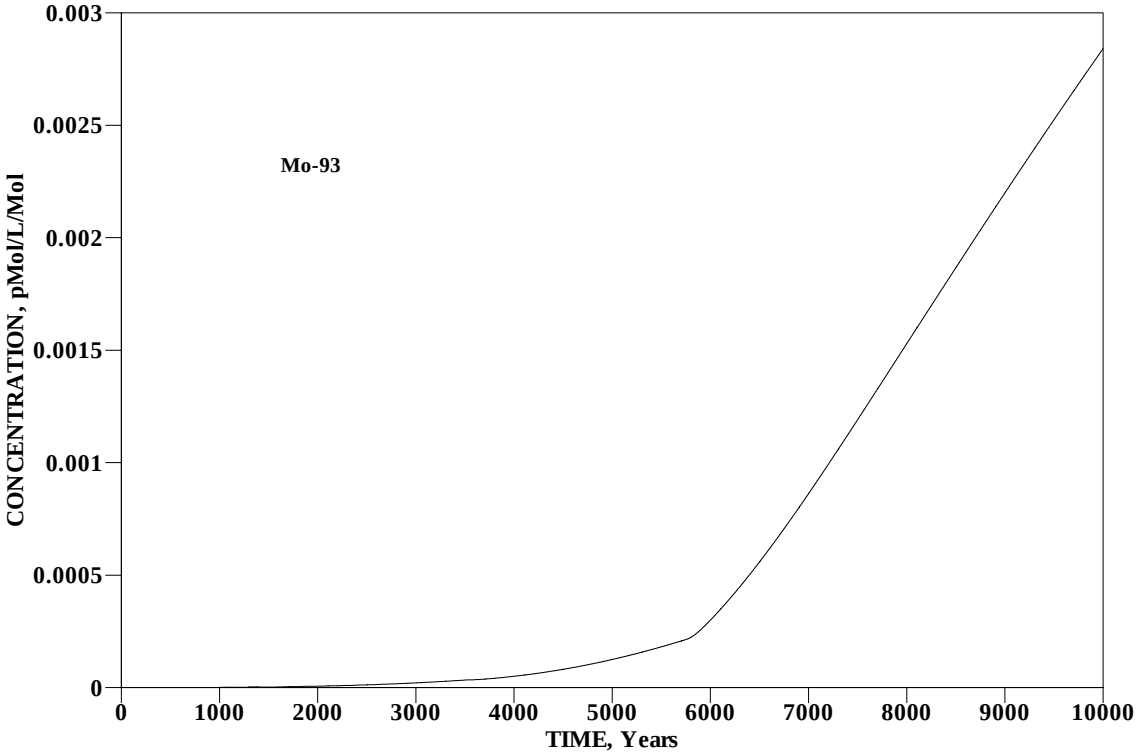

Figure A-66. Concentration of Mo-93 vs Time for 10,000 Years

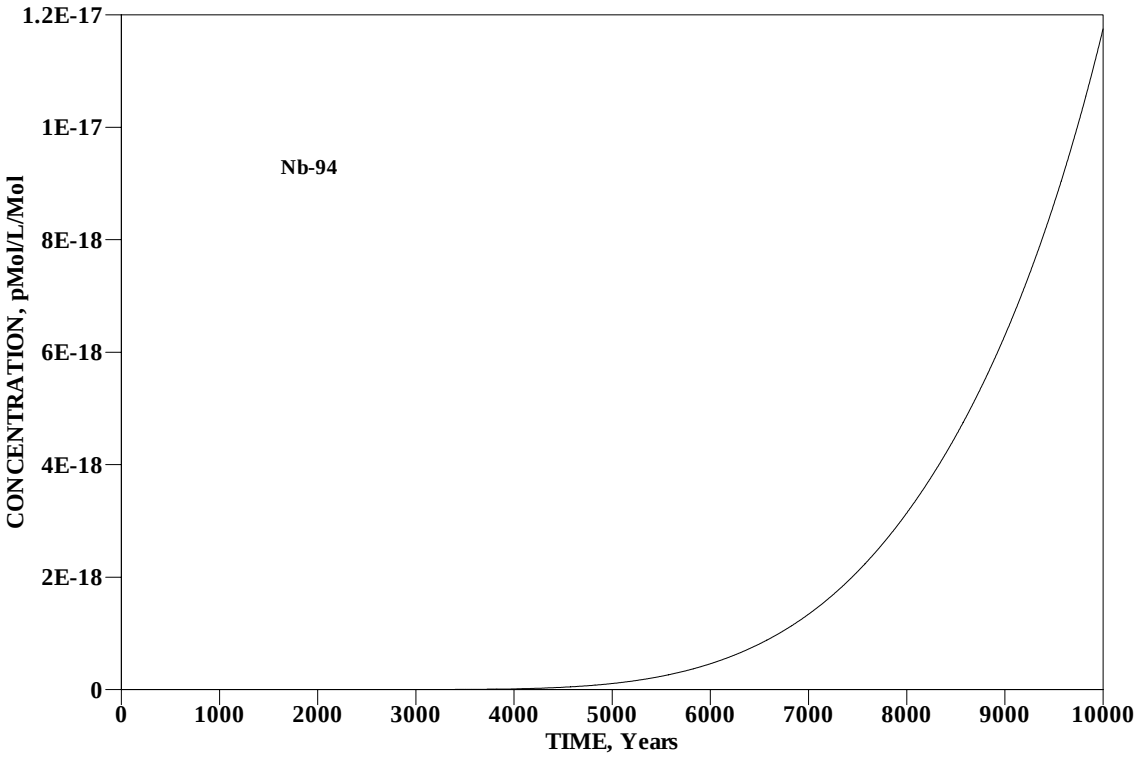

Figure A-67. Concentration of Nb-94 vs Time for 10,000 Years

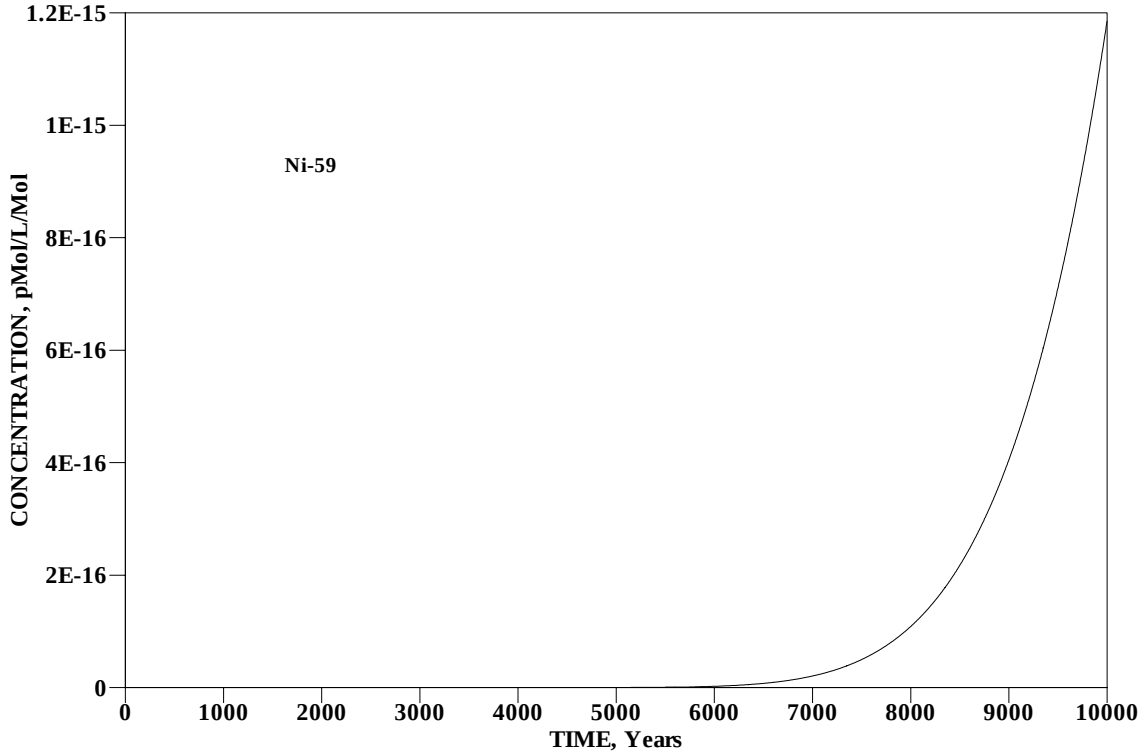

Figure A-68. Concentration of Ni-59 vs Time for 10,000 Years

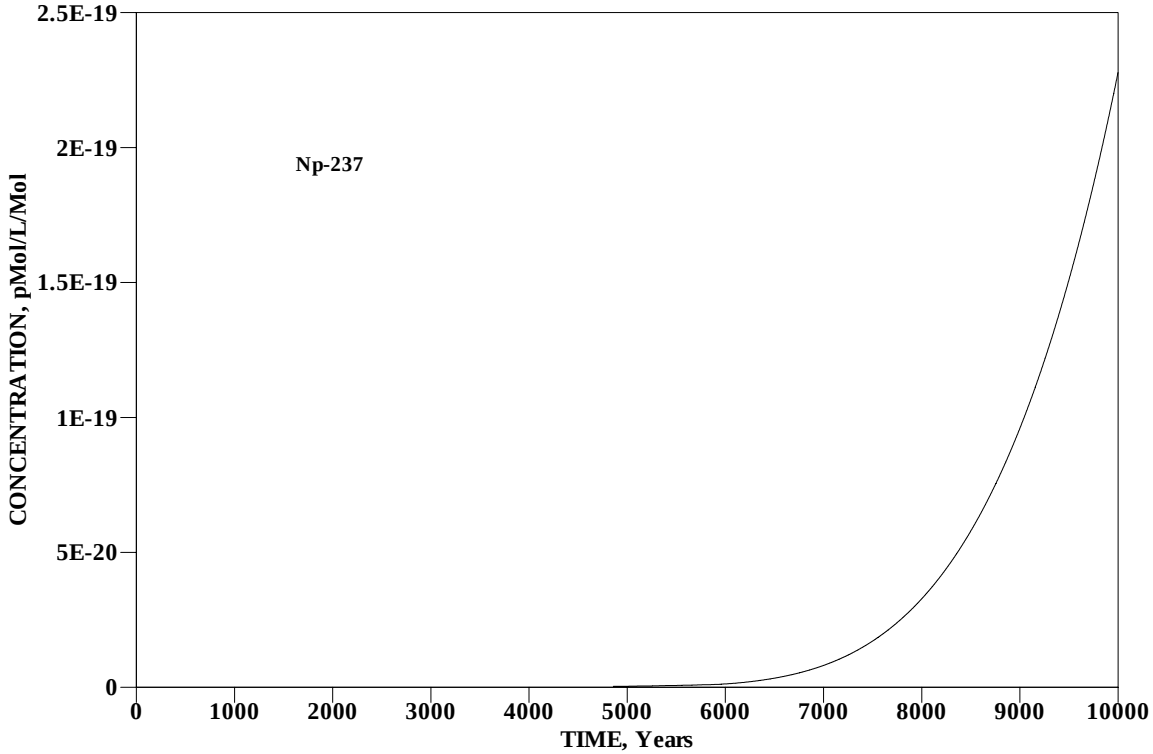

Figure A-69. Concentration of Np-237 vs Time for 10,000 Years

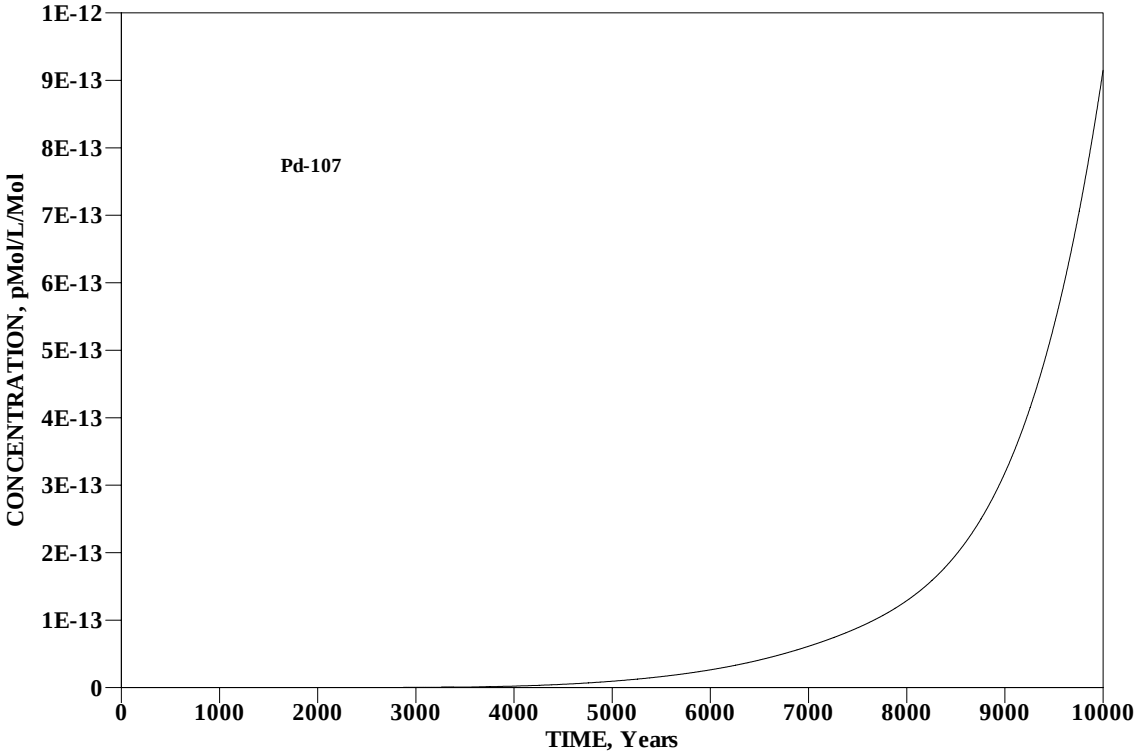

Figure A-70. Concentration of Pd-107 vs Time for 10,000 Years

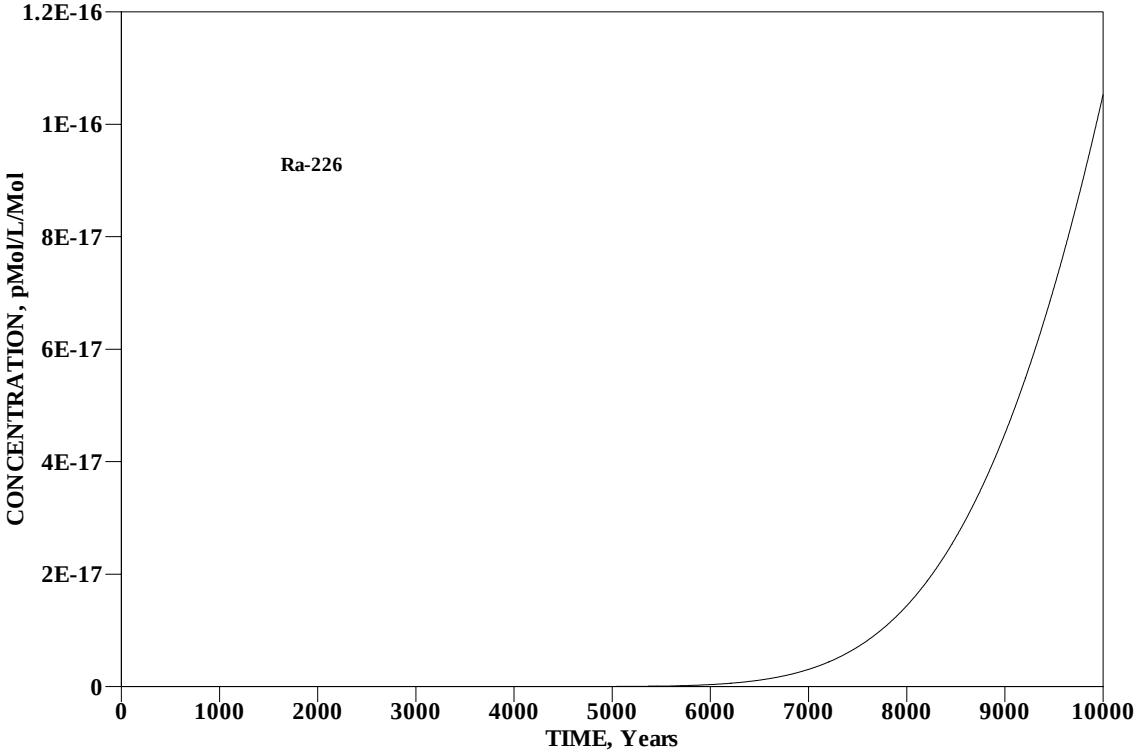

Figure A-71. Concentration of Ra-226 vs Time for 10,000 Years

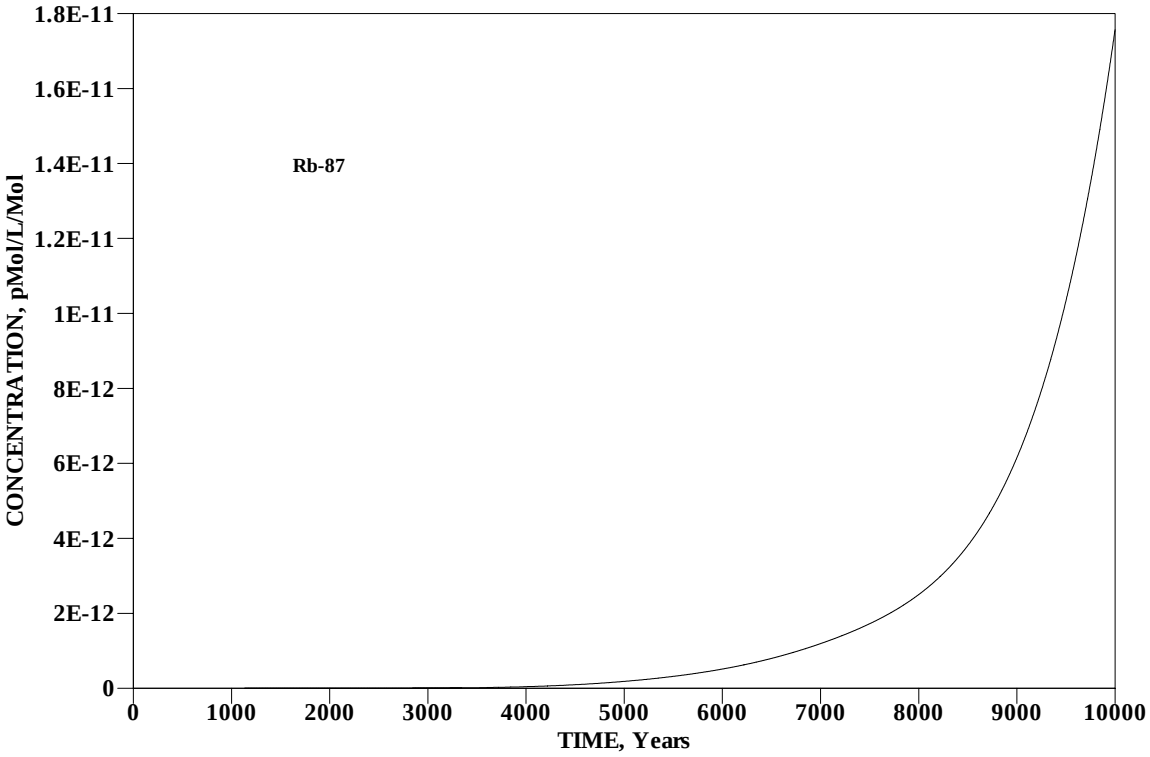

Figure A-72. Concentration of Rb-87 vs Time for 10,000 Years

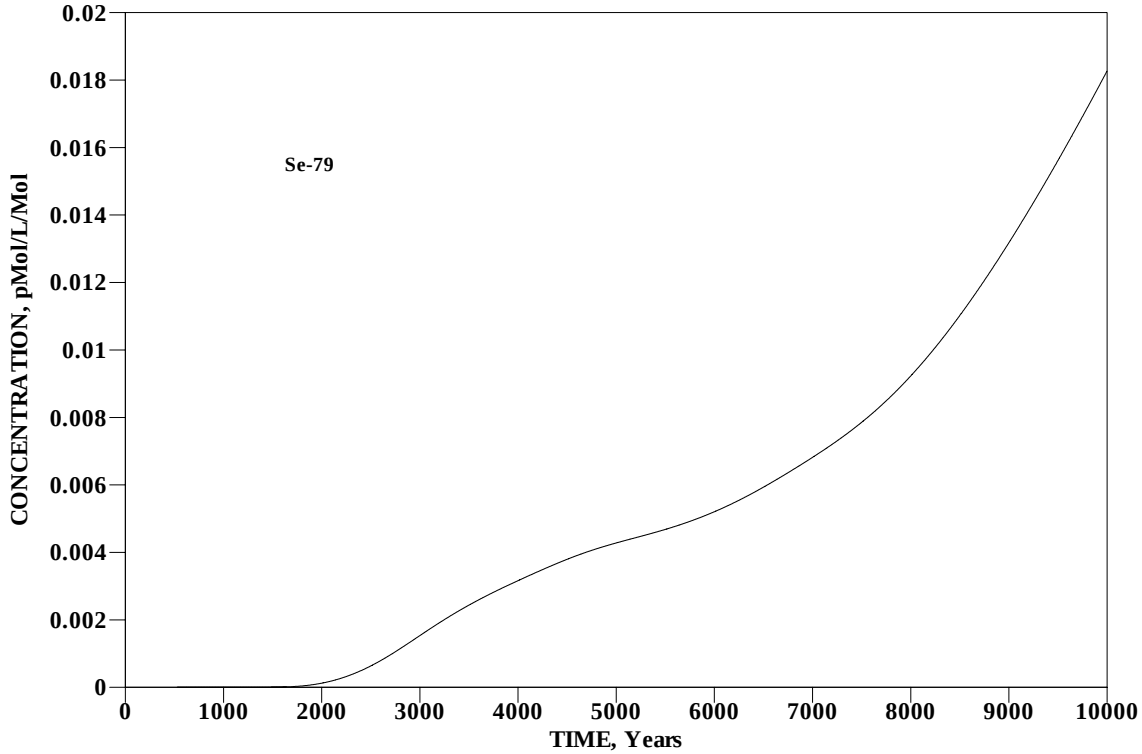

Figure A-73. Concentration of Se-79 vs Time for 10,000 Years

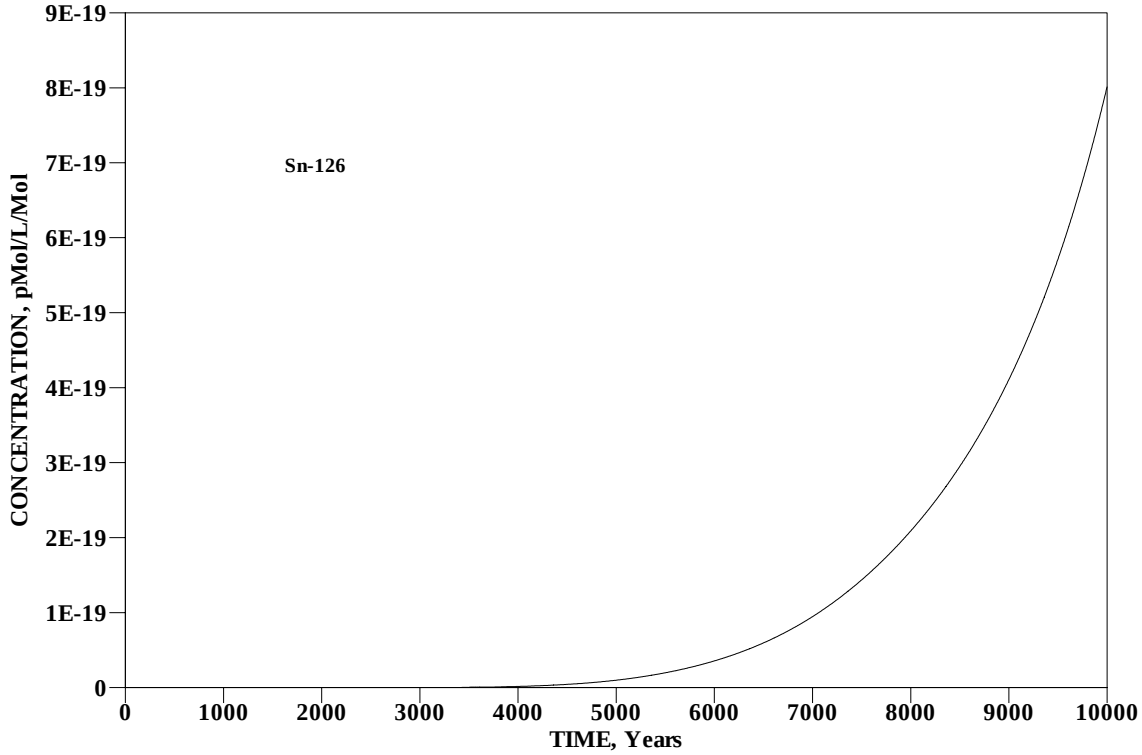

Figure A-74. Concentration of Sn-126 vs Time for 10,000 Years

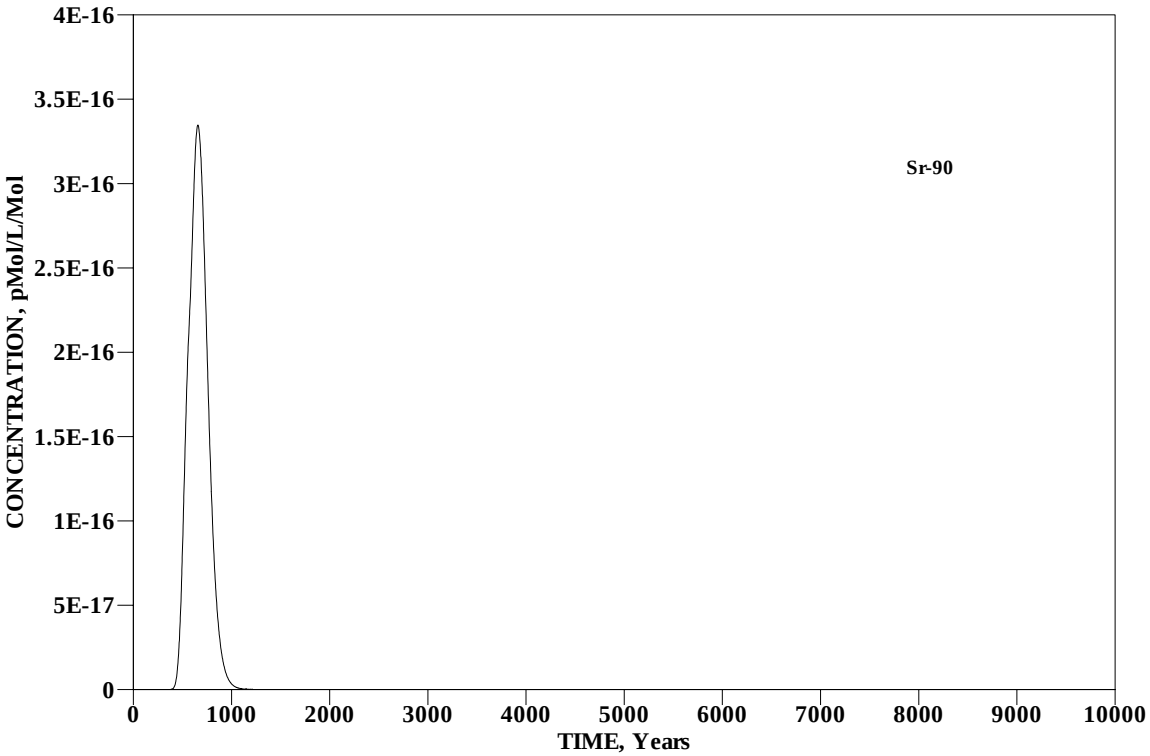

Figure A-75. Concentration of Sr-90 vs Time for 10,000 Years

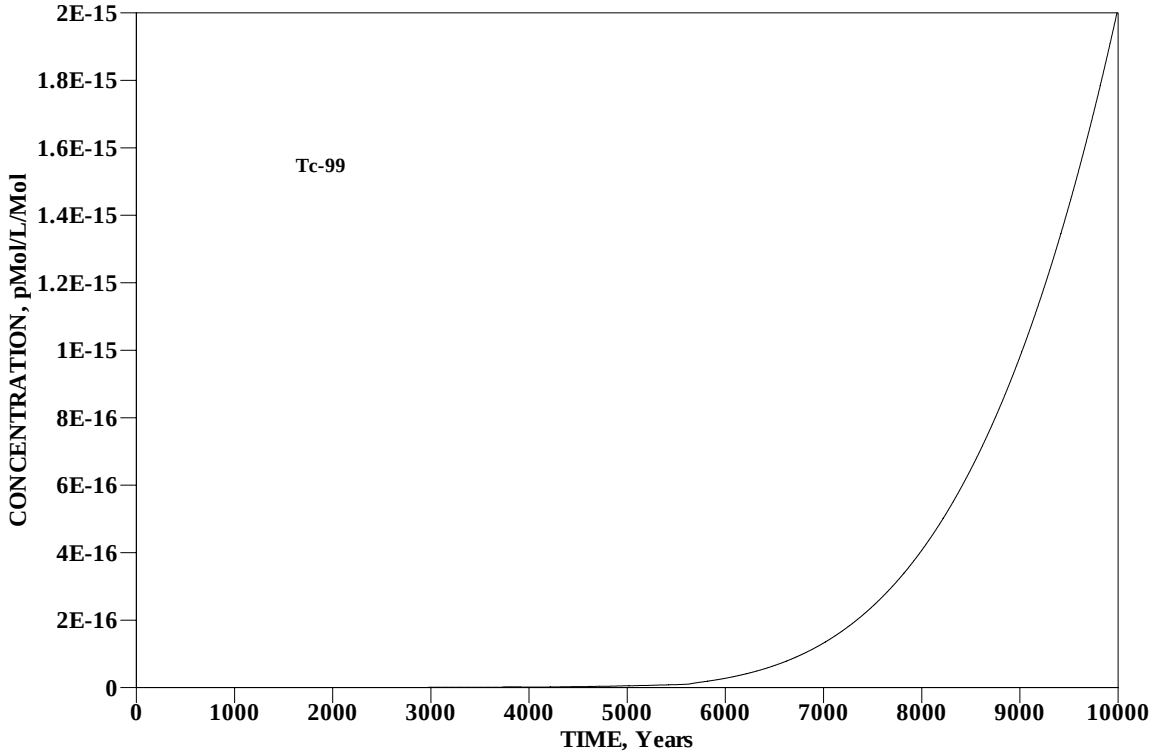

Figure A-76. Concentration of Tc-99 vs Time for 10,000 Years

Inventory Limits for Nitrate

The inventory limit for a contaminant is the Maximum Contaminant Level (MCL) divided by the peak groundwater concentration within the time and location of compliance:

$$I_L = MCL / C_{Peak} \qquad \text{(A-17)}$$

The MCL for nitrate is 1.0×10^4 parts per billion (ppb) as nitrogen. In Table A-14, the predicted nitrate peak concentrations are in pMole/L/Mole, which is equivalent to pico-Kg/L/Kg. If we assume the density of groundwater is 1.00 Kg/L, the concentrations in Table A-14 are changed to ppb/Kg as nitrogen by multiplying by 0.001. The converted peak concentrations, MCL and calculated inventory limits for nitrate are shown in Table A-17.

Table A-17. Converted Peak Concentrations, Peak Times, and Peak Nodes and Inventory Limit for Nitrate (MCL=1.0×10^4 ppb as nitrogen)

Contaminant	Peak Conc. ppb/Kg	Peak Time Years	Peak Node	Inventory Limit Kg as Nitrogen
NO_3	3.46E-05	1.00E+03	15,15,11	2.89E+08
NO_3	2.80E-03	9.80E+03	15,15,11	3.57E+06

As indicated in Table A-17, the calculated inventory limit for nitrate in Saltstone Vault 4 is 2.89E+08 Kg (as nitrogen) for a 1,000 year time of compliance and 3.57E+06 Kg (as nitrogen) for a 10,000 year time of compliance.

A.3.4 Inventory Limits for the Radionuclides

The peak concentrations shown in Tables A-14 and A-15 are in pico-mole/L/mole parent. Since the Maximum Contaminant Levels (MCL) for radionuclides are given in pCi/L, we converted the peak concentrations to pCi/L/Ci parent and entered them in Tables A-18 and A-19. As expected, the parent radionuclide peak concentrations remain the same. The daughter peak concentrations are calculated as:

$$C_{Ci} = C_{mol} \times \lambda_d / \lambda_p \qquad \text{(A-18)}$$

where λ_d and λ_p are the specific activity of the daughter and parent radionuclides, respectively. The MCLs used to calculate the inventory limits are also listed. The inventory limit is calculated by:

$$I_{Lim} = MCL / C_{Ci} \qquad \text{(A-19)}$$

Table A-18 and A-19 present the radionuclide inventory limits for Vault 4 based on 1,000 and 10,000 year times of compliance, respectively. In these tables, all concentrations that were less than 1.0×10^{-30} are shown as <1.E-30; no limits are calculated for these radionuclides. These concentrations are too low to produce meaningful limits. For radionuclides in a decay chain, the inventory limit for a parent may be determined by the peak concentration and MCL of a daughter.

Table A-18. Maximum Contaminant Levels and Calculated Inventory Limits for the Radionuclides - Time of Compliance = 1,000 years

Nuclide	Peak Conc. pCi/L/Ci	Peak Time Years	MCL pCi/L	Inv. Limit Ci
Al-26	2.94E-17	1.00E+03	4.00E+02	1.36E+19
Am-243	1.70E-75	1.00E+03	1.50E+01	8.82E+75
Np-239	7.94E-73	1.00E+03	3.00E+02	3.78E+74
Pu-239	2.73E-53	1.00E+03	1.50E+01	5.49E+53
Pu5-239	1.14E-56	1.00E+03	1.50E+01	1.32E+57
Bi-210	0.00E+00		9.00E+02	
Po-210	0.00E+00		1.50E+01	
C-14	5.34E-25	1.00E+03	2.00E+03	3.75E+27
Cf-249	1.41E-56	1.00E+03	1.50E+01	1.06E+57
Cm-245	3.73E-60	1.00E+03	1.50E+01	4.02E+60
Pu-241	7.07E-59	1.00E+03	3.00E+02	4.24E+60
Pu5-241	3.14E-62	1.00E+03	3.00E+02	9.55E+63
Am-241	6.17E-61	1.00E+03	1.50E+01	2.43E+61
Np-237	6.54E-31	1.00E+03	1.50E+01	2.29E+31
Cl-36	1.24E-24	1.00E+03	7.00E+02	5.65E+26
Cm-245	1.60E-87	1.00E+03	1.50E+01	9.38E+87
Pu-241	9.43E-63	1.00E+03	3.00E+02	3.18E+64
Pu5-241	4.25E-66	1.00E+03	3.00E+02	7.06E+67
Am-241	2.10E-64	1.00E+03	1.50E+01	7.14E+64
Np-237	3.61E-29	1.00E+03	1.50E+01	4.16E+29
Cm-246	1.13E-87	1.00E+03	1.50E+01	1.33E+88
Cm-247	1.53E-87	1.00E+03	1.50E+01	9.80E+87
Am-243	5.72E-77	1.00E+03	1.50E+01	2.62E+77
Np-239	2.69E-74	1.00E+03	3.00E+02	1.12E+76
Pu-239	4.64E-55	1.00E+03	1.50E+01	3.23E+55
Pu5-239	1.95E-58	1.00E+03	1.50E+01	7.69E+58
Cm-248	1.57E-87	1.00E+03	1.50E+01	9.55E+87
Pu-244	8.38E-57	1.00E+03	1.50E+01	1.79E+57
Pu5-244	3.51E-60	1.00E+03	1.50E+01	4.27E+60
Cs-135	9.24E-38	1.00E+03	9.00E+02	9.74E+39
Cs-137	5.08E-48	1.00E+03	2.00E+02	3.94E+49
H-3	1.10E-08	1.25E+02	2.00E+04	1.82E+12
I-129	5.69E-08	1.00E+03	1.00E+00	1.76E+07
K-40	2.83E-08	1.00E+03	3.00E+02	1.06E+10
Mo-93	5.07E-07	1.00E+03	4.00E+03	7.89E+09
Nb-93m	9.01E-09	1.00E+03	1.00E+03	1.11E+11
Nb-94	7.93E-36	1.00E+03	1.00E+03	1.26E+38
Nb-95m	0.00E+00		1.00E+03	
Nb-95	0.00E+00		3.00E+02	
Ni-59	7.66E-44	1.00E+03	3.00E+02	3.92E+45
Np-237	2.65E-25	1.00E+03	1.50E+01	5.66E+25
Pd-107	1.22E-22	1.00E+03	4.00E+04	3.28E+26
Pu-238	8.12E-55	1.00E+03	1.50E+01	1.85E+55
Pu5-238	3.40E-58	1.00E+03	1.50E+01	4.41E+58
U-234	5.85E-59	1.00E+03	1.30E+02*	2.22E+60
Pu-239	2.75E-51	1.00E+03	1.50E+01	5.45E+51
Pu5-239	1.15E-54	1.00E+03	1.50E+01	1.30E+55
U-235	5.06E-59	1.00E+03	6.50E+01*	1.28E+60

Pu-240	2.54E-51	1.00E+03	1.50E+01	5.91E+51
Pu5-240	1.06E-54	1.00E+03	1.50E+01	1.42E+55
U-236	1.41E-57	1.00E+03	1.40E+02*	9.93E+58
Pu-241	1.21E-72	1.00E+03	3.00E+02	2.48E+74
Pu5-241	5.15E-76	1.00E+03	3.00E+02	5.83E+77
Am-241	1.02E-73	1.00E+03	1.50E+01	1.47E+74
Np-237	1.38E-30	1.00E+03	1.50E+01	1.09E+31
Pu-242	2.83E-51	1.00E+03	1.50E+01	5.30E+51
Pu5-242	1.18E-54	1.00E+03	1.50E+01	1.27E+55
U-238	8.18E-60	1.00E+03	1.00E+01*	1.22E+60
Pu-244	2.83E-51	1.00E+03	1.50E+01	5.30E+51
Pu5-244	1.18E-54	1.00E+03	1.50E+01	1.27E+55
Ra-226	1.24E-45	1.00E+03	5.00E+00	4.03E+45
Rb-87	2.42E-21	1.00E+03	3.00E+02	1.24E+23
Se-79	3.50E-07	1.00E+03	7.00E+02	2.00E+09
Sn-126	4.64E-35	1.00E+03	3.00E+02	6.47E+36
Sr-90	3.35E-16	6.57E+02	8.00E+00	2.39E+16
Tc-99	3.59E-21	1.00E+03	9.00E+02	2.51E+23
Th-228	0.00E+00		1.50E+01	
Ra-224	0.00E+00		1.50E+01	
Th-229	5.93E-84	1.00E+03	1.50E+01	2.53E+84
Ra-225	3.99E-83	1.00E+03	2.00E+01	5.01E+83
Ac-225	4.50E-83	1.00E+03	1.00E+00	2.22E+82
Th-230	7.78E-84	1.00E+03	1.50E+01	1.93E+84
Ra-226	3.15E-47	1.00E+03	5.00E+00	1.59E+47
Pb-210	4.38E-45	1.00E+03	1.00E+00	2.28E+44
Po-210	8.26E-45	1.00E+03	1.50E+01	1.82E+45
Th-232	6.99E-84	1.00E+03	1.50E+01	2.15E+84
Ra-228	1.51E-75	1.00E+03	5.00E+00	3.31E+75
Th-228	2.46E-76	1.00E+03	1.50E+01	6.10E+76
Ra-224	1.63E-75	1.00E+03	1.50E+01	9.20E+75
U-232	9.25E-65	1.00E+03	2.60E+01*	2.81E+65
Th-228	2.21E-65	1.00E+03	1.50E+01	6.79E+65
Ra-224	1.46E-64	1.00E+03	1.50E+01	1.03E+65
U-233	2.99E-60	1.00E+03	1.30E+02*	4.35E+61
Th-229	1.88E-63	1.00E+03	1.50E+01	7.98E+63
Ra-225	1.25E-62	1.00E+03	2.00E+01	1.60E+63
U-234	3.12E-60	1.00E+03	1.30E+02*	4.17E+61
Th-230	1.93E-64	1.00E+03	1.50E+01	7.77E+64
Ra-226	1.50E-50	1.00E+03	5.00E+00	3.33E+50
Pb-210	2.44E-48	1.00E+03	1.00E+00	4.10E+47
Po-210	4.61E-48	1.00E+03	1.50E+01	3.25E+48
U-235	3.00E-60	1.00E+03	6.50E+01*	2.17E+61
Pa-231	2.94E-57	1.00E+03	1.50E+01	5.10E+57
Ac-227	5.69E-57	1.00E+03	1.00E+00	1.76E+56
Th-227	7.98E-58	1.00E+03	1.50E+01	1.88E+58
Ra-223	5.29E-57	1.00E+03	1.50E+01	2.84E+57
U-236	3.00E-60	1.00E+03	1.40E+02*	4.67E+61
U-238	3.00E-60	1.00E+03	1.00E+01*	3.33E+60
Th-234	7.72E-61	1.00E+03	4.00E+02	5.18E+62
U-234	9.04E-63	1.00E+03	1.30E+02	1.44E+64
Zr-93	5.05E-58	1.00E+03	2.00E+03	3.96E+60
Nb-93m	1.17E-49	1.00E+03	1.00E+03	8.55E+51
Zr-95	0.00E+00		2.00E+02	
Nb-95	0.00E+00		3.00E+02	

* Uranium “MCL” is based on 25 mrem/year rather than the 30 μg/L MCL

Table A-19. Maximum Contaminant Levels and Calculated Inventory Limits for the Radionuclides - Time of Compliance = 10,000 years

Nuclide	Peak Conc. pCi/L/Ci	Peak Time Years	MCL pCi/L	Inv. Limit Ci
Al-26	6.19E-09	1.00E+04	4.00E+02	6.46E+10
Am-243	5.78E-34	1.00E+04	1.50E+01	2.60E+34
Np-239	2.23E-31	1.00E+04	3.00E+02	1.35E+33
Pu-239	6.70E-25	1.00E+04	1.50E+01	2.24E+25
Pu5-239	2.46E-28	1.00E+04	1.50E+01	6.10E+28
Bi-210	0.00E+00		9.00E+02	
Po-210	0.00E+00		1.50E+01	
C-14	1.18E-19	1.00E+04	2.00E+03	1.69E+22
Cf-249	5.47E-33	7.58E+03	1.50E+01	2.74E+33
Cm-245	3.67E-34	1.00E+04	1.50E+01	4.09E+34
Pu-241	4.35E-33	1.00E+04	3.00E+02	6.90E+34
Pu5-241	1.61E-36	1.00E+04	3.00E+02	1.86E+38
Am-241	1.04E-33	1.00E+04	1.50E+01	1.44E+34
Np-237	2.13E-23	1.00E+04	1.50E+01	7.04E+23
Cl-36	6.77E-19	1.00E+04	7.00E+02	1.03E+21
Cm-245	4.94E-42	1.00E+04	1.50E+01	3.04E+42
Pu-241	1.41E-40	1.00E+04	3.00E+02	2.13E+42
Pu5-241	5.63E-44	1.00E+04	3.00E+02	5.33E+45
Am-241	3.71E-38	1.00E+04	1.50E+01	4.04E+38
Np-237	5.18E-22	1.00E+04	1.50E+01	2.90E+22
Cm-246	2.60E-42	1.00E+04	1.50E+01	5.77E+42
Cm-247	1.12E-41	1.00E+04	1.50E+01	1.34E+42
Am-243	1.61E-34	1.00E+04	1.50E+01	9.32E+34
Np-239	6.22E-32	1.00E+04	3.00E+02	4.82E+33
Pu-239	1.96E-25	1.00E+04	1.50E+01	7.65E+25
Pu5-239	7.18E-29	1.00E+04	1.50E+01	2.09E+29
Cm-248	1.10E-41	1.00E+04	1.50E+01	1.36E+42
Pu-244	3.11E-28	1.00E+04	1.50E+01	4.82E+28
Pu5-244	1.14E-31	1.00E+04	1.50E+01	1.32E+32
Cs-135	1.11E-11	1.00E+04	9.00E+02	8.11E+13
Cs-137	3.85E-44	1.67E+03	2.00E+02	5.19E+45
H-3	1.10E-08	1.25E+02	2.00E+04	1.82E+12
I-129	4.62E-03	1.00E+04	1.00E+00	2.16E+02
K-40	2.39E-03	1.00E+04	3.00E+02	1.26E+05
Mo-93	2.84E-03	1.00E+04	4.00E+03	1.41E+06
Nb-93m	5.53E-05	1.00E+04	1.00E+03	1.81E+07
Nb-94	1.17E-17	1.00E+04	1.00E+03	8.55E+19
Nb-95m	0.00E+00		1.00E+03	
Nb-95	0.00E+00		3.00E+02	
Ni-59	1.19E-15	1.00E+04	3.00E+02	2.52E+17
Np-237	2.28E-19	1.00E+04	1.50E+01	6.58E+19
Pd-107	9.15E-13	1.00E+04	4.00E+04	4.37E+16
Pu-238	1.17E-42	3.16E+03	1.50E+01	1.28E+43
Pu5-238	4.37E-46	3.16E+03	1.50E+01	3.43E+46
U-234	1.86E-28	1.00E+04	1.30E+02*	6.99E+29
Pu-239	5.12E-24	1.00E+04	1.50E+01	2.93E+24
Pu5-239	1.88E-27	1.00E+04	1.50E+01	7.98E+27
U-235	4.75E-30	1.00E+04	6.50E+01*	1.37E+31
Pu-240	2.37E-24	1.00E+04	1.50E+01	6.33E+24
Pu5-240	8.70E-28	1.00E+04	1.50E+01	1.72E+28

U-236	8.08E-29	1.00E+04	1.40E+02*	1.73E+30
Pu-241	1.76E-72	1.16E+03	3.00E+02	1.70E+74
Pu5-241	7.40E-76	1.16E+03	3.00E+02	4.05E+77
Am-241	5.22E-42	1.00E+04	1.50E+01	2.87E+42
Np-237	1.56E-24	1.00E+04	1.50E+01	9.62E+24
Pu-242	6.71E-24	1.00E+04	1.50E+01	2.24E+24
Pu5-242	2.46E-27	1.00E+04	1.50E+01	6.10E+27
U-238	9.23E-31	1.00E+04	1.00E+01*	1.08E+31
Pu-244	6.83E-24	1.00E+04	1.50E+01	2.20E+24
Pu5-244	2.51E-27	1.00E+04	1.50E+01	5.98E+27
Ra-226	1.05E-16	1.00E+04	5.00E+00	4.76E+16
Rb-87	1.76E-11	1.00E+04	3.00E+02	1.70E+13
Se-79	1.83E-02	1.00E+04	7.00E+02	3.83E+04
Sn-126	8.01E-19	1.00E+04	3.00E+02	3.75E+20
Sr-90	3.35E-16	6.57E+02	8.00E+00	2.39E+16
Tc-99	2.01E-15	1.00E+04	9.00E+02	4.48E+17
Th-228	0.00E+00		1.50E+01	
Ra-224	0.00E+00		1.50E+01	
Th-229	1.85E-39	1.00E+04	1.50E+01	8.11E+39
Ra-225	1.22E-38	1.00E+04	2.00E+01	1.64E+39
Ac-225	1.36E-38	1.00E+04	1.00E+00	7.35E+37
Th-230	4.36E-39	1.00E+04	1.50E+01	3.44E+39
Ra-226	4.04E-17	1.00E+04	5.00E+00	1.24E+17
Pb-210	9.13E-17	1.00E+04	1.00E+00	1.10E+16
Po-210	1.65E-16	1.00E+04	1.50E+01	9.09E+16
Th-232	4.78E-39	1.00E+04	1.50E+01	3.14E+39
Ra-228	3.63E-38	1.00E+04	5.00E+00	1.38E+38
Th-228	5.67E-39	1.00E+04	1.50E+01	2.65E+39
Ra-224	3.75E-38	1.00E+04	1.50E+01	4.00E+38
U-232	4.99E-51	3.27E+03	2.60E+01*	5.21E+51
Th-228	1.30E-51	3.27E+03	1.50E+01	1.15E+52
Ra-224	8.58E-51	3.27E+03	1.50E+01	1.75E+51
U-233	5.68E-25	1.00E+04	1.30E+02*	2.29E+26
Th-229	9.66E-27	1.00E+04	1.50E+01	1.55E+27
Ra-225	6.39E-26	1.00E+04	2.00E+01	3.13E+26
U-234	5.77E-25	1.00E+04	1.30E+02*	2.25E+26
Th-230	1.00E-27	1.00E+04	1.50E+01	1.50E+28
Ra-226	2.96E-19	1.00E+04	5.00E+00	1.69E+19
Pb-210	6.72E-19	1.00E+04	1.00E+00	1.49E+18
Po-210	1.21E-18	1.00E+04	1.50E+01	1.24E+19
U-235	5.94E-25	1.00E+04	6.50E+01*	1.09E+26
Pa-231	1.87E-24	1.00E+04	1.50E+01	8.02E+24
Ac-227	2.39E-24	1.00E+04	1.00E+00	4.18E+23
Th-227	3.35E-25	1.00E+04	1.50E+01	4.48E+25
Ra-223	2.22E-24	1.00E+04	1.50E+01	6.76E+24
U-236	5.94E-25	1.00E+04	1.40E+02*	2.36E+26
U-238	5.94E-25	1.00E+04	1.00E+01*	1.68E+25
Th-234	1.53E-25	1.00E+04	4.00E+02	2.61E+27
U-234	1.71E-26	1.00E+04	1.30E+02*	7.60E+27
Zr-93	1.61E-25	1.00E+04	2.00E+03	1.24E+28
Nb-93m	6.60E-25	1.00E+04	1.00E+03	1.52E+27
Zr-95	0.00E+00		2.00E+02	
Nb-95	0.00E+00		3.00E+02	

* Uranium “MCL” is based on 25 mrem/year rather than the 30 μg/L MCL

A.4 Impact of Macroscopic Cracks on Saltstone Vault 4 Performance

Vertical cracks or fractures spanning the entire Saltstone Vault 4 width and height are predicted to occur at 30 ft intervals, coinciding with construction joints, in response to static settlement and earthquakes. For the assumed properties of saltstone (10^{-11} cm/s conductivity), the literature indicates cracks can be neglected when the suction head exceeds approximately 200 cm in saltstone. Such conditions are predicted to occur during the 0-10,000 year period. This conclusion applies regardless of crack geometry, i.e., open at top, open at bottom, or through-crack.

A.4.1 Introduction

Peregoy (2003) analyzed the structural behavior of Saltstone Vault 4 in response to forecast static settlement and earthquakes. Approximately vertical cracks or fractures spanning the entire Vault 4 width and height were predicted to occur at 30 ft intervals, coinciding with construction joints. In the structural simulations, these macroscopic cracks were observed to open at either the top or bottom, while remaining in close contact at the opposite end of the fracture face, the latter forming a "hinge" of sorts. The cracks developed gradually over time (Peregoy 2003, Figure 9, Figure 10 and Table 2). Predicted mean crack sizes are summarized in Table A-20.

Table A-20. Summary of mean crack sizes at specific times.

Cracks open at bottom

Time (yr)	Crack width at open end (in)	Average width (in)
100	0.06	0.03
500	0.18	0.09
1000	0.30	0.15
2500	0.63	0.31
5000	1.15	0.58
10000	2.18	1.09

Cracks open at top

Time (yr)	Crack width at open end (in)	Average width (in)
100	0.01	0.004
500	0.03	0.015
1000	0.06	0.03
2500	0.16	0.08
5000	0.31	0.16
10000	0.62	0.31

Under a positive pressure condition, cracks or fractures in the saltstone monolith would be liquid-filled and form preferential pathways for infiltrating water compared to the surrounding low permeability matrix (10^{-11} cm/s). Under negative pressure or suction, the impact of cracks on saltstone performance is not immediately clear. The purpose of this Section is to assess the effect of macroscopic cracks on moisture movement through Saltstone Vault 4 under a range of hydraulic conditions and crack dimensions.

A.4.2 Flow Regimes

Water flow through a rough walled crack in a porous medium occurs in at least three distinct regimes:

1. Saturated flow, that is, liquid completely filling the aperture.
2. "Thick" film flow on each crack wall, where water is present as a film completely filling surface pits and grooves and the air-water interface is relatively flat.
3. "Thin" film flow, where water recedes into surface pits/grooves by capillary forces and adheres to flat surfaces by adsorption.

The saturated flow regime occurs at positive or very slightly negative pressures. The "thick" and "thin" film flow regimes occur at increasing negative pressures or suction in the surrounding porous medium. Each flow regime is analyzed separately below in the context of a uniform crack width.

An implicit assumption in these analyses is that the source of liquid to the crack is steady rather than episodic/transient, and that the resulting fracture flow is steady. Unsteady fracture flow has been observed at laboratory scale and inferred at field scale (Persoff and Pruess 1995; Su et al. 2001; Nativ et al. 1995; Fabryka-Martin et al. 1996; Pruess 1999). At laboratory scale, unsteady flow appears to be associated with relatively low suctions in a variable aperture setting. Under these conditions, water fills the smaller apertures while larger apertures are desaturated. At field scale (e.g. Yucca Mountain), unsteady flow has been inferred under high matrix suction. Temporal and spatial variations in infiltration and physical heterogeneity are thought to be factors leading to episodic flow.

The planned Saltstone closure cover system is expected to insulate cracks from episodic rainfall and lead to a relatively steady influx of water. Saltstone itself is expected to exhibit uniform properties in comparison with fractured geologic media. Cracks forming from differential settlement and seismic events are expected to be unsaturated. All of these conditions favor steady flow in Saltstone Vault 4.

A.4.3 Saturated Flow

The height of capillary liquid rise H between two parallel surfaces of aperture b is given by (e.g. Looney and Falta 2000)

$$H = \frac{2\sigma}{\rho g b} \tag{A-20}$$

where σ is surface tension, ρ is liquid density, and g is gravitational acceleration. In the context of a fracture subject to a given pressure P in the surrounding matrix, the aperture will be liquid filled under the condition

$$P > -\frac{2\sigma}{b} \tag{A-21}$$

where suction is indicated by a negative pressure value (e.g. Wang and Narasimhan 1985). The equivalent permeability of the fracture is

$$k = \frac{b^2}{12} \tag{A-22}$$

and the hydraulic conductivity is

$$K = \frac{\rho g k}{\eta} = \frac{\rho g b^2}{12\eta} \tag{A-23}$$

where η is liquid viscosity. Figure 1 shows hydraulic conductivity as a function of aperture for water at 20°C. Note that even narrow cracks have a high conductivity compared to cementitious materials.

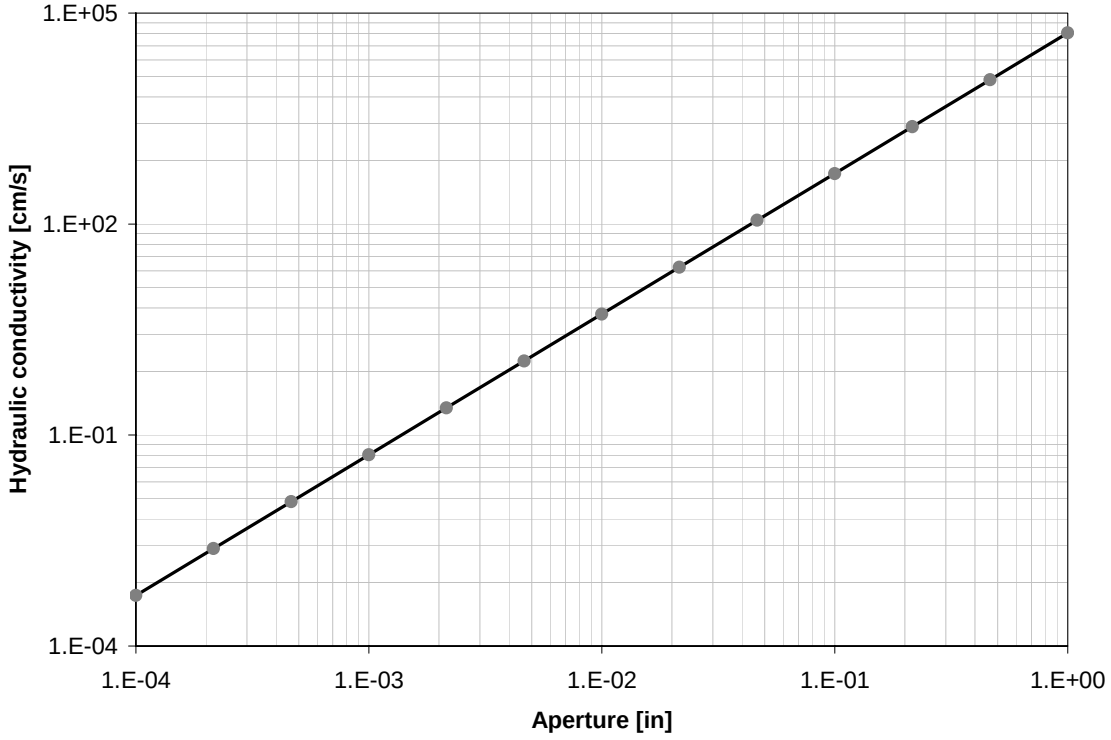

Figure A-77. Hydraulic conductivity of saturated cracks as a function of aperture.

A.4.4 Film Flow

When $P < -2\sigma/b$, liquid can no longer span an aperture and the crack will desaturate. For this condition, a rough fracture face can be conceptually simplified as a repeating series of vertical flat surfaces and V-shaped grooves to facilitate further analysis, following Or and Tuller (2000, Figure 1). At pressures slightly below $-2\sigma/b$, liquid will completely fill a groove and form a flat liquid-vapor interface. At a sufficiently low pressure, liquid will recede into the corner of the groove and be retained by capillary forces. Under this condition, the matric potential

$$\mu = \frac{P}{\rho} = gH \tag{A-24}$$

determines the radius of the liquid vapor interface in a groove (Or and Tuller 2000, Figure 2):

$$r(\mu) = -\frac{\sigma}{\rho\mu} \tag{A-25}$$

For a groove of depth L and angle γ, the maximum radius accommodated by the groove geometry is

$$r_c = \frac{L\tan(\gamma/2)}{\cos(\gamma/2)} \tag{A-26}$$

The critical pressure defining the transition between flat and curved interfaces is

$$P_c = -\frac{\sigma}{r_c} \tag{A-27}$$

and is the result of combining equations (A-24) through (A-26). Thus the three flow regimes identified earlier occur over the following pressure ranges for the assumed geometry of the fracture face:

1. Saturated flow: $P > -\frac{2\sigma}{b}$
2. "Thick" film flow: $-\frac{\sigma}{r_c} < P < -\frac{2\sigma}{b}$
3. "Thin" film flow: $P < -\frac{\sigma}{r_c}$

Liquid not being held by capillary suction will adhere to the remaining surfaces of the fracture face as a thin film. Considering only van der Waal forces, liquid adsorption on solid surfaces can be characterized by

$$h(\mu) = \left[\frac{A_{svl}}{6\pi\rho\mu}\right]^{1/3} \tag{A-28}$$

where h is film thickness and A_{svl} is a Hamaker constant.

Liquid held in groove corners by capillary suction and adhering as a thin film to remaining surfaces flows downward under the force of gravity. Or and Tuller (2000) present a detailed analysis of the liquid area and average velocity associated with corner and film flows, which is summarized in the Appendix. Figures A-78a and A-78b illustrate equivalent film thickness and average hydraulic conductivity for a representative "rough" fracture surface (Or and Tuller 2000, Figure 6a). The critical matric potential defining the transition between "thick" and "thin" film flow is $\mu_c = -0.22$ J/kg or approximately 2 cm of suction head. A discontinuity in film thickness is observed in Figure 6a at this matric potential.

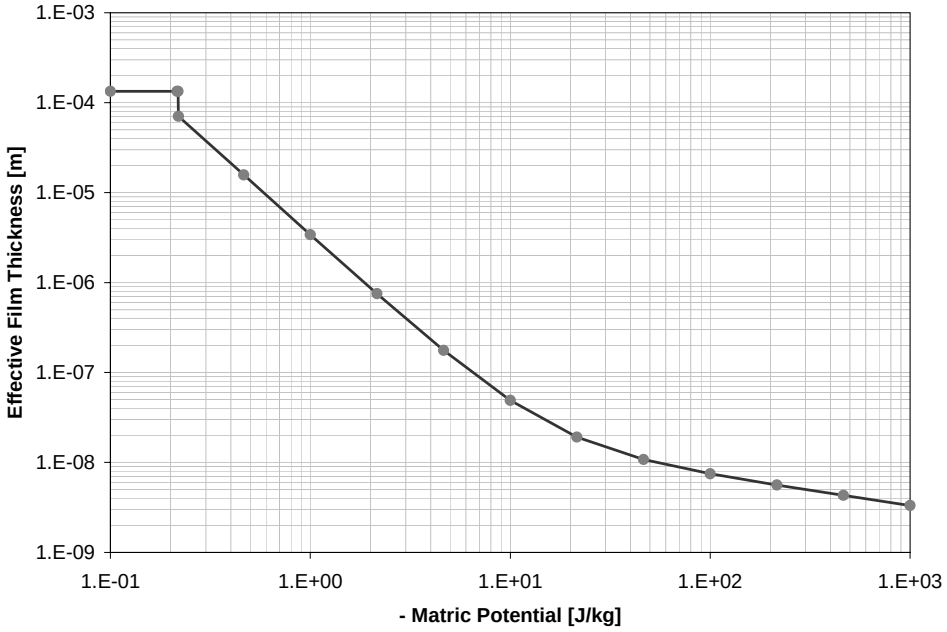

(a)

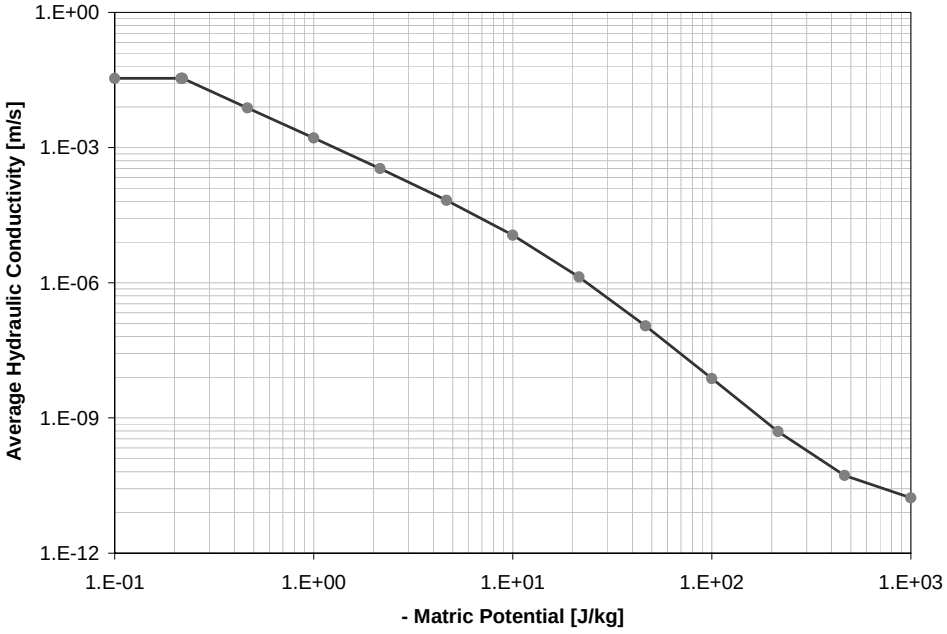

(b)

Figure A-78. Predicted film flow behavior for a representative "rough" fracture face with $L = 5 \times 10^{-4}$ m and $\gamma = 60°$: a) equivalent film thickness, and b) average hydraulic conductivity.

A.4.5 Application to Saltstone Vault 4

Under saturated flow conditions, the thickness of saltstone transmitting the same flow as a saturated crack under the same hydraulic gradient is

$$D_{saltstone} = \frac{K_{crack} b}{K_{saltstone}} \tag{A-29}$$

where b is the aperture and K_{crack} is defined by Figure A-77. For the assumed Saltstone Vault 4 hydraulic conductivity of 10^{-11} cm/s, even a small crack is significant because of the extreme conductivity contrast. During the 10,000-50,000 year period, Saltstone Vault 4 is predicted to experience ponding on the upper surface. Cracks should be considered under these positive pressure conditions.

Similarly, the equivalent thickness of saltstone for unsaturated flow is

$$D_{saltstone} = \frac{2K_A D_A}{K_{saltstone}} \tag{A-30}$$

where the factor of two results from consideration of flow down both sides of the crack, D_A the average film thickness (e.g. Figure A-78a), and K_A is average conductivity (e.g. Figure 2b). Figure 3 defines the suction head required to desaturate a fixed width crack and the equivalent saltstone thickness, for the aperture conditions assumed in Figure A-78.

For example, at a suction of 100 cm, cracks larger than 6×10^{-4} inches will be unsaturated according to equation (A-27). Therefore the exact geometry of the crack, i.e. open at top or bottom, has little impact on the end result. The equivalent saltstone thickness, assuming a conductivity of 10^{-11} cm/s, would be about 3 ft. At lower suctions, the equivalent thickness increases rapidly. Conversely, thickness rapidly decreases at higher suction. During the 0-10,000 year period, Saltstone Vault 4 is predicted to experience a suction of around 1200 cm. At this suction, unsaturated crack flow is predicted to be negligible ($D_{saltstone} \approx 10^{-3}$ ft from Figure A-79). An informal sensitivity study that varied groove depth (L), angle (γ), and spacing (β in Or and Tuller (2000)) indicates this conclusion is not sensitive to the particular values assumed in Figure A-79.

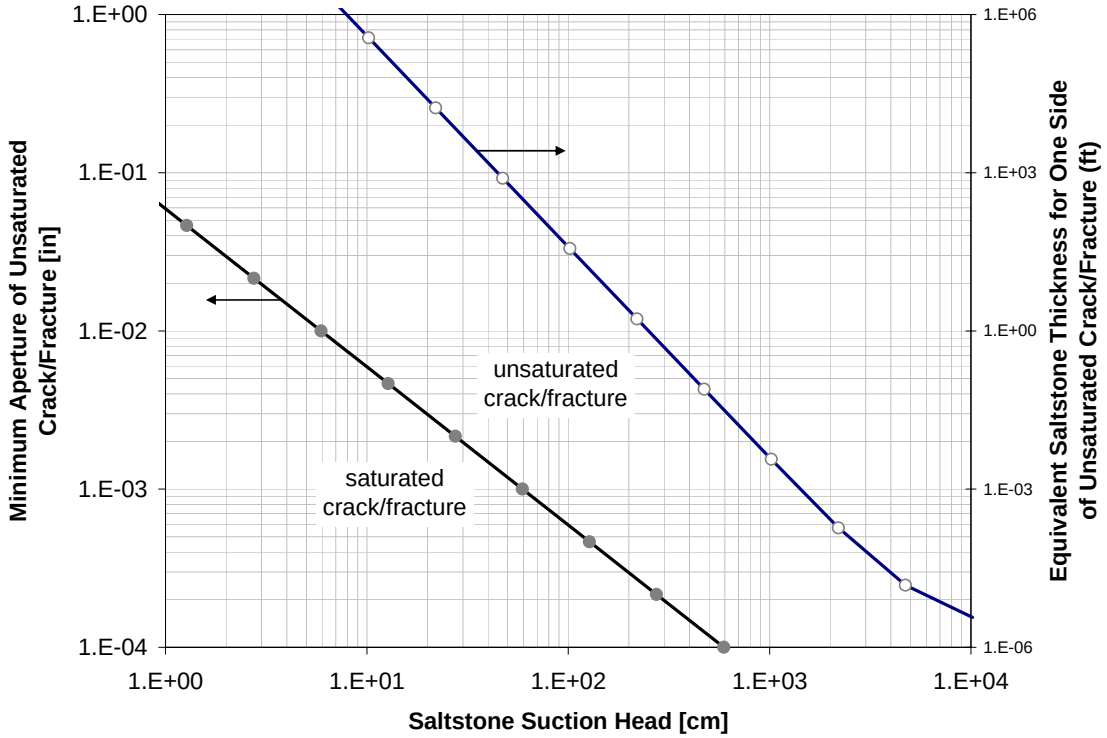

Figure A-79. Minimum unsaturated aperture and equivalent saltstone thickness for film flow down crack faces.

A.4.6 Conclusions

Macroscopic cracks forming in Saltstone Vault 4, whether pinched at top or bottom or through-wall, can be neglected when the suction head exceeds approximately 200 cm. Such conditions are predicted to occur during the 0-10,000 year period. At lower suction or positive pressure conditions, crack flow may be significant.

A.4.7 Details from Or and Teller Reference

The key equations and relationships needed to reproduce Figure 6a in Or and Tuller (2000) are summarized below:

Matric potential

$$\mu = \frac{P}{\rho} = gH \tag{A-31}$$

Film thickness adsorbed to surface under tension

$$h(\mu) = \left[\frac{A_{svl}}{6\pi\rho\mu}\right]^{1/3} \tag{A-32}$$

Corner radius under capillary retention

$$r(\mu) = -\frac{\sigma}{\rho\mu} \tag{A-33}$$

Critical matric potential

$$\mu_c = -\frac{\sigma\cos(\gamma/2)}{\rho L\tan(\gamma/2)} \tag{A-34}$$

Critical radius of curvature ($r < r_c$)

$$r_c = \frac{L\tan(\gamma/2)}{\cos(\gamma/2)} \tag{A-35}$$

Corner area for $\mu < \mu_c$

$$A_{C1}(\mu) = r(\mu)^2\left[\frac{1}{\tan(\gamma/2)} - \frac{\pi(180-\gamma)}{360}\right] \tag{A-36}$$

Corner area for $\mu \geq \mu_c$

$$A_{C2} = L^2\tan(\gamma/2) \tag{A-37}$$

Film area for $\mu < \mu_c$

$$A_{F1}(\mu) = h(\mu)\left\{\beta L + 2\left[\frac{L}{\cos(\gamma/2)} - \frac{r(\mu)}{\tan(\gamma/2)}\right]\right\} \tag{A-38}$$

Film area for $\mu \geq \mu_c$

$$A_{F2}(\mu) = h(\mu)\{\beta L + 2(1-\delta)L\tan(\gamma/2)\} \tag{A-39}$$

Smooth vertical surface film flow (Tokunaga and Wan 1997; Or and Tuller 2000)

$$\bar{v} = \frac{\rho g}{3\eta}h^2 \tag{A-40}$$

Corner vertical flow (Or and Tuller 2000)

$$\bar{v} = \frac{\rho g}{\varepsilon\eta}r^2 \tag{A-41}$$

where

$$\varepsilon = \exp\left[\frac{b + d\gamma}{1 + c\gamma}\right] \tag{A-42}$$

and $b = 2.124$, $c = -0.00415$ and $d = 0.00783$ for $10° < \gamma < 150°$.

Hydraulic conductivity

$$K \equiv \bar{v} \tag{A-43}$$

Average hydraulic conductivity (velocity) for $\mu < \mu_c$

$$K_{Al} = \frac{K_F A_{F1} + K_C A_{C1} \delta}{A_{F1} + A_{C1}} \tag{A-44}$$

Average hydraulic conductivity (velocity) for $\mu \geq \mu_c$

$$K_{Al} = \frac{K_F A_{F2} + K_C A_{C2} \delta}{A_{F2} + A_{C2}} \tag{A-45}$$

Width of representative surface element

$$W = \beta L + 2L \tan(\gamma / 2) \tag{A-46}$$

Effective film thickness

$$D = \frac{A_F + A_C}{W} \tag{A-47}$$

A.5 QUALITY ASSURANCE

The major quality assurance issues are addressed below.

A.5.1 Assumptions and Input Data

The data employed in the modeling work, as well as the relevant assumptions are presented in either the main groundwater chapter or the Appendix.

A.5.2 Pre- and Post-Processing

Most of the input data are directly read in from tables. The data are carefully selected to ensure numerical stability. A Fortran program generates the PORFLOW transport run input file for each of the contaminants to eliminate transcription errors. The PORFLOW 5.97.0 solver is drastically improved over previous versions such that very small initial time steps can now be used to achieve solutions with reasonable run times. The improvements also facilitate solutions with much smaller mass balance errors.

The post-processing capabilities were developed to facilitate information transfer between runs and to generate tables and plots for reporting and design check purposes. The time history of contaminant fluxes to the water table was used as the source term for the saturated-zone modeling.

A.5.3 Steady-State Flow Field Simulation

PORFLOW 5.97.0 has implemented a change of convergence criteria from global sum of errors to sum of percentage errors at each of the nodes. This change puts more emphasis on the nodes of low conductivity (Saltstone and concrete). Consequently, the steady-state flow field will produce fewer mass balance errors for the transport runs. This is a significant improvement of the simulation methodology.

A.6 REFERENCES

ACRI (Analytical & Computational Research, Inc.). 2004. *PORFLOW Version 5.0 User's Manual*, Revision 5, Analytical & Computational Research, Inc., Los Angeles, California.

Cook, J. R. and E.L. Wilhite, *Special Analysis: Radionuclide Screening Analysis for E-Area*, WSRC-TR-2004-00294, June 1, 2004.

Domenico, P.A., and F.W. Schwartz, 1990. *Physical and Chemical Hydrogeology*, John Wiley & Sons, New York, NY.

Fabryka-Martin, J. T., P. R. Dixon, S. Levy, B. Liu, H. J. Turin, and A. V. Wolfsburg. 1996. *Summary Report of Chlorine-36 Studies: Systematic Sampling for Chlorine-36 in the Exploratory Studies Facility*. Los Alamos National Laboratory Milestone Report 3783AD. Los Alamos, N.M.: Los Alamos National Laboratory.

Flach, G. P. 2004. *Groundwater Flow Model of the General Separations Area Using PORFLOW*, WSRC-TR-2004-00106, Revision 0, Westinghouse Savannah River Company, Aiken, South Carolina.

Freeze, R. A. and J. A. Cherry. 1979. *Groundwater*, Prentice-Hall, Inc. Englewood Cliffs, New Jersey.

Kaplan, D. I. 2004. *Recommended Geochemical Input Values for the Special Analysis of the Slit/Engineered Trenches and Intermediate Level Vault*, WSRC-RP-2004-00267, Revision 0. Westinghouse Savannah River Company, Aiken, South Carolina.

Looney, B. and R. Falta, 2000, *The vadose zone; What it is, Why it Matters, and How it Works*, in B. B. Looney and R. W. Falta eds., Vadose Zone Science and Technology Solutions, Volume 1, Battelle Press, Columbus OH.

MMES (Martin Marietta Energy Systems, Inc., EG&G Idaho, Inc., Westinghouse Hanford Company, and Westinghouse Savannah River Company). 1992. *Radiological Performance Assessment for the Z-Area Saltstone Disposal Facility*, WSRC-RP-92-1360, Westinghouse Savannah River Company, Aiken, South Carolina.

Nativ, R., E. Adar, O. Dahan and M. Geyh. 199., *Water Recharge and Solute Transport Through the Vadose Zone of Fractured Chalk under Desert Conditions*, Water Resources Research, v. 31 n. 2, 253-261.

Or, D. and M. Tuller. 2000. *Flow in unsaturated fractured porous media: Hydraulic conductivity of rough surfaces*, Water Resources Research, v. 36, n. 5, 1165-1177.

Peregoy, W. 2003. *Saltstone Vault Structural Degradation Prediction*, T-CLC-Z-00006, July 2003. Westinghouse Savannah River Company, Aiken, South Carolina.

Persoff, P. and K. Pruess. 1995. *Two-Phase Flow Visualization and Relative Permeability Measurement in Natural Rough-Walled Rock Fractures*, Water Resources Research, v. 31 n. 5, 1175-1186.

Phifer, M. A. 2004. Interoffice Memorandum to J. R. Cook, et al, *Vault 4 Infiltration and Hydraulic Conductivity Input for the Vadose Zone PORFLOW Modeling*, SRT-EST-2004-00068, February 26, 2004. Westinghouse Savannah River Company, Aiken, South Carolina.

Pruess, K. 1999. *A Mechanistic Model for Water Seepage Through Thick Unsaturated Zones in Fractured Rrocks of Low Matrix Permeability*, Water Resources Research, v. 35 n. 4, 1039-1051.

Su, G. W., J. T. Geller, K. Pruess and J. R. Hunt, 2001, *Solute Transport along Preferential Flow Paths in Unsaturated Fractures*, Water Resources Research, v. 37 n. 10, 2481-2491.

USDOE. 1999. "Low-Level Waste Requirements," Chapter IV in *Radioactive Waste Management Manual,* USDOE Manual 435.1-1. U.S Department of Energy, Washington, DC.

USEPA (U.S. Environmental Protection Agency). 1994a. *The Hydrologic Evaluation of Landfill Performance (HELP) Model User's Guide for Version 3*, EPA/600/R-94/168a, September 1994, Office of Research and Development, United States Environmental Protection Agency, Washington, DC.

USEPA (U.S. Environmental Protection Agency). 1994b. *The Hydrologic Evaluation of Landfill Performance (HELP) Engineering Documentation for Version 3*, EPA/600/R-94/168b, September 1994. Office of Research and Development, United States Environmental Protection Agency, Washington, DC.

Wilhite, E. L. 2003. Performance Assessment Position Paper: *Time for Compliance*, WSRC-RP-2003-00390, October 23, 2003. Westinghouse Savannah River Company, Aiken, South Carolina.

Yu, A. D., C. A. Langton, and M. G. Serrato. 1993. *Physical Properties Measurement,* WSRC-RP-93-894, June 30, 1993. Westinghouse Savannah River Company, Aiken, South Carolina.

THIS PAGE INTENTIONALLY LEFT BLANK

APPENDIX B
ADDITIONAL INFORMATION ON INTRUDER ANALYSIS

THIS PAGE INTENTIONALLY LEFT BLANK

B.1 ADDITIONAL INFORMATION ON INTRUDER ANALYSIS

This section presents an assessment of potential radiation doses to a hypothetical inadvertent intruder onto the site of the Saltstone Disposal Facility (SDF) at the Savannah River Site (SRS). Results of the dose assessment are used to derive a set of limits on allowable average concentrations and total inventories of radionuclides in waste at the time of disposal in Vault 4.

Doses to a hypothetical inadvertent intruder are estimated based on assumptions about credible exposure scenarios at different times after disposal and their associated exposure pathways. The scenarios for inadvertent intrusion at different times are based on an assumed design and performance of the cover system above a disposal vault. Results of the dose assessment for the assumed scenarios are expressed in terms of annual effective dose equivalents (EDE) per unit concentration of radionuclides in a disposal vault; these doses per unit concentration are referred to as scenario dose conversion factors (SDCFs). Limits on allowable concentrations and inventories of radionuclides at the time of disposal are then calculated based on the SDCFs for each radionuclide of concern, a specified performance measure for exposure of inadvertent intruders, assumptions about the time of occurrence of the assumed scenarios, and assumptions about the degradation of the cover system above a vault over time. The methodology used in this report is the same as that used in pervious SRS performance assessments. The previous analyses used either hand calculations or spreadsheets, which underwent extensive external peer review during the approval process. The same methodology has been incorporated into a computer program, which was used in this analysis. The program (Koffman 2004) and the data used to implement it (Lee 2004) have both been documented and reviewed.

The specified performance measures for inadvertent intruders (USDOE 1999) include (1) an annual effective dose equivalent of 100 mrem (1 mSv) for scenarios involving chronic exposure and (2) an effective dose equivalent of 500 mrem (5 mSv) for scenarios involving a single acute exposure (see Section 2.3.2). In both performance measures for inadvertent intruders, potential doses due to inhalation of radon and its short-lived decay products are excluded (USDOE 1999). The relevant scenarios for inadvertent intrusion involve exposure to residual solidified waste in a disposal facility, and scenarios that involve exposure to contaminated groundwater or surface water on the disposal site are excluded (USDOE 1996). A study of intruder scenarios prepared for the USDOE Low Level waste Management Program found that when both acute and chronic scenarios are applied to the same disposal facility, the chronic scenarios are more limiting, because the exposure times are longer and the dose criterion is smaller (Kennedy and Peloquin 1988). The scenarios for inadvertent intrusion assumed in this analysis therefore only involve chronic exposure.

For the purpose of establishing limits on allowable disposals of radionuclides in a near-surface facility, a time frame for assessments of inadvertent intrusion of 1,000 years after facility closure is specified (USDOE 1999), and the assessments also should assume that active institutional control will be maintained over a disposal site for at least 100 years (USDOE 1999). In this analysis, limits on allowable disposals of radionuclides in the SDF are calculated based on a longer time frame of 10,000 years for assessments of inadvertent intrusion. Use of the 10,000-year time frame demonstrates compliance with Nuclear Regulatory Commission (NRC) performance objectives, as well as the time frame of 1,000 years specified by USDOE (1999).

It is assumed in this analysis that the overall disposal system will perform as an effective barrier to inadvertent intrusion over 10,000 years. The erosion barrier is constructed of material sized to remain in place during a rainfall event with a 10,000-year recurrence interval (3.3 inches of rain in a 15 minute time span, [see Phifer and Nelson 2003, Appendix K]). The cover system therefore provides a distance of greater than 10 feet from the top of the erosion barrier to the Saltstone waste form of the 10,000-year time frame and therefore the basement construction portion of the

Agricultural Scenario is not possible. The Agricultural Scenario then becomes the Resident Scenario, where a home is constructed with a basement that does not bring up waste material. The reinforced concrete vault roof and the Saltstone waste form itself are assumed to provide a deterrent to drilling activities by an inadvertent intruder. The persistent, thick cover system provides protection from physical weathering. The concrete and Saltstone will undergo chemical degradation over time, which will slowly alter the nature of the cementitious materials. Initially and for many years afterward, the roof and Saltstone will present a dramatically more difficult media through which to drill than an Aiken County well installer would be prepared to deal with. The rational response would be to move to a nearby location where his equipment could penetrate to the desired depth. In later times, the nature of the altered concrete and Saltstone will still present a sharp contrast to the native sand and clays, which should provide enough information to an inadvertent intruder so that he would conclude he is not dealing with naturally occurring materials.

B.1.1 Radionuclides Considered in the Intruder Analysis

Low-level radioactive waste that may be sent to the SDF contains many radionuclides. However, the number of radionuclides that need to be included in a dose analysis for inadvertent intruders can be reduced substantially based on considerations of radionuclide half-lives and the processes by which low-level waste at the SDF is generated.

The results of a screening analysis (Cook and Wilhite 2004) using a methodology developed by the NCRP (NCRP 1996) were used to determine the radionuclides to be considered in the intruder analysis. The radionuclides considered in the analysis, their half-lives, and daughter products are listed in Table B-1.

Table B-1. Radionuclides Considered in Dose Analysis for Inadvertent Intruders

Nuclide	Half Life[1]	Units	Daughter1	Branch1	Daughter2	Branch2
Ac-225	1.0000E+01	days	Fr-221	1		
Ac-227	2.1773E+01	years	Fr-223	0.0138	Th-227	0.9856
Ac-228	6.1500E+00	hours	Th-228	1		
Ag-108	2.3700E+00	minutes				
Ag-108m	4.1800E+02	years	Ag-108	0.089		
Al-26	7.1700E+05	years				
Am-241	4.3220E+02	years	Np-237	1		
Am-242	1.6020E+01	hours	Pu-242	0.173	Cm-242	0.827
Am-242m	1.4100E+02	years	Np-238	0.00476	Am-242	0.995
Am-243	7.3700E+03	years	Np-239	1		
Ar-39	2.6900E+02	years				
At-217	3.2300E-02	seconds	Bi-213	1		
At-218	1.5000E+00	seconds	Bi-214	1		
Ba-133	3.8489E+03	days				
Ba-137m	2.5520E+00	minutes				
Bi-207	3.1550E+01	years				
Bi-210	5.0130E+00	days	Po-210	1		
Bi-211	2.1400E+00	minutes	Tl-207	0.9972	Po-211	0.0028
Bi-212	6.0550E+01	minutes	Tl-208	0.3593	Po-212	0.6407
Bi-213	4.5590E+01	minutes	Tl-209	0.0216	Po-213	0.9784
Bi-214	1.9900E+01	minutes	Po-214	0.9998		
Bk-249	3.3000E+02	days	Cf-249	1		
C-14	5.7300E+03	years				
Ca-41	1.0300E+05	years				
Cd-113m	1.4100E+01	years				
Cf-249	3.5100E+02	years	Cm-245	1		
Cf-250	1.3080E+01	years	Cm-246	0.9992		
Cf-251	8.9800E+02	years	Cm-247	1		
Cf-252	2.6450E+00	years	Cm-248	0.9691		
Cl-36	3.0100E+05	years				
Cm-242	1.6280E+02	days	Pu-238	1		
Cm-243	2.9100E+01	years	Pu-239	0.9976	Am-243	0.0024
Cm-244	1.8100E+01	years	Pu-240	1		
Cm-245	8.5000E+03	years	Pu-241	1		
Cm-246	4.7600E+03	years	Pu-242	0.9997		
Cm-247	1.5600E+07	years	Pu-243	1		
Cm-248	3.4800E+05	years	Pu-244	0.9174		
Co-60	1.9251E+03	days				
Cs-134	7.5450E+02	days				
Cs-135	2.3000E+06	years				
Cs-137	3.0070E+01	years	Ba-137m	0.946		
Eu-152	1.3516E+01	years	Gd-152	0.278		
Eu-154	8.5920E+00	years				
Eu-155	4.7611E+00	years				
Fr-221	4.9000E+00	minutes	At-217	1		
Fr-223	2.2000E+01	minutes	Ra-223	1		
Gd-152	1.0800E+14	years				

Table B-1. Radionuclides Considered in Dose Analysis for Inadvertent Intruders

Nuclide	Half Life[1]	Units	Daughter1	Branch1	Daughter2	Branch2
H-3	1.2330E+01	years				
I-129	1.5700E+07	years				
K-40	1.2770E+09	years				
Kr-85	3.9344E+03	days				
Mo-93	4.0000E+03	years	Nb-93m	1		
Na-22	2.6019E+00	years				
Nb-93m	1.6130E+01	years				
Nb-94	2.0300E+04	years				
Ni-59	7.6000E+04	years				
Ni-63	1.0010E+02	years				
Np-237	2.1440E+06	years	Pa-233	1		
Np-238	2.1170E+00	days	Pu-238	1		
Np-239	2.3565E+00	days	Pu-239	1		
Np-240	6.1900E+01	minutes	Pu-240	1		
Np-240m	7.2200E+00	minutes	Pu-240	1		
Pa-231	3.2760E+04	years	Ac-227	1		
Pa-233	2.6967E+01	days	U-233	1		
Pa-234	6.7000E+00	hours	U-234	1		
Pa-234m	1.1700E+00	minutes	Pa-234	0.0013	U-234	0.9987
Pb-209	3.2530E+00	hours				
Pb-210	2.2300E+01	years	Bi-210	1		
Pb-211	3.6100E+01	minutes	Bi-211	1		
Pb-212	1.0640E+01	hours	Bi-212	1		
Pb-214	2.6800E+01	minutes	Bi-214	1		
Pd-107	6.5000E+06	years				
Po-210	1.3838E+02	days				
Po-211	5.1600E-01	seconds				
Po-212	2.9800E-07	seconds				
Po-213	3.6500E-06	seconds	Pb-209	1		
Po-214	1.6430E-04	seconds	Pb-210	1		
Po-215	1.7810E-03	seconds	Pb-211	1		
Po-216	1.4500E-01	seconds	Pb-212	1		
Po-218	3.1000E+00	minutes	Pb-214	0.9998	At-218	0.0002
Pu-238	8.7700E+01	years	U-234	1		
Pu-239	2.4110E+04	years	U-235	1		
Pu-240	6.5640E+03	years	U-236	1		
Pu-241	1.4290E+01	years	Am-241	1		
Pu-242	3.7330E+05	years	U-238	1		
Pu-243	4.9560E+00	hours	Am-243	1		
Pu-244	8.0000E+07	years	U-240	0.9988		
Ra-223	1.1435E+01	days	Rn-219	1		
Ra-224	3.6600E+00	days	Rn-220	1		
Ra-225	1.4900E+01	days	Ac-225	1		
Ra-226	1.6000E+03	years	Rn-222	1		
Ra-228	5.7500E+00	years	Ac-228	1		
Rb-87	4.7500E+10	years				
Re-188	1.7005E+01	hours				
Rn-219	3.9600E+00	seconds	Po-215	1		
Rn-220	5.5600E+01	seconds	Po-216	1		

Table B-1. Radionuclides Considered in Dose Analysis for Inadvertent Intruders

Nuclide	Half Life[1]	Units	Daughter1	Branch1	Daughter2	Branch2
Rn-222	3.8235E+00	days	Po-218	1		
S-35	8.7380E+01	days				
Sb-125	2.7586E+00	years	Te-125m	0.228		
Sb-126	1.2460E+01	days				
Sb-126m	1.9150E+01	minutes	Sb-126	0.14		
Sc-46	8.3790E+01	days				
Se-79	1.1000E+06	years				
Sm-151	9.0000E+01	years				
Sn-121	2.7060E+01	hours				
Sn-121m	5.5000E+01	years	Sn-121	0.76		
Sn-126	1.0000E+05	years	Sb-126m	1		
Sr-90	2.8790E+01	years	Y-90	1		
Tc-99	2.1110E+05	years				
Te-125m	5.7400E+01	days				
Th-227	1.8720E+01	days	Ra-223	1		
Th-228	1.9116E+00	years	Ra-224	1		
Th-229	7.3400E+03	years	Ra-225	1		
Th-230	7.5380E+04	years	Ra-226	1		
Th-231	2.5520E+01	hours	Pa-231	1		
Th-232	1.4050E+10	years	Ra-228	1		
Th-234	2.4100E+01	days	Pa-234m	1		
Tl-207	4.7700E+00	minutes				
Tl-208	3.0530E+00	minutes				
Tl-209	2.2000E+00	minutes	Pb-209	1		
U-232	6.8900E+01	years	Th-228	1		
U-233	1.5920E+05	years	Th-229	1		
U-234	2.4550E+05	years	Th-230	1		
U-235	7.0380E+08	years	Th-231	1		
U-236	2.3420E+07	years	Th-232	1		
U-238	4.4680E+09	years	Th-234	1		
U-240	1.4100E+01	hours	Np-240m	1		
W-181	1.2120E+02	days				
W-185	7.5100E+01	days				
W-188	6.9400E+01	days	Re-188	1		
Y-90	6.4000E+01	hours				
Zr-93	1.5300E+06	years	Nb-93m	1		

NOTES:
[1] Tuli 2000

Many radionuclides listed in Table B-1 have shorter-lived decay products. All such decay products are taken into account in the dose analysis for inadvertent intruders based on an assumption of activity equilibrium with the parent radionuclide. Buildup of radioactive decay products in disposed waste over time, including decay products that are longer-lived than their parent radionuclide (e.g., Am-241 produced in decay of Pu-241) as well as decay products that are shorter-lived than their parent (e.g., Ra-226 produced in decay of Th-230), is taken into account in the dose analysis for inadvertent intruders. The importance of a decay product depends on its half-life, the radiological properties of the parent, and decay product, and the time frame for the analysis. The half-life of the parent also is important when the decay product is longer-lived.

B.2 SCENARIOS FOR EXPOSURE OF INADVERTENT INTRUDERS

This section discusses the exposure scenarios and associated exposure pathways that are assumed in the dose analysis for inadvertent intruders at the SDF. The discussion is divided into two parts. The present design of the cover system is described in Section B.2.1. Section B.2.2 discusses the assumed exposure scenarios for inadvertent intruders.

B.2.1 Design of Cover System for Disposal Vault

The design of the cover system above Vault 4 has been documented (Phifer and Nelson 2003). The thicknesses of the cover system layers are: 36" soil cover, 12" erosion barrier and 107" backfill. At least 16 inches of clean grout will be poured on top of the Saltstone. The reinforced concrete vault roof will be 4 inches thick.

B.2.2 Exposure Scenarios and Pathways for Inadvertent Intruders

In estimating doses to inadvertent intruders after the period of active institutional control (i.e., at any time beyond 100 years after closure of the disposal facility), it is assumed that such individuals could establish a permanent homestead on the site. Furthermore, it is assumed that an intruder has no *a priori* knowledge of waste disposal activities at the site. Inadvertent intruders are assumed to receive radiation exposures directly from the saltstone waste in the resident scenario and from waste removed in the post-drilling scenario, which is assessed as a sensitivity case.

For direct intrusion into disposal units after loss of active institutional control, exposures are assumed to occur according to one of three scenarios, which are called the agriculture, resident, and post-drilling scenarios. The three scenarios considered in this analysis and their associated exposure pathways are described as follows.

In the agriculture scenario, an intruder is assumed to build a home directly on top of disposal units, and the foundation is assumed to extend into the units themselves. Radioactive wastes exhumed during excavation for the foundation are assumed to be indistinguishable from native soil, and some of the exhumed waste is assumed to be mixed with native soil in the intruder's vegetable garden. The following pathways involving exposure to radionuclides in solid waste then are assumed to occur:

- ingestion of vegetables grown in contaminated garden soil,
- direct ingestion of contaminated soil, primarily in conjunction with intakes of vegetables from the garden,
- external exposure to contaminated soil while working in the garden or residing in the home on top of the disposal units,
- inhalation of radionuclides attached to soil particles that are suspended into air from contaminated soil while working in the garden or residing in the home.

In the resident scenario, an intruder also is assumed to excavate at the location of disposal units, but is assumed to encounter an intact engineered barrier (e.g., a reinforced concrete roof) used in constructing the disposal units which cannot readily be penetrated by the types of excavation equipment normally used near the SRS or because the depth of the disposed waste is greater than the typical maximum depth of an excavation in digging a foundation for a home. Therefore, instead of excavating into the waste, the intruder is assumed to build a home immediately on top of the intact engineered barrier. Since waste in the disposal facility is not directly accessed during excavation, due to the assumed impenetrability of the engineered barriers, the only exposure pathway of concern for this scenario is external exposure to photon-emitting radionuclides in the waste while residing in the home.

In the post-drilling scenario, an intruder is assumed to access solid waste by drilling through a disposal unit (e.g., for the purpose of constructing a well for the intruder's domestic water supply.) During drilling, a small volume of waste is brought to the surface, and all of the drilling waste is assumed to be mixed with native soil in the intruder's vegetable garden. The following pathways involving exposure to radionuclides in the solid waste then are assumed to occur:

- ingestion of vegetables grown in contaminated soil,
- direct ingestion of contaminated soil, primarily in conjunction with intakes of vegetables from the garden,
- external exposure to contaminated soil while working in the garden,
- inhalation of radionuclides attached to soil particles that are suspended into air from contaminated soil while working in the garden.

The pathways listed above for the post-drilling scenario correspond to some of the pathways for the agriculture scenario. However, in the post-drilling scenario, external and inhalation exposures while residing in the home are not relevant, because all drilling waste is assumed to be mixed with soil in the intruder's vegetable garden and the intruder's home is not located on top of disposal units.

B.2.3 Selection of Credible Exposure Scenarios for Inadvertent Intruders

B.2.3.1 Credibility of Agriculture Scenario

The key assumption in the agriculture scenario is that an inadvertent intruder excavates into Saltstone in digging a foundation for a home at the location of a disposal vault. An essential function of the cover system is to preclude the occurrence of the agriculture scenario during the 10,000-year time frame of concern to this analysis. The assumption that the agriculture scenario is not credible during this time frame is based on the existence of an erosion barrier so that an intruder basement will never excavate into Saltstone.

B.2.3.2 Definition of Credible Resident Scenarios

A second exposure scenario for inadvertent intruders referred to as the resident scenario was included in the intruder dose analysis. As in the agriculture scenario, the resident scenario assumes that an intruder excavates a foundation for a home on top of a disposal vault. However, the resident scenario assumes that excavation into Saltstone is precluded, either because the intruder encounters an intact engineered barrier (e.g., vault roof) that cannot be readily penetrated by the types of excavation equipment normally used in the vicinity of the SRS, or because the depth of buried waste (Saltstone) is greater than a typical maximum depth of an excavation in digging a foundation for a home (i.e., 3 m). The resident scenario then occurs after the home is constructed, and the only relevant pathway is external exposure to photon-emitting radionuclides in the waste while residing in the home on top of shielded waste. The presence of uncontaminated material above the waste would preclude inhalation or ingestion exposure. Based on the conclusion discussed in the previous section that the agriculture scenario involving excavation into Saltstone is not a credible occurrence within the 10,000-year time frame of concern to the intruder dose analysis, the only credible scenarios during this time frame are resident scenarios at different times after disposal and involving different thicknesses of shielding above the waste.

The resident scenario is a credible occurrence at any time after institutional control over the site is assumed to be relinquished at 100 years after disposal. However, the external dose in the resident scenario can increase over time due to a decrease in the thickness of shielding between Saltstone and the depth of an excavation. The thickness of shielding can decrease as the cover material above the engineered barriers erodes and the engineered barriers above the waste lose their

physical integrity and no longer deter excavation. Thus, the resident scenario was evaluated for times between 100 and 10,000 years after disposal.

At 100 years after disposal, which is the earliest time the resident scenario can occur, all engineered barriers above the waste are assumed to be intact. An assumption that the barriers to excavation will not degrade by a significant amount during the 100-year period of institutional control is reasonable when surveillance and maintenance of the cover system presumably will be performed during that time. An inadvertent intruder then is assumed to excavate to the depth of 3 m, a typical maximum depth of an excavation in digging a foundation for a home. Over time erosion will lower the ground elevation, until the erosion barrier becomes exposed. Thus the amount of shielding will decrease and radioactive decay of long-lived radionuclides will produce increasing quantities of daughter products. The intruder analysis tool used (Koffman 2004) was set to perform an analysis in ten-year steps from year 100 to year 10,000 to find the maximum contribution from each radionuclide.

The residential scenario dose coefficient is estimated by:

$$DC_R = DC_{ie}(R) \qquad \text{(Eq. B-1)}$$

$DC_{ie}(R)$ = residential exposure dose coefficient (rem*cm^3/μCi*year)

B.2.3.3 Definition of Post-Drilling Scenario as a Sensitivity Case

The post-drilling scenario assumes that an intruder who resides permanently on the disposal site drills through a disposal unit in constructing a well for a domestic water supply. Following construction of the well, the contaminated material brought to the surface during drilling operations, which is assumed to be indistinguishable from native soil, is assumed to be mixed with native soil in the intruder's vegetable garden. The exposure pathways involving ingestion of contaminated vegetables, ingestion of contaminated soil, and external and inhalation exposures while working in the garden then are the same as the pathways described previously for the agriculture scenario. In the post-drilling scenario, however, external and inhalation exposures while residing in the home on the disposal site, which are important in the agriculture scenario, are considered insignificant. All drilling waste is assumed to be mixed with native soil in the garden, which is considered to be at a sufficient distance from the home that indoor exposures are minor relative to those in the garden.

As stated earlier, the concrete vault and saltstone are assumed to remain a barrier to drilling over the 10,000-year analysis period. However, to test the sensitivity of the results to this assumption, a post-drilling scenario is assessed. In this sensitivity analysis it is assumed that the reinforced concrete vault roof remains a barrier to excavation and drilling for only 1,000 years. Therefore, at any time after 1,000 years the post-drilling scenario is analyzed and a transient analysis was performed for times from 1,000 year to 10,000 years.

For the post-drilling scenario, inadvertent intruders are assumed to be exposed after drilling through the disposal unit mixing the drilling waste with the native soil in the vegetable garden. Potential exposure scenarios for this scenario include:

- ingestion of vegetables grown in the garden soil mixed with exhumed waste,
- direct ingestion of contaminated soil,
- external exposure to the contaminated soil while working in the garden, and
- inhalation of contaminated particulates while working in the garden.

The post-drilling residential scenario dose coefficient is estimated by:

$$DC_{PD} = 0.1 * \left(DC_{iv} + DC_{is} + DC_{ie} + DC_{ia}(g)\right) \quad \text{(Eq. B-2)}$$

where

0.1 = factor to adjust dilution factor for mixture of exhumed waste in vegetable garden to account for more dilution in post drilling because drilling brings less waste to the surface than excavation (McDowell Boyer et al. 2000).

B.3 EXPOSURE PATHWAYS

B.3.1 Ingestion Pathway

Potential ingestion pathways include consumption of vegetables grown in the contaminated native soil, and incidental ingestion of soil.

The vegetable consumption dose coefficient is estimated by:

$$DC_{iv} = \frac{B_{iv} * U_v * f_s * DCF_i}{\rho_s} \quad \text{(Eq. B-3)}$$

where

B_{iv} = plant-to-soil ratio for radionuclide i

U_v = annual consumption of vegetables (kg/year)

f_s = dilution factor for mixture of exhumed waste in vegetable garden

ρ_s = bulk density of soil (kg/cm^3)

DCF_i = DCF for ingestion of radionuclide i (rem/μCi).

The soil ingestion dose coefficient is estimated by:

$$DC_{is} = \frac{U_s * f_s * DCF_i}{\rho_s} \quad \text{(Eq. B-4)}$$

where

U_s = annual consumption of soil (kg/year).

B.3.2 External Pathway

External exposure is assumed to occur while working in the vegetable garden, residing in the home on top of the disposal unit with no shielding other than the foundation of the home, and with shielding of a thickness dependent on the design of the disposal unit.

The external dose coefficient while working in the vegetable garden is estimated by:

$$DC_{ie} = U_g * f_s * DCF_{ie} \quad \text{(Eq. B-5)}$$

where

U_g = fraction of a year exposed to contaminated soil in vegetable garden

DCF_{ie}= DCF for external exposure to 15 cm of soil uniformly contaminated with radionuclide i (rem*cm^3/μCi*year)

External dose coefficient while residing in the home directly on top of the disposal unit is estimated by:

$$DC_{ie}(0) = U_h * DCF_{it}(0) * S \quad \text{(Eq. B-6)}$$

where

U_h = fraction of a year spent in home

$DCF_{it}(0)$ = DCF for external exposure to waste containing radionuclide i with no shielding (rem*cm^3/μCi*year)

S = shielding factor for radionuclides during indoor residence

External dose coefficient while residing in the home on top of the disposal unit shielded by a known thickness (t) is estimated by:

$$DC_{ie}(t) = U_h * DCF_{it}(t) * S \quad \text{(Eq. B-7)}$$

where

$DCF_{it}(t)$ = DCF for external exposure to waste containing radionuclide i with a known amount of shielding (t) (rem*cm^3/μCi*year)

B.3.3 Inhalation Pathway

The inadvertent intruder is assumed to inhale suspended radionuclides while working in the vegetable garden and residing in the home.

Inhalation dose coefficients for garden exposure are estimated by:

$$DC_{ia}(g) = \frac{f_a(g) * U_a * L_a(g) * DCF_{ia}}{\rho_s} \quad \text{(Eq. B-8)}$$

where

$f_a(g)$ = fraction of the year spent in garden

U_a = annual air intake (cm^3/year)

$L_a(g)$ = garden mass loading (kg/cm^3)

DCF_{ia} = DCF for inhalation of radionuclide i (rem/μCi).

Inhalation dose coefficients while residing in the home are estimated by:

$$DC_{ia}(h) = \frac{f_a(h) * f_s * U_a * L_a(h) * DCF_{ia}}{\rho_s} \quad \text{(Eq. B-9)}$$

where

$f_a(h)$ = fraction of the year spent in home

U_a = annual air intake (cm^3/year)

$L_a(h)$ = home mass loading (kg/cm^3)

DCF_{ia} = DCF for inhalation of radionuclide i (rem/μCi).

The values for each of the parameters used in these equations can be found in Lee, 2004.

B.4 LIMIT CALCULATIONS

After the radionuclide- and scenario-specific dose coefficients have been determined, the concentration limit for each radionuclide based on each scenario can be calculated by:

$$DL_i = \frac{H}{DC_{iS}} \quad \text{(Eq. B-10)}$$

where

DL_i = the disposal limit for radionuclide i (μCi /cm^3)

H = Effective dose equivalent (0.1 rem/year), and

DC_{iS} = radionuclide- and scenario- specific dose coefficient (rem*cm^3/μCi*year).

The concentration limits can be converted to disposal unit limits in curies using appropriate unit conversions to express the limit in units of Ci/m^3 (in this case, (μCi /cm^3 is equivalent to Ci/m^3) and then multiplying by the volume of the disposal unit (78,800 m^3 for Vault 4).

B.5 RESULTS

The parameters specific to Vault 4 used in the intruder analysis are given in Table B-2.

Table B-2. Intruder Parameters for Vault 4

Resident Geometry Factor	0.6	Cook et al. 2002
Post-Drilling Geometry Factor	1	Cook et al. 2002
Waste Volume (m^3)	78800	Cook et al. 2002
Resident Analysis Start Time (yr)	100	
Post-Drilling Analysis Start Time (yr)	1000	
Resident Shielding Thickness (cm)	100	

Transient Layer Model (Surface to Top of Waste) (Phifer and Nelson 2004)

Layer	Thickness (m)	Description	Erosion Rate (mm/yr)	Degradation Time (yr)
1	0.9144	Soil cover (36")	1.4	0
2	0.3048	Erosion barrier (12")	1.00E-10	0
3	2.7178	Soil backfill (107")	1.4	0
4	0.5080	Concrete/Grout Min (20")	1.4	1000

The results of the analysis of the resident scenario for the period 100 to 1,000 years and 100 to 10,000 years are presented in Tables B-3 and B-4, respectively. Table B-5 gives the results for the post-drilling scenario for the period 1,000 to 10,000 years. In Tables B-3 through B-5 the entry "---" in the Time of Limit column means that the dose calculation is always zero so there is no limit. For cases where there is a time given, there may be an entry "---" in one or both of the limit columns. In this case the entry "---" indicates a limit value greater than or equal to the threshold value of 1E+20.

Table B-3. Intruder-Based Radionuclide Disposal Limits for Vault 4 – Resident Scenario with Transient Calculation for 100 - 1000 Years

Radionuclide	Time of Limit (Years)	Concentration Limit ($\mu Ci/m^3$)	Inventory Limit (Ci/Unit)
H-3	---	---	---
C-14	---	---	---
Na-22	100	9.90E+16	7.80E+15
Al-26	760	2.05E+03	1.61E+02
S-35	---	---	---
Cl-36	---	---	---
Ar-39	---	---	---
K-40	760	4.00E+04	3.15E+03
Ca-41	---	---	---
Sc-46	100	---	---
Co-60	100	7.29E+10	5.75E+09
Ni-59	---	---	---
Ni-63	---	---	---
Se-79	---	---	---
Kr-85	100	3.46E+12	2.73E+11
Rb-87	---	---	---
Sr-90	---	---	---
Zr-93	---	---	---
Nb-93m	---	---	---
Nb-94	760	1.28E+04	1.01E+03
Mo-93	---	---	---
Tc-99	760	4.64E+14	3.66E+13
Pd-107	---	---	---
Ag-108m	760	7.21E+04	5.68E+03
Cd-113m	---	---	---
Sn-121m	---	---	---
Sn-126	760	1.48E+04	1.17E+03
Sb-125	100	1.79E+18	1.41E+17
I-129	760	---	---
Cs-134	100	---	4.12E+19
Cs-135	---	---	---
Cs-137	100	7.61E+07	5.99E+06
Ba-133	100	1.53E+11	1.21E+10
Sm-151	---	---	---
Eu-152	100	8.15E+07	6.42E+06
Eu-154	100	1.46E+09	1.15E+08
Eu-155	100	---	1.12E+19
W-181	100	---	---
W-185	100	---	---
W-188	100	---	---
Pb-210	100	4.99E+12	3.94E+11
Bi-207	100	3.91E+06	3.08E+05
Ra-226	760	5.34E+03	4.21E+02
Ra-228	100	4.72E+09	3.72E+08

Table B-3. Intruder-Based Radionuclide Disposal Limits for Vault 4 – Resident Scenario with Transient Calculation for 100 - 1000 Years

Radionuclide	Time of Limit (Years)	Concentration Limit ($\mu Ci/m^3$)	Inventory Limit (Ci/Unit)
Ac-227	100	1.11E+09	8.78E+07
Th-228	100	---	1.88E+19
Th-229	760	1.09E+05	8.61E+03
Th-230	1000	1.10E+04	8.66E+02
Th-232	760	1.98E+03	1.56E+02
Pa-231	760	2.73E+05	2.15E+04
U-232	100	1.14E+05	9.00E+03
U-233	1000	1.13E+06	8.92E+04
U-234	1000	2.23E+06	1.76E+05
U-235	1000	7.29E+06	5.75E+05
U-236	1000	4.06E+10	3.20E+09
U-238	1000	1.02E+06	8.01E+04
Np-237	1000	9.74E+05	7.68E+04
Pu-238	1000	7.90E+09	6.22E+08
Pu-239	1000	3.80E+11	3.00E+10
Pu-240	1000	2.86E+15	2.25E+14
Pu-241	1000	1.85E+11	1.46E+10
Pu-242	1000	6.56E+12	5.17E+11
Pu-244	760	4.64E+04	3.65E+03
Am-241	1000	6.05E+09	4.77E+08
Am-242m	750	1.99E+08	1.57E+07
Am-243	760	3.75E+06	2.96E+05
Cm-242	1000	1.56E+12	1.23E+11
Cm-243	100	8.88E+10	7.00E+09
Cm-244	1000	1.09E+18	8.60E+16
Cm-245	760	1.07E+08	8.42E+06
Cm-246	1000	7.41E+15	5.84E+14
Cm-247	1000	3.26E+05	2.57E+04
Cm-248	1000	5.84E+09	4.60E+08
Bk-249	760	6.24E+08	4.92E+07
Cf-249	760	1.61E+06	1.27E+05
Cf-250	1000	2.80E+18	2.21E+17
Cf-251	760	2.33E+07	1.83E+06
Cf-252	1000	7.96E+14	6.27E+13

Table B-4. Intruder-Based Radionuclide Disposal Limits for Vault 4 – Resident Scenario with Transient Calculation for 100 - 10000 Years

Radionuclide	Time of Limit (Years)	Concentration Limit ($\mu Ci/m^3$)	Inventory Limit (Ci/Unit)
H-3	---	---	---
C-14	---	---	---
Na-22	100	9.90E+16	7.80E+15
Al-26	760	2.05E+03	1.61E+02
S-35	---	---	---
Cl-36	---	---	---
Ar-39	---	---	---
K-40	760	4.00E+04	3.15E+03
Ca-41	---	---	---
Sc-46	100	---	---
Co-60	100	7.29E+10	5.75E+09
Ni-59	---	---	---
Ni-63	---	---	---
Se-79	---	---	---
Kr-85	100	3.46E+12	2.73E+11
Rb-87	---	---	---
Sr-90	---	---	---
Zr-93	---	---	---
Nb-93m	---	---	---
Nb-94	760	1.28E+04	1.01E+03
Mo-93	---	---	---
Tc-99	760	4.64E+14	3.66E+13
Pd-107	---	---	---
Ag-108m	760	7.21E+04	5.68E+03
Cd-113m	---	---	---
Sn-121m	---	---	---
Sn-126	760	1.48E+04	1.17E+03
Sb-125	100	1.79E+18	1.41E+17
I-129	760	---	---
Cs-134	100	---	4.12E+19
Cs-135	---	---	---
Cs-137	100	7.61E+07	5.99E+06
Ba-133	100	1.53E+11	1.21E+10
Sm-151	---	---	---
Eu-152	100	8.15E+07	6.42E+06
Eu-154	100	1.46E+09	1.15E+08
Eu-155	100	---	1.12E+19
W-181	100	---	---
W-185	100	---	---
W-188	100	---	---
Pb-210	100	4.99E+12	3.94E+11
Bi-207	100	3.91E+06	3.08E+05
Ra-226	760	5.34E+03	4.21E+02
Ra-228	100	4.72E+09	3.72E+08

Table B-4. Intruder-Based Radionuclide Disposal Limits for Vault 4 – Resident Scenario with Transient Calculation for 100 - 10000 Years

Radionuclide	Time of Limit (Years)	Concentration Limit ($\mu Ci/m^3$)	Inventory Limit (Ci/Unit)
Ac-227	100	1.11E+09	8.78E+07
Th-228	100	---	1.88E+19
Th-229	760	1.09E+05	8.61E+03
Th-230	9090	4.18E+03	3.29E+02
Th-232	760	1.98E+03	1.56E+02
Pa-231	760	2.73E+05	2.15E+04
U-232	100	1.14E+05	9.00E+03
U-233	10000	1.71E+05	1.35E+04
U-234	10000	5.69E+04	4.48E+03
U-235	10000	1.30E+06	1.03E+05
U-236	10000	4.02E+09	3.17E+08
U-238	10000	8.38E+05	6.60E+04
Np-237	10000	8.55E+05	6.73E+04
Pu-238	10000	1.62E+08	1.27E+07
Pu-239	10000	1.74E+11	1.37E+10
Pu-240	10000	3.75E+13	2.96E+12
Pu-241	10000	1.30E+11	1.02E+10
Pu-242	10000	6.23E+11	4.91E+10
Pu-244	760	4.64E+04	3.65E+03
Am-241	10000	4.29E+09	3.38E+08
Am-242m	10000	1.25E+08	9.83E+06
Am-243	760	3.75E+06	2.96E+05
Cm-242	10000	3.18E+10	2.51E+09
Cm-243	100	8.88E+10	7.00E+09
Cm-244	10000	1.37E+16	1.08E+15
Cm-245	760	1.07E+08	8.42E+06
Cm-246	10000	1.06E+14	8.34E+12
Cm-247	10000	3.11E+05	2.45E+04
Cm-248	10000	5.89E+08	4.64E+07
Bk-249	760	6.24E+08	4.92E+07
Cf-249	760	1.61E+06	1.27E+05
Cf-250	10000	3.87E+16	3.05E+15
Cf-251	760	2.33E+07	1.83E+06
Cf-252	10000	8.00E+13	6.31E+12

Table B-5. Intruder-Based Radionuclide Disposal Limits for Vault 4 – Post-Drilling Scenario with Transient Calculation for 1000 - 10000 Years

Radionuclide	Time of Limit (Years)	Concentration Limit ($\mu Ci/m^3$)	Inventory Limit (Ci/Unit)
H-3	1000	---	---
C-14	1000	7.49E+04	5.91E+03
Na-22	1000	---	---
Al-26	1000	5.42E+04	4.27E+03
S-35	---	---	---
Cl-36	1000	8.56E+02	6.74E+01
Ar-39	1000	1.24E+10	9.75E+08
K-40	1000	1.73E+04	1.37E+03
Ca-41	1000	4.08E+05	3.21E+04
Sc-46	---	---	---
Co-60	1000	---	---
Ni-59	1000	1.43E+07	1.12E+06
Ni-63	1000	5.23E+09	4.12E+08
Se-79	1000	8.01E+05	6.32E+04
Kr-85	1000	---	---
Rb-87	1000	5.18E+05	4.08E+04
Sr-90	1000	1.45E+14	1.14E+13
Zr-93	1000	3.22E+07	2.54E+06
Nb-93m	1000	---	---
Nb-94	1000	9.57E+04	7.54E+03
Mo-93	1000	1.87E+07	1.48E+06
Tc-99	1000	8.28E+04	6.53E+03
Pd-107	1000	2.96E+07	2.33E+06
Ag-108m	1000	3.49E+05	2.75E+04
Cd-113m	1000	---	---
Sn-121m	1000	3.35E+12	2.64E+11
Sn-126	1000	7.07E+04	5.57E+03
Sb-125	1000	---	---
I-129	1000	1.29E+04	1.01E+03
Cs-134	1000	---	---
Cs-135	1000	8.27E+05	6.51E+04
Cs-137	1000	8.31E+14	6.55E+13
Ba-133	1000	---	---
Sm-151	1000	2.07E+11	1.63E+10
Eu-152	1000	6.13E+18	4.83E+17
Eu-154	1000	---	---
Eu-155	1000	---	---
W-181	---	---	---
W-185	---	---	---
W-188	---	---	---
Pb-210	1000	1.02E+17	8.01E+15
Bi-207	1000	3.37E+14	2.66E+13
Ra-226	1000	3.48E+03	2.75E+02
Ra-228	1000	---	---

Table B-5. Intruder-Based Radionuclide Disposal Limits for Vault 4 – Post-Drilling Scenario with Transient Calculation for 1000 - 10000 Years

Radionuclide	Time of Limit (Years)	Concentration Limit ($\mu Ci/m^3$)	Inventory Limit (Ci/Unit)
Ac-227	1000	3.93E+17	3.10E+16
Th-228	1000	---	---
Th-229	1000	1.85E+04	1.46E+03
Th-230	9090	2.46E+03	1.94E+02
Th-232	1000	5.03E+03	3.96E+02
Pa-231	1000	4.21E+03	3.32E+02
U-232	1000	2.73E+08	2.15E+07
U-233	10000	2.32E+04	1.83E+03
U-234	10000	2.67E+04	2.10E+03
U-235	10000	1.83E+04	1.45E+03
U-236	1000	1.33E+05	1.05E+04
U-238	10000	1.26E+05	9.95E+03
Np-237	10000	3.69E+03	2.91E+02
Pu-238	10000	7.55E+07	5.95E+06
Pu-239	1000	5.12E+04	4.04E+03
Pu-240	1000	5.53E+04	4.36E+03
Pu-241	1000	5.81E+06	4.58E+05
Pu-242	1000	5.25E+04	4.14E+03
Pu-244	10000	2.92E+04	2.30E+03
Am-241	1000	1.98E+05	1.56E+04
Am-242m	1000	2.16E+06	1.70E+05
Am-243	1000	4.14E+04	3.26E+03
Cm-242	10000	1.49E+10	1.17E+09
Cm-243	1000	4.21E+07	3.32E+06
Cm-244	1000	2.00E+07	1.58E+06
Cm-245	1600	2.51E+04	1.98E+03
Cm-246	1000	5.67E+04	4.46E+03
Cm-247	10000	2.59E+04	2.04E+03
Cm-248	1000	1.34E+04	1.05E+03
Bk-249	1000	7.51E+07	5.92E+06
Cf-249	1000	1.94E+05	1.53E+04
Cf-250	1000	2.06E+07	1.62E+06
Cf-251	1000	7.91E+04	6.23E+03
Cf-252	1000	1.82E+09	1.43E+08

Table B.6 Intruder-Based Radionuclide Disposal Limits for Vault 4 – Agriculture Scenario with Transient Calculation for 10000 Years

Radionuclide	Time of Limit (Years)	Concentration Limit ($\mu Ci/m^3$)	Inventory Limit (Ci/Unit)
H-3	1150	---	---
C-14	3275.0	1.64E+04	1.30E+03
Na-22	1132.1	---	---
Al-26	3275.0	4.37E+01	3.44E+00
S-35	---	---	---
Cl-36	3275.0	1.43E+02	1.13E+01
Ar-39	1132.1	1.63E+07	1.29E+06
K-40	3275.0	5.84E+02	4.60E+01
Ca-41	3275.0	6.90E+04	5.44E+03
Sc-46	---	---	---
Co-60	1132.1	---	---
Ni-59	3275.0	2.43E+06	1.91E+05
Ni-63	1280	8.72E+10	6.87E+09
Se-79	3275.0	1.33E+05	1.05E+04
Kr-85	1132.1	---	---
Rb-87	3275.0	8.50E+04	6.70E+03
Sr-90	1132.1	2.11E+16	1.66E+15
Zr-93	3275.0	2.61E+06	2.06E+05
Nb-93m	1132.1	---	---
Nb-94	1132.1	8.18E+01	6.45E+00
Mo-93	1720	1.31E+06	1.03E+05
Tc-99	3275.0	1.39E+04	1.09E+03
Pd-107	3275.0	4.89E+06	3.85E+05
Ag-108m	1132.1	5.17E+02	4.07E+01
Cd-113m	1150	---	---
Sn-121m	1132.1	5.67E+11	4.47E+10
Sn-126	1132.1	6.48E+01	5.11E+00
Sb-125	1132.1	---	---
I-129	3275.0	2.07E+03	1.63E+02
Cs-134	1132.1	---	---
Cs-135	3275.0	1.37E+05	1.08E+04
Cs-137	1132.1	4.82E+13	3.79E+12
Ba-133	1132.1	---	---
Sm-151	1132.1	9.51E+11	7.50E+10
Eu-152	3275.0	4.12E+17	3.25E+16
Eu-154	1132.1	---	---
Eu-155	1132.1	---	---
W-181	---	---	---
W-185	---	---	---
W-188	---	---	---
Pb-210	1150	---	9.56E+18
Bi-207	1132.1	5.15E+12	4.06E+11

Table B.6 Intruder-Based Radionuclide Disposal Limits for Vault 4 – Agriculture Scenario with Transient Calculation for 10000 Years

Radionuclide	Time of Limit (Years)	Concentration Limit ($\mu Ci/m^3$)	Inventory Limit (Ci/Unit)
Ra-226	1132.1	1.11E+02	8.76E+00
Ra-228	1132.1	---	---
Ac-227	1132.1	1.18E+18	9.32E+16
Th-228	1132.1	---	---
Th-229	1132.1	4.51E+02	3.55E+01
Th-230	9080	6.25E+01	4.92E+00
Th-232	3275.0	4.39E+01	3.46E+00
Pa-231	3275.0	1.87E+02	1.48E+01
U-232	1132.1	6.34E+06	5.00E+05
U-233	10000	5.70E+02	4.49E+01
U-234	10000	8.03E+02	6.33E+01
U-235	10000	4.64E+02	3.66E+01
U-236	3275.0	1.50E+04	1.18E+03
U-238	10000	4.01E+03	3.16E+02
Np-237	10000	3.13E+02	2.47E+01
Pu-238	10000	2.28E+06	1.80E+05
Pu-239	3275.0	5.65E+03	4.45E+02
Pu-240	3275.0	7.28E+03	5.73E+02
Pu-241	1132.1	1.33E+06	1.05E+05
Pu-242	3275.0	5.44E+03	4.28E+02
Pu-244	10000	3.37E+02	2.65E+01
Am-241	1132.1	4.55E+04	3.58E+03
Am-242m	1132.1	8.32E+05	6.56E+04
Am-243	1132.1	8.88E+02	7.00E+01
Cm-242	10000	4.49E+08	3.53E+07
Cm-243	3275.0	4.48E+06	3.53E+05
Cm-244	3275.0	2.63E+06	2.07E+05
Cm-245	3275.0	1.37E+03	1.08E+02
Cm-246	3275.0	8.01E+03	6.31E+02
Cm-247	10000	2.85E+02	2.24E+01
Cm-248	3275.0	1.37E+03	1.08E+02
Bk-249	1132.1	1.33E+06	1.05E+05
Cf-249	1132.1	3.43E+03	2.70E+02
Cf-250	3275.0	2.91E+06	2.29E+05
Cf-251	1132.1	3.02E+03	2.38E+02
Cf-252	3275.0	1.87E+08	1.47E+07

B.6 SENSITIVITY AND UNCERTAINTY ANALYSIS OF MODEL TO ESTIMATE DOSE

Current USDOE guidance on performance assessment (USDOE 1996) indicates that a sensitivity and uncertainty analysis of the assumed exposure scenarios for inadvertent intrusion should be limited to qualitative arguments including, for example, discussions of the rationale for selecting particular scenarios and parameter values. The guidance on sensitivity and uncertainty analysis of intrusion scenarios is based on an assumption that active institutional control will be maintained over disposal sites until they can be safely released in accordance with requirements in Order 5400.5 (USDOE 1990).

The following discussion of uncertainties in the model used to estimate external dose to inadvertent intruders in the resident scenarios goes beyond the requirements in current guidance (USDOE 1996). The purpose of these discussions is to provide insight into the magnitude of uncertainties in estimates of annual effective dose equivalents per unit concentration of radionuclides in the assumed resident scenarios.

Limits on allowable disposals in Tables B-3 and B-4 are based on estimates of dose for the pathway involving external exposure during indoor residence in a home located on top of a disposal vault. As indicated by equations B-6 and B-7 in Section B.3.2, the external dose factor during indoor residence of a radionuclide in a disposal vault is proportional to the exposure time, the shielding factor during indoor residence, and the dose conversion factor for external exposure. For purposes of radiation protection, external dose coefficients are treated as fixed parameters for reference individuals and reference conditions of exposure and, thus, essentially have no uncertainty. Even if uncertainties in external dose coefficients were treated rigorously, they probably are less than a factor of two for radionuclides that are high-energy photon emitters (Eckerman and Ryman 1993; ICRP 1996). The exposure time is uncertain, but the value of 50% of the time during the year assumed in this analysis is intended to be conservative for most individuals and would not underestimate the exposure time in the worst case by more than a factor of two. The shielding factor during indoor residence also is uncertain, but the assumed value of 0.7 would not underestimate the actual value by more than 50%, and it probably does not overestimate values for typical homes in the vicinity of the SRS by more than a factor of two (Kocher 1980). Substantially lower shielding factors and, thus, lower external doses would result if a home were assumed to be constructed with a thick foundation of uncontaminated material, such as concrete. However, it does not seem reasonable to assume that such a foundation would be used in any home that would be constructed at the disposal site.

Based on these considerations, uncertainties in the model used to assess external dose to inadvertent intruders should not be significant. Rather, the definition of exposure scenarios and an ability to obtain sufficiently accurate estimates of radionuclide inventories in waste prior to disposal are likely to be more important factors in determining acceptable disposals of radionuclides based on the results of an intruder dose analysis. These factors are discussed in the following section.

B.6.1 General Consideration of Uncertainties in Determining Acceptable Disposals

In evaluating uncertainties in models used to estimate dose to an inadvertent intruder, the most important consideration may be the definitions of the exposure scenarios. Dose assessments for the different scenarios are based on an assumption that the scenarios will occur as postulated, but many of the assumptions used in defining the scenarios are likely to be pessimistic.

In defining exposure scenarios for inadvertent intruders at the SDF, it is reasonable to assume that individuals will establish a homestead within the site boundary at some time after loss of active institutional control. However, several of the assumptions used in developing the exposure

scenarios are less certain and probably pessimistic. For example, all scenarios for inadvertent intrusion assume that individuals will have no prior knowledge of waste disposal activities at the site, but this assumption seems unreasonable at times soon after loss of active institutional control. Furthermore, all exposure scenarios assume that an intruder will build a home at the location of disposed waste, but there is some probability that all homes constructed on the SRS at future times will be located elsewhere.

An assumption that active institutional control will be relinquished at 100 years after disposal also may be pessimistic. Controls over waste disposal or other contaminated sites will not be relinquished until such sites can be released safely (USDOE 1996), and conditions that define safe release may be more restrictive than the performance measure for inadvertent intruders assumed in this analysis (Luftig and Weinstock 1997). Thus, active institutional control may be required for considerably longer than 100 years to provide adequate protection of the public, and some assumed scenarios, such as the resident scenario at 100 years, may be precluded.

By the way they are defined, assumed exposure scenarios for inadvertent intruders tend to maximize estimates of dose that reasonably could be experienced by individuals who might come onto the disposal site after loss of active institutional control. It is important to recognize that a dose assessment for inadvertent intruders is not intended to provide either best estimates of doses that likely would be received or a quantification of uncertainties in estimated doses. Rather, the primary purpose of a dose assessment is to indicate whether planned disposal practices at a site would be adequately protective of future inadvertent intruders. This is accomplished mainly by using the results of a dose assessment to establish waste acceptance criteria in the form of limits on average concentrations or inventories of radionuclides in waste prior to disposal. If these limits are not exceeded, it may be assumed that future inadvertent intruders will be protected, and there is no need to be concerned about the magnitude of doses that any such individuals might actually receive. Furthermore, quantitative estimates of uncertainties in calculated doses based on parameter uncertainty analysis may not be particularly meaningful, because the results are conditional on the occurrence of assumed exposure scenarios. Therefore, an important factor in determining the acceptability of waste disposals is the credibility of assumed exposure scenarios for inadvertent intruders, rather than any estimates of uncertainties in the results due to uncertainties in parameters in the dose assessment models.

A second important factor in determining the acceptability of waste disposals is the capability of estimating inventories of radionuclides in disposed waste with sufficient accuracy. In a PA for a disposal facility at another site (ORNL 1997), uncertainties in estimating inventories of radionuclides in waste were judged to be an important, if not the most important, source of uncertainty in assessing long-term performance, even when all sources of uncertainty in the various models and parameters were considered. It usually is not difficult to estimate the inventories of high-energy photon-emitting radionuclides, such as Co-60 and Cs-137. However, it can be a major challenge to estimate inventories of beta- and alpha-emitting radionuclides based on measurement, rather than process knowledge. Furthermore, depending on the scenarios for inadvertent intrusion that are assumed to be credible occurrences, inventories of some of these radionuclides, such as Tc-99, uranium, and alpha-emitting transuranic radionuclides (e.g., Pu-239, Am-241) may be comparable to, or a substantial fraction of the limits on, allowable inventories, in which case there is a clear need of accurate estimates of inventories. Therefore, the problem of determining inventories of important radionuclides in waste may override any considerations of uncertainties in the models used to assess dose to inadvertent intruders.

B.7 REFERENCES

Cook, James R. and Wilhite, Elmer L. 2004. *Special Analysis: Radionuclide Screening Analysis for E Area*. WSRC-TR-2004-00294. Westinghouse Savannah River Company, Aiken, SC.

Cook, J. R., Kocher, D. C. McDowell-Boyer, L., and Wilhite, E. L., 2002, *Special Analysis: Reevaluation of the Inadvertent Intruder, Groundwater, Air and Radon Analyses for the Saltstone Disposal Facility,* WSRC-TR-2002-00456, Westinghouse Savannah River Company, Aiken, South Carolina.

Eckerman, K.F., and Ryman, J.C. 1993. *External Exposure to Radionuclides in Air, Water, and Soil*, Federal Guidance Report No. 12, USEPA 402-R-93-081, U.S. Environmental Protection Agency, Washington, DC.

ICRP (International Commission on Radiological Protection). 1996. *Conversion Coefficients for Use in Radiological Protection Against External Exposure*, ICRP Publication 74, *Ann. ICRP* 26, No. 3/4.

Kennedy, W. E. and Peloquin, R. A. 1988. *Intruder Scenarios for Site Specific Low-Level Radioactive Waste Classification*. DOE/LLW-71T, U. S. Department of Energy, Idaho Falls, ID.

Kocher, D.C. 1980. "Effects of Indoor Residence on Radiation Doses from Routine Releases of Radionuclides to the Atmosphere," *Nuclear Technology.* 48, 171.

Koffman, L. D. 2004. *An Automated Inadvertent Intruder Analysis Application.* WSRC-TR-2004-00293. Westinghouse Savannah River Company, Aiken, SC.

Lee, Patricia L. 2004. *Inadvertent Intruder Analysis Input for Radiological Performance Assessments*. WSRC-TR-2004-00295. Westinghouse Savannah River Company, Aiken, SC.

Luftig, S.D., and Weinstock, L. 1997. "Establishment of Cleanup Levels for CERCLA Sites with Radioactive Contamination," Directive 9200.4-18, Office of Solid Waste and Emergency Response, U.S. Environmental Protection Agency, Washington, DC.

McDowell-Boyer, L., Yu, A.D., Cook, J.R., Kocher, D.C., Wilhite, E.L., Holmes-Burns, H., and Young, K.E. 2000. *Radiological Performance Assessment for the E-Area Low-Level Waste Facility*, WSRC-RP-94-218, Revision 1, Westinghouse Savannah River Company, Aiken, South Carolina.

NCRP 1996. *Screening Models for Releases of Radionuclides to Atmosphere, Surface Water and Ground.* NCRP Report 123, Volumes I and II. Bethesda, MD.

ORNL (Oak Ridge National Laboratory). 1997. *Performance Assessment for Continuing and Future Operations at Solid Waste Storage Area 6*, ORNL-6783/R1, Volume 1 and 2, Oak Ridge National Laboratory, Oak Ridge, Tennessee.

Phifer, M. A. and Nelson, E. A., 2003, *Saltstone Disposal Facility Closure Cap Configuration and Degradation Base Case: Institutional Control to Pine Forest Scenario*, WSRC-TR-2003-00436, Revision 0, Westinghouse Savannah River Company, Aiken, South Carolina.

Tuli, J. K. 2000. *Nuclear Wallet Cards*, sixth edition. Brookhaven National Laboratory, Upton, NY.

USDOE (U.S. Department of Energy). 1990. *Radiation Protection of the Public and the Environment*, USDOE Order 5400.5, U.S. Department of Energy, Washington, DC.

USDOE 1996. *Interim Format and Content Guide and Standard Review Plan for U.S. Department of Energy Low-Level Waste Disposal Facility Performance Assessments*, U.S. Department of Energy, Washington, DC.

USDOE 1999. "Low-Level Waste Requirements," Chapter IV in *Radioactive Waste Management Manual*, USDOE M 435.1-1, U.S. Department of Energy, Washington, DC.

THIS PAGE INTENTIONALLY LEFT BLANK

APPENDIX C
ATMOSPHERIC PATHWAY ANALYSIS

THIS PAGE INTENTIONALLY LEFT BLANK

C.1 ADDITIONAL INFORMATION ON ATMOSPHERIC PATHWAY ANALYSIS

This section describes the investigation conducted to evaluate the potential magnitude of gaseous release of radionuclides from Vault 4 of the Saltstone Disposal Facility over the 10,000-year performance assessment (PA) period of interest.

A screening analysis was conducted to produce a list of radionuclides requiring a more thorough analysis to derive disposal limits for the Saltstone Disposal Facility based on the atmospheric pathway. This study, described in Crapse and Cook, 2004, used a methodology developed by the National Council on Radiation Protection and Measurements, professional judgment and process knowledge to determine this list. The list of potential radionuclides includes C-14, Cl-36, H-3, I-129, Sb-125, Se-79, Sn-121m and Sn-126.

This analysis considers the diffusion of these radionuclides upward from the Saltstone vault through the overlying soil material (anticipated closure cap) to determine emanation rates at the land surface. The atmospheric pathway exposure standard deriving from USDOE Order 435.1 is 10 mrem/yr.

The analysis presented here uses accepted computer programs for chemical interactions (MINTEQ), diffusion (PORFLOW) and atmospheric transport and dose calculations (CAP88).

C.2 SALTSTONE CLOSURE CONSIDERATIONS

The concepts for closure of the Saltstone Vault 4 are relevant to the determination of the flux of gaseous radionuclides at the land surface. Therefore, Vault 4 construction specifics and closure concept described in Cook, J. R. et al., 2002 are summarized below.

The current Vault 4 is a concrete vault with a base constructed 11.5 ft. below grade. Its footprint dimensions are approximately 600 ft. by 200 ft. and it contains 12 individual cells, each having approximate dimensions of 100 ft. by 100 ft by 25 ft. high. Individual cells will be filled with approximately 24 ft. of Saltstone and then approximately 16 in. of uncontaminated grout over which a concrete vault roof will be placed.

For the purposes of this investigation, it is assumed that there will be a 30-year operational period during which the unit is loaded with waste. After an individual vault cell is filled with Saltstone, interim closure will be performed which consists of the placement of a 16-inch (0.41 m) clean grout layer between the Saltstone and the overlying concrete roof. Final closure will occur when all Saltstone vaults are filled, and will consist of the placement of a closure cap over all of the vaults. This will be followed by a 100-year period of institutional control, as described in Phifer and Nelson, 2003. The final closure cap will exist far into the future and is the configuration that must be considered in evaluating gaseous releases at the land surface. A conceptual drawing of a Saltstone vault and closure cap is shown in Figure C-1 and the vertical section over which gaseous diffusion was evaluated is indicated.

C.2.1 Closure Configuration

The closure configuration utilized in this analysis includes all materials, as constructed, including the final closure cap placed over all of the filled vaults at the end of the operations period.

Table C-1 lists the individual components of the vault materials and closure cap. Materials are indicated with the associated thickness of each component in inches, feet and meters. The composite thickness of the non-waste material below the top of the erosion barrier is 11.5 ft. (3.5 m).

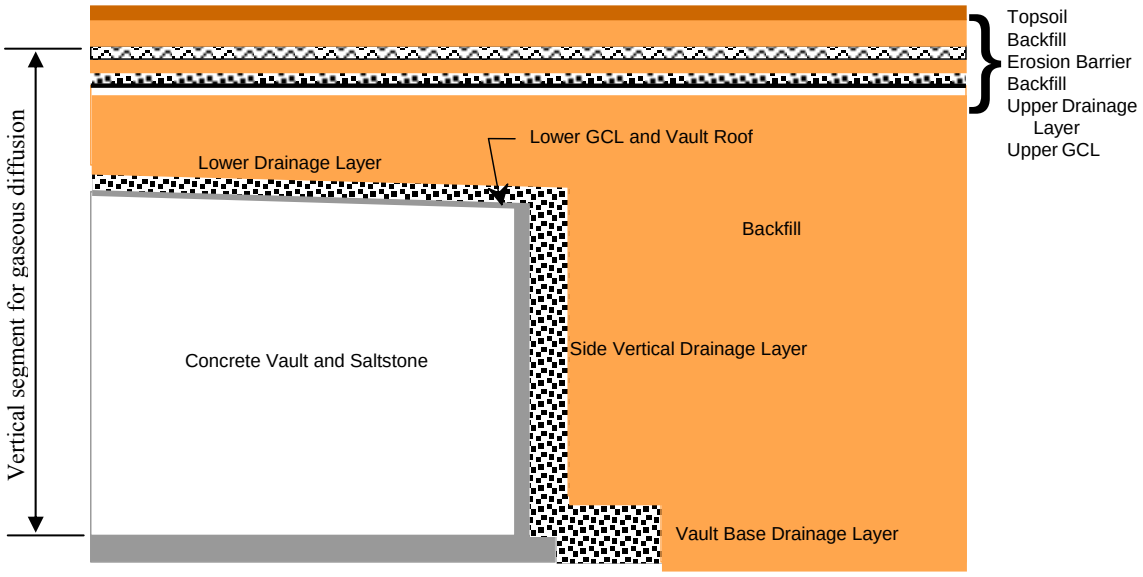

Figure C-1. Conceptual Closure Configuration for Vault 4

Table C-1. Vertical Layer Sequence and Associated Thickness for Saltstone Cover Material (Adapted from Phifer And Nelson, 2003)

Layer	Thickness (inches)	Thickness (ft.)	Thickness (m)
Topsoil	6	0.5	0.15
Upper backfill	30	2.5	0.76
Erosion barrier	12	1	0.3
Middle backfill layer	12	1	0.3
Middle drainage layer	12	1	0.3
Lower backfill layer	58.7	4.89	1.5
Lower drainage layer	24	2	0.61
Vault concrete roof	4	~0.3	~0.1
Vault clean grout layer	16	~1.3	~0.41
Vault Waste Zone	288	~24	~7.3

C.3 MODEL DEVELOPMENT

C.3.1 Conceptual Model

The flux of radioactive gasses at the land surface above the Saltstone Vault 4 was evaluated for its specific closure configuration. Gaseous radionuclides introduced within the waste zone diffuse outward from this zone into the air-filled soil pores surrounding the vault, eventually resulting in some of the radionuclides emanating at the land surface. As such, air is the fluid through which they diffuse. It is assumed that fluctuations in atmospheric pressure at the land surface that could induce small pulses of air movement into and out of the shallow soil profile over relatively short periods of time will have a zero net effect when averaged over longer time periods. Thus, advective transport of these radionuclides in air-filled soil pores is not considered to be a significant process when compared to the rate of air diffusion.

The radionuclides present as gasses are those identified in the screening process described in Crapse and Cook, 2004. Certain gaseous radionuclides will not likely remain in the monatomic elemental form but combine with other gaseous elements or form diatomic molecules. The state of existence of each of these radionuclides in the gaseous phase is important in evaluating their transport to the land surface because the diffusion coefficient associated with each is related to its molecular weight.

In this investigation it is assumed that:

- C-14 exists as part of the CO_2 molecule
- Cl-36, H-3 and I-129 exist as diatomic gasses
- Sb-125, Se-79, Sn-121m, and Sn-126 exist as monatomic gasses.

A related investigation was undertaken to quantify the gaseous phase activity of the above mentioned radionuclides when allowed to equilibrate between the aqueous phase and gaseous phases within the Saltstone pores, taking into account the chemical compounds the radionuclides would tend to occur as in the gaseous phase and the residual saturation of Saltstone. A specific activity of each radionuclide was calculated in the air-filled pore space within Saltstone per Ci of source. This investigation is documented in Denham and Crapse, 2005.

C.3.2 Numerical Model

The mathematical model utilized in this report is provided by the PORFLOW simulation package. PC-based PORFLOW Version 5.97.0 was used to conduct a series of simulations. PORFLOW is developed and marketed by Analytic & Computational Research, Inc. to solve problems involving transient and steady-state fluid flow, heat and mass transport in multi-phase, variably saturated, porous or fractured media with dynamic phase change. PORFLOW has been widely used at the SRS and in the USDOE complex to address major issues related to the groundwater and nuclear waste management.

The governing equation for mass transport of species *k* in the fluid phase is given by

$$\frac{\partial C_k}{\partial t} + \frac{\partial}{\partial x_i}(V_i C_k) = \frac{\partial}{\partial x_i}(D_{ij}\frac{\partial C_k}{\partial x_j}) + \gamma_k \qquad \text{Eqn. C-1}$$

Where

C_k	concentration of species *k*
V_i	fluid velocity in the i^{th} direction
D_{ij}	effective diffusion coefficient for the species
γ_k	net decay of species *k*
i, j	direction index
t	time
x	distance coordinate

This equation is solved within PORFLOW to evaluate transient radionuclide transport through the soil cover above Saltstone Vault 4 and to determine gaseous radionuclide flux at the land surface over time. For this exercise the advection term was disabled within PORFLOW and only the diffusive and net decay terms were evaluated.

C.3.3 Model Development and Assumptions

The numerical representation of the conceptual model is as a 1-dimensional vertical stack of elements configured to correspond to the vertical dimensions of the Saltstone vault and overlying cover material associated with final closure of Vault 4.

The radionuclides evaluated are C-14, Cl-36, H-3, I-129, Sb-125, Se-79, Sn-121m and Sn-126.

Since source radionuclides exist as gases, air was taken to be the fluid within which transport occurs. The flow field was assumed to be isobaric and isothermal. The impact of naturally occurring fluctuations of atmospheric pressure is likely to have a zero net effect and only a very shallow zone of influence at the land surface. Therefore, for the relatively long periods of time evaluated in this investigation, air-diffusion was the only transport mechanism simulated in the model and advective air-transport was assumed to be negligible.

A small percentage of the radionuclides dissolve in residual pore water but since diffusion proceeds more slowly in that fluid, air-diffusion is regarded as the only transport process by which they can reach the land surface from the Saltstone waste zone. This assertion is substantiated in Yu et al. 2001. In that report the radon effective diffusion coefficient, D_{eff}, for soil is reported to range from the open-air diffusion coefficient of 1.0E-6 m^2/sec to that of fully saturated soil, 1.0E-10 m^2/sec. This 4-order of magnitude difference is consistent with the

comparison of water diffusion coefficients to air diffusion coefficients of other common molecular compounds and reported in many references. Thus, the larger volume of water-filled pore space compared to air-filled pore space (maximum of 2 orders of magnitude difference) is inconsequential, in terms of the ability of water-dissolved compounds to diffuse through water-filled pores as compared to the ability of the same compounds to diffuse as gas in the vapor-filled pore spaces. Furthermore, there is vertical downward movement of the pore water which acts to offset or overcome any vertical upward diffusion of dissolved constituents. Consequently, in this investigation radionuclide transport was allowed to proceed only through air-filled pore space and, therefore, residual pore water was treated as if it was part of the solid matrix material within the flow field. No accounting was made of the partitioning of the gaseous radionuclides into the pore water as diffusive vapor transport proceeded from the waste zone to the land surface. By ignoring this mechanism, diffusive fluxes at the land surface were slightly overestimated.

The boundary conditions imposed on the model domain included:

- No-flux specified for all radionuclides along sides and bottom
- Radionuclide concentrations set to 0 at land surface.

These boundary conditions force all of the gaseous radionuclides to move upward from the waste disposal zone to the land surface. In reality, some lateral and downward diffusion occurs in the air-filled pores surrounding the waste zone; hence ignoring this has the effect of increasing the flux at the land surface, thus introducing a significant measure of conservatism in the calculated results. Simulations were conducted in transient mode for diffusive transport in air, with results being obtained over 10,125 years.

A summary of the radionuclides and compounds of interest in this investigation are summarized below in Table C-2.

Table C-2. Radionuclides and Compounds of Interest.

Radionuclide	Half-life (yrs)	Atomic Wt.	Molecular form in gaseous state	Molecular Wt.
C-14	5.73E+03	14	CO_2	45.99
Cl-36	3.01E+05	36	Cl_2	72
H-3	12.33	3	H_2	6
I-129	1.57E+07	129	I_2	258
Sb-125	2.76	125	Sb	125
Se-79	1.1E+06	79	Se	79
Sn-121m	55	121	Sn	121
Sn-126	1.00E+05	126	Sn	126

C.3.4 Grid Construction

The model grid was constructed as a node mesh 3 nodes wide by 36 nodes high. This mesh creates the vertical stack of 34 model elements. The grid extends upward only as far as the erosion barrier, anticipating that this is the cover thickness that will prevail over the majority of the PA assessment period. A set of consistent units were employed in the simulations for length, mass and time, these being meters, grams and years, respectively.

C.3.5 Material Zones

The model domain was divided into two primary zones, the Saltstone waste zone occupying the lower 24 ft. (7.3 m) of the domain and the cover zone, extending ~11.5 ft. (~3.5 m) above the

waste zone to the top of the domain. The cover zone includes the vault concrete roof as well as the different closure cap layers. The upper model elements were scaled to correspond to the geometry of the closure cap thickness while the lower model elements were scaled to correspond to the Saltstone waste zone. The land surface for the evaluation period of interest is assumed to be the top of the erosion resistant layer.

C.3.6 Material Zone Properties and Other Input Parameters

Material properties utilized within the 1-D numerical model were specified for 7 material zones defined within the model domain. Each material zone was assigned values for total porosity, residual saturation, air-filled porosity, matrix density, air density, and an effective air-diffusion coefficient for each source element or compound. Tortuosity was assigned a unit value since an effective diffusion coefficient was employed. The rock (matrix) density was selected based on the density of quartz, and is regarded to be representative of most SRS soils.

Values for total porosity and long-term residual saturation for Saltstone and concrete were obtained from vadose zone 2-D simulations conducted to evaluate the groundwater pathway as a part of this Special Analysis and which are presented in Appendix A. Saltstone and concrete porosities were established at 0.42 and 0.18, respectively in that analysis. The steady-state residual saturations were obtained from representative nodes in the simulation domain. These values were found to be 0.99 for both materials at reference nodes (35,50) and (35,67) for Saltstone and concrete, respectively.

Values for total porosity and long-term residual saturation of the closure cap materials were selected based on a series of HELP model simulations conducted as part of the investigation summarized in Phifer and Nelson, 2003. HELP model analyses were conducted at different points in time, these being at 100, 300, 550, 1000, 1800, 3400, 5600 and 10,000 years in the future. Porosities of the different materials changed slightly through time as a result of leaching and residual saturations varied as porosities and expected recharge rates varied. Porosities changed less conspicuously than residual saturations, and by plotting residual saturation versus time representative values could then be selected. A summary of the selected values of porosity, long-term residual saturation and air-filled porosity are listed for each material type in Table C-3.

Air-filled porosity was estimated by subtracting the residual moisture content from the total porosity. A value for the density of air was obtained from the Bolz, R.E., et al., CRC Handbook of Tables for Applied Engineering Science.

Table C-3. Porosity, Residual Saturation and Air-Filled Porosity Values

Layer Material	Representative Porosity	Long-term Residual Saturation	Air-filled Porosity
Erosion Barrier	0.07	0.83	1.19E-02
Upper Backfill	0.38	0.63	1.39E-01
Upper Drainage	0.38	0.58	1.58E-01
Lower Backfill	0.37	0.72	1.04E-01
Lower Drainage	0.31	0.5	1.60E-01
Concrete	0.18	0.99	2.00E-03
Saltstone	0.42	0.99	4.00E-03

Molecular diffusion coefficients for each of the radionuclides evaluated were calculated based on the effective open air diffusion coefficient of radon, as reported in Nielson, et. al. 1984. That study used a soil pore size distribution model that allowed the selection of effective radon air-diffusion coefficients based on the degree of residual water saturation.

Using the effective radon air-diffusion coefficient calculated for each material zone in the model domain as the reference, the effective diffusion coefficients for each of the radionuclides in their gaseous compound was then calculated using the following relationship:

$$D = D' \sqrt{\frac{MWT'}{MWT}} \qquad \text{Eqn. C-2}$$

Where: D = the diffusion coefficient of the radionuclide of interest (m^2/yr)

D' = the diffusion coefficient of the reference radionuclide (m^2/yr)

MWT' = the molecular weight of the reference radionuclide (Rn-222)

MWT = the molecular weight of the element or compound of interest

A summary of the calculated effective air-diffusion coefficients, calculated for each radionuclide or compound by material zone, is presented below in Table C-4.

Table C-4. Effective Air-Diffusion Coefficients for Each Radionuclide/Compound, by Material.

Radionuclide	Saltstone and Concrete (m^2/yr)	Lower Drainage (m^2/yr)	Lower Backfill (m^2/yr)	Upper Drainage and Upper Backfill (m^2/yr)	Erosion Barrier (m^2/yr)
$^{14}CO_2$	4.86E-01	1.39E+01	6.24E+00	1.04E+01	1.73E+00
$^{36}Cl_2$	3.88E-01	1.11E+01	4.99E+00	8.31E+00	1.39E+00
$^{3}H_2$	1.34E+00	3.84E+01	1.73E+01	2.88E+01	4.80E+00
$^{129}I_2$	2.05E-01	5.85E+00	2.63E+00	4.39E+00	7.32E-01
^{125}Sb	2.95E-01	8.41E+00	3.78E+00	6.30E+00	1.05E+00
^{126}Sb	2.93E-01	8.38E+00	3.77E+00	6.28E+00	1.05E+00
^{79}Se	3.70E-01	1.06E+01	4.76E+00	7.93E+00	1.32E+00
^{121m}Sn	2.99E-01	8.55E+00	3.85E+00	6.41E+00	1.07E+00
^{126}Sn	2.93E-01	8.38E+00	3.77E+00	6.28E+00	1.05E+00

In developing the vapor phase source term for the simulations, it was assumed that 1 curie of each of the potentially gaseous radionuclides was available to partition between the residual pore water and the vapor-filled pore space. Furthermore, it was assumed that the concentration of each radionuclide in the residual pore water was in equilibrium with the source material, e.g., solid Saltstone, and continued to add vapor phase activity proportional to the water concentration as the gaseous phase radionuclides diffused away. The residual pore water concentration was assumed to decrease through time at a rate proportional to the decay constant for each radionuclide, hence the source term in the vapor phase decreased similarly over time.

C.4 MODEL RESULTS

Model simulations were conducted to evaluate the peak flux of each radionuclide emanating from the top of the domain. Results were output in Ci/yr, consistent with the set of units employed in the model, and are presented for C-14, Cl-36, H-3, I-129 and Se-79 in Figures C-2, C-3, C-4, C-5 and C-6, respectively. The peak fluxes emanating at the land surface are presented for two time periods, 0-100 years and for the period of 100-10,125 years and are presented in Table C-5. The results are reported in this way to facilitate calculation of human exposure at the different locations defined for these time periods. Graphs showing the flux rates at the land surface for Sn-126, Sn-121m, and Sb-125 are not shown because the extremely low tendency to partition into vapor phase resulted in the calculation of extraordinarily low flux rates at the land surface and correspondingly high facility disposal limits. The results for these radionuclides are shown, however, in Table C-5.

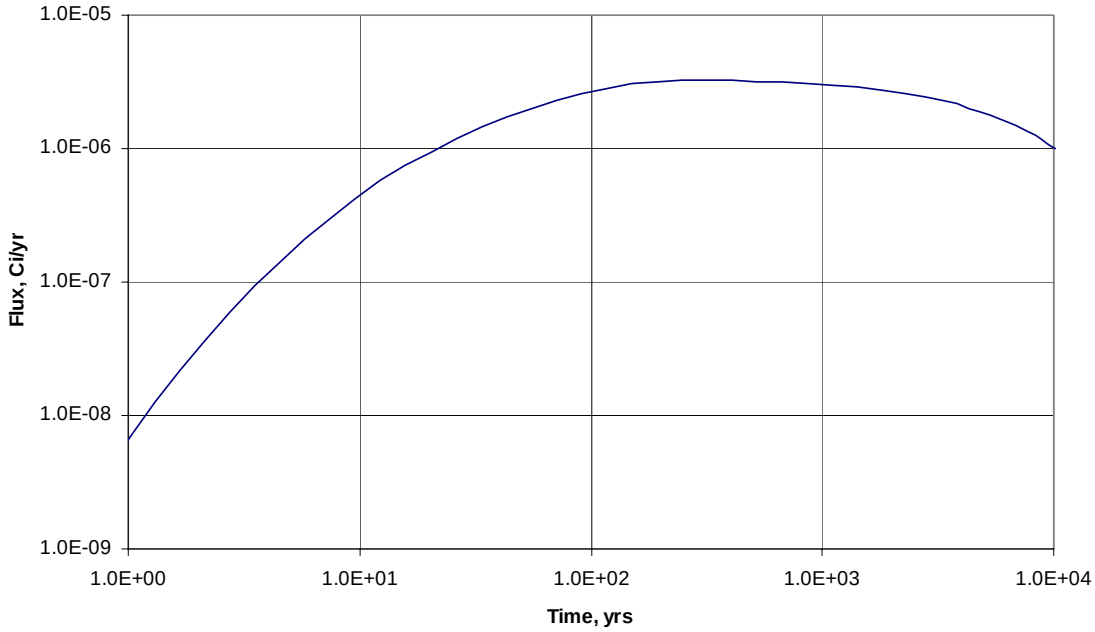

Figure C-2. Flux Rate at Land Surface for C-14

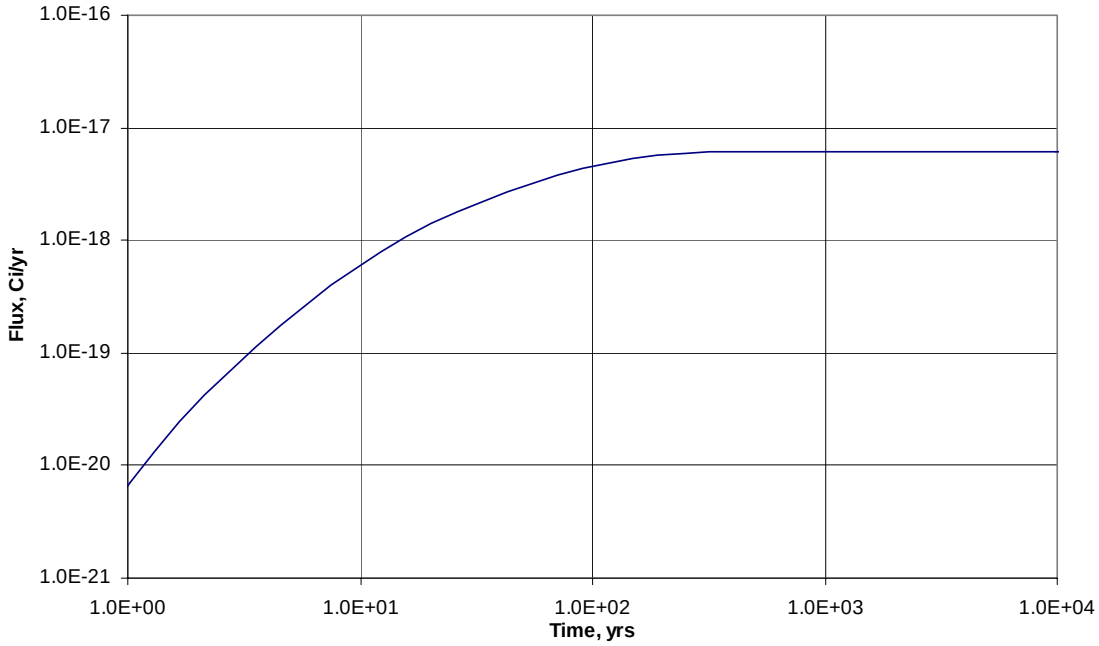

Figure C-3. Flux Rate at Land Surface for Cl-36

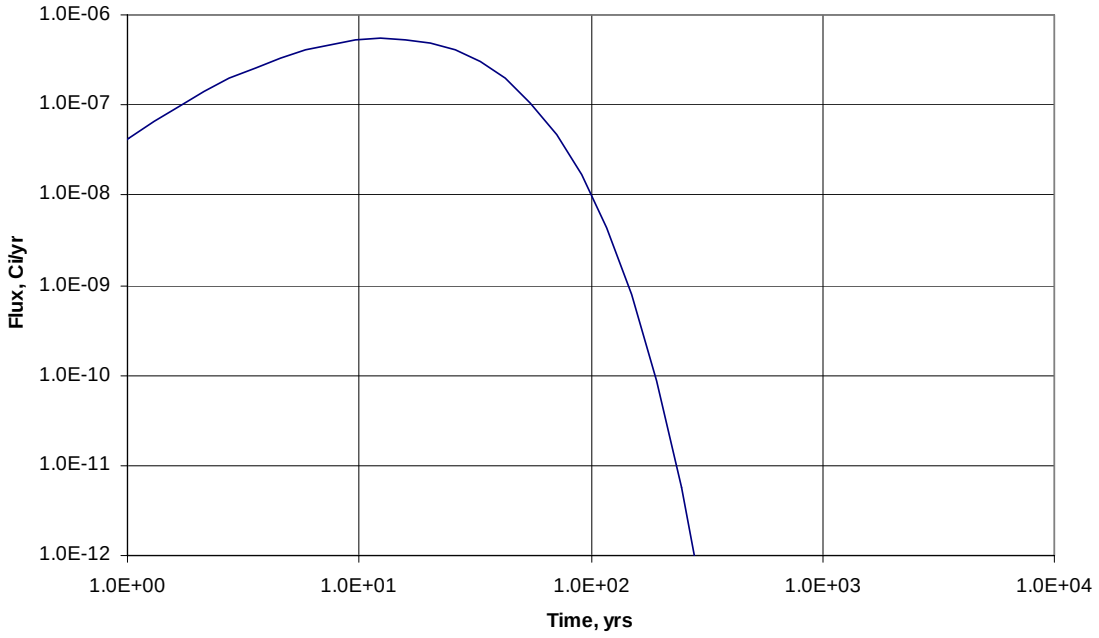

Figure C-4. Flux Rate at Land Surface for H-3

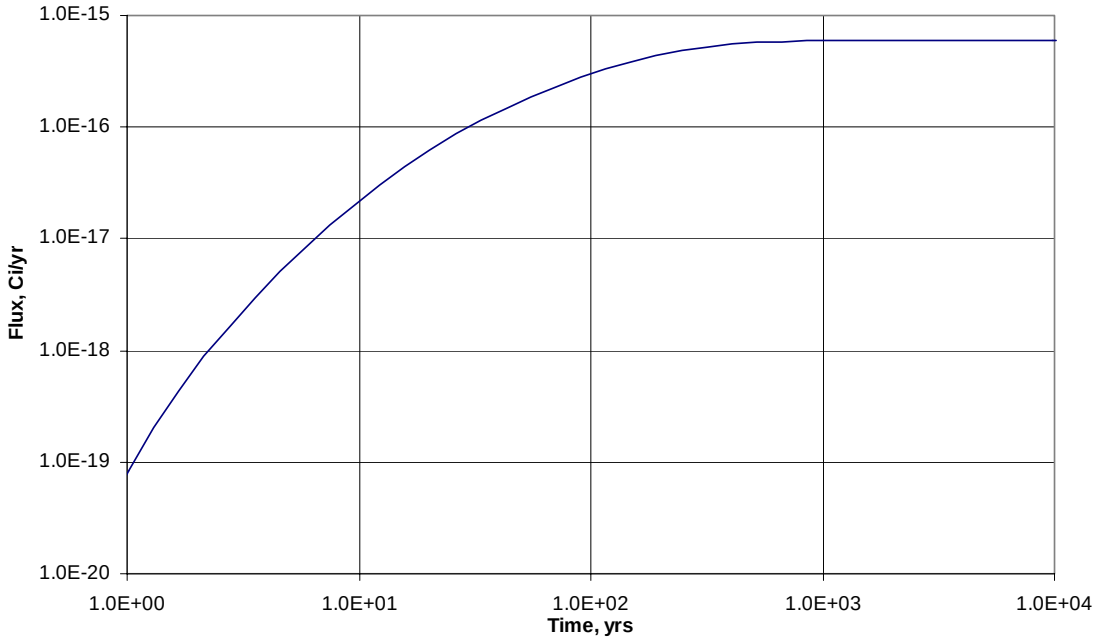

Figure C-5. Flux Rate at Land Surface for I-129

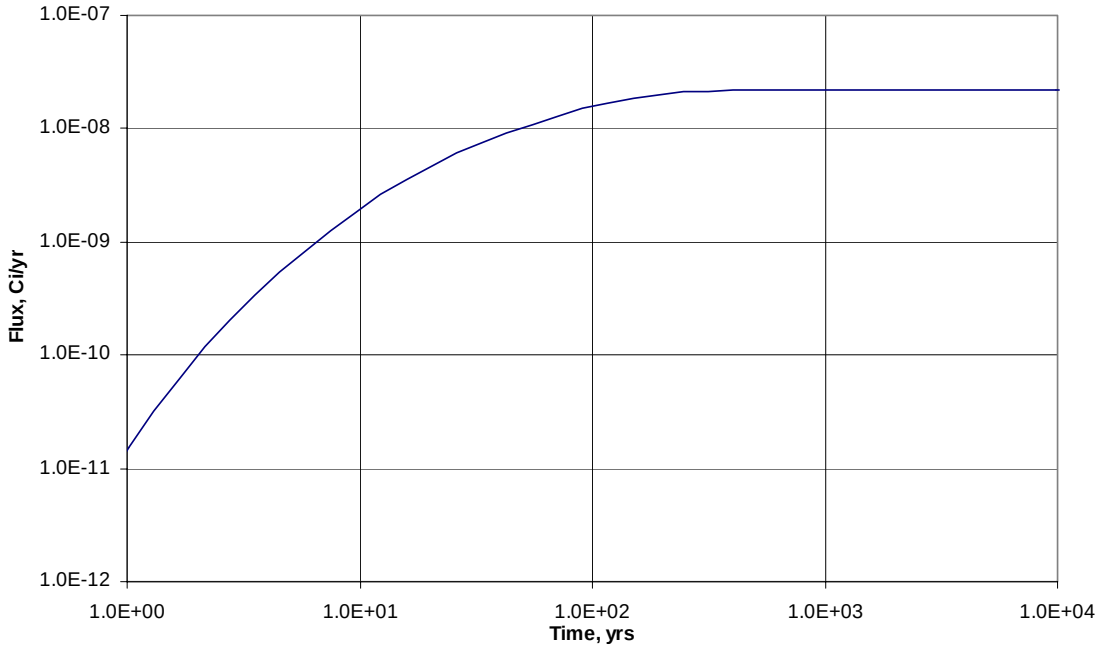

Figure C-6. Flux Rate at Land Surface for Se-79

Table C-5. Summary of the Peak Flux Rates for Each Radionuclide

Radionuclide	Activity Level in Gas Phase (Ci/Ci)	Max. Flux Before 100 years (Ci/yr)	Time of Peak (yr)	Max. Flux after 100 years (Ci/yr)	Time of Peak (yr)
C-14	3.40E-06	2.70E-06	3.16E+02	3.25E-06	3.16E+02
Cl-36	6.20E-08	4.51E-18	8.57E+02	6.19E-18	8.57E+02
H-3	2.5E-06	5.42E-07	1.23E+01	1.22E-08	1.00E+02
I-129	5.90E-06	2.96E-16	1.81E+03	5.90E-16	1.81E+03
Sb-125	8.40E-43	5.34E-45	1.00E+02	4.92E-54	1.00E+02
Se-79	2.20E-08	1.56E-08	8.57E+02	2.20E-08	8.57E+02
Sn-121m	1.70E-64	3.67E-65	1.00E+02	3.08E-65	1.00E+02
Sn-126	1.70E-64	1.07E-64	6.68E+02	1.69E-64	6.68E+02

An evaluation was conducted to assess the potential dose to a maximally exposed individual (MEI) at both the SRS boundary and at the 100 m locations using 1) the peak flux rates realized in the 0-100-year and 100-10,125-year time periods and 2) dose release factors (DRF) that were calculated for each radionuclide at the exposure point associated with each time period. These DRFs were calculated in a separate investigation and documented in Simpkins, A.A., 2004. DRFs represent the dose to the receptor for 1 Ci of the specified radionuclide being released to the atmosphere. Specific DRFs and the calculated exposure levels for the MEI are presented in Table C-6. It should be noted that no DRF was calculated for Sb-126, but its contribution to dose is included with its parent radionuclide, Sn-126.

Also listed in Table C-6 are the Saltstone Vault 4 disposal limits calculated for each of the radionuclides associated with the atmospheric pathway. The Vault 4 limits were calculated by dividing the maximum permissible exposure level (10 mrem/yr) by the highest dose received by the MEI from the 1 Ci source, whether that occurred in the 0-100-year period or the 100-10,125-year period.

Table C-6. Dose Calculations and Saltstone Vault 4 Disposal Limits

Radionuclide	SRS Boundary Dose Release Factor (mrem/Ci)	Dose to MEI at SRS Boundary from 1 Ci in the vault (mrem/yr)	100-meter Dose Release Factor (mrem/Ci)	Dose to MEI at 100 meters from 1 Ci in the vault (mrem/yr)	Saltstone Vault 4 Disposal Limit (Ci)
C-14	1.00E-04	2.70E-10	7.00E-02	2.28E-07	4.39E+07
Cl-36	2.20E-04	9.93E-22	1.10E-01	6.81E-19	1.47E+19
H-3	2.20E-06	1.19E-12	1.50E-03	1.83E-11	5.46E+11
I-129	4.70E-02	1.39E-17	1.00E+02	5.90E-14	1.70E+14
Sb-125	6.30E-03	3.36E-47	2.00E+00	9.83E-54	2.97E+47
Se-79	1.30E-01	2.03E-09	9.40E+01	2.07E-06	4.84E+06
Sn-121m	4.10E-05	1.50E-69	1.40E-02	4.32E-67	2.32E+67
Sn-126	2.90E-01	3.09E-65	9.20E+01	1.55E-62	6.44E+62

C.5 REFERENCES

Bolz, R.E. and G.L. Tuve, (Editors), 1973. *Handbook of Tables for Applied Engineering Science, 2nd Edition*. CRC Press, 18901 Cranwood Parkway, Cleveland, OH.

Crapse, K.P. and J.R. Cook, 2004. *Atmospheric Pathway Screening Analysis for Saltstone Disposal Facility Vault 4*, WSRC-TR-2004-00555, Westinghouse Savannah River Company, Aiken, SC 29808. 11/09/2004.

Cook, J.R., D.C. Kocher, L. McDowell-Boyer and E.L. Wilhite, 2002. *Special Analysis: Reevaluation of the Inadvertent Intruder, Groundwater, Air, and Radon Analyses for the Saltstone Disposal Facility*, WSRC-TR-2002-00456, Westinghouse Savannah River Company, Aiken, SC 29808. 10/23/2002.

Denham, M. and Crapse, K. 2005. *Activity Estimates of Various Radionuclides in Saltstone Vapor Phase*. WSRC-TR-2005-00046. Westinghouse Savannah River Company, Aiken, SC.

Nielson, K.K., V.C. Rogers and G.W. Gee, 1984. *Diffusion of Radon through Soils: A Pore Distribution Model*, Soil Science Society of America, J. 48:482-487

Phifer, M.A. and E.A. Nelson, 2003. *Saltstone Disposal Facility Closure Cap Configuration and Degradation Base Case: Institutional Control to Pine Forest Scenario (U).* WSRC-TR-2003-00436. Westinghouse Savannah River Company, Aiken, SC 29808. 9/2003.

Simpkins, A.A. 2004. *Modeling of Air Releases from the Saltstone Disposal Facility for NESHAP Compliance Considering an Area Source,* SRNL-EST-2004-00071, Inter-Office Memorandum, Westinghouse Savannah River Company, Aiken SC 29808. 12/02/2004.

Yu, C., A.J. Zielen, J.J. Cheng, D.J. LePoire, E. Gnanapragasam, S. Kamboj, J. Arnish, A. Wallo III, W.A. Williams, and H. Peterson, 2001. *Users Manual for RESRAD Version 6*, Environmental Assessment Division, Argonne National Laboratory. Chicago, Illinois.

APPENDIX D
RADON PATHWAY ANALYSIS

THIS PAGE INTENTIONALLY LEFT BLANK

D.1 INTRODUCTION

This section describes the investigation conducted to evaluate the potential magnitude of radon release from Vault 4 of the Saltstone Disposal Facility over the 10,000-year performance assessment period of interest. The permissible radon flux for USDOE facilities is addressed in DOE G 435.1-1 Appendix A. In this Appendix, Section IV. P.(c) states the radon flux limitations associated with the development of a disposal facility and maintenance of a performance assessment and the closure of the disposal facility. This requirement is that the release of radon shall be less than an average flux of 20 $pCi/m^2/sec$ at the surface of the disposal facility. The requirements analysis states that this standard was adopted from the uranium mill tailings requirements in 40 CFR Part 192 and 10 CFR Part 40. 10 CFR Part 40 discusses both Rn-222 from uranium and Rn-220 from thorium, therefore the performance objective refers only to radon, and the correct species must be analyzed depending on the characteristics of the waste stream.

This guidance forms the basis for the investigation to evaluate radon flux above the Saltstone Vault 4. The scope of the investigation involved defining a decay chain of parent radionuclides to evaluate with a 1-D, vertical, numerical model. The model was customized to represent the vertical dimension of Vault 4 and the anticipated cover material described in Phifer and Nelson, 2003. The instantaneous Rn-222 flux at the land surface was evaluated for the Performance Assessment (PA) time period of 10,000 years and this flux was then compared to the USDOE performance objective.

This investigation addresses only Rn-222 from uranium because screening calculations, using the numerical model developed in this analysis, indicates that the short half-life of Rn-220 (55.6 seconds) renders it unable to escape the Saltstone waste form and migrate to the land surface via air-diffusion before it is transformed by radioactive decay.

The potential parent radionuclides that can contribute to the creation of Rn-222 are illustrated in Figure D-1. The diagram indicates the specific decay chains that lead to the formation of Rn-222, as well as the half-lives for each radionuclide. The extremely long half-life of U-238 (4.468E+9 years) cause the other radionuclides higher up on the chain of parents to be of little concern with regard to their potential to contribute significantly to the Rn-222 flux at the land surface over the period of interest.

The methodology used in this analysis is far more quantitative than that used in the existing SRS performance assessments. This analysis applies the capability of the standard SRS groundwater simulation program (PORFLOW) to model gas phase transport through partially saturated porous media to the ground surface.

D.2 SALTSTONE CLOSURE CONSIDERATIONS

The concepts for closure of the Saltstone Vault 4 are relevant to the determination of the radon flux at the land surface during the PA evaluation period (10,000 years). Vault 4 construction specifics and closure concept are described in Cook et al., 2002 and are summarized below.

The current Vault 4 is a concrete vault with a base is constructed 11.5 ft. below grade. Its footprint dimensions are approximately 600 ft. by 200 ft. and it contains 12 individual cells, each having approximate dimensions of 100 ft. by 100 ft by 25 ft. high. Individual cells will be filled with approximately 24 ft. of Saltstone and then approximately 16 in. of uncontaminated grout over which a concrete vault roof will be placed.

D.2.1 Closure Configuration

For the purposes of this investigation, it is assumed that there will be a 30-year operational period during which the unit is loaded with waste. After an individual vault cell is filled with Saltstone, interim closure will be performed which consists of the placement of a 16-inch (0.41 m) clean

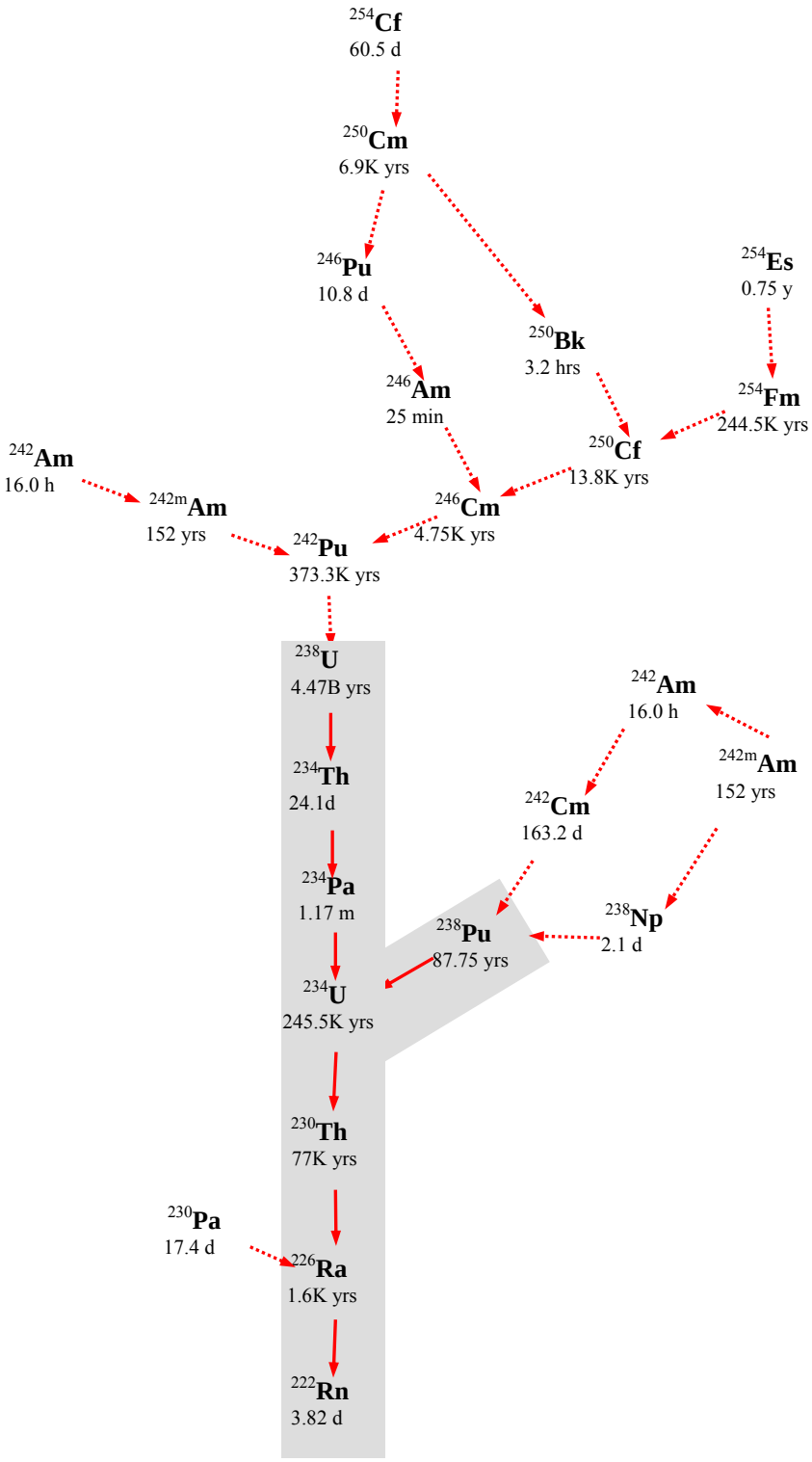

Figure D-1. Radioactive Decay Chains Leading to Rn-222

grout layer between the Saltstone and the overlying concrete roof. Final closure will occur when all Saltstone vaults are filled, and will consist of the placement of a closure cap over all of the vaults. This will be followed by a 100-year period of institutional control, as described in Phifer and Nelson, 2003. The final closure cap will exist far into the future and is the configuration that must be considered in evaluating the long-term radon release at the land surface. A conceptual drawing of a Saltstone vault and closure cap is shown in Figure D-2 and the vertical section over which Rn-222 diffusion was evaluated is indicated.

The closure configuration utilized in this analysis includes all materials, as constructed, including the final closure cap placed over all of the filled vaults at the end of the operations period.

Table D-1 lists the individual components of the vault materials and closure cap. Materials are indicated with the associated thickness of each component, in inches, ft. and m.

Table D-1. Vertical Layer Sequence and Associated Thickness for Saltstone Cover Material

Layer	Thickness (inches)	Thickness (ft)	Thickness (m)
Topsoil	6	0.5	0.15
Upper backfill	30	2.5	0.76
Erosion barrier	12	1	0.3
Middle backfill layer	12	1	0.3
Middle drainage layer	12	1	0.3
Lower backfill layer	58.7	4.89	1.5
Lower drainage layer	24	2	0.6
Vault concrete roof	4	~0.3	~0.1
Vault clean grout layer	16	~1.3	~0.4
Vault Waste Zone	288	~24.7	~7.5

SOURCE: Adapted from Phifer and Nelson, 2003.

The components of concern for the long-term radon performance calculation are those that will persist over the 10,000-year evaluation period. These components are situated below the top of the erosion barrier. The composite thickness of the non-waste material below the top of the erosion barrier is 3.5 m (11.5 ft).

D.3 MODEL DEVELOPMENT

D.3.1 Conceptual Model

The Rn-222 flux at the land surface above the Saltstone Vault 4 was evaluated for its specific closure configuration. Rn-222 is generated within the Saltstone waste zones by radioactive decay of different parent radionuclides following along the decay chains that lead to the formation of Rn-222. The decay chains for all possible parent radionuclides of Rn-222 are shown in Figure D-1. In this figure the parent radionuclides that were individually evaluated are indicated with the gray shaded area (i.e., beginning with Pu-238 and U-238). Rn-222 generated within the waste zone is in the gaseous phase and diffuses outward from this zone into the air-filled soil pores surrounding the vault, eventually resulting in some of the radon emanating at the land surface. As such, air is the fluid through which Rn-222 diffuses, although some Rn-222 may dissolve in residual pore water. It is assumed that fluctuations in atmospheric pressure at the land surface that could induce small pulses of air movement into and out of the shallow soil column will have a zero net effect over the long-term period of evaluation in this study, thus advective transport of Rn-222 in air-filled soil pores is not considered to be a significant process when compared to air

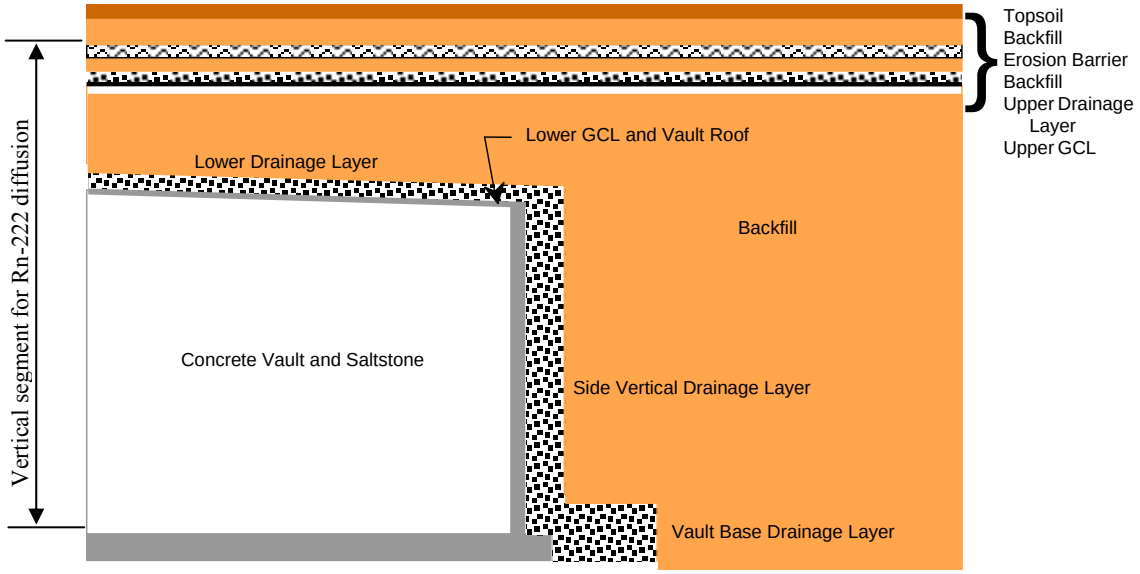

Figure D-2. Conceptual Closure Configuration for Vault 4

diffusion. The parent radionuclides exist in the solid phase and therefore do not migrate upward through the air-filled pore space, although they could be leached and transported downward from the waste zone by pore water movement.

The time period of interest for which the flux of Rn-222 at the land surface was evaluated is 10,000 years. An additional 125 years were added to this to account for any possible Rn-222 buildup during the operational period and 100-year institutional control period.

D.3.2 Numerical Model

The mathematical model utilized in this report is provided by the PORFLOW simulation package. PC-based PORFLOW Version 5.97.0 was used to conduct a series of simulations. PORFLOW is developed and marketed by Analytic & Computational Research, Inc. to solve problems involving transient and steady-state fluid flow, heat and mass transport in multi-phase, variably saturated, porous or fractured media with dynamic phase change. PORFLOW has been widely used at the SRS and in the DOE complex to address major issues related to the groundwater and nuclear waste management.

The governing equation for mass transport of species *k* in the fluid phase is given by

$$\frac{\partial C_k}{\partial t} + \frac{\partial}{\partial x_i}(V_i C_k) = \frac{\partial}{\partial x_i}(D_{ij}\frac{\partial C_k}{\partial x_j}) + \gamma_k$$

Where

C_k	concentration of species *k*
V_i	fluid velocity in the i^{th} direction
D_{ij}	effective diffusion coefficient for the species
γ_k	net decay of species *k*
i, j	direction index
t	time
x	distance coordinate

This equation is solved using PORFLOW to evaluate transient Rn-222 transport through the soil cover above Saltstone Vault 4 to evaluate Rn-222 flux at the land surface over time. For this exercise the advection term was disabled within PORFLOW and only the diffusive and net decay terms were evaluated.

D.3.3 Model Development and Assumptions

The numerical representation of the conceptual model is as a 1-dimensional vertical stack of elements configured to represent the thickness of the Saltstone and overlying cover material associated with final closure of Vault 4.

Decay chains evaluated were U-238→Th-234→Pa-234m→U-234→Th-230→Ra-226→Rn-222 and Pu-238 →U-234→Th-230→Ra-226→Rn-222. Each parent in these chains, except Th-234 and Pa-234m, were simulated separately as the starting point of the decay chain. Th-234 and Pa-234m have extremely short half-lives compared to the other parent radionuclides in these chains. Only a fraction of the Rn-222 generated by the decay of each parent is available for migration away from its source and into open pore space. Since the Rn-222 parent radionuclides exist as oxides or in other crystalline forms, only a fraction of Rn-222 generated by decay of Ra-226 has sufficient energy to migrate away from its original location into adjacent pore space before further decay occurs (3.82 day half-life for Rn-222). The fraction of radon escaping its

source and migrating into adjacent pore space is approximated by the use of a radon emanation coefficient. This coefficient has been shown to vary between 0.02 and 0.7 in soils but is typically 0.25 (Yu et al. 2001). This value is taken as the default factor value for the RESRAD program, developed for the USDOE. To account for this effect in this model, an effective source term of 0.25 Ci of parent radionuclide was utilized as the source term for each Ci disposed within the facility.

Since Rn-222 exists as a gas, air was assumed to be the fluid within which radon transport occurs. The flow field was assumed to be isobaric and isothermal. The impact of naturally occurring fluctuations of atmospheric pressure is likely to have a zero net effect and only a very shallow zone of influence at the land surface. Therefore, for the relatively long periods of time evaluated in this investigation, air-diffusion was the only transport mechanism simulated in the model and advective air-transport was assumed to be negligible.

Some radon dissolves in pore water but since diffusion proceeds more slowly in that fluid, air diffusion is the only transport process by which Rn-222 can reach the land surface from the Saltstone waste zone. This assertion is substantiated in Yu, et al. 2001. In that report the D_{eff} for soil is reported to range from the radon open air diffusion coefficient of 1.0E-6 m^2/sec to that of fully saturated soil, 1.0E-10 m^2/sec. This 4-order of magnitude difference is consistent with the comparison of water diffusion coefficients to air diffusion coefficients of other common molecular compounds and reported in many references. Thus, the larger volume of water-filled pore space compared to air-filled pore space (maximum of 1 order of magnitude difference) is inconsequential, in terms of the ability of water-dissolved radon to diffuse through water-filled pores as compared to the ability of the same compounds to diffuse as gas in the vapor-filled pore spaces. In this investigation, transport was allowed to proceed only through air-filled pore space and, therefore, residual pore water was treated as if it was part of the solid matrix material within the flow field. No credit was taken for airborne radon dissolving in pore water as it proceeds from the vault to the land surface although it has been observed to partition between air and water in the ratio of 4 to 1, respectively, at 20° C (Nazaroff, W.W. and A.V. Nero 1988).

The boundary conditions imposed on the domain included:

- No-flux specified for all parent radionuclides at perimeter of the domain
- No-flux specified for Rn-222 along sides and bottom
- Rn-222 concentration set to 0 at land surface.

Simulations were conducted in transient mode for diffusive transport in air, with results being obtained over 10,125 years.

D.3.4 Measures Implemented to Assure Conservative Results

In this analysis, several conditions introduce a significant measure of conservatism into the calculations. These include:

- The use of boundary conditions that force all of the Rn-222 to move upward from the waste disposal zone to the land surface. In reality, some of the Rn-222 diffuses sideways and downward in the air-filled pores surrounding the waste zone, hence ignoring this has the effect of increasing the radon flux at the land surface.
- Not taking credit for the removal of either Rn-222 or of the parent radionuclides by pore water moving vertically downward through the model domain. This mechanism would likely carry off some dissolved Rn-222 in addition to the parent radionuclides, and therefore its omission has the effect of increasing the estimate of instantaneous Rn-222 flux at the land surface in simulations conducted as a part of this investigation.

- The addition of an extra 125 years to the required 10,000-year evaluation period to account for any Rn-222 generated during the operations and institutional control period, thus incrementally increasing the instantaneous Rn-222 flux. The extra time means slightly higher instantaneous fluxes for all parent radionuclides except Ra-226 and Th-230.
- Use of the top of the erosion layer in the soil cover as the land surface for the purpose of calculating Rn-222 flux. No credit is taken for the additional distance Rn-222 must migrate above the erosion layer prior to that portion of the Soil Cover Zone eroding away. This assumption impacts only Ra-226.

D.3.5 Grid Construction

The model grid was constructed as a node mesh 3 nodes wide by 36 nodes high. This mesh creates the vertical stack of 34 model elements. The grid extends upward only as far as the erosion barrier, anticipating that this is the cover thickness that will prevail over the majority of the 10,125-year evaluation period. A set of consistent units was employed in the simulations for length, mass and time, these being meters, grams and years, respectively.

D.3.6 Material Zones

The model domain was divided into two primary zones, the Saltstone waste zone occupying the lower 24.7 ft. (7.5 m) of the domain and the cover zone, extending ~11.4 ft. (~3.5 m) above the waste zone to the top of the domain. The cover zone includes the vault concrete roof as well as the different closure cap layers. The upper model elements were scaled to correspond to the geometry of the closure cap thickness while the lower model elements were scaled to correspond to the Saltstone waste zone. The land surface for the evaluation period of interest is assumed to be the top of the erosion resistant layer, within the closure cap, and no credit is taken for the compacted soil and topsoil above that layer.

D.3.7 Material Zone Properties and Other Input Parameters

Material properties utilized within the 1-D numerical model were specified for 7 material zones defined within the model domain. Each material zone was assigned values of total porosity, residual saturation, air-filled porosity, matrix density, air density, and an effective air-diffusion coefficient for Rn-222. Selection of effective Rn-222 diffusion coefficients was based on a soil pore size distribution model that allowed the selection of effective Rn-222 air-diffusion coefficients based on the degree of residual water saturation (Nielson et al. 1984). With the use of an effective air-diffusion coefficient, tortuosity was assigned a unit value in each material zone. The rock (matrix) density was selected based on the density of quartz, and is regarded to be representative of most SRS soils.

Values for total porosity and long-term residual saturation for concrete and Saltstone were obtained from vadose zone 2-D simulations conducted to evaluate the groundwater pathway as a part of this Special Analysis which are presented in Appendix A. Concrete and Saltstone porosities were established at 0.18 and 0.42, respectively in that analysis. The steady-state residual saturations were obtained from representative nodes in the simulation domain. These values were found to be 0.99 for both materials at reference nodes (35,50) and (35,67) for Saltstone and concrete, respectively.

Values for total porosity and long-term residual saturation for the closure cap materials were selected based on a series of HELP model simulations conducted as part of the investigation summarized in Phifer, M.A. and E.A. Nelson, 2003. HELP model analyses were conducted at different points in time, these being at 100, 300, 550, 1000, 1800, 3400, 5600 and 10,000 years in the future. Porosities of the different materials changed slightly through time as a result of leaching and residual saturations varied as porosities and expected recharge rates varied.

Porosities changed less conspicuously than residual saturations, and by plotting residual saturation versus time, representative values could then be selected. The values selected were chosen to be more representative of the 5,600 to 10,000-year time frame because that is when most of the peak instantaneous Rn-222 fluxes occur. A summary of the values of porosity, long-term residual saturation, air-filled porosity and the effective Rn-222 air-diffusion coefficients are listed for each material type in Table D-2.

Table D-2. Porosity, Residual Saturation, and Air-filled Porosity Values

Layer Material	Representative Porosity	Long-term Residual Saturation	Air-filled Porosity	Eff. Diffusion Coefficient (m^2/yr)
Erosion Barrier	0.07	0.83	1.19E-02	7.89E-01
Upper Backfill	0.38	0.63	1.39E-01	4.73E+00
Upper Drainage	0.38	0.58	1.58E-01	4.73E+00
Lower Backfill	0.37	0.72	1.04E-01	2.84E+00
Lower Drainage	0.31	0.5	1.60E-01	6.31E+00
Concrete	0.18	0.99	2.00E-03	7.89E-01
Saltstone	0.42	0.99	4.00E-03	7.89E-01

Air-filled porosity was calculated by subtracting the residual moisture content from the total porosity. A value for the density of air was obtained from the Bolz, R.E. et al., CRC Handbook of tables for Applied Engineering Science.

D.4 MODEL RESULTS

Model simulations were conducted to evaluate the peak instantaneous Rn-222 flux at the land surface over the 10,125-year period. This time period includes the 25-year operations cycle, 100 years of institutional control, and the 10,000-year compliance period. Model results were output in Ci/m^2/yr, consistent with the set of units employed in the model. A graph of these results is shown in Figure D-3, although the units are converted to pCi/m^2/sec, which are the units used to define the regulatory flux limit in 40 CFR Part 61, Rev. 4.

The peak fluxes represent the peak Rn-222 flux per square meter at the top of the closure cap erosion barrier and are listed below in Table D-3. The top of the erosion barrier is expected to represent the land surface 10,125 years in the future. Also shown in Table D-3, for each of the 5 parent radionuclides, are the calculated disposal limits per unit area and the Vault 4 disposal limits. The unit-area disposal limit was calculated as follows:

Disposal Limit per unit area (Ci/m^2) =

Regulatory limit (20 pCi/m^2/s) / Inst. flux per unit area per unit inventory of parent radionuclide per unit area ([pCi/m^2/s]/Ci/m^2])).

The unit area limits for each of the 5 parent radionuclides was converted to Vault 4-specific disposal limit by multiplying the unit area limit for each by the area of the Vault 4 footprint. This area is calculated to be 182m × 61m = 11,102 m^2. The calculated results are presented in Table D-3.

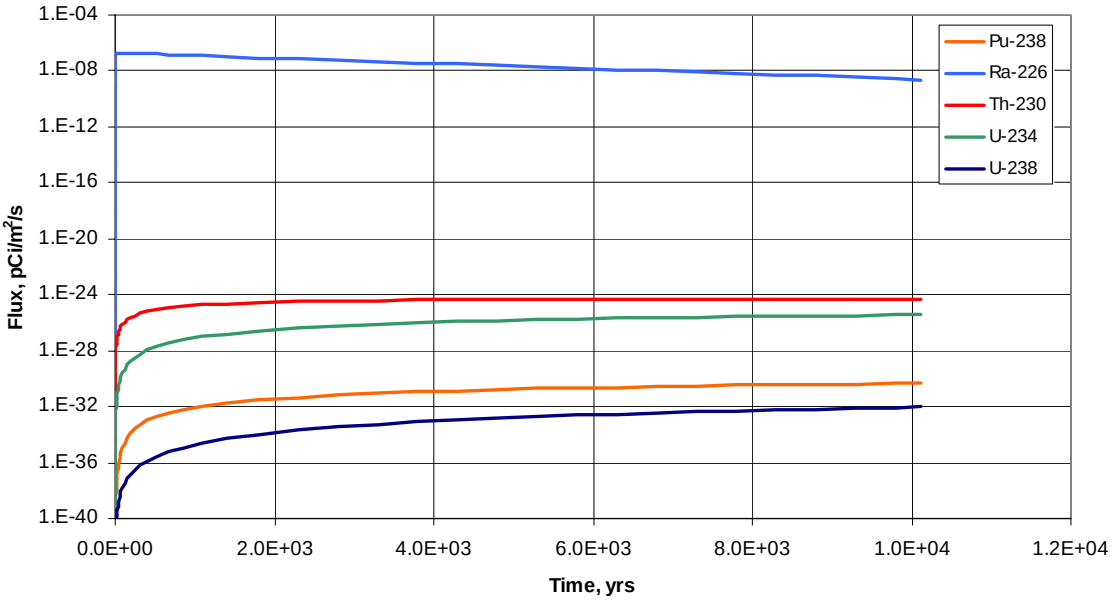

Figure D-3. Rn-222 Flux at Land Surface Resulting from Unit Source Terms

Table D-3. Simulated Peak Instantaneous Rn-222 Flux Over 10,125-Years at the Land Surface and Associated Disposal Limits for Parent Radionuclides

Parent Source (1 Ci)	Peak Instantaneous Rn-222 Flux at Land Surface ($pCi/m^2/s$)	Disposal Limit Per Unit Area (Ci/m^2)	Vault 4 Disposal Limit (Ci/Vault 4)
Pu-238	4.61E-31	4.34E+31	4.82E+35
U-238	9.25E-33	2.16E+33	2.40E+37
U-234	3.78E-26	5.29E+26	5.88E+30
Th-230	4.90E-25	4.08E+25	4.53E+29
Ra-226	1.95E-07	1.03E+08	1.14E+12

D.5 REFERENCES

Bolz, R.E. and G.L. Tuve, (Editors), 1973. *Handbook of tables for APPLIED ENGINEERING SCIENCE, 2'nd Edition*. CRC Press, 18901 Cranwood Parkway, Cleveland, OH.

Phifer, M.A. and E.A. Nelson, 2003. *Saltstone Disposal Facility Closure Cap Configuration and Degradation Base Case: Institutional Control to Pine Forest Scenario (U).* WSRC-TR-2003-00436. Westinghouse Savannah River Company, Aiken, SC 29808. 9/2003.

Cook, J.R., D.C. Kocher, L. McDowell-Boyer and E.L. Wilhite, 2002. *Special Analysis: Reevaluation of the Inadvertent Intruder, Groundwater, Air, and Radon Analyses for the Saltstone Disposal Facility*, WSRC-TR-2002-00456, Westinghouse Savannah River Company, Aiken, SC 29808. 10/23/2002.

Nazaroff, W.W., and A.V. Nero (editors), 1998, *Radon and its Decay Products in Indoor Air*, John Wiley & Sons, New York, N.Y.

Nielson, K.K., V.C. Rogers and G.W. Gee, 1984. *Diffusion of Radon through Soils: A pore distribution Model*, Soil Science Society of America, J. 48:482-487.

Yu, C., A.J. Zielen, J.J. Cheng, D.J. LePoire, E. Gnanapragasam, S. Kamboj, J. Arnish, A. Wallo III, W.A. Williams, and H. Peterson, 2001. *Users Manual for RESRAD Version 6*, Environmental Assessment Division, Argonne National Laboratory. Chicago, Illinois.